Title
Ecological Aspects of the Diversity Dynamics of North American Fossil Mammals

Author
Tomiya, Susumu

Publication Date
2012

Peer reviewed|Thesis/dissertation

Ecological Aspects of the Diversity Dynamics of North American Fossil Mammals

By

Susumu Tomiya

A dissertation submitted in partial satisfaction of the

requirements for the degree of

Doctor of Philosophy

in

Integrative Biology

in the

Graduate Division

of the

University of California, Berkeley

Committee in charge:

Professor Anthony D. Barnosky, Chair
Professor David R. Lindberg
Professor Wayne M. Getz

Fall 2012

Ecological Aspects of the Diversity Dynamics of North American Fossil Mammals

by Susumu Tomiya

Abstract

Ecological Aspects of the Diversity Dynamics of North American Fossil Mammals

by

Susumu Tomiya

Doctor of Philosophy in Integrative Biology

University of California, Berkeley

Professor Anthony D. Barnosky, Chair

The dissertation research presented herein addresses two questions on possible ecological drivers of mammalian diversity dynamics at macroevolutionary time scales. The first question is whether key intrinsic biological traits that are tightly correlated with body size (e.g., reproductive rates) have strong influence on the extinction probability of mammalian taxa at the generic level. The second question is whether, within a regional mammalian fauna, the ecological composition of carnivores (as inferred from their dental morphology) responds in predictable manners to shifts in the ecological composition of non-carnivores that represent their potential prey.

In preparation for the ecological analyses of carnivore and non-carnivore compositional changes through time, concentrated effort was made to advance the taxonomy of carnivorous mammals from the middle Eocene of southern California. As part of this effort, the first chapter describes a carnivoramorphan that sheds a new light on the origin and early evolution of crown-group carnivorans. The new taxon, *Lycophocyon hutchisoni*, exhibits stages of dental and basicranial evolution that are intermediate between earlier carnivoramorphans and the earliest representatives of canoid carnivorans. The evolutionary affinity of the new taxon was determined by a cladistic analysis of previously-published and newly-acquired morphological data for 30 Paleogene carnivoramorphans. The most-parsimonious trees identified *L. hutchisoni* as a basal caniform carnivoran, and placed (1) *Tapocyon robustus*, *Quercygale angustidens*, "*Miacis*" *sylvestris*, "*M.*" *uintensis*, and "*M.*" *gracilis* inside or outside the Carnivora, (2) nimravids within the Feliformia, and (3) the amphicyonid *Daphoenus* outside the crown-group Canoidea. Parsimony reconstructions of ancestral character states suggest that loss of the upper third molars and development of well-ossified entotympanics that are firmly fused to the basicranium (neither condition is observed in *L. hutchisoni*) are not associated with the origin of the Carnivora as traditionally thought, but instead occurred independently in the Caniformia and the Feliformia. A discriminant analysis of the estimated body weight and dental ecomorphology predicted a mesocarnivorous diet for *L. hutchisoni*, and the postcranial morphology suggests a scansorial habit. Thus, *Lycophocyon hutchisoni* illuminates the morphological evolution of early caniforms leading to the origin of crown-group canoids. Nevertheless, considerable uncertainty remains with respect to the phylogenetic origin of the Carnivora. The minimum date of caniform-feliform divergence is provisionally suggested to be either 47 million years ago or 38 million years ago, depending on the position of "*Miacis*" *sylvestris* within or outside the Carnivora, respectively.

The second chapter investigates the relationship between body size as a proxy for various intrinsic biological traits of key importance and extinction probability as measured by durations of genera in the fossil record. Preservation of mammalian diversity requires a concentrated effort to identify biological correlates of vulnerability to environmental perturbations. Studies of living mammals and late-Quaternary extinctions frequently point to large body size as a correlate—if not necessarily a determinant—of elevated extinction risk in mammalian species, and this correlation is often attributed to slow reproductive rates and lower population densities of large taxa. At the same time, biological patterns of extinction risk above the level of species have received much less attention, despite their relevance to conservation of evolutionary history embedded in ecological types that are more inclusive than individual species. I examined the North American fossil record of modern and some extinct families of terrestrial mammals to test whether extinction probability (or, more precisely, inter-regional extirpation probability) of genera, as measured by their durations in geologic time, scales with body size across 7 orders of magnitude in body weight. After adjusting observed generic durations for significant paleontological sampling bias against small taxa, generalized least-squares regression analyses showed no correlation between estimated body weights and durations in 221 Oligo-Pleistocene genera ranging from shrews to rhinoceroses. The same lack of correlation was observed for subsets of the data that (a) approximated basic trophic divisions (small/large herbivores, "insectivores," and carnivores) or (b) were grouped by the timing of extinctions, suggesting that the overall pattern is not clouded by trophic and temporal variations in the relationship between size and vulnerability. The only notable deviation from this pattern was the significantly shorter durations of carnivorans compared to other taxonomic/ecological groups. Qualitatively identical results were obtained by analyses of durations and inter-birth interval lengths expected from body weights. Thus, in general, the population-biological expectation of higher extinction risk for large and slow-reproducing mammals was not supported for the genera that lived prior to significant anthropogenic influence. Two non-exclusive hypotheses are offered to explain this apparent mismatch: (1) the size-biased extinctions since the late Quaternary and elevated extinction risk for living large mammals signify an abnormal state of diversity dynamics brought about by human-induced reduction of large-mammal populations to critical levels, below which demographic or environmental stochasticity alone can threaten slow-reproducing taxa of low population density; (2) large mammalian species indeed have higher probabilities of extinction, but replacement of lost species within genera compensates for this pattern, resulting in comparable durations of large and small taxa at the genus level. The corollary of the first hypothesis is that, in normal times, thriving large mammals are no more likely—and perhaps less likely—to reach the critical population size than small mammals. The second hypothesis, if true, would indicate that extinction processes are distinct across levels of phylogenetic hierarchy and that prediction of future extinctions at supraspecific levels should not simply rely on extrapolation of extinction risk for individual species, especially if some of the species constituting a genus of interest are poorly known.

Building on the taxonomic work on the middle-Eocene carnivores of southern California, I investigate in the final chapter the matches and mismatches between shifts in the ecological compositions of mammalian carnivores and other mammals that constitute their potential prey at the macroevolutionary time scale of approximately 6-9 million years. The middle-Eocene fossil record of southern California, which includes a diverse array of carnivores and particularly rich

record of small mammals, was analyzed. Appearance event ordination was used to estimate the relative ages of fossil-bearing localities and their associated assemblages. Using the predicted temporal ranges of carnivore taxa and locality-level occurrence data for non-carnivores (ultimately grouped into time bins), it was found that changes in the distribution of taxa, and possibly taxonomic abundance as well, across morphological categories (defined by estimated body weight, arboreal versus non-arboreal habit, and ecologically-informative dental morphology) are largely discordant between carnivores and non-carnivores in the study system, except for the overall increase in the number of taxa in both groups. Analysis of morphological-compositional variation and factors that correlate with taphonomic disparity lend support to the interpretation of observed diversity fluctuations through time in non-carnivores. The findings raise additional questions about the controls of carnivore diversity—for example, what promotes the appearance of new morphotypes—and predictability of their extinctions.

Table of Contents

*Reproduced with modification from the original publication (under the Creative Commons Attribution License): Tomiya, S. 2011. A new caniform (Carnivora: Mammalia) from the middle Eocene of North America and remarks on the phylogeny of early carnivorans. PLoS ONE 6:e24146. Available at http://www.plosone.org/article/info:doi/10.1371/journal.pone.0024146.

Acknowledgements

Various aspects of this dissertation were improved through illuminating discussions with, and insightful comments from, Anthony D. Barnosky, William A. Clemens, Alan B. Shabel, Patricia A. Holroyd, Elizabeth A. Wommack, Michelle Spaulding, David R. Lindberg, Wayne M. Getz, Charles R. Marshall, Marc A. Carrasco, Alex Hubbe, M. Allison Stegner, Emily L. Lindsey, Kaitlin C. Maguire, Natalia Villavicencio, Jenny L. McGuire, Anthony R. Friscia, Paul C. Murphey, Diane M. Erwin, Jeffrey A. Myers, and K. E. Beth Townsend. In addition, I am indebted to Juliana K. Olsson for her exquisite drawings of the dentition of *Lycophocyon hutchisoni* (Figure 1.4) and Vanessa E. Van Zerr for assistance with data collection for the analysis of dental size variation in carnivorans.

For access to museum collections, I thank Christopher J. Conroy and Eileen A. Lacey (Museum of Vertebrate Zoology, University of California, Berkeley), Maureen E. Flannery (California Academy of Sciences, San Francisco), Vanessa R. Rhue, Samuel A. McLeod, and Xiaoming Wang (Natural History Museum of Los Angeles County, Los Angeles), Mark A. Norrell and Judy Galkin (AMNH), Michael K. Brett-Surman (National Museum of Natural History, Washington, D.C.), Daniel L. Brinkman (Yale Peabody Museum of Natural History, New Haven), Amy C. Henrici and Alan R. Tabrum (CM), and Kenneth D. Rose (Johns Hopkins University, Baltimore). I am particularly grateful to Kesler A. Randall and Thomas A. Deméré (SDSNH) for allowing my use of their collection record and making my numerous visits to San Diego both productive and enjoyable.

For hospitality during my museum visits, I thank J. Galkin and Brian P. Kraatz (AMNH), E. Bruce Lander (Paleo Environmental Associates, Inc., Altadena), Z. Jack Tseng and Xiaoming Wang (Natural History Museum of Los Angeles County, Los Angeles), Samantha S. B. Hopkins, Edward B. Davis, and John D. Orcutt (University of Oregon), and Kaitlin C., Clare C., and John X. Maguire.

The research for the first and last chapters of this dissertation was in part funded by the National Science Foundation grant DDIG-1011474, the Grant-in-Aid-of-Research program of the Berkeley Chapter of Sigma Xi, and various graduate-student research grants from the UCMP and the Department of Integrative Biology. In addition, I was supported by the Annie M. Alexander Fellowship of the UCMP and a grant from the UC Berkeley Graduate Division during the preparation of this dissertation.

It is not possible here to express my gratitude to all the individuals—from my fellow graduate students and past and present lab mates to the staff of the UCMP and the Department of Integrative Biology—who have contributed to my well-being in the last six years, but I must state that I owe my most sincere thanks to Tony Barnosky for all his support, inspiration, and encouragement, Pat Holroyd for sage advice, and Jenny L. McGuire, Emily L. Lindsey, and Kaitlin C. Maguire for their friendship.

Chapter 1

A new basal caniform (Mammalia: Carnivora) from the middle Eocene of North America and remarks on the phylogeny of early carnivorans

Introduction

The first major effort to reconstruct the ancestry of the mammalian order Carnivora goes back over a century. As early as 1898, Scott (1898) took particular note of numerous skeletal similarities among carnivorans from the late Eocene to early Oligocene of western North America, such as the nimravid *Dinictis*, the amphicyonid *Daphoenus* (then regarded as a canid), and the canid *Hesperocyon*. He interpreted these similarities as an indication for basal divergences of carnivoran lineages not long before the Oligocene. Around the same time, Wortman and Matthew (1899), working on the systematics of carnivoramorphans (carnivorans and their close relatives) from the middle-Eocene Bridger and Uinta Formations of Wyoming and Utah, inferred largely linear series of descent from such fossil taxa as *Uintacyon* and *Procynodictis* to some of the extant canids based on what they recognized as progressive stages of skeletal evolution. Matthew (1909) later expanded upon this study and presented a more complex phylogeny, portraying the early radiation of carnivoramorphans as divergent adaptations to various habitats and diets. His monumental work was soon followed by that of Teilhard de Chardin (1914-1915) on early carnivorans from the Eocene-Oligocene fissure-fill deposits of Quercy, France. Through a detailed study of dental morphology, Teilhard proposed that many of the lineages leading to extant families had already separated by the Miocene. These early workers were keenly aware of the difficulty of distinguishing phylogenetically-informative traits from parallel or convergent similarities, but lacked an analytical framework to deal with this problem.

The introduction of cladistics in paleontology thus provided an impetus for renewed investigations of the carnivoran origin, and precipitated in the last 30 years the seminal works of Flynn and Galiano (1982), Wang and Tedford (1994), and most recently, Wesley-Hunt and Flynn (2005). Respectively, these studies advanced foundational hypotheses on carnivoramorphan clades (Flynn and Galiano, 1982), unraveled the intricacies of basicranial evolution from early carnivoramorphans to early canids (Wang and Tedford, 1994), and clarified the relationships of some of the basal carnivoramorphan groups to carnivorans (Wesley-Hunt and Flynn, 2005). Still, a holistic understanding of the phylogenetic, biogeographic, and ecological context of the carnivoran origin has yet to emerge, owing to the paucity of well-preserved basicranial and postcranial remains for many of the Paleogene taxa, as well as the limited spatial sampling of fossils both at the continental and global scales (Hunt, 1996*b*; Flynn and Wesley-Hunt, 2005).

This paper presents a taxonomic description of a new genus of carnivoramorphan from the Eocene Epoch, which constitutes a critical period of major cladogenetic events within the Carnivora (Bininda-Emonds et al., 2007, 2008; Eizirik et al., 2010). Cladistic analyses were conducted to assess the phylogenetic affinity of the new taxon and to further elucidate the evolutionary relationships among early carnivorans and their close carnivoramorphan relatives. In addition, the diet and locomotor habit of the new taxon are discussed to facilitate future studies of carnivoramorphan evolution from the ecological perspective.

In this paper, I follow Bryant's (1996:p. 184) phylogenetic definitions of higher taxa emended

from Wyss and Flynn (1993): the crown-group Carnivora is defined as the "most recent common ancestor of Feloidea, all species referred to Canidae by Wilson and Reeder (1993), and Arctoidea and all of its descendants"; the name Carnivoramorpha is applied to the more inclusive, stem-based group consisting of the "Carnivora and all members of Mammalia (Rowe, 1988) that are more closely related to Carnivora than to taxa referred to Creodonta by Carroll (1988)." It should be noted, however, that the sister-group relationship of the Carnivora and Creodonta is yet to be demonstrated in a comprehensive cladistic study of eutherian mammals (Polly, 1996). Phylogenetically, the origin of Carnivora is the point of divergence of its two major lineages, the Caniformia and the Feliformia. Within the stem-group Caniformia, the crown group Canoidea encompasses the "most recent common ancestor of Arctoidea and the species referred to Canidae by Wilson and Reeder (1993) and all of its descendants" (Bryant, 1996:p. 184).

Accurate estimates of lineage divergence dates are essential for studies of trait evolution (Garland et al., 1992), diversity dynamics and biogeographic histories of major groups (Arnason et al., 2006; Gaubert and Cordeiro-Estrela, 2006; Koepfli et al., 2007, 2008; Eizirik et al., 2010), and ecological community assembly (Cooper et al., 2008), as well as for the evaluation of biological conservation priorities (Diniz-Filho, 2004; Isaac et al., 2007). The node that marks the caniform-feliform divergence is important in mammalian phylogenetics because it is frequently selected as one of multiple fossil calibration points used in deriving the time scale for a molecular tree (Eizirik et al., 2001; Murphy et al., 2001; Corneli, 2003; Springer et al., 2003; Woodburne et al., 2003; Yoder et al., 2003; Arnason et al., 2006, 2007, 2008; Johnson et al., 2006; Kitazoe et al., 2007; Poux et al., 2008; Wan et al., 2009; Fulton and Strobeck, 2010). Judicious selection of a fossil constraint in this context requires the knowledge of cladistic relationships of relevant fossil taxa, and must be updated according to the advancement of phylogenetic hypotheses in paleontology.

Geographical and Geological Context

All currently-known specimens of the new carnivoramorphan come from the middle-Eocene non-marine sediments of "member C" (an informally-designated unit) (Wilson, 1972) of the Santiago Formation in San Diego County, California (Fig. 1.1). The holotype and a paratype (UCMP 170713) were collected in 1968 by personnel of the University of California Museum of Paleontology (UCMP; Berkeley, California, U.S.A.) at the Laguna Riviera housing subdivision in Carlsbad, California. Golz (1976) reported the lithology of the holotype locality, V6839, as successive layers of sand and mudstone, in which most of the vertebrate fossils were concentrated in the sand-mud transitional zone. Based on this and the occurrence of reed impressions and brackish to freshwater invertebrates in the mudstone, he interpreted the depositional environment for the vertebrate remains to have been transitional between fluvial and lagoonal. The locality V6885, which yielded UCMP 170713, is a small sedimentary pocket of sandstone with a high concentration of vertically-oriented skeletal elements, and is located roughly 2 meters below the level of V6839 (D. P. Whistler, field notes for August 8, 1968, on file at the UCMP).

Golz (1976) described the mammalian assemblages from V6839 and other localities in its vicinity as the Laguna Riviera Local Fauna, and considered them to be of the late Uintan North American Land Mammal Age (NALMA) based on the occurrence of the leporid *Mytonolagus* and the composition of artiodactyls similar to that in the Myton Member of the Uinta Formation, Utah. However, in the most-recent summary of middle-Eocene mammalian assemblages from San Diego County, Walsh (1996) suggested the possibility of an early Duchesnean NALMA for the Laguna

Riviera Local Fauna based partly on the occurrence of the rhinocerotoid *Amynodontopsis bodei* and the pantolestan *Simidectes merriami*.

The remaining specimens are from the San Diego Natural History Museum (SDSNH; San Diego, California, U.S.A.) localities at the Ocean Ranch Corporate Centre, Oceanside, California. Most of the localities are associated with sandy channel-deposits, and all are assigned to the Duchesnean NALMA based on the taxonomic composition of mammals (Mihlbachler and Deméré, 2009).

A diverse array of vertebrate taxa are known from the holotype locality V6839, including fish, turtles, snakes, crocodiles, and birds. The mammalian component of the assemblage is numerically dominated by small to medium-sized selenodont artiodactyls such as *Leptoreodon* and *Protoreodon*, but also includes: erinaceomorph lipotyphlans; ischyromyid, cylindrodontid, and dipodid rodents; omomyid primates; and members of the enigmatic groups Apatotheria (*Apatemys* sp.) and Pantolesta (*Simidectes merriami*).

Materials and Methods

All currently-known specimens of *Lycophocyon hutchisoni* are housed at the University of California Museum of Paleontology and the San Diego Natural History Museum. A list of comparative specimens directly examined by the author is provided in Appendix S1.1. Skeletal comparisons with extant carnivorans are based on the author's direct observation of modern specimens. The taxonomic classification of extant carnivorans follows Wilson and Reeder (2005).

Anatomical Terminology and Measurements

The anatomical terminology used in this paper follows primarily: Mac Intyre (1966), Van Valen (1966), Flynn and Galiano (1982), and Heinrich et al. (2008) for dentition; Wang and Tedford (1994) for basicranium; and Gingerich (1983) and Heinrich and Rose (1997) for postcrania. All measurements were taken with digital calipers with the accuracy of 0.01 mm, and are reported to the nearest 0.1 mm. Dental measurements follow Gingerich (1983), and measurements of humerus and ulna follow Meachen-Samuels and Van Valkenburgh (2009).

Statistical Comparisons of Size Variation

The comparative samples consisted of 27 specimens of the earliest-known canid *Hesperocyon gregarius* from the late Eocene to early Oligocene (Chadronian to Whitneyan NALMA) of the northern and central Great Plains, 51 specimens of *Urocyon cinereoargenteus townsendi* from California, U.S.A., and 29 specimens of *Martes pennanti columbiana* from British Columbia, Canada. All measurements are reported in Appendix S1.2. For the fossil taxa, only the specimens that could be confidently assigned to separate individuals were measured to avoid data duplication. Both the differences among the sample means (not exceeding an order of magnitude) and the percent measurement errors (0.8 to 5.5%) are sufficiently small for proper comparisons of CVs (cf. Polly, 1998).

Because the conventional F-ratio test is sensitive to non-normal distribution of data (Plavcan and Cope, 2001), the randomization procedure of Lockwood et al. (1996) was adopted for

the present analysis. From each comparative sample, 10,000 bootstrap replicates (Efron, 1979) of 9 m1L measurements (to make the subsample size equal to the sample size of *Lycophocyon hutchisoni*) were produced, and the CV was calculated for each replicate. Finally, the frequency distribution of 10,000 CVs was compared to the CV of *L. hutchisoni*; if the latter fell outside the bias-corrected 95% confidence interval (Efron, 1981) of the former, the sample of *L. hutchisoni* was considered to be significantly more (or less) variable than that of the comparative taxon. All computations were performed in the R programming environment Version 2.10.1 for Windows (R Developement Core Team, 2009).

Dietary Inference

The body weight of the individual represented by the holotype UCMP 85202 was estimated using a rescaled version of the least-squares regression equation of Van Valkenburgh (1990): $LBW = 2.97\ln(m1L)+1.68$, where LBW is the natural log-transformed body weight in grams. This equation was derived from data on extant placental carnivorans (69 species) and marsupial carnivores (2 species), including representatives of all carnivoran families other than the Herpestidae and Eupleridae, and ranging in body weight from roughly 140 g to 400 kg. A more accurate body-weight estimate based on the condylobasal length of a cranium is available for the referred specimen SDSNH 107465 ($LBW = 3.13\ln(105.3(\mathrm{mm})) \times 5.96 = 5.50 \times 10^3(\mathrm{g})$; rescaled equation from Van Valkenburgh (1990)), but it is practically identical to the estimate obtained for UCMP 85202. Body weight estimates based on cross-sectional areas of proximal limb bones would be ideal but are not possible with the available specimens, in which diaphyses are crushed.

The dietary inference for *Lycophocyon hutchisoni* is based on a linear discriminant analysis of estimated body weight and craniodental morphology. Data on the diet (divided into three groups: carnivorous, insectivorous, and omnivorous/durophagous), body weight, and ecomorphological indices of 82 extant species of small to medium-sized carnivorans (body weight $\leq$ 30 kg) were adopted from Friscia et al. (2007; *Poiana richardsonii* was excluded from the data set because of a missing datum). To generate a set of classification functions for the prediction of the diet of *L. hutchisoni*, all possible subsets of 10 predictor variables (consisting of log-transformed body weight and 9 variables that were shown by Friscia et al. (2007) to differ significantly among the dietary groups) were subjected to the linear discriminant analysis, whereby the success rate of jackknife re-classification was evaluated for each subset of variables.

A set of dietary classification functions with 6 predictor variables was then chosen based on the highest overall jackknife re-classification success rate of 88%, with correct dietary identification of 93% of the carnivores, 93% of the insectivores, and 71% of the omnivores/hard-object feeders in the data set (see Table 1.3 for additional information and abbreviations). The first and second discriminant functions are given as:
$LD1 = -0.098LBW - 42.430m1BS + 51.671m2S - 1.043RBL + 2.167RUGA - 3.559UM21$
$LD2 = 0.553LBW + 22.923m1BS - 25.780m2S - 5.264RBL + 3.228RUGA - 2.373UM21$,
and account for 69% and 31% of the between-group variance, respectively.

The dietary classification of *Lycophocyon hutchisoni* is based on measurements of the holotype UCMP 85202, from which the following values were obtained: $LBW = 8.73, RBL = 0.682, RUGA = 1.068, M1BS = 0.074, M2S = 0.058, UM21 = 0.638$. The linear discriminant analysis was performed with the *MASS* package Version 7.3-5 (Venables and Ripley, 2010) in the R programming environment.

Cladistic Analysis

Character matrix data. The morphological character matrix of Wesley-Hunt and Flynn (2005) and additional data from subsequent studies (Wesley-Hunt and Werdelin, 2005; Polly et al., 2006; Spaulding and Flynn, 2009; Spaulding et al., 2010) were adopted for the cladistic analysis in this paper. The numbering of characters and the treatment of Character 40 as an additive character (all others are non-additive) follow these previous studies, and the identification of operational taxonomic units (OTUs) represented by referred specimens (indicated by "cf.") follows Polly et al. (2006). For the present analysis, Character 43 was eliminated (cf. Spaulding and Flynn, 2009), and the OTUs originally identified (Wesley-Hunt and Flynn, 2005) as *Hyaenodon cruentus*, *Prohesperocyon wilsoni*, and *Protictis schaffi* are considered to represent *Hyaenodon horridus* (Mellet, 1977), *"Miacis" gracilis* (cf. Spaulding and Flynn, 2009; *"M." gracilis* is possibly a junior synonym of *Procynodictis vulpiceps* (Wang, 1994; Wang and Tedford, 1994)), and *Viverravus politus* (Polly, 1997), respectively. The matrix data for *Lycophocyon hutchisoni* are based on the holotype UCMP 85202 and paratypes UCMP 170713, SDSNH 107443, SDSNH 107444, and SDSNH 107659. Character matrix data for the following additional taxa were collected by the author and were included in the analysis: *Amphicticeps shackelfordi*, *Broiliana nobilis*, *Daphoenus*, *Mustelavus priscus*, *Plesictis genettoides*, and *Pseudobassaris riggsi* (see Appendix S1.1 for a list of the specimens examined). Of these, the data for *Daphoenus* replaced those for the composite amphicyonid OTU in the previous studies (Wesley-Hunt and Flynn, 2005; Wesley-Hunt and Werdelin, 2005; Polly et al., 2006; Spaulding and Flynn, 2009; Spaulding et al., 2010). The composite OTU for *Daphoenus* is represented by specimens referred to *D. hartshornianus*, *D. vetus*, and undetermined species of the genus (most likely *D. hartshornianus* or *D. vetus*); the two currently-recognized species are skeletally quite similar except for size (Hunt, 1996*a*) and difficult to distinguish when comparing large individuals of *D. hartshornianus* with small individuals of *D. vetus* (Hough, 1948; Hunt, 1996*a*), making their specific distinction questionable (Hough, 1948). The state of Character 89 (size of baculum) for *Daphoenus* was determined based on a published account and figures of *D. vetus* (CM 492) (Hatcher, 1902). Appendix S1.3 contains the complete character matrix analyzed for the present study.

Analytical procedure. Parsimony analysis was conducted with the program TNT Version 1.1 (Goloboff et al., 2003, 2008) for (1) the full data set of 98 characters and 50 OTUs, in which *Leptictis dakotensis*, *Erinaceus concolor*, and *Echinosorex gymnura* were placed in the outgroup and (2) its subset consisting of 33 OTUs that represent taxa known from the Paleogene Period. The most-parsimonious trees were heuristically searched for using the "traditional search" function of the program with the tree bisection and reconnection algorithm and 3,000 random-addition sequence replicates. The nodal support for the consensus tree was assessed in two ways: (1) the Bremer support value for each node (Bremer, 1994) was determined by step-wise inspection of the consensus of suboptimal trees in TNT and, for well-supported groups, using the Bremer.run script of Goloboff et al. (2008) (available at tnt.insectmuseum.org/images/0/08/Bremer.run); (2) using 1,000 pseudo-replicates of the character matrix, bootstrap support values were obtained to evaluate the effect of differential weighting of characters (Felsenstein, 1985).The ensemble consistency index (CI; Kluge and Farris, 1969) and ensemble retention index (RI; Farris, 1989) for the most-parsimonious trees were calculated using the program Mesquite Version 6.72 (Maddison and Maddison, 2009). Synapomorphies were identified by the optimization function of TNT and the parsimony reconstruction of ancestral character states using Mesquite.

Results

Systematic Paleontology

Mammalia sensu Rowe, 1988
Carnivoramorpha sensu Bryant, 1996
Carnivora sensu Bryant, 1996
Caniformia sensu Bryant, 1996
Family-group indet.
Lycophocyon, gen. nov.
urn:lsid:zoobank.org:act:CCD7EEE0-1EE9-4C73-A207-3F2CB9C49F42

Type species. *Lycophocyon hutchisoni*, gen. et sp. nov.

Diagnosis. As for type species.

Etymology. From the Greek $\lambda\upsilon\kappa\acute{o}\phi\omega\varsigma$, twilight, and $\kappa\upsilon\acute{o}\nu$, dog; in references to its occurrence on the west coast of North America, and its probable affiliation with caniform carnivorans.

Distribution. As for type species.

Lycophocyon hutchisoni, gen. et sp. nov.
urn:lsid:zoobank.org:act:7186E061-58AC-49D6-8499-CDF41ECF21FC

Diagnosis. Differs from canoid carnivorans in absence of well-ossified entotympanics that are firmly attached to basicranium. Differs from other non-canoid carnivoramorphans in broad and flat anterior extension of petrosal promontorium. Further differs from: (1) both amphicyonids and canids in greater anterolabial extension of M1 parastylar region such that distance between paracone and anterolabial tooth margin roughly equals distance between paracone and protocone, and M1 posterior lingual cingulum that is not as raised as protocone; (2) arctoids in swelling of M1 posterior lingual cingulum (though not as raised as in amphicyonids and canids), and presence of M3; (3) feliforms in presence of unreduced postglenoid foramen, presence of unreduced M1, presence of M3, and presence of moderately-developed m1 talonid; (4) *"Miacis" cognitus* in P3 with well-defined posterior accessory cusp, greater anterolabial extension of M1 parastylar region, and more reduced M2; (5) both *Procynodictis* and *"Miacis" gracilis* in having proportionately longer M1 (M1L/M1W $>$ 0.60), less-developed cuspulids on anterior and posterior cingulids of p3 and p4, and more lingually-directed m1 paraconid (giving trigonid more closed appearance); (6) Procynodictis in more rounded anterolabial corner of P4, and more posterior placement of M1 protocone; (7) *"M." gracilis* in anterior tilt of M1 parastylar region, more reduced M2 protocone, and less-pronounced lingual protrusion of m1 metaconid; (8) *"Miacis" uintensis* in having p4 that is shorter than m1 (p4L $\geq$ m1L in *"M." uintensis*) and more straight posterior slope of p4 owing to less-developed cuspulid on posterior cingulid; (9) *"Miacis" sylvestris* in larger size (m1 $>$ 20% longer), presence of posterior accessory cusp/cuspid on P3 and p4, better-developed posterior lingual cingulum of M1, more reduced m2 trigonid cuspids, more reduced and simplified m3, and absence of sulci on petrosal promontorium for promontory and stapedial branches of internal carotid artery; (10) *Miacis parvivorus* in larger size (m2 $>$ 25% longer), greater anterolabial extension of M1 parastylar region, more triangular outline of M1 in occlusal view, and m1 and m2 with

more open trigonid; (11) *Quercygale* in wide shelf between mastoid process and paroccipital process that does not form a trough, better-developed M1 posterior lingual cingulum, and presence of M3; (12) *Tapocyon* in less-pronounced labial extension of M1 parastylar region, larger M2 relative to M1 (M2W/M1W $>$ 0.60), presence of M3, larger m1 talonid relative to trigonid, less-developed cuspulid on posterior cingulid of p4, larger m2 relative to m1 (m2L/m1L $>$ 0.55), and more gradual tapering of dentary toward its anterior end; (13) *Dawsonicyon* in larger size (m1 $>$ 40% longer) and p4 with more dorsally-positioned posterior accessory cuspid; (14) viverravids in having M1 with protocone that is shorter than paracone, presence of M3 and m3, and low trigonid and short talonid of m2; (15) all other known carnivoramorphans in the combination of: well-ossified tegmen tympani; petrosal promontorium in medial contact with basioccipital; slight ventral deflection of ventral floor of basioccipital along middle ear chamber; absence of sulci on petrosal promontorium for promontory and stapedial branches of internal carotid artery; P3, p3, and p4 with well-defined posterior accessory cusp/cuspid located between main cusp and posterior cingulum/cingulid; M1 and M2 with pronounced anterolabial extension of parastylar region; M1 protocone located near anterolingual border of tooth; M1 anterior lingual cingulum forming very thin band rather than shelf; crescentic M1 posterior lingual cingulum that is at least twice as wide in occlusal view as anterior lingual cingulum; M2 approximately one-third to one-half the size of M1 (when measured as the product of length and width in occlusal view); M2 and M3 with increasingly-reduced occlusal surficial relief; presence of diminutive M3; cuspulid on anterior cingulid of p2-p4 small or absent; p4 shorter than m1; and gradual tapering of dentary toward its anterior end.

Etymology. Specific name after J. Howard Hutchison, who led a UCMP team in a 1968 excavation that yielded the holotype and a paratype (UCMP 170713), and in honor of his contribution to the study of fossil vertebrates of California. Distribution. Upper portions of "member C" (Wilson, 1972) of the Santiago Formation, San Diego County, California, corresponding to the early Duchesnean and possibly also to the late Uintan NALMAs (Golz, 1976; Walsh, 1996; Mihlbachler and Deméré, 2009).

Holotype. UCMP 85202, right dentary fragment with p2-m1, left dentary with p2-m2, and cranial fragments with right P4-M2 and left P3-M2.

Holotype locality. UCMP locality V6839, Laguna Riviera 1, Santiago Formation, member C, Carlsbad, San Diego County, California, U.S.A.

Paratypes. UCMP locality V6885, Half-day Pocket, Santiago Formation, member C, Carlsbad, San Diego County, California, U.S.A.: UCMP 170713, right dentary with c1, p2-m2, left dentary fragments with c1, p1, m1, and cranial fragment with right P2, P4-M3. SDSNH locality 5416, Ocean Ranch Phase 2C Bone Sands, Santiago Formation, member C, Oceanside, San Diego County, California, U.S.A.: SDSNH 107658, right dentary with m1-m3; SDSNH 107659, cranium with right P2, P4-M2, and left P2-M2. SDSNH locality 5721, Ocean Ranch Phase 1B, Santiago Formation, member C, Oceanside, San Diego County, California, U.S.A.: SDSNH 107442, articulated cranium and mandible; SDSNH 107443, cranium with right P2-M2 and left P3-M1; SDSNH 107444, cranium with left P4-M2, left dentary fragments with c1, p2-p3; SDSNH 107446, cranium, dentary, caudal vertebra, left ulna, left femur, right tibia, right astragalus, middle phalanx; SDSNH 107447, left dentary with p1-m1, left humerus. Referred specimens. UCMP locality RV6830 (same quarry as UCMP locality V6839; Golz, 1976), Laguna Riviera Quarry, Santiago Formation, member C, Carlsbad, San Diego County, California, U.S.A.: UCMP 313994, left m1. SDSNH locality 4821, Rancho Del Oro Road Extension, Santiago Formation, member C, Oceanside, San Diego County, California, U.S.A.: SDSNH 92094, right dentary with p2-m1, left dentary

with c1-p4. SDSNH locality 5415, Ocean Ranch Phase 2A Bone Sands, Santiago Formation, member C, Oceanside, San Diego County, California, U.S.A.: SDSNH 105783, right dentary with c1, p4-m2. SDSNH locality 5721, Ocean Ranch Phase 1B, Santiago Formation, member C, Oceanside, San Diego County, California, U.S.A.: SDSNH 107448, left dentary with p2-m2; SDSNH 107449, right dentary with c1, p2-m2; SDSNH 107450, left dentary with c1, p2-m2; SDSNH 107452, left dentary with c1-m1; SDSNH 107453, left dentary with m2; SDSNH 107455, left dentary fragment with m1; SDSNH 107456, right dentary; SDSNH 107457, left dentary with m1 and m2; SDSNH 107458, right dentary with p2-m1; SDSNH 107460, left dentary with c1-p4; SDSNH 107461, left dentary with c1-m2; SDSNH 107462, right P4; SDSNH 107465, edentulous cranium, right dentary with m2; SDSNH 107467, edentulous left dentary; SDSNH 107468, edentulous left dentary; SDSNH 107538, partial cranium.

Remarks. *Lycophocyon hutchisoni* is here classified as a caniform carnivoran based on the result of a cladistic analysis in the present study, as discussed below. The familial affiliation of *L. hutchisoni* is indeterminate with the current knowledge of the species and basal carnivoran phylogeny.

Description

Unless otherwise noted, the description of the cranium is based on the holotype UCMP 85202. The descriptions of caudal vertebra, ulna, femur, tibia, astragalus, and intermediate phalanx are based on the paratype SDSNH 107446 with an associated skull, and the description of humerus is based on the paratype SDSNH 107447 with an associated left dentary fragment with p1-m1 that can be confidently identified as belonging to Lycophocyon hutchisoni. Craniodental and postcranial measurements are reported in Table 1.1 and Table 1.2, respectively. A list of comparative specimens directly examined by the author is provided in Appendix S1.1. Comparisons with published accounts and figures of other taxa should be considered preliminary. References to character numbers pertain to the cladistic analysis discussed below; the characters, character states, and their numbering follow those of Wesley-Hunt and Flynn (2005).

Cranium. The crania of UCMP 85202 (Fig. 1.2A, B) and SDSNH 107659 (Fig. 1.2E, F) are missing the rostrum and much of the occipital region, respectively, and both are dorsoventrally crushed. The cranium of SDSNH 107442 (Fig. 1.2D) is nearly complete but crushed transversely. In all three specimens, frontals and parietals are fused. In SDSNH 107659, the sutures surrounding the pair of nasals are visible. The cranium of SDSNH 107444 (Fig. 1.3B) is missing much of the palate and the right maxilla, but preserves some details of the basicranium that are obscure in the holotype; the remaining bones are highly fragmented but largely held together by the sedimentary matrix.

While the type and referred specimens exhibit considerable craniodental size variation, the cranial length of *Lycophocyon hutchisoni* is comparable to those of such extant carnivorans as *Urocyon cinereoargenteus* (gray fox), *Martes pennanti* (fisher), and *Procyon lotor* (raccoon), and intermediate between those of the early canid *Hesperocyon gregarius* and the early amphicyonid *Daphoenus*. The rostrum (preorbital region) is wide and tall as in *M. pennanti* and *P. lotor* but proportionately longer (Fig. 1.2D-F). The braincase of *L. hutchisoni* is short (roughly 40% of the cranial length or smaller) and almost as narrow as the interorbital breadth measured between the anterior extremities of orbits (Fig. 1.2E). The dorsal border of braincase in profile is nearly horizontal in SDSNH 107442 (Fig. 1.2D). The cranial form in dorsal and ventral views closely

resembles that of *Cynodictis lacustris* (cf. Teilhard de Chardin, 1914-1915:plate 2, figs. 1, 3), known from the late Eocene of Europe.

The premaxilla of SDSNH 107442 is short in dorsal aspect, and does not extend beyond the C1. The anterior end of the premaxilla bearing the alveoli for the upper incisors is mediolaterally highly compressed. Narrow incisive foramina are located immediately posterior to the I1 and I2, and extend slightly beyond the anterior margin of C1. In SDSNH 107443, the posterior border of premaxilla lateral to the incisive foramen is located next to the C1 (Character 2, state 0). The nasals maintain roughly the same width along most of their lengths, with tapered posterior extremities located above the anterior margins of the orbits (Character 63, state 0). Turbinal bones (Character 62) cannot be observed in any of the currently-known specimens. The maxilla is relatively long and bears a round (UCMP 85202) to dorsally-elongate (UCMP 170713) infraorbital foramen (Character 3; coded as state 0/elongate because UCMP 170713 appears to preserve the original shape more accurately) above the P3 (Character 4, state 0). The maxillary roof of the oral cavity is deeply excavated between the P4 and M1 to accommodate the relatively tall trigonid of M1 characteristic of early carnivoramorphans.

The pair of palatines forms a wedge-shaped anterior margin located as anteriorly as the protocone of P4. The midline-length of palatine is shorter than that of maxilla (19.6 mm and $>$ 29 mm, respectively, in SDSNH 107659; Character 60, state 0). The right and left tooth rows diverge gradually from their anterior ends to the posterior ends of P4s, such that the maximum palatal width is roughly 270% of the palatal width between the upper canines (Character 61, state 0). In SDSNH 107659, two openings of the palatine canal are discernible essentially along the left maxillopalatine suture (Character 6, state 1); the posterior end of palate on the median line is more or less aligned with the posterior end of the upper tooth row (Character 5, state 1). The extent of palatines on the lateral faces of the cranium (Character 65) is unclear.

The lacrimal is mostly broken and missing in the holotype, but is preserved intact in SDSNH 107659, showing a small exposure on the rostrum (lacrimal facial process; Character 1, state 1). The lacrimal foramen in UCMP 85202 is nearly circular and approximately 2 mm in diameter. In the holotype, the anterodorsal end of the jugal bears a probable contact surface with the lacrimal (Character 64, state 0). The large orbit bears a short, pointed postorbital process (Character 8, state 1), which gives rise to a ridge that connects to a well-delineated sagittal crest formed by the frontals and the parietals. The relative lengths of the frontal and the parietal are unclear because the fronto-parietal suture is apparently fused in all available crania (cf. Characters 7 and 66). In UCMP 85202 and SDSNH 107538, expansive lambdoidal crests are present. The zygomatic arch is particularly deep in UCMP 85202, suggesting the presence of a powerful masseter muscle. The large glenoid fossa is associated with a well-developed postglenoid process, but is laterally more open than in extant mustelids.

Morphological details of the basicranium (Fig. 1.3) are difficult to discern in the holotype because of poor preservation. The basisphenoid region is rather narrow, reflecting the constriction of the braincase. The fused basioccipital and basisphenoid form a somewhat fusiform floor. A pair of muscular tubercles presumably for the insertion of the longus capitis muscles is located at the posterolateral ends of this fusiform floor medial to the posterior lacerate foramina. In the early amphicyonids *Cynodictis* (cf. Petter, 1966:fig. 2; Hunt, 2001:fig. 8) and *Daphoenus*, the fusiform floor terminates somewhat more anteriorly, and the muscular tubercles are correspondingly positioned medial to the petrosal promontoria. Although less pronounced than in *Hesperocyon gregarius*, the lateral edge of the ventral surface of the basioccipital shows slight ventral

deflection (Character 34, state 1), and so it was likely in contact with the presumably unossified auditory bulla (see below). There is, however, no indication on the basioccipital and basisphenoid of pronounced medial inflation of the entotympanic as has been noted for some early and extant feliforms (Wesley-Hunt and Flynn, 2005) (Character 35, state 0). Notably, the basioccipital bears a laterally-extended flange dorsal to the ventral floor. This flange is in contact with the medial face of promontorium, and forms a broad trough anterior to the posterior lacerate foramen ("foramen lacerum posterius primitivum" of Petter, 1966). Similar basioccipital morphology has been reported for *"Miacis" sylvestris* (cf. Wang and Tedford, 1994:fig. 3) and *Cynodictis* (Petter, 1966; see also Hunt, 2001:fig. 8), in which the flange presumably formed the roof of inferior petrosal sinus. The broad trough of *L. hutchisoni* (broader than that of *"M." sylvestris*) may reflect an inferior petrosal sinus with a relatively large diameter. However, a very deep excavation of the basioccipital as in amphicyonids and ursids (known to accommodate a double-looped internal carotid artery in ursids; Hunt, 1977) seems unlikely because there is little vertical space, if any, between the promontorium and the underlying ventral floor of basioccipital in both the holotype and SDSNH 107659 (Character 31, state 0); in *Daphoenus* and *Ursus*, the promontoria are deeply (i.e. in the dorsal direction) embedded in the middle ear chambers relative to the level of the ventral floor of basioccipital.

Of the 4 known crania of *Lycophocyon hutchisoni* in which at least part of the middle-ear region can be observed, none preserves the auditory bulla, malleus, incus, or stapes. The bulla is therefore tentatively assumed to have been either made of a soft tissue or ossified but not as firmly attached to the basicranium as in more derived carnivorans (Character 68, state 0). Because no bulla is preserved, presence of an ectotympanic or entotympanic septum in the bulla cannot be determined (Characters 70 and 71). The petrosal promontorium (Fig. 1.3) is posterolaterally somewhat globular, and appears to have been medially in contact with the lateral edge of the ventral surface of basioccipital (Character 21, state 1). In SDSNH 107444, the promontorium is anteromedially elongate and flat (Fig. 1.3B; Character 28, state 3), resembling those of early canids and arctoids but differing from those of early amphicyonids with distinct, round anterior margins (cf. Hunt, 2001:figs. 3, 9). The ventral surface of the promontorium in SDSNH 107444 is smooth except for a slightly rugose medial portion ("R" in Fig. 1.3B; Character 30, state 1). Rugose areas of similar extent in *"Miacis" sylvestris* and *Amphicticeps shackelfordi* have been interpreted as attachment areas for entotympanics (Wang and Tedford, 1994; Wang et al., 2005). Unlike in earlier carnivoramorphans such as *Vulpavus profectus*, *Miacis parvivorus*, and *"M." sylvestris* (Wang and Tedford, 1994), the promontorium does not bear any arterial sulcus, suggesting an extrabullar passage of the internal carotid artery (Character 25, state 2), which is otherwise first known in *Hesperocyon gregarius* among caniform carnivorans (Wang and Tedford, 1994). The promontorium of *L. hutchisoni* resembles those of early arctoids such as *A. shackelfordi*, *Plesictis genettoides*, and *Broiliana nobilis* in having a moderately-expanded shelf posterior to the fenestra cochlea (Character 26, state 1); in contrast, the extent of this shelf is very limited in early amphicyonids such as *Daphoenus* and *Paradaphoenus*, presumably inheriting the primitive condition in carnivoramorphans (Wesley-Hunt and Flynn (2005); see also Wang and Tedford (1994)). Unlike in early feliforms such as *Palaeoprionodon lamandini*, *Stenogale julieni*, and *Proailurus lemanensis* (Wesley-Hunt and Flynn, 2005), the promontorium of *L. hutchisoni* does not have a ventral process (Character 27, state 0) or a facet for the attachment of ectotympanic (Character 29, state 0). The fenestra vestibuli is elliptical, with the long axis pointing anteromedially. The similarly-sized fenestra cochlea (Character 72, state 0; clearly seen only in SDSNH 107444) is somewhat more

circular in shape.

The deep fossa for stapedius muscle is approximately 2 mm in diameter, and is anteriorly bounded by the mastoid tubercle (Character 37, state 0). Similar size and depth characterize the clearly-demarcated posterior lacerate foramen (Character 17, state 1). The small, elongate condyloid foramen is located anterior to the groove between the occipital condyle and the paroccipital process (Character 16, state 1) and behind the posterior lacerate foramen such that their medial margins are more or less aligned; the latter two foramina are separated by a distance of more than the diameter of the condyloid foramen (Character 15, state 0). The mastoid tubercle is composed of the petrosal (Character 22, state 0), and the mastoid process is similar in size to the paroccipital process (Character 13, state 0). The precise orientation of the mastoid process (Character 14) is unclear because the extremity is missing on the left process, and the right process appears to have been ventrally reoriented distal to a breakage at its base. The mastoid tubercle in SDSNH 107444 is tightly appressed to the promontorium slightly anterior to the fenestra cochlea (Character 18, state 0). In comparison, the mastoid tubercles in *Daphoenus* are mediolaterally shorter and do not contact the promontoria, whereas those in *Cynodictis* are long and apparently lie ventral to the fenestra cochlea (cf. Petter, 1966:fig. 2; Hunt, 2001:fig. 8). Because of poor preservation, it is unclear whether the mastoid tubercle of *Lycophocyon hutchisoni* bears an articular facet for the posterior limb of ectotympanic as in *"Miacis" cognitus*, *Miacis parvivorus*, and *Tapocyon robustus* (Gustafson, 1986; Wesley and Flynn, 2003). In the holotype and SDSNH 107444, a very shallow depression on the dorsal wall of the external auditory meatus appears to represent an incipient suprameatal fossa (Character 24, state 1) as in *Hesperocyon gregarius* (Wang and Tedford, 1994), and is in contrast to the deep fossae in some of the early mustelidans such as *Plesictis genettoides* and *Broiliana nobilis*. No bony tube is preserved in association with the external auditory meatus, but the possibility of a tube formed by a cartilaginous bullar element cannot be discounted (Character 69).

The oblong postglenoid foramen is located lateral to the trough-like Glaserian fissure (but not near the lateral edge of skull; Characters 11 and 12, state 0), which, in turn, ascends steeply into the deeply-excavated epitympanic recess. There does not appear to be a deep, clearly-defined fossa on the squamosal for the contact with the anterior crus of ectotympanic (Character 32, state 0). The fossa for tensor tympani muscle is deep (Character 39, state 1). While the details are difficult to discern, there is no sign of an exposed canal for the facial nerve anterior to the promontorium, and it seems likely that the facial nerve was floored by the well-ossified tegmen tympani (Character 20, state 2). The promontory foramen cannot be identified in the available specimens. In SDSNH 107444, the middle lacerate foramen is anteriorly bounded by the tympanic wing of basisphenoid and posteriorly by the petrosal (Character 40, state 1); the tympanic wing of basisphenoid bears a depression with a well-delineated round anterior margin, suggesting the presence of an anterior loop of the internal carotid artery (Character 23, state 1). Presence of an epitympanic wing of the petrosal near the anteromedial corner of the fossa for tensor tympani muscle (Character 38) cannot be determined. In SDSNH 107659, the posterior opening of alisphenoid canal and the foramen ovale are respectively located at the anterior and the posterior ends of a groove (approximately 5 mm in length, 2 mm in width) behind the pterygoid, and are separated by a distance that is greater than the diameter of the alisphenoid opening (Character 19, state 0).

The long (9 mm in SDSNH 107465), pointed paroccipital process (Characters 9 and 10, state 0) is posteriorly-directed, and its ventral surface appears flat, resembling that of the early arctoid *Amphicticeps shackelfordi*. The shelf between the mastoid process and paroccipital process is

laterally wide, but lacks a smooth, curved trough that has been noted for early carnivoramorphans such as *Oodectes herpestoides* (Wesley-Hunt and Flynn, 2005) (Character 33, state 1). There is no indication of an extensive attachment area for the entotympanic posterior to the petrosal that would suggest pronounced posterior inflation of entotympanic (Character 36, state 0). The right and left occipital condyles are as distinct as in extant canids, and in SDSNH 107465, each condyle measures approximately 11 mm along its long axis.

Mandible. The moderately-deep dentary (Fig. 1.2C, D) has a gently arching ventral border and gradually-tapering anterior end. The mandibular symphysis of UCMP 170713 is relatively smooth. The location of the anterior mental foramen varies from below the posterior end of p1 in UCMP 85202 to between p1 and p2 in UCMP 170713. Likewise, the posterior mental foramen is located below the posterior border of p2 in UCMP 85202, but between p2 and p3 in UCMP 170713. The anteroposteriorly-expansive coronoid process rises steeply behind m3, and attains the maximum height along its posterodorsal border. The deep masseteric fossa is anteriorly delineated by a well-developed coronoid crest. The mandibular condyle is cylindrical and medially rather robust, but gradually flattens toward the lateral end. The dentary bears a long and dorsoventrally flat angular process that extends as far posteriorly as the mandibular condyle.

Dentition. The dental formula for *Lycophocyon hutchisoni* is 3.1.4.3/?.1.4.3 (Characters 78, 79, 84, 88, state 0). The P1 and lower incisors are not preserved in any of the known specimens. Overall, the dentition of *L. hutchisoni* (Fig. 1.4) is characterized by: (1) a posterior accessory cusp on P3; (2) well-developed, somewhat blade-like posterior accessory cuspsid on p3 and p4; (3) M1 with a labially extended parastylar region, a protocone with the base that is nearly or partially in contact with the anterolingual margin of the tooth, and an anteroposteriorly asymmetrical lingual cingulum; (4) reduced M2/m2 and diminutive M3/m3 (Character 86, state 1); and (5) m1 and m2 with relatively open trigonids compared to those of earlier carnivoramorphans but without notable reduction (as in *Tapocyon* and feliform carnivorans) or expansion (as in more derived caniform carnivorans) of the talonid.

The upper incisors and canines are preserved in SDSNH 107442. Because of the anterior constriction of the rostrum, the upper incisors (especially I1 and I2) are tightly appressed. The I1 and I2 are subequal in size, mediolaterally compressed as in *Martes pennanti*, and have somewhat spatulate crowns. The I3 is markedly larger than I1 and I2; its crown shows a slight posterior bulging at the base, has a sharp ridge running along its length on the posterolabial side, and is somewhat caniniform in overall morphology. The C1 is of moderate size, and is slightly larger in anteroposterior length than c1.

The P1, P2, and P3 are each preceded by a small diastema (Fig. 1.4D). Based on the alveolus of SDSNH 107659, P1 appears to have been single-rooted and shorter than P2. The size of upper premolars gradually increases from P1 to P4. The double-rooted P2 of UCMP 170713 (Fig. 1.4D) is mediolaterally compressed and has a simple triangular profile, with the main cusp showing slight posterior inclination. The tooth lacks a clearly-defined anterior cingulum, but has a small, blade-like posterior accessory cusp that is aligned with the posterior ridge of the main cusp. The posterior accessory cusp is flanked by two small notches, and is followed by a trenchant ridge on the moderately-broad posterior cingulum.

The P3 (Fig. 1.4G) is labiolingually robust, and has a more asymmetrical profile than P2 because of the better-developed posterior accessory cusp (Character 58, state 0). As in P2, the posterior accessory cusp of P3 is surrounded by a pair of small notches, but the accessory cusp itself is slightly more conical. The anterior cingulum is weakly-developed as a small bulge at the

anterior base of the main cusp. In UCMP 85202, the base of the crown bulges out lingually behind the main cusp, but this bulging is less conspicuous in SDSNH 107659. No lingual cusp is present on P3 (Character 80, state 0).

The protocone of P4 (Fig. 1.4D, G) is located anterior to the paracone (Character 82, state 0); it has approximately one-third of the height of the paracone, and is comparable in size to those of *Daphoenus* and *Amphicticeps shackelfordi* but not as reduced as in *Hesperocyon gregarius* (Character 56, state 1). The parastyle is a diminutive swelling located at the base of the well-defined preparacrista (Character 55, state 2), and is contiguous with the anterior cingulum. The prominent paracone is more posteriorly inclined than the main cusps of P2 and P3, and bears a postparacrista that is nearly as long as the metasylar blade. The sharp metastylar blade is separated from the postparacrista by a deep carnassials notch, and forms a large surface for shearing against the anterior surface of m1 (Character 81, state 0; Characters 54 and 57, state 1). In UCMP 170713 and the right P4 of UCMP 85202, the posterior end of the metasylar blade is labially deflected, but this is less apparent in SDSNH 107659 and the left P4 of UCMP 85202, and appears to reflect variation in individual tooth development. The lingual shearing surface consisting of the postparacrista and the metasylar blade forms an angle of approximately 45º with the long axis of upper tooth row. In UCMP 170713 and UCMP 85202, the cingulum is well delineated around the tooth except at the base of the protocone, and is particularly well-developed at the lingual base of the metasylar blade, contributing to the somewhat inflated appearance of this region in occlusal view. In SDSNH 107659, the cingulum on the posterolingual surface is limited to the base of metastylar blade. No hypocone is present on the P4 (Character 83, state 0).

The unreduced M1 (Fig. 1.4D, G; Character 46, state 0) is marked by the anterolabially elongate parastylar region (Character 44, state 1) that bears a trenchant preparacrista and a parastylar blade extending straight in the labial direction (Character 45, state 1). The parastylar region of *Lycophocyon hutchisoni*, however, is not as labially elongate as in *Tapocyon robustus* and *Procynodictis vulpiceps*, and the parastylar shelf appears relatively broad (Character 51, state 1). In UCMP 85202 and SDSNH 107659, substantial tooth wear is observed along the anterior surface of preparacrista and parastylar blade, as well as along the anterior lingual cingulum. The paracone is noticeably taller than the metacone (Character 48, state 1), but the two cusps are subequal in anteroposterior length. The apices of the paracone and the metacone are connected by a trenchant ridge consisting of the postparacrista and premetacrista. In UCMP 85202 and UCMP 170713, the paraconule is well developed and is considerably larger than the metaconule (Character 49, state 0), the latter of which is present as a somewhat angular projection at the posterolabial corner of trigon basin. The paraconule is separated from the protocone by a notch. The labial cingulum is well developed and forms a relatively thick ridge along the labial margin of the broad stylar shelf, giving the latter a somewhat basined appearance. The height of the protocone is shorter than that of the paracone but is subequal to that of the metacone (Character 42, state 0). The lingual cingulum is continuous around the protocone in UCMP 85202 (Character 41, state 1). In UCMP 170713 and SDSNH 107659, however, the base of protocone is partly confluent with the anterolingual margin of the tooth, thus interrupting the continuity of lingual cingulum around the protocone. In all specimens, the anterior portion of lingual cingulum is a narrow strip, and the posterior portion forms a crescentic shelf that bulges posterolingually, resulting in the characteristically asymmetrical appearance of the lingual portion of the tooth (Character 47, state 1). The development of posterior lingual cingulum is less pronounced than in early caniform carnivorans such as *Daphoenus* and *Hesperocyon*, and whether to identify this structure as a "hypocone" (Character 50; coded as state

2) is a matter of subjective judgment; however, the edge of posterior lingual cingulum in SDSNH 107659 is slightly worn, suggesting its contact with the anterior portion of the m2 trigonid and involvement in mastication.

The parastylar region of M2 (Fig. 1.4D, G) projects labially and bears a broad stylar shelf posterior to the parastyle. The short parastyle extends anterolabially until it reaches the anterior margin of tooth, and is separated from the preparacrista by a small notch. A diminutive caspule is present on the anterolabial margin of the stylar shelf and labial to the parastyle. The labial margin of the stylar shelf forms a raised ridge as in M1. The paracone is slightly taller and longer than the metacone. The notched ridge formed by the postparacrista and premetacrista is less trenchant than in M1. In UCMP 85202 and SDSNH 107659, a narrow wear facet is present along the margin of tooth anterior to the paracone. The broad trigon basin is mostly flat because of the diminutive size of paraconule and the absence of metaconule. The protocone is a low, round ridge that is anteriorly more or less confluent with the broad, bulbous lingual cingulum. No hypocone is present on the M2 (Character 87, state 0). Considerable variation in the size of M2 (Character 52; coded as state 0 to be consistent with the coding for other carnivoramorphans in Wesley-Hunt and Flynn (2005)) exists among known specimens: the M2 of UCMP 85202, for example, is approximately 29% longer and 22% wider than that of UCMP 170713. Likewise, the size of M2 (measured as the product of anteroposterior length and transverse width) relative to that of M1 ranges from approximately 0.33 in UCMP 170713 to 0.44 in UCMP 85202.

The diminutive M3 (Fig. 1.4D; Character 53, state 0) is preserved only in UCMP 170713. It has an oval outline in occlusal view, and a slightly concave anterior margin that closely fits the convex posterolingual margin of M2. The round trigon basin is bordered anteriorly by a slightly crenulated ridge, and labially by two small ridges that may represent reduced paracone and metacone. The single root of the tooth is attached to a groove at the posterior extremity of maxilla along the upper tooth row, such that its posterior surface is not in contact with any bone. This does not seem to be a result of breakage, since none of the known maxillae of *Lycophocyon hutchisoni* has an M3 alveolus that is completely enclosed by the bone. In UCMP 85202, for instance, a posteriorly-exposed M3 alveolus is present at the apparent posterior end of maxilla.

The crown of c1 (Figs. 1.2D, 1.4E) at its base is slightly bulbous and anteriorly inclined. In SDSNH 107442, the crown curves rather abruptly at mid-length, such that its tip is oriented more or less vertically. The c1 is labiolingually compressed and has an oval cross section. All lower premolars (Fig. 1.4A-C, E) are mediolaterally compressed and bear a well-developed posterior cingulid. Well-defined central ridges are present on the anterior and posterior slopes of the crowns. The size of crown increases gradually from p1 to p4. The single-rooted p1 of UCMP 170713 (Fig. 1.4E) has an anteriorly-projecting main cuspid and lacks an anterior cingulid. The sharp, highly-tilted posterior ridge of the main cuspid is connected to an anteroposterior ridge on the posterior cingulid that divides the cingulid into a relatively flat, broad lingual portion and a more inclined, narrow labial portion. A pointed cuspulid is located at the posterior end of this ridge on the cingulid.

The double-rooted p2 (Fig. 1.4A-C) has a main cuspid that rises vertically. A small bulge on the anterolingual margin of the main cuspid forms the poorly-defined anterior cingulid. The trenchant posterior ridge of the main cuspid is followed by a longitudinal ridge on the broad posterior cingulid. As in p1, the posterior cingulid is flatter and broader lingual to this ridge.

The p3 (Fig. 1.4A-C) has a short anterior cingulid with a diminutive cuspulid that is connected to the anterior ridge of the main cuspid. The sharp posterior ridge of the main cuspid is succeeded

by a notch and a posterior accessory cuspid. The posterior accessory cuspid is roughly conical in occlusal view, and is located slightly more labially than the main cuspid. Like the main cuspid, the posterior accessory cuspid bears a ridge along its length, which is followed by a short ridge on the posterior cingulid. The transverse asymmetry of the posterior cingulid across this ridge is more pronounced than in p1 and p2. In occlusal view, the posterior portion of the tooth appears inflated relative to its anterior portion because of the broad posterior cingulid.

The p4 (Fig. 1.4A-C) has the same basic form as the smaller p3, but is distinguished by a better-developed, trenchant cuspulid on the anterior cingulid, and a longer, more blade-like posterior accessory cuspid. A deep notch is present both anterior and posterior to the posterior accessory cuspid. In labial view, the posterior cingulid ascends posteriorly, and is therefore more elevated than in p3. The posterolingual surface of the main cuspid and the lingual surface of the posterior accessory cuspid form a slight concavity to accommodate the protocone of P4.

The m1 and m2 (Fig. 1.4A-C, F) are both characterized by a trigonid with relatively robust cuspids and the angle between the paralophid and the protolophid (approximately 65°in UCMP 85202) that is intermediate between those of earlier carnivoramorphans such as *Miacis parvivorus* (with closed trigonid) and early crown-group carnivorans such as *Hesperocyon* (with open trigonid). The trigonid of m1 is roughly 80% longer than the talonid. In contrast to early canids, the metaconid of m1 is unreduced and has nearly the same height as the paraconid. The angle between the paralophid and the line connecting the apices of paraconid and metaconid is approximately 44°. A deep notch is present between the paraconid and the protoconid, and between the protoconid and the metaconid. A deep, wedge-shaped cleft is present between the paraconid and the metaconid. The talonid basin (Character 85, state 0) is relatively narrow but moderately deep, and is demarcated by a continuous ridge, in which the sharp cristid obliqua runs roughly parallel to the paralophid. Vestigial cuspids and cuspulids give a crenulated appearance to this ridge encircling the talonid basin: While the pointed hypoconid is readily recognizable, the rather tightly-appressed entoconid and hypoconulid are diminutive, and are flanked by a distinct bulge on the labial side and two small cuspulids on the lingual side. In UCMP 170713, the entoconid and hypoconulid are barely discernible, and the accessory cuspulids are essentially absent. The labial surface of talonid descends less steeply than in *H. gregarius* to meet the posterior labial cingulid near the base of the crown. The well-defined anterior labial cingulid forms a thin strip.

The trigonid and talonid of m2 (Fig. 1.4A-C, F) are subequal in length and, together with the well-developed anterior labial cingulid, give the tooth a nearly rectangular outline in occlusal view (Character 59, state 1). The trigonid is considerably more closed than in m1. The trigonid cuspids are low in height but retain pointed apices. The protoconid and metaconid are subequal in height and slightly taller than the paraconid, which has approximately the same height as the hypoconid and is not as markedly reduced as in early canids. A small notch separates each pair of trigonid cuspids. In UCMP 85202, wear facets are present along the posterior cingulum of M1 and the anterior cingulum of M2, indicating shearing against the paralophid and the protolophid of m2, respectively. The talonid is similar in shape to that of m1, but the basin is shallow, in part because the hypoconid is short. The hypoconulid and entoconid are not recognizable as individual structures.

The single-rooted m3 of SDSNH 107658 (Fig. 1.4F) is low-crowned and is oval in occlusal view. The crown morphology is obscured by heavy wear, but the unworn portions are suggestive of a simple, button-like crown with no clear distinction between the trigonid and the talonid. Comparison with UCMP 170713 suggests that the tooth occluded mostly with M3, with little contact

with M2.

In comparison to other North American carnivoramorphans, the dental morphology of *Lycophocyon hutchisoni* appears most similar to those of *Procynodictis vulpiceps*, *P. progressus*, *"Miacis" gracilis* (considered by some authors to be synonymous with *P. vulpiceps* (Wang, 1994; Wang and Tedford, 1996)), and *Prohesperocyon wilsoni* (morphologically the most-primitive, but not the earliest-known, stem canid; Wang, 1994). Of these, the first three species are known from the Uintan NALMA, while *P. wilsoni* is known from the Chadronian NALMA. Interestingly, however, even greater resemblance is observed with specimens of *Cynodictis lacustris* from the late Eocene of France. Comparisons with UCMP 62709 and UCMP 63054 from La Débruge, Vaucluse, and AMNH FM 10056 (in collection of the American Museum of Natural History, New York, New York, U.S.A.; identified as *C. intermedius*, which may be conspecific with *C. lacustris* (Kotsakis, 1980)) from a locality of Phosphorites du Quercy in Escamps, Lot, reveals striking similarities in the size and structure of lower premolars (with weakly-developed cuspulids on cingulids and well-developed posterior accessory cuspids on p3 and p4), lower molars (with similar, intermediate openness of m1 trigonid and reduction of m2), and the dentary (including the locations of mental foramina and diastema). The only major differences between the two genera are the better-developed (though still small) entoconid of m1, which makes the posterolingual corner of talonid appear more orthogonal, and the somewhat more elongate talonid of m2 in *C. lacustris*.

As for the upper dentition, UCMP 63173, an isolated P4 of *Cynodictis* sp. from Escamps, is essentially indistinguishable from that of UCMP 170713. An isolated M1 (UCMP 63175) from the same locality also closely resembles that of *Lycophocyon hutchisoni* in the configuration and development of cusps and cingulae, although the labial extension of parastylar region is less pronounced and the posterior lingual cingulum is enlarged in the specimen from France. In addition, the presence of a posterior accessory cusp on P3 (also present in *L. hutchisoni*, *Daphoenus*, and early canids) can be confirmed for a specimen of *Cynodictis* sp. from Quercy (cf. Hunt, 2001:fig. 8). The phylogenetic affinity of *Cynodictis* to amphicyonids (and, in early studies, canids) has been suggested based on the dental (Teilhard de Chardin, 1914-1915; Kotsakis, 1980; Hunt, 2001) and basicranial morphological similarities (Petter, 1966; Hunt, 1998*a*, 2001). Hunt (1998*a*) considered *Cynodictis* to be the earliest known genus of amphicyonine amphicyonids, a Eurasian lineage that is distinct from the North American daphoenine amphicyonids.

Caudal vertebra. Based on the size of transverse processes and the apparent lack of zygapophyses, the caudal vertebra of SDSNH 107446 (Fig. 1.5F) appears to belong to the proximal portion of the distal caudal vertebral series, but the poor preservation of processes precludes definitive identification. The vertebra is similar to the 8th caudal vertebra of *Nasua narica* (white-nosed coati) in overall size and the development of proximal processes. Its robusticity index of 23 (calculated as the percent proportion of the transverse width of the centrum at its mid-length to the length of the vertebra; Youlatos, 2003) is comparable to those obtained for the 8th caudal vertebrae of *Nasua*, *Procyon*, and *Genetta* (genets), and is suggestive of a long, relatively robust tail (Youlatos, 2003).

Humerus. The left humerus of SDSNH 107447 (Fig. 1.5A, B) shows deformation along the proximal one-third of its length due to compression, and the proximoposterior part of diaphysis is shattered. The total length of the humerus (10.5 cm) is comparable to those of *Procyon lotor* and *Urocyon cinereoargenteus* among extant carnivorans. Compared to other Paleogene carnivoramorphans, it is roughly 40% shorter than those of *Daphoenus vetus* (18.5 cm in CM 492 in collection of the Carnegie Museum of Natural History, Pittsburgh, Pennsylvania, U.S.A.; Hatcher,

1902) and *Tapocyon robustus* (17.1 cm in SDSNH 36000), nearly identical to that of *"Miacis" uintensis* (10.2 cm in AMNH FM 1964 (Spaulding and Flynn, 2009)), and 40-50% longer than those of *"Miacis" gracilis* (7.6 cm in CM 11900; Clark, 1939) and *Hesperocyon gregarius* (7.1 cm in UCMP 126095).

The greater and the lesser tuberosities have roughly the same height as the humeral head. Due to the crushing, however, the precise orientations of these tuberosities, as well as the form of the humeral head cannot be determined. The morphology of the intertubercular groove is likewise obscured, but it appears to have been well defined. The deltoid and the pectoral ridges converge near the mid-shaft and extend further distally as a prominent deltopectoral crest similar to those in other Paleogene carnivoramorphans such as *Vulpavus* (Heinrich and Rose, 1997), *"Miacis" uintensis* (Spaulding and Flynn, 2009), and *Tapocyon robustus*. In comparison, the deltopectoral crests of *Hesperocyon gregarius* and all the extant carnivorans examined are much less developed, generally forming a low ridge rather than a flange.

The supinator crest forms a large flange that merges proximally with the diaphysis at approximately 40% of the length of humerus from its distal end, and is comparable to that of *Nasua narica* in this regard. A similarly well-developed supinator crest is present in *Tapocyon robustus* and *Daphoenus vetus* (cf. Scott, 1898:plate 20, fig. 15); the same crests in *"Miacis" gracilis* (Clark, 1939) and *Hesperocyon gregarius* are much less prominent. The medial epicondyle is well developed and has a rugose surface. A large, elliptical entepicondylar foramen is present proximal to the trochlea. The trochlea, which may be slightly bent due to compression, is approximately half as wide as the capitulum, nearly semicircular in medial view, and projects slightly more distally than the capitulum. The capitulum is rather bulbous and shows slight proximodistal constriction toward its medial end, where it merges with the trochlea. Both the trochlea and the capitulum are relatively shallow in the anteroposterior direction. On the posterior side of the distal humerus, a deep, groove-like depression is present between the medial epicondyle and the trochlea, probably representing the attachment site for the ulnar collateral ligament (Heinrich and Rose, 1997). The olecranon fossa is well defined but notably shallow as in *Nasua narica*, *Potos flavus* (kinkajou), *Arctictis binturong* (binturong), and apparently *Uintacyon* (cf. Heinrich and Rose, 1997:text-fig. 2C). This is in contrast to the deep fossae in *"M." gracilis*, *Daphoenus vetus* (cf. Hatcher, 1902:plate 19, fig. 7), *H. gregarius* (supratrochlear foramen is present in UCMP 126095), and reportedly *"M." uintensis* (Spaulding and Flynn, 2009), as well as the extant terrestrial, semi-fossorial, and some of the scansorial carnivorans examined. The coronoid fossa immediately proximal to the trochlea on the anterior side is shallow but well delineated as in *Uintacyon* (Heinrich and Rose, 1997). A similarly shallow radial fossa is present lateral to the coronoid fossa and proximal to the capitulum.

Ulna. The left ulna of SDSNH 107446 (Fig. 1.5C) is missing the distal end, and the proximolateral surface of the olecranon process is abraded. The olecranon process is relatively straight and does not project any more anteriorly than the anconeal process (the latter, however, may be broken in the specimen). The morphology of the tendinal groove is mostly unrecognizable due to the abrasion, but a flat surface of the proximomedial end of olecranon process suggests the presence of a shallow groove. The semilunar notch appears to have a greater radius of curvature than that in any of the carnivoramorphans examined and *"Miacis" uintensis* (cf. Spaulding and Flynn, 2009:fig. 1), but is comparable to that of *Vulpavus* (Heinrich and Rose, 1997). A thin stretch of shallow depression is present on the medial surface distal to the semilunar notch, likely representing the insertion site for the antebrachial flexor muscles brachialis and clavobrachialis (Leach, 1977). The morphology of the radial notch may be slightly obscured by crushing, but it appears to have been

relatively wide and flat as in most of the extant mustelids and viverrids examined. The diaphysis is mediolaterally narrow, and its anterior surface flattens toward the distal end, giving rise to a well-developed, medially-projecting flange for the insertion of the pronator quadratus muscle (Leach, 1977). Shallow grooves run on the medial and the lateral sides of diaphysis along its length, delineating the sites of attachment for the flexor and extensor muscles of the manus and manual digits (Leach, 1977).

Femur. The left femur of SDSNH 107446 (Fig. 1.5D) exhibits anteroposterior and mediolateral crushing along the proximal and the distal halves, respectively. It is missing most of the medial condyle, and the lesser trochanter is broken. The length of the femur (13.4 cm) is nearly identical to that reported for *"Miacis" uintensis* (Spaulding and Flynn, 2009) and approximately 50% longer than that of *"M." gracilis* (Clark, 1939). The shape of the patellar groove is obscured by the crushing. The femoral neck is rather short as in Potos flavus and *"M." gracilis* (cf. Clark, 1939:fig. 2), and the greater trochanter projects only as far proximally as the femoral head. The presence of the third trochanter cannot be determined due to poor preservation.

Tibia. The right tibia of SDSNH 107446 (Fig. 1.5E) is mediolaterally crushed and is missing both the proximal and distal epiphyses. The diaphysis is mediolaterally narrower than is anteroposteriorly deep, and is intermediate in robusticity between those of *Nasua narica* and *Arctictis binturong*. The prominent ridges on the posterior and posterolateral surfaces of the diaphysis are suggestive of a strong flexor longus hallucis muscle for the flexion of pedal digits (Taylor, 1976).

Astragalus. The right astragalus of SDSNH 107446 (Fig. 1.5H-M) is missing a portion of the dorsolateral margin and the proximomedial end of trochlea due to breakage, but is otherwise well preserved. The overall size of the astragalus is similar to that of *"Miacis" uintensis* (Spaulding and Flynn, 2009).

The medial portion of the trochlea bears a round, very low ridge that smoothly merges into the shallow trochlear groove and the gently-sloping medial side of trochlea (Fig. 1.5H). The lateral portion of the trochlea, on the other hand, forms a sharp ridge, with a slightly concave fibular facet on its lateral side. In these features, the astragalus of *Lycophocyon hutchisoni* is similar to those of *Martes pennanti*, *Gulo gulo* (wolverine), and *Ailurus fulgens* (red panda). A broad and shallow astragalar trochlea has also been reported for *"Miacis" uintensis* (Spaulding and Flynn, 2009); the trochlear groove in Daphoenus vetus, however, is noticeably deeper (cf. Scott, 1898:plate 20, fig. 22). The dorsal excursion of the plantar tendinal groove (Fig. 1.5I, L) indicates that the lateral aspect of the trochlear groove does not extend as far proximally as the medial aspect, and the lateral margin of the trochlea has a markedly smaller radius of curvature than the medial margin of the trochlea (Fig. 1.5J, K). Unlike in basal carnivoramorphans such as *Didymictis*, *Miacis*, *Uintacyon*, and *Vulpavus*, the astragalus appears to lack both the dorsal and ventral astragalar foramina (Heinrich and Rose, 1997; Gingerich, 1983; Heinrich and Houde, 2006). A relatively long, narrow, and deep plantar tendinal groove for the tendons of the plantarflexor muscles is present proximal to the lateral aspect of the trochlear groove, and extends to the ventral side of astragalus. This groove is oriented slightly oblique to the trochlear groove as in *Vulpavus* and *Didymictis* (Heinrich and Rose, 1997). Similar to *Vulpavus* and unlike *Didymictis* (Heinrich and Rose, 1997), the astragalus lacks the cotylar fossa.

The sustentacular facet is mediolaterally wide and relatively flat (Fig. 1.5I), resembling those of *Vulpavus* (Heinrich and Rose, 1997) and, among extant carnivorans, *Nasua narica*. The ectal facet is similar to those of *N. narica* and *Ailurus fulgens* in the shape of its outline and the concave curvature; it also resembles those of *A. fulgens* and *Paradoxurus hermaphroditus* (Asian palm

civet) in the slightly helical arrangement of its proximal and the dorsal aspects. The sustentacular and the ectal facets are separated by a deep, narrow depression, and their relative sizes and positions are quite similar to those of *N. narica*. In addition, the outline shapes and relative sizes of these facets are generally similar to those of ‘*‘Miacis” uintensis* (cf. Spaulding and Flynn, 2009:fig. 2).

In the distal view (Fig. 1.5M), the astragalar head is dorsoventrally shallower than in any of the extant carnivorans examined, and its long axis is more or less parallel to the transverse axis of trochlea as in *Vulpavus* (Heinrich and Rose, 1997), *Hesperocyon gregarius* (Wang, 1993), and the extant procyonids and mustelids examined, but in contrast to the markedly more tilted astragalar heads in *Didymictis* (Heinrich and Rose, 1997), ‘*‘Miacis” gracilis*, *Atilax paludinosus* (marsh mongoose), and extant canids (Wang, 1993). The dorsoventral and mediolateral convexity of the navicular facet is comparable to those in *Nasua narica* and *Procyon lotor*.

Phalanx. The middle phalanx of SDSNH 107446 (Fig. 1.5G) is characterized by the asymmetrical diaphysis with one side of the dorsal aspect forming a much broader slope than the other. This phalanx cannot be sided on the basis of the asymmetry because the sloping dorsal aspect may face medially or laterally in extant carnivorans, depending on the taxon and the digit. The asymmetry is not associated with deep excavation of the diaphysis or lateral protrusion of the articular condyle as seen in extant felids and, to a lesser degree, in *Tapocyon robustus* (cf. Wesley and Flynn, 2003:fig. 7), in which these features enable full retraction of the claws (Gonyea and Ashworth, 1975). In dorsal view, the outline of phalanx as a whole is essentially symmetrical. Overall, these conditions are similar to those found in some digits of *Daphoenus vetus* (cf. Scott, 1898:plate 20, fig. 21), *Ailurus fulgens* and extant canids such as *Vulpes vulpes* (red fox) and *Urocyon cinereoargenteus*.

Assessment of Size Variation for Taxonomic Consideration

Specimens of *Lycophocyon hutchisoni* exhibit notable size variation (Fig. 1.6A). For example, the anteroposterior length of the lower first molar (m1L) ranges from 9.1 mm in SDSNH 107450 to 10.8 mm in SDSNH 107458, representing a difference of 19%. Because size difference is sometimes the only observable distinction between closely-related species of fossil mammals (Gingerich, 1974; Gingerich and Winkler, 1979), the possibility that the known specimens of *L. hutchisoni* in fact represent more than one species was evaluated by comparing the coefficient of variation (CV) (Simpson et al., 1960) in m1L to those of the earliest known stem canid, *Hesperocyon gregarius*, an extant canid, *Urocyon cinereoargenteus* (gray fox), and an extant mustelid, *Martes pennanti* (fisher). These comparative taxa were selected based on their sizes (Fig. 1.6B-D) and m1 morphology (with well-developed carnassial shear and talonid) that are reasonably similar to those of *L. hutchisoni*. In addition, *H. gregarius* represents a fossil species with an adequate sample size that is phylogenetically close to *L. hutchisoni* (see the result of a cladistic analysis presented below); *U. cinereoargenteus* and *M. pennanti* represent species with low and high degrees of sexual size dimorphism, respectively (Fig. 1.6D). Since diagnosis of fossil taxa is prone to subjective lumping or splitting of morphotypes by researchers, the comparison with another fossil species, *H. gregarius*, may appear circular for the purpose of recognizing the species boundary of *L. hutchisoni*. However, the morphological integrity both in size and form of *H. gregarius* (i.e., the species is not clearly divisible into smaller sets of morphotypes) has been well established by comparison to extant species of canids (Wang, 1994). As may well be the case for the sample of *L. hutchisoni*, the sample of *H. gregarius* consists of geologically-diachronous individuals, providing a useful reference for exploring possible accumulation of size variation over the history of an evo-

lutionary lineage segment. At the least, comparison with well-sampled, clearly-delineated fossil species such as *H. gregarius* should contribute to consistency in taxonomic practice by establishing reasonable size ranges for closely-related fossil species. It should also be noted that, because different species in a sample (paleontological or otherwise) need not differ in size, presence of a single species in a sample cannot be demonstrated by statistical hypothesis testing; instead, the purpose of cross-taxonomic comparison here is to inform a taxonomic decision by testing whether the observed within-sample variation of *L. hutchisoni* is too great to be interpreted as solely intraspecific variation.

The sample-size adjusted coefficient of variation (CV) (Haldane, 1955) in m1L is 6.3% for 9 specimens belonging to separate individuals of *Lycophocyon hutchisoni*. Statistical hypothesis tests using randomization procedure (Lockwood et al., 1996) show that the CV of 6.3% for *L. hutchisoni* falls within the bootstrap estimates of bias-corrected 95% confidence intervals for *Hesperocyon gregarius* (95% CI = [2.9%, 6.7%], mean = 4.7%, median = 4.7%; Fig. 1.6E) and *Martes pennanti* (95% CI = [1.3%, 8.4%], mean = 7.2%, median = 7.5%; Fig. 1.6G), but outside that for *Urocyon cinereoargenteus* (95% CI = [2.4%, 6.1%], mean = 4.1%, median = 4.0%; Fig. 1.6F). Thus, at the confidence level of $\alpha = 0.05$, the within-sample variation in m1L of *L. hutchisoni* is statistically indistinguishable from those of *H. gregarius* and *M. pennanti*, but is significantly greater than that of *U. cinereoargenteus*.

Dietary Inference

The body weight of the individual represented by the holotype UCMP 85202 was estimated from its m1L to be roughly 6 kg. A linear discriminant analysis of dietary categories using 6 morphological variables and the data set of Friscia et al. (2007) predicted a carnivorous diet for *Lycophocyon hutchisoni*, with the posterior probabilities of 83%, 10%, and 7% for carnivory, omnivory/durophagy, and insectivory, respectively (Fig. 1.7). This prediction reflects the long m1 trigonid and the small m2, features indicating the relative importance of shearing over crushing when compared to extant carnivorans that are not major consumers of vertebrates (Table 1.3).

Cladistic Analysis

Building on the currently most-extensive character matrix in the literature for basal carnivoramorphans and early carnivorans (Spaulding et al., 2010; see also Wesley-Hunt and Flynn, 2005; Wesley-Hunt and Werdelin, 2005; Polly et al., 2006; Spaulding and Flynn, 2009), a parsimony analysis of 50 taxa (including 2 hyaenodontid creodonts and 3 outgroup taxa represented by *Leptictis dakotensis*, *Erinaceus concolor*, and *Echinosorex gymnura*) and 98 morphological characters was performed to determine the cladistic position of *Lycophocyon hutchisoni*. This analysis yielded 132 most-parsimonious trees (length = 488 steps, ensemble consistency index = 0.289, ensemble retention index = 0.667; Appendix S1.3), and failed to resolve the relationships among the carnivoramorphans surrounding the base of crown-group Carnivora, including *L. hutchisoni* (Fig. 1.8A).

Consequently, a second parsimony analysis was conducted for a subset of the same character matrix consisting of only the taxa that are known from the Paleogene Period (see Discussion) and *Leptictis dakotensis* as the outgroup taxon. The strict consensus of 32 most-parsimonious trees

thus obtained (length = 280 steps, ensemble consistency index = 0.382, ensemble retention index = 0.664; Appendix S1.3) placed *Lycophocyon hutchisoni* on the caniform branch within the Carnivora, and immediately outside the crown-group Canoidea (Fig. 1.8B). Addition of *Nandinia binotata*, which is consistently identified by molecular studies as belonging to the earliest-splitting lineage among extant feloids (Flynn and Nedbal, 1998; Flynn et al., 2005; Gaubert and Cordeiro-Estrela, 2006; Eizirik et al., 2010), does not alter the relationships of other taxa in the strict consensus tree; when included in the cladistic analysis, *N. binotata* is positioned as the sister taxon to the monophyletic group B7 (Fig. 1.8B). Likewise, the selection of *Thinocyon* sp. or *Hyaenodon horridus* (*"Hyaenodon cruentus"* in Wesley-Hunt and Flynn (2005)) as the outgroup taxon (instead of *Leptictis dakotensis*) does not affect the topology of the consensus tree with respect to the non-viverravid carnivoramorphans.

The topology of the consensus tree for Paleogene taxa broadly agrees with those reported in the recent studies (Wesley-Hunt and Flynn, 2005; Wesley-Hunt and Werdelin, 2005; Polly et al., 2006; Spaulding and Flynn, 2009; Spaulding et al., 2010) in that (1) the viverravids form a monophyletic group (B2 in Fig. 1.8B) outside all other carnivoramorphans, and (2) the earliest non-viverravid carnivoramorphans are located outside the crown-group Carnivora. However, it differs in the ambiguous placement of *Quercygale angustidens*, *"Miacis"* cf. *"M." sylvestris*, *"M." gracilis*, *"M." uintensis*, and *Tapocyon robustus* either inside or outside the crown-group Carnivora. As a result, the precise phylogenetic origin of the crown-group Carnivora cannot be located. In the most-parsimonious trees in which *"M." sylvestris*, *"M." gracilis*, and *"M." uintensis* are included in the Carnivora (18 out of 32 most-parsimonious trees), *Q. angustidens* is invariably positioned as a basal feliform, whereas *T. robustus* is variably located in the Caniformia or the Feliformia (Appendix S1.3).

Lycophocyon hutchisoni shares with the canoids (B11 in Fig. 1.8B) the derived trait of the broad and flat anterior extension of the petrosal promontorium (Character 28, state 3), but lacks the canoid synapomorphies (though none is unique to the Canoidea) of: (1) the infraorbital foramen positioned above the anterior edge of P4 (Character 4, state 1); (2) loss of M3 (Character 53, state 1); and (3) well-ossified entotympanics firmly fused to the basicranium (Character 68, state 1). The monophyletic group consisting of the canoids, *L. hutchisoni*, *"Miacis" cognitus*, and *Daphoenus* (B8 in Fig. 1.8B) is united by a wide shelf between the mastoid process and the paroccipital process that does not form a trough (Character 33, state 1). Synapomorphies for other selected monophyletic groups in the consensus tree are as follows (see node numbers in Fig. 1.8B): B1 (Carnivoramorpha), M1 with broad parastylar shelf (Character 51, state 1), carnassials consisting of P4 and m1 (Character 54, state 1), P4 protocone anterior to paracone (Character 82, state 1), pronounced size decrease from m1 to m3 (Character 86, state 1); B2 (Viverravidae), small flange along middle-ear chamber formed by ventral floor of basioccipital (Character 34, state 1), subequal heights of protocone and paracone (Character 42, state 1), absence of m3 (Character 88, state 1); B3, round infraorbital foramen (Character 3, state 1), fenestra cochlea located at the same level or anterior to mastoid tubercle (Character 18, state 1), elongate promontorium with round anterior end (Character 28, state 1), rugose surface for entotympanic attachment on anteromedial promontorium or tympanic wing of basisphenoid (Character 30, state 1), deep fossa for tensor tympani muscle (Character 39, state 1), short m2 talonid (Character 59, state 1); B4, no synapomorphy exists for this clade that is common to all most-parsimonious trees; B5 (part of Feliformia), postglenoid foramen reduced or absent (Character 12, state 1), short promontorium with blunt anterior end (Character 28, state 2), promontorium with facet for ectotympanic attachment (Character 29,

state 1), absence of lingual cingulum on M1 (Character 41, state 0; derived among non-viverravid carnivoramorphans but reversal among all taxa considered in the analysis), reduced M1 (Character 46, state 1), pronounced reduction of m1 talonid (Character 85, state 1); B6 (Nimravidae), reduced paroccipital process (Character 9, state 1), mastoid process extending farther than paroccipital process (Character 13, state 0; derived among non-viverravid carnivoramorphans but may represent a reversal within the Carnivoramorpha), M1 with narrow parastylar shelf (Character 51, state 2), well-ossified entotympanic firmly attached to basicranium (Character 68, state 1), absence of p1 (Character 84, state 1); B7 (Feloidea), absence of lacrimal exposure on rostrum (Character 1, state 2), condyloid foramen close to posterior lacerate foramen (Character 15, state 1), extensive attachment area for entotympanic on promontorium posterior to fenestra cochlea (Character 26, state 1), narrow shelf between mastoid process and paroccipital process (Character 33, state 2), middle lacerate foramen located anterior to basisphenoid-basioccipital suture (Character 40, state 2), anterior entry of carotid artery into auditory capsule not enclosed in bony tube (Character 67, state 3); B9, anteriorly open fossa for stapedius muscle (Character 37, state 1); B12 (stem-group Canidae), condyloid foramen close to posterior lacerate foramen (Character 15, state 1), anterior lingual cingulum of M1 reduced or absent (Character 41, state 2), absence of parastylar shelf on M1 (Character 51, state 0; derived within the Carnivoramorpha but a reversal among all taxa considered in the analysis); B13 (Arctoidea), absence of hypocone on M1 (Character 50, state 0; derived within the Canoidea but a reversal within the Carnivoramorpha).

Finally, the tree length increases by at least: (1) 2 steps when *Lycophocyon hutchisoni* is paired with *Daphoenus* or the group consisting of *Daphoenus* and *"Miacis" cognitus*; (2) 6 steps when *L. hutchisoni* is placed in the Feliformia; (3) 5 steps when *L. hutchisoni* is placed immediately outside the Carnivora; and (4) 5 steps when the group consisting of *Daphoenus* and *"M." cognitus* is either paired with or placed among the basal arctoids in the analysis.

Discussion

Intraspecific Variations in Dental Morphology

While the size variation among known specimens of *Lycophocyon hutchisoni* is notable, it does not significantly exceed that of *Martes pennanti*, an extant mustelid with a high degree of sexual size dimorphism, or that of *Hesperocyon gregarius*, an extinct canid (Fig. 1.6E, G). From the perspective of hypothesis testing, this should be viewed not as direct support for the presence of a single species in the sample of fossil specimens but as failure to detect the presence of more than one species. A comprehensive assessment of intraspecific size variation in carnivorans was not attempted in the present study, in part to minimize the statistical problem of multiple comparisons; nevertheless, CVs in m1L of other carnivorans available in the literature (Table 1.4) are consistent with the interpretation that the size variation of *L. hutchisoni* is not unusually high compared to those of extant carnivoran species.

The significantly-greater CV in m1L of *Lycophocyon hutchison*i compared to that of *Urocyon cinereoargenteus* (Fig. 1.6F) merits discussion. Because the geographic area encompassed by the sample of *U. cinereoargenteus* is much greater than that of *L. hutchisoni* (approximately 73,000 km2 versus 3 km2), the difference in CV is not attributable to geographic variation. Instead, it may partly be explained as phyletic variation in size of *L. hutchisoni*. Indeed, Hunt (2004*b*) demon-

strated that greater time-averaging of fossil samples significantly increased the observed variance in quantitative morphological traits as predicted under the Markovian random-walk model of phenotypic evolution. However, Hunt (2004*b*, 2004*a*) also showed that, for a variety of organisms and traits (including m1L of mammals), the increase in within-sample variance caused by time-averaging of 104-105 years was typically on the order of 1%. This would result in 0.5 to 4% increase in CV, whereas the observed difference is roughly 50%. Therefore, considering that much of the size variation in *L. hutchisoni* is captured by specimens from the same horizon (SDSNH locality 5721; Fig. 1.6A), it seems likely that the difference in CV between the samples of *L. hutchisoni* and *U. cinereoargenteus* primarily reflects greater intrapopulational variation of the former independent of time.

With regard to qualitative dental morphology, it is notable that the subtle variations among the specimens of *Lycophocyon hutchisoni*, such as the degree of development of accessory cuspids on lower premolars and the continuity of M1 lingual cingulum around the protocone, are well documented both within and across populations of an extant canid, *Vulpes vulpes* (Szuma, 2007). Indeed, the increasing knowledge of intraspecific dental morphological variation in extant carnivorans (Dayan et al., 2002; Szuma, 2004; Daitch and Guralnick, 2007; Szuma, 2007) is especially pertinent to the taxonomy of fossil species, and should inform the selection of morphological characters and categorization of character states in future cladistic analyses. In summary, the dental morphological variations among the known specimens of *Lycophocyon* appear insufficient for establishing multiple species within the genus.

Ecomorphological Interpretations

Dentition. In addition to predicting a carnivorous diet for *Lycophocyon hutchisoni*, the linear discriminant analysis of ecomorphology produced similar posterior probabilities of dietary-group affiliations for such extant carnivorans as *Urocyon littoralis* (island fox), *Genetta maculata* (rusty-spotted genet), *Martes americana* (American marten), and *Herpestes ichneumon* (Egyptian mongoose; Fig. 1.7). While the obvious correlations among the predictor variables must be noted, the coefficients of linear discriminants indicate that these taxa are united among ecological carnivores by their relatively large m2 occlusal areas and relatively short m1 trigonid lengths. Indeed, as would be expected from such dental morphology, insects and plants may constitute a significant portion of the diet of *U. littoralis*, *G. maculata*, and *M. americana* (Angelici, 2000; Crooks and Van Vuren, 1995; Zielinski and Duncan, 2004; Phillips et al., 2007). Likewise, *H. ichneumon*, while most heavily dependent on small terrestrial vertebrates (as measured in consumed biomass), often feeds on insects, and its opportunistic diet may also include fish, hard-shelled aquatic invertebrates, and plants (Palomares, 1993; Angelici, 2000; Rosalino et al., 2009). Notable similarity in dietary composition between *G. maculata* and *H. ichneumon* where they are sympatric has been reported (Angelici, 2000). Thus, the observable ecomorphology suggests *L. hutchisoni* to have been a generalist mesocarnivore (sensu Van Valkenburgh, 2007).

Postcranial skeleton. The locomotor inference for fossil mammals is necessarily based on comparison of their skeletal forms with those of their extant relatives, for which direct behavioral observations are available (cf. Van Valkenburgh, 1987; Wang, 1993; Heinrich and Rose, 1997). To alleviate the potential problem of allometry, comparisons were made primarily with extant carnivorans of similar body size. Decoupling the phylogenetic and adaptive components of postcranial skeletal morphology is difficult at present, but it is plausible that, in some cases, relatively minor

skeletal modifications can provide sufficient adaptations for highly divergent locomotor habits; for example, postcranial elements of the extant *Urocyon cinereoargenteus* (gray fox) are clearly recognizable as belonging to a canid (author's pers. obs.), yet this species, unlike other canids, is highly capable of climbing trees (Fritzell and Haroldson, 1982). In light of the recent advancement in molecular phylogenetics of carnivorans, comprehensive studies of their locomotor morphology in explicitly phylogenetic frameworks (cf. Garland and Janis, 1993) are awaited.

The humeral morphology of *Lycophocyon hutchisoni* (Fig. 1.5A, B) is suggestive of an adept climber. The mobility of the glenohumeral joint is enhanced by the low height of the greater tuberosity (Larson and Stern, 1989; Heinrich and Rose, 1997). The distal extension of the prominent deltopectoral crest resembles the condition in *Vulpavus* (Heinrich and Rose, 1997) and arboreal *Nandinia binotata* (African palm civet) (Taylor, 1974), and suggests the presence of powerful musculature that generated large force at the expense of speed (Hildebrand and Goslow, 2001). The well-developed medial epicondyle and the expansive supinator crest are similar to those of *Nasua narica* (white-nosed coati) and *Gulo gulo* (wolverine), which are both skilled climbers (Jenkins and McClearn, 1984; Gompper, 1995; Pasitschniak-Arts and Larivière, 1995), and are indicative of strong flexor and extensor muscles for the manus and the manual digits that are necessary for habitual climbing (Taylor, 1974). The muscle attachment areas on the humerus of *L. hutchisoni*, however, are not expanded to the same degree as in the semi-fossorial *Taxidea taxus* (American badger). The well-demarcated coronoid fossa similar to that of *N. narica* may reflect frequently flexed position of the ulna, as has been suggested for *Vulpavus* (Heinrich and Rose, 1997). The very shallow olecranon fossa as seen in *Potos flavus* (kinkajou) and *Arctictis binturong* (binturong) and the limited projection of the humeral trochlea distal to the capitulum suggest a relatively wide range of mediolateral movement of the ulna at the humeroulnar joint, and are in contrast to the typical morphology in extant terrestrial carnivorans that restricts the ulnar movement mostly to the anteroposterior direction (Taylor, 1974).

Features of the ulna (Fig. 1.5C) are consistent with the mode of locomotion inferred from the humeral morphology. The lateral orientation of radial notch enhances the rotation of radius (Taylor, 1974). The relatively straight olecranon process of *Lycophocyon hutchisoni* compared to those of extant terrestrial carnivorans maximizes the force generated by the triceps muscle when the ulna is highly flexed, as often occurs during climbing (Taylor, 1974; Van Valkenburgh, 1987).

With regard to the hind limb, the relatively round head (similar to *Paradoxurus hermaphroditus* (Asian palm civet) and more spherical than in *Urocyon cinereoargenteus* (gray fox) and *Vulpes vulpes* (red fox)) and the short neck of femur (Fig. 1.5D) suggest its wide range of rotational movement at the hip joint (Heinrich and Houde, 2006).

The shallow trochlear groove and the low, round ridge of the medial trochlear margin of astragalus (Fig. 1.5H, M) are comparable to those of *Martes pennanti* (fisher), *Gulo gulo*, *Nasua narica*, and *Ailurus fulgens* (red panda), and are suggestive of enhanced pedal inversion concomitant with plantarflexion (Jenkins and McClearn, 1984; Heinrich and Rose, 1997). The dorsolateral extension of the navicular facet (Fig. 1.5H, K, M) may have enhanced the eversion of the foot at the astragalonavicular joint (Szalay and Decker, 1974). In addition, the ectal facet with a smoothly round concavity and the slightly helical arrangement of its proximal and distal aspects (Fig. 1.5I) would, together with the mediolateral orientation of the astragalar head (Fig. 1.5M) and the ventrally-facing sustentacular facet (Fig. 1.5I), further facilitate the pedal inversion by subtalar joint movement (Jenkins and McClearn, 1984). At the same time, although the proximal extent of the medial trochlear margin (Fig. 1.5H, J) and the apparent lack of the dorsal astragalar foramen

may have allowed the maximum angle between the tibial diaphysis and the long axis of the astragalus to be greater than 90°(cf. Heinrich and Rose, 1997), the presence of the dorsally-extensive plantar tendinal groove slightly in angle with the trochlear groove (Fig. 1.5L) likely limited the range of plantarflexion (Wang, 1993). The astragalar morphology is thus indicative of a plantigrade posture and substantial hindfoot flexibility, but the ability to completely reverse the hindfoot as in the arboreal *Potos flavus* is unlikely, since it would have required a greater range of plantarflexion (Jenkins and McClearn, 1984). It should be noted, however, that complete reversal of hindfeet is not necessary for descending trees headfirst: the scansorial *N. narica*, for example, is known to compensate for the relatively limited hindfoot flexibility with pronounced abduction of the femora (Jenkins and McClearn, 1984).

Taken together, the known postcranial elements of *Lycophocyon hutchisoni* point to a scansorial habit of an animal that was likely as adept at climbing as the extant *Nasua narica* (Jenkins and McClearn, 1984; Gompper, 1995) and *Gulo gulo* (Pasitschniak-Arts and Larivière, 1995; although the substantial weight difference between *L. hutchisoni* and *G. gulo* makes the latter comparison less conclusive), but was probably not as dependent on the arboreal habitat as *Potos flavus*.

Cladistic Position of Lycophocyon hutchisoni *and Remarks on the Phylogeny of Early Carnivorans*

Following recent studies of early carnivoramorphans (Wesley-Hunt and Flynn, 2005; Wesley-Hunt and Werdelin, 2005; Polly et al., 2006; Spaulding and Flynn, 2009; Spaulding et al., 2010), with which the present study shares many of the same character matrix data, the initial cladistic analysis here included 12 operational taxonomic units (OTUs) represented partly or entirely by extant carnivorans (Fig. 1.8A; also see Wesley-Hunt and Flynn, 2005). However, this analysis failed to (1) resolve the cladistic position of *Lycophocyon hutchisoni* and (2) recover well-established relationships of extant arctoids (Flynn et al., 2005; Arnason et al., 2007; Finarelli, 2008; Eizirik et al., 2010). In re-examining the results of the recent studies (Wesley-Hunt and Flynn, 2005; Wesley-Hunt and Werdelin, 2005; Spaulding and Flynn, 2009; Spaulding et al., 2010), it is notable that they consistently reported most-parsimonious trees in which many of the extant (partially or entirely) OTUs clustered together, showing topologies that are in major conflict with those that are strongly supported by recent molecular and combined molecular and morphological studies (Gaubert and Veron, 2003; Flynn et al., 2005; Arnason et al., 2007; Finarelli, 2008; Eizirik et al., 2010); interestingly, the same pattern is observed when comparing the morphological tree and the combined morphological and molecular tree of fossil and extant arctoids reported by Finarelli (2008). In the present and previous studies (Wesley-Hunt and Flynn, 2005; Wesley-Hunt and Werdelin, 2005; Spaulding and Flynn, 2009; Spaulding et al., 2010), this problem may be attributable to the insufficient sampling of fossil taxa from the Neogene that would fill the morphological gaps between the basal carnivorans and their extant relatives, predisposing the cladistic analysis to long branch attraction (cf. Wang et al., 2005; Donoghue et al., 1989; Bergsten, 2005). Temporally-long branches in parsimony analysis are of particular concern in light of the growing evidence that, at least in parts of the carnivoran phylogeny, the types of craniodental characters considered here have evolved more rapidly and flexibly than had traditionally been assumed (Koepfli et al., 2007; Gaubert and Veron, 2003; Gaubert et al., 2005). Furthermore, the morphological characters analyzed in the present and recent studies (Wesley-Hunt and Flynn, 2005; Wesley-Hunt and Werdelin, 2005; Polly et al., 2006; Spaulding and Flynn, 2009; Spaulding et al., 2010) may not be suitable for

analyses that include highly-derived extant carnivorans because they were originally selected primarily to resolve the relationships of early carnivoramorphans (Wesley-Hunt and Werdelin, 2005). In any case, the phylogenetic locus of interest in the present study is not the entire carnivoramorphan tree but the branches surrounding *Lycophocyon hutchisoni*, and so basal carnivorans, rather than extant carnivorans that are morphologically far removed from the carnivoran origin (see e.g., Finarelli, 2008, for morphological transformations that separate extant arctoids from their extinct basal relatives), should provide more appropriate and sufficient data for the polarization of character states in this region of the carnivoramorphan tree. For these reasons, the discussion below of basal carnivoran phylogeny is based on the result of the second analysis that focused on the Paleogene carnivoramorphans (Fig. 1.8B).

The following interpretations of the strict consensus tree for the Paleogene taxa (Fig. 1.8B) rest on the assumptions that (1) at least *Hesperocyon gregarius* or *Otarocyon macdonaldi* is a caniform, (2) at least one among *Stenogale julieni*, *Proailurus lemanensis*, and *Palaeoprionodon lamandini* is a feliform, and (3) at least one among *Mustelavus priscus*, *Pseudobassaris riggsi*, *Amphicticeps shackelfordi*, *Plesictis genettoides*, and *Broiliana nobilis* is an arctoid. These assumptions are deemed secure in light of detailed studies of their skeletal anatomy and previously-conducted cladistic analyses (Hunt, 1989; Wang, 1994; Wang, X. and Tedford, R. H. and Taylor, B. E., 1999; Wang et al., 2005; Wesley-Hunt and Flynn, 2005; Wesley-Hunt and Werdelin, 2005; Finarelli, 2008; Spaulding and Flynn, 2009; Spaulding et al., 2010). As in the recent studies that share many of the same character matrix data (Wesley-Hunt and Flynn, 2005; Wesley-Hunt and Werdelin, 2005; Spaulding and Flynn, 2009; Spaulding et al., 2010), the nodal support values for the consensus tree are generally low (Fig. 1.8B), but such information cannot simply be taken as evidence against particular phylogenetic hypotheses when morphological variations among the taxa of interest are limited, as might be expected for basal branches that have been divergent for a relatively short period of time (cf. Wang et al., 2005). It is hoped that further progress in mammalian molecular phylogenetics and developmental genetics will help formulate probabilistic models of skeletal evolution that can be incorporated into future cladistic analyses of the taxa considered here.

The proximity of *Lycophocyon hutchisoni* to one of the earliest-known amphicyonids, *Daphoenus*, agrees with its notable similarity in dental morphology to another early amphicyonid, *Cynodictis lacustris*. Further testing of the hypothesized cladistic position of *L. hutchisoni* would, therefore, benefit from increased sampling of early amphicyonids (*Cynodictis* could not be incorporated into the present cladistic analysis because of the limited availability of specimens that preserve morphological details of the basicranium).

The placement of *Daphoenus* outside the Canoidea (Fig. 1.8B, node group B11) corroborates the findings of some of the recent studies (Wesley-Hunt and Flynn, 2005; Polly et al., 2006), and is consistent with its earlier first appearance than those of almost all other caniforms (see below). It also implies that the deep excavation of the lateral margin of basioccipital in amphicyonids and ursids—a trait that is often considered as a potential synapomorphy uniting the two groups (Hunt, 1977; Wyss and Flynn, 1993)—may have evolved convergently. In fact, distribution of this trait among the most basal ursids appears to be poorly known at present (cf. Finarelli, 2008). Furthermore, this phylogenetic arrangement is most parsimonious with regard to loss of M3 and ossification of entotympanics in early caniforms. Because early amphicyonids such as *Daphoenus* possess M3s and lack well-ossified entotympanics firmly fused to the basicranium, their inclusion in the Canoidea (regardless of their precise affiliation with ursids) would require (1) an additional loss (two independent losses within canoids) or a regeneration of M3s and, similarly, (2) an ad-

ditional instance of entotympanic ossification (two independent ossifications within canoids) or a reversal to unossified (or poorly-ossified) entotympanics. Of these possibilities, multiple losses of M3s within the Canoidea are not implausible, but no basal caniform of unquestionable canoid affinity is currently known that retains M3s. On the other hand, a regeneration of M3s as part of the regular dentition seems yet more improbable considering that almost no such case is known among living and extinct caniforms of unquestionable canoid affiliation, the sole exception being *Otocyon megalotis* (bat-eared fox) (Clark, 2005); the remarkably well-developed "M3s" of *O. megalotis*, whose diet consists mainly of termites (Clark, 2005), are suggestive of an unusual molar developmental system (Wood and Wood, 1933; Guilday, 1962; Van Valen, 1964) and are a questionable comparison to the highly-reduced M3s of early amphicyonids that are morphologically similar to those of the non-canoid caniform *Lycophocyon hutchisoni*.

The feliform affiliation of nimravids (*Dinictis felina* and *Hoplophoneus* sp.) is in accord with the findings of several previous studies (Bryant, 1991; Wyss and Flynn, 1993; Wesley-Hunt and Flynn, 2005). The monophyletic subgroup of the Feliformia consisting of the nimravids, *Stenogale julieni*, *Proailurus lemanensis*, and *Palaeoprionodon lamandini* (Fig. 1.8B, Group B5) has the highest nodal support values of all the monophyletic groups in the cladogram, and is supported by at least five probable synapomorphies (see Results).

Recent studies (Wesley-Hunt and Flynn, 2005; Wesley-Hunt and Werdelin, 2005; Polly et al., 2006; Spaulding and Flynn, 2009; Spaulding et al., 2010) consistently placed *Tapocyon robustus*, *Quercygale angustidens*, *"Miacis"* cf. *"M." sylvestris*, *"M." uintensis*, and *"M." gracilis* outside the crown-group Carnivora, suggesting a phylogenetically-shallow origin of carnivorans consisting mostly of the taxa that have long been recognized as definitive carnivorans. Considered in this light, the equivocal relationships of the above-mentioned taxa to crown-group carnivorans in the most-parsimonious trees obtained here are an important finding of the present study, providing an alternative hypothesis of a phylogenetically-deeper origin of carnivorans. Thus, with regard to the timing of caniform-feliform divergence, the consensus tree of Paleogene taxa (Fig. 1.8B) suggests two possible minimum divergence dates (see Benton and Donoghue, 2007, for the protocol for deriving minimum constraints on lineage divergence dates):

(1) If *"Miacis" sylvestris* is located outside the Carnivora, the conservative minimum divergence date will be 38 million years ago (Ma) based on the first appearance of the amphicyonid *Daphoenus lambei* in the early-Duchesnean Hendry Ranch Member of the Wagon Bed Formation, Wyoming, and assuming that the locality is older than the Buckshot Ignimbrite of Texas, which has yielded a $^{40}\mathrm{Ar}/^{39}\mathrm{Ar}$ date of 37.8 $\pm$ 0.2 Ma (Hunt, 1996*a*; Robinson et al., 2004), or based on the first appearance of the canid *Hesperocyon* cf. *H. gregarius* in the Duchesnean Lac Pelletier Lower Fauna of the Cypress Hills Formation, Saskatchewan, Canada (Bryant, 1992; Wang, 1994) (N.B. an earlier study (Wesley-Hunt and Flynn, 2005) noted the first appearance date of ca. 43 Ma for *Daphoenus* and *Hesperocyon*, but the derivation of this date is unclear; no unambiguous occurrence of a canid or amphicyonid is currently known prior to the Duchesnean NALMA). A less-secure minimum divergence date of 40 Ma may instead be proposed for the same cladistic topology based on the occurrence of an unidentified nimravid in the Hancock Mammal Quarry of the Clarno Formation, Oregon, below a welded tuff layer in the Member A of the John Day Formation, which has yielded $^{40}\mathrm{Ar}/^{39}\mathrm{Ar}$ dates of 39.5-40.0 Ma (Hanson, 1996; Lander and Hanson, 2006).

(2) If *"Miacis" sylvestris* is located inside the Carnivora, the conservative minimum divergence date will be approximately 47 Ma based on its first appearance near the top of the Upper Blacks

Fork Member (Matthew, 1909; Robinson et al., 2004) of the Bridger Formation, Wyoming, below the Henrys Fork Tuff in the overlying Twin Buttes Member, which has yielded a $^{40}\mathrm{Ar}/^{39}\mathrm{Ar}$ date of 46.9 $\pm$ 0.2 Ma (Murphey et al., 1999; Robinson et al., 2004).

Comparison of these minimum dates of caniform-feliform divergence with divergence-date estimates reported in molecular phylogenetic studies is hampered by the fact that most of the published molecular-clock estimates depend on a fossil constraint placed on this very node of interest. The problem is further complicated by the frequent selection of fossil constraints (Eizirik et al., 2001; Murphy et al., 2001; Springer et al., 2003; Woodburne et al., 2003; Kitazoe et al., 2007; Poux et al., 2008; Wan et al., 2009) using taxonomic classifications that either do not distinguish between crown and stem groups or implicitly assume the inclusion of all carnivoramorphans in the crown-group Carnivora (Stucky and McKenna, 1993; McKenna and Bell, 1997). The few estimates that do not depend on a fossil constraint placed on the node of carnivoran origin are widely divergent, ranging from 63 $\pm$ 2 (standard error) Ma (Bininda-Emonds et al., 2007, 2008) to 46 $\pm$ 6 (standard error) Ma (Kumar and Hedges, 1998). The accuracies of both of these estimates may be questioned, however, because of the choice of *Procynodictis vulpiceps* to constrain the base of Canidae in the former case (Bininda-Emonds et al., 2007, 2008; following McKenna and Bell, 1997, but not supported by the present or past cladistic analyses (Wang and Tedford, 1994)), and because of the reliance on a single fossil calibration point (310 Ma for the synapsids-diapsid split) in the latter case (Kumar and Hedges, 1998) in deriving the time scale for a vertebrate phylogeny (cf. Graur and Martin, 2004; Hug and Roger, 2007).

Lycophocyon hutchisoni sheds an additional light on the morphological evolution of caniforms surrounding the origin of the crown-group Canoidea. In the middle to late Eocene, early caniforms such as *L. hutchisoni*, *Cynodictis* (e.g. *C. lacustris*), and *Daphoenus* (e.g. *D. lambei*) were generally characterized by M1s with labially-extended parastylar regions, diminutive M3s, relatively closed m1 trigonids with well-developed metaconids, and absence of well-ossified entotympanics that were firmly fused to the basicranium. With minor modifications, the features of M1 and m1 were inherited by the most-basal canoids from the late Eocene to the early Oligocene, such as *Prohesperocyon wilsoni* (putatively the most primitive, though not the earliest-known, stem canid (Wang, 1994)), *Mustelavus priscus*, and *Amphicticeps shackelfordi* (Wang et al., 2005). On the other hand, loss of M3 and development of well-ossified entotympanics seem to be closely associated with the canoid origin sometime before 38 Ma; this implies that the same transformations independently took place among early feliforms. Apparently very early in the history of the canid lineage, the parastylar extension of M1 was suppressed, the metaconid of m1 was substantially reduced, the m1 trigonid became quite open (i.e., much longer than wide), and a partial septum was formed inside the ossified auditory bulla, as seen in the earliest-known canid *Hesperocyon gregarius*. Similar modifications of M1 and m1 are seen within early arctoids (e.g. "amphicynodonts") and amphicyonids, respectively.

Consideration of the biogeographic and ecological context of the carnivoran origin depends on a clear understanding of the phylogenetic relationships of the early carnivorans and their close carnivoramorphan relatives outside the crown group. Cladistic analyses of wider arrays of Paleogene carnivoramorphans are thus awaited.

(Supporting Material)

Appendix S1.1. List of comparative specimens examined. Available at http://www.plosone.org/article/fetchSingleRepresentation.action?uri=info:doi/10.1371/journal.pone.0024146.s00

Appendix S1.2. Measurements of the lower first molars of *Lycophocyon hutchisoni*, *Hesperocyon gregarius*, *Urocyon cinereoargenteus townsendi*, and *Martes pennanti columbiana* used for the analysis of size variation. Available at http://www.plosone.org/article/fetchSingleRepresentation.action?uri=info:doi/10.1371/journal.pone.0024146.s00

Appendix S1.3. Nexus file for the program Mesquite (Maddison and Maddison, 2009) containing the character matrix for the cladistic analysis, most-parsimonious trees for the full set of 50 OTUs (labeled as MPT50-1 through MPT50-132) and the subset consisting of 33 OTUs (labeled as MPT33-1 through MPT33-32), and the strict consensus for each set of taxa (labeled Consensus50 and Consensus33, respectively). For the full set of 50 OTUs, only the trees with *Leptictis dakotensis* as the primary outgroup taxon are shown; as noted in the Results, the choice of either Thinocyon sp. or *Hyaenodon horridus* as the primary outgroup taxon does not affect the topology of non-viverravid carnivoramorphans. The character numbers of Wesley-Hunt and Flynn (2005) are denoted with the prefix "whf." The parsimony reconstruction of ancestral character states can be viewed in the Tree Window of Mesquite. Available at http://www.plosone.org/article/fetchSingleRepresentation.action?uri=info:doi/10.1371/journal.pone.0024146.s00

Table 1.1: Craniodental measurements (in mm) of *Lycophocyon hutchisoni*

Measurement	UCMP 85202	UCMP 170713	SDSNH 107442	SDSNH 107443	SDSNH 107444	SDSNH 107447	SDSNH 107465	SDSNH 107658	SDSNH 107659
Cranium									
Length[1]			105				105.3		
W_{int}									31
WC1									18.4
WM1									34.1
Mandible									
Length[2]	98.7		91						
Dm1	16.1					16.5		13.6	
Dentition									
I1W			1.3						
I2W			1.2						
I3L			3.3						
C1L			7.0						
P2L		5.5	6.4	6					5.6
P2W		2.5		2.6					2.4
P3L	6.7		6.7	7.6					6.4
P3W	4.3			4.3					3.5
P4L	10.9	10.3	10.6	10.5					9.4
P4W	7.6	7.4		7.6					6.4
M1L	8.1	6.8	8	7.4	6.8				6.5
M1W	11.9	10.9		11.4	11				9.9
M2L	4.9	3.8		4.3	4.6				4.5
M2W	8	6.6		7.7	7.6				7.2
M3L		1.8							
M3W		2.9							
c1L		5.5	5.8						
c1W		3.4	4.1						
p1L		3.2				2.4			
p1W		1.8				2			
p2L	5.8	5	5.5			5.5			
p2W	2.6	2.4				2.6			
p3L	7	6.5	7.6			7.2			
p3W	3.5	3.2				3.1			
p4L	8.3	8.1	8.7			8.9			
p4W	4.3	3.9				3.8			
m1L	10.7	9.6				9.5			
m1W	6.5	5.7				6.2			
m2L	6.8	5.4	7					6.3	
m2W	4.9	4.1						4.1	
m3L								3.2	
m3W								2.6	

[1]Length from the anterior end of premaxilla to the posterior end of occipital condyle. [2]Length from the anterior end of c1 alveolus to the posterior end of mandibular condyle. Where applicable, dental measurements are the arithmetic means of the right and left teeth. **Abbreviations**: **Dm1**, depth below m1; **L**, anteroposterior length; **W**, labiolingual width; **WC1**, rostral width between labial margins of right and left C1; $\mathbf{W_{int}}$, interorbital width; **WM1**, palatal width between labial margins of right and left M1.

Table 1.2: Postcranial measurements (in mm) of *Lycophocyon hutchisoni*

Measurement	SDSNH 107446	SDSNH 107447
Caudal vertebra		
TL	35.2	
MW	8	
Humerus[1]		
HD		9.2
HDAB		21.1
HDAP		11.5
HEB		28.9
HL		105.2
Ulna[1]		
ULO	16.2	
UOD	10.0	
UPA	15.1	
Femur		
TL	134.4	
Astragalus		
PDL	20.4	
TW	13	
HW	10.4	
Phalanx		
TL	13.6	
MW	3.9	

[1]Measurements and abbreviations follow Meachen-Samuels and Van Valkenburgh (2009). **Abbreviations**: **HD**, minimum transverse diameter of diaphysis; **HDAB**, distal width of trochlea and capitulum combined; **HDAP**, anteroposterior depth of distal humerus; **HEB**, maximum mediolateral width of distal humerus; **HL**, maximum length; **HW**, mediolateral width of astragalar head; **MW**, transverse width at mid-length; **PDL**, proximodistal length of astragalus; **TL**, total length; **TW**, mediolateral width of astragalar trochlea; **ULO**, length of olecranon process; **UOD**, anteroposterior depth of olecranon process; **UPA**, anteroposterior depth measured from anconeal process and parallel to UOD.

Table 1.3: Dental ecomorphological statistics for *Lycophocyon hutchisoni* and comparative extant carnivorans

Taxon/Dietary group	N	LBW	$m1BS$	$m2S$	RBL	$RUGA$	$UM21$
Lycophocyon hutchisoni† (holotype)	1	8.73	0.074	0.058	0.682	1.068	0.638
Carnivores	46	7.71	0.101	0.052	0.66	0.807	0.327
Omnivores/Hard-object feeders	21	8.26	0.085	0.069	0.573	1.107	0.334
Insectivores	15	7.01	0.074	0.077	0.63	1.025	0.556

Data on extant carnivorans (mean values) from Friscia et al. (2007). **Abbreviations**: LBW, natural log-transformed body weight in grams; *m1BS*, length of the m1 trigonid relative to the length of dentary ("$M1BS$" of Friscia et al. (2007)); $m2S$, square-root transformed m2 occlusal area relative to the length of dentary ("$M2S$" of Friscia et al. (2007)); RBL, length of the m1 trigonid relative to the length of m1; $RUGA$, square-root transformed occlusal areas of M1 and M2 combined, relative to the length of P4; $UM21$, square-root transformed occlusal area of M2 relative to that of M1.

Table 1.4: Coefficients of variation in m1L of selected carnivorans

Taxon	N	Mean (mm)	CV (%)[1]	Source
Lyocphocyon hutchisoni†	9	9.88	6.3	This study
Canidae				
Hesperocyon gregarius†	27	9.35	4.8	This study
Urocyon cinereoargenteus	51	12.15	4.1	This study
Urocyon cinereoargenteus	81	12.41	5.2	Polly (1998)
Vulpes lagopus	58	13.8	4.5	Szuma (2008)
Vulpes vulpes	50	15.38	4.2	Gingerich and Winkler (1979)
Mustelidae				
Martes americana	121	8.84	7.2	Polly (1998)
Martes pennanti	29	12.89	7.3	This study
Felidae				
Felis sylvestris	21	8.18	7.4	Dayan et al. (2002)

[1]Adjusted for sample size (Haldane, 1955).

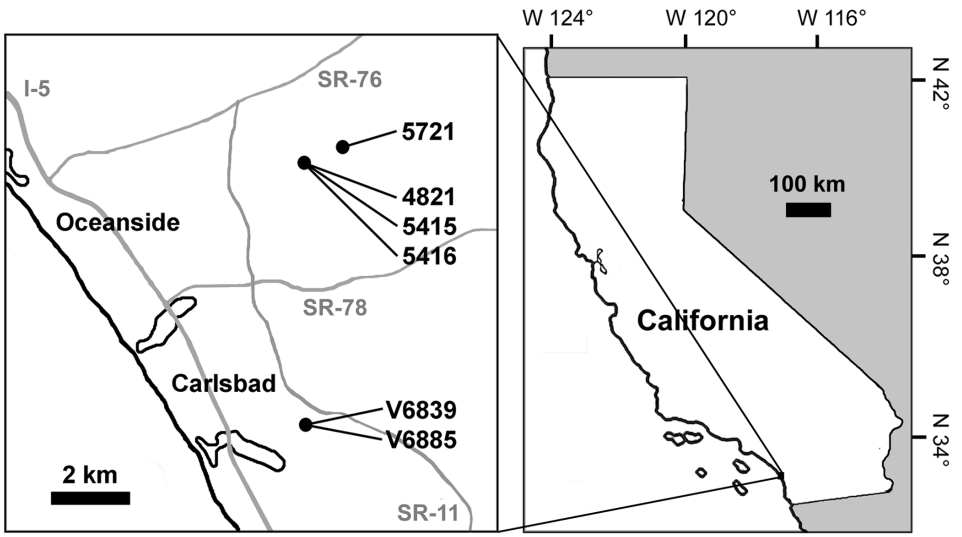

Figure 1.1: Map of localities that have yielded specimens of *Lycophocyon hutchisoni*. Localities with the prefix "V" are UCMP localities, and the rest are SDSNH localities.

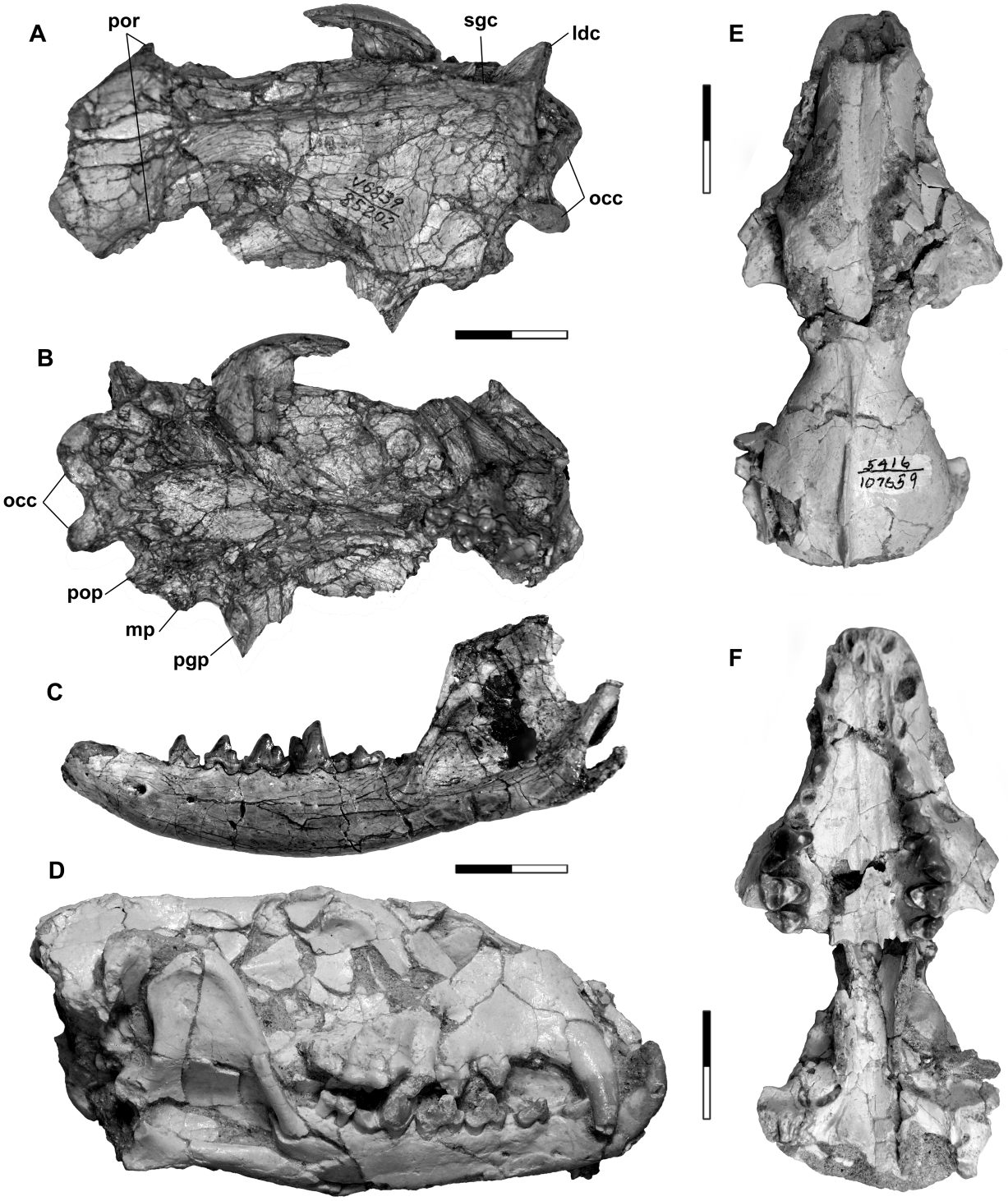

Figure 1.2: Crania and mandibles of *Lycophocyon hutchisoni*. Holotype UCMP 85202 (*A*-*C*), SDSNH 107442 (*D*), and SDSNH 107659 (*E, F*), showing cranium in dorsal (*A*) and ventral (*B*) views, left dentary (*C*), cranium articulated with mandible (*D*), and cranium in dorsal (*E*) and ventral (*F*) views. Scale bars equal 2 cm. **Abbreviations**: **ldc**, lambdoidal crest; **mp**, mastoid process; **occ**, occipital condyle; **pgp**, postglenoid process; **pop**, paroccipital process; **por**, postorbital process; **sgc**, sagittal crest.

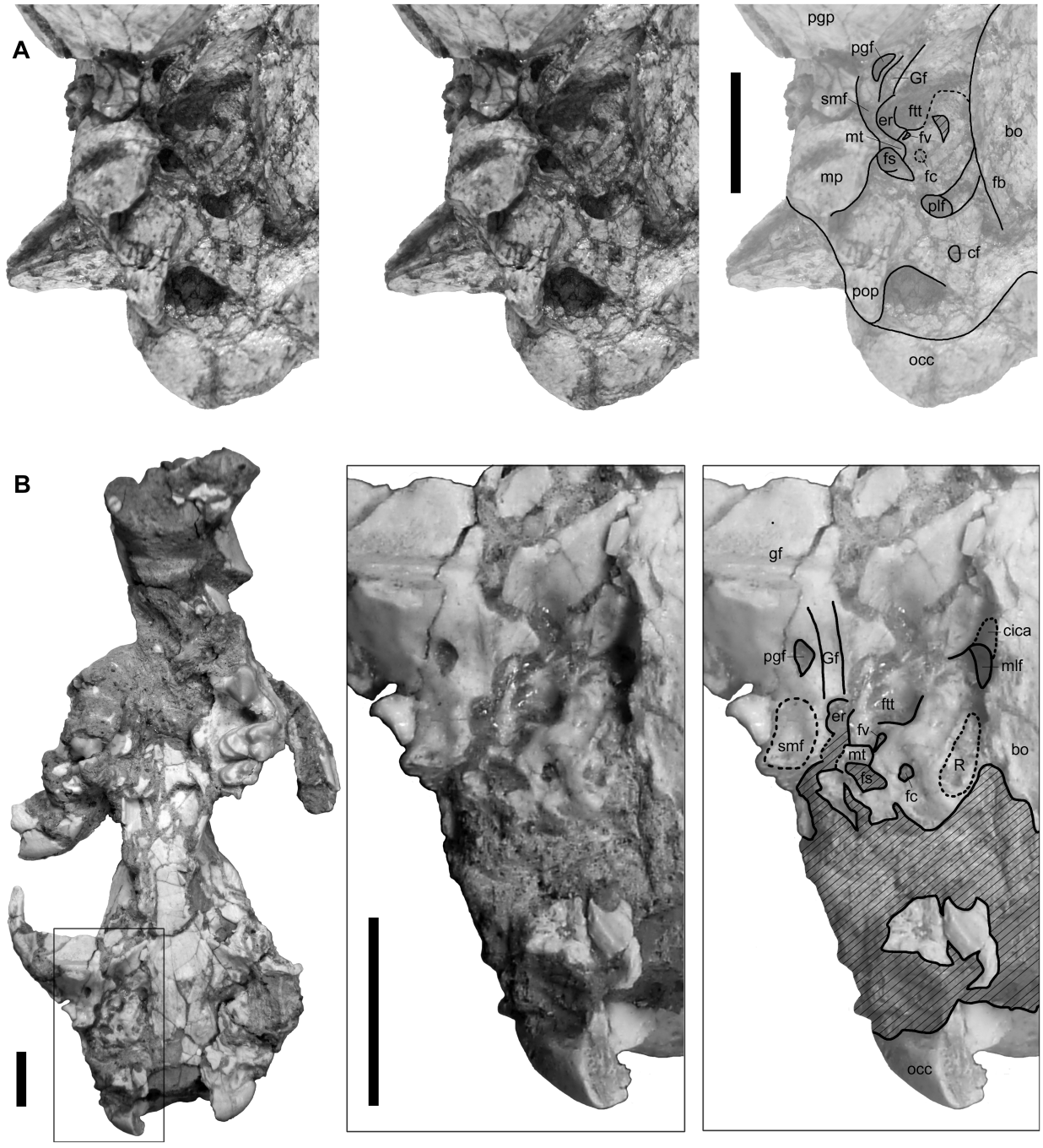

Figure 1.3: Right basicranial regions of *Lycophocyon hutchisoni*. Holotype UCMP 85202 (*A*, stereo pair) and SDSNH 107444 (*B*). **Abbreviations**: **bo**, basioccipital, **cf**, condyloid foramen; **cica**, canal for internal carotid artery; **er**, epitympanic recess; **fb**, lateral flange of basioccipital; **fc**, fenestra cochlea; **fs**, fossa for stapedius muscle; **ftt**, fossa for tensor tympani muscle; **fv**, fenestra vestibuli; **gf**, glenoid fossa; **Gf**, Glaserian fissure; **mlf**, middle lacerate foramen; **mp**, mastoid process; **mt**, mastoid tubercle; **occ**, occipital condyle; **pgf**, postglenoid foramen; **pgp**, postglenoid process; **plf**, posterior lacerate foramen; **pop**, paroccipital process; **R**, rugose area on petrosal promontorium; **smf**, suprameatal fossa. Scale bars equal 1 cm. Anterior to the top.

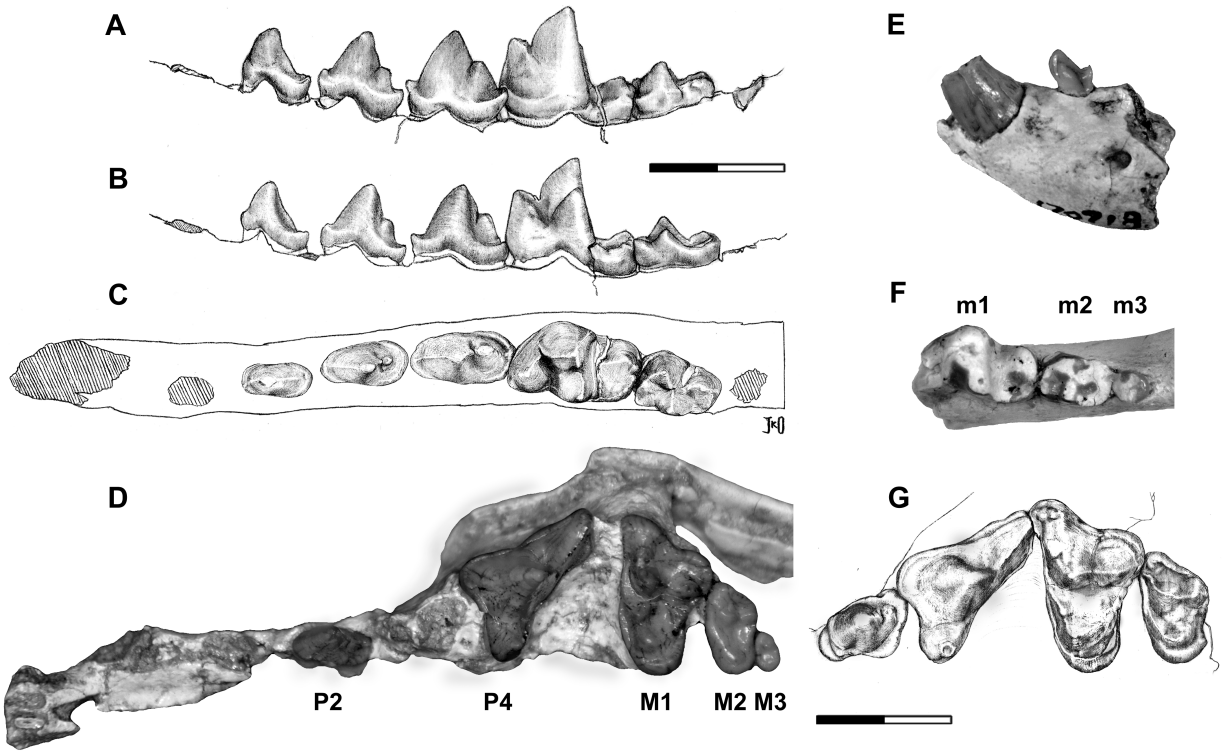

Figure 1.4: Dentition of *Lycophocyon hutchisoni*. Holotype UCMP 85202 (*A-C, G*), UCMP 170713 (*D, E*), and SDSNH 107658 (*F*), showing left p2-m2 in labial (*A*), lingual (*B*, inverted), and occlusal (*C*, inverted) views, right P2, P4-M3 in occlusal view (*D*, inverted), left c1 and p1 in labial view (*E*), right m1-m3 in occlusal view (*F*), and left P3-M2 in occlusal view (*G*). Scale bars equal 1 cm.

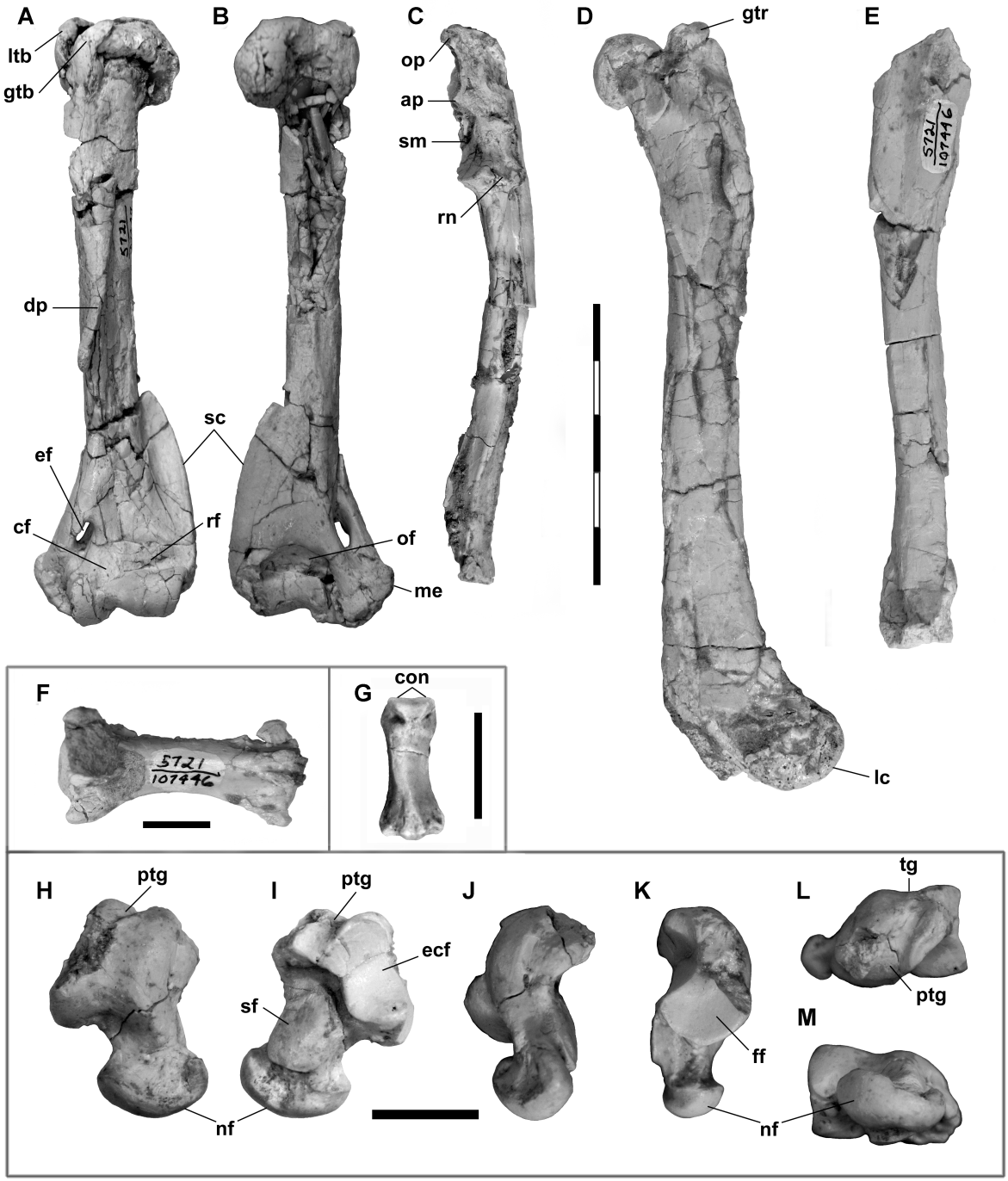

Figure 1.5: Postcrania of *Lycophocyon hutchisoni*. SDSNH 107447 (*A-B*) and SDSNH 107446 (*C-M*), showing left humerus in anterior (*A*) and posterior (*B*) views, left ulna in lateral view (*C*), left femur in lateral view (*D*), right tibia in medial view (*E*), caudal vertebra in dorsal view (*F*; proximal end to the left), middle phalanx in dorsal view (*G*; distal end to the top), and right astragalus in dorsal (*H*), ventral (*I*), medial (*J*), lateral (*K*), proximal (*L*), and distal (*M*) views. **Abbreviations**: **ap**, anconeal process; **cf**, coronoid fossa; **con**, phalangeal condyles; **dp**, deltopectoral crest; **ecf**, ectal facet; **ef**, entepicondylar foramen; **ff**, fibular facet; **gtb**, greater tuberosity; **gtr**, greater trochanter; **lc**, lateral condyle; **ltb**, lesser tuberosity; **me**, medial epicondyle; **nf**, navicular facet; **of**, olecranon fossa; **op**, olecranon process; **ptg**, plantar tendinal groove; **rf**, radial fossa; **rn**, radial notch; **sc**, supinator crest; **sf**, sustentacular facet; **sm**, semilunar notch; **tg**, trochlear groove. Scale bar equals 5 cm for *A-E*, 1cm for *F-M*.

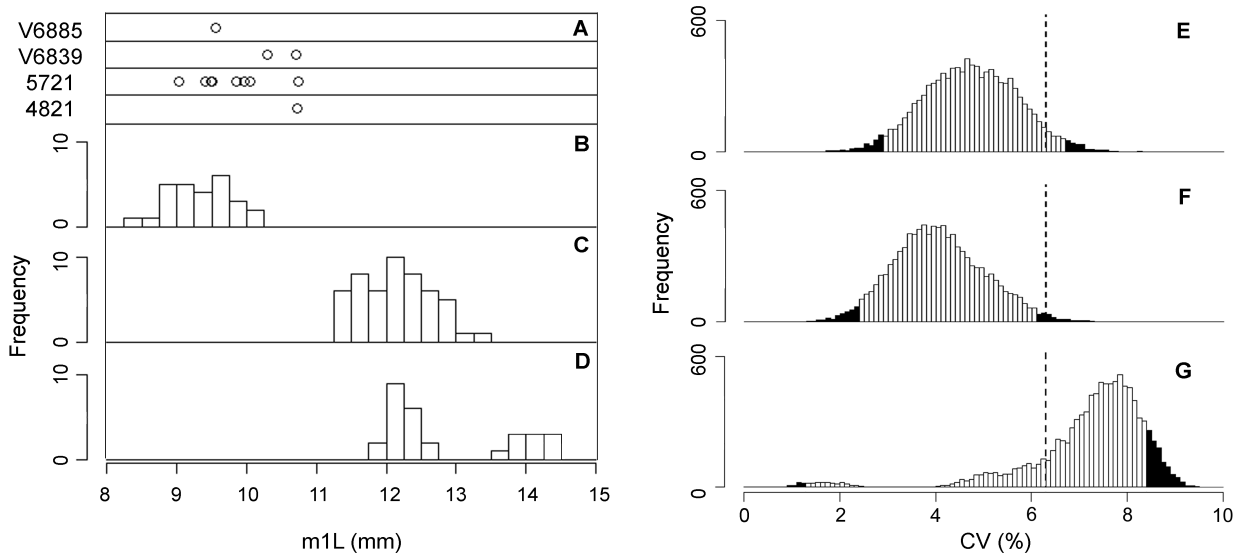

Figure 1.6: Comparisons of within-sample variation in m1L of *Lycophocyon hutchisoni* and selected carnivorans. Measurements of *L. hutchisoni* from UCMP localities V6839 (=RV6830) and V6885, and SDSNH localities 4821 and 5721 (*A*) are plotted on the same scale as the histograms for samples of *Hesperocyon gregarius* (*B*), *Urocyon cinereoargenteus townsendi* (*C*), and *Martes pennanti columbiana* (*D*). Histograms of CV values for 10,000 bootstrapped pseudo-replicates (each consisting of 9 specimens) of *H. gregarius* (*E*), *U. c. townsendi* (*F*), and *M. p. columbiana* (*G*) are compared to observed CV for 9 specimens of *L. hutchisoni* (6.3%; dashed lines); bootstrap-based CV values that fall outside the 95% confidence intervals are shaded in black.

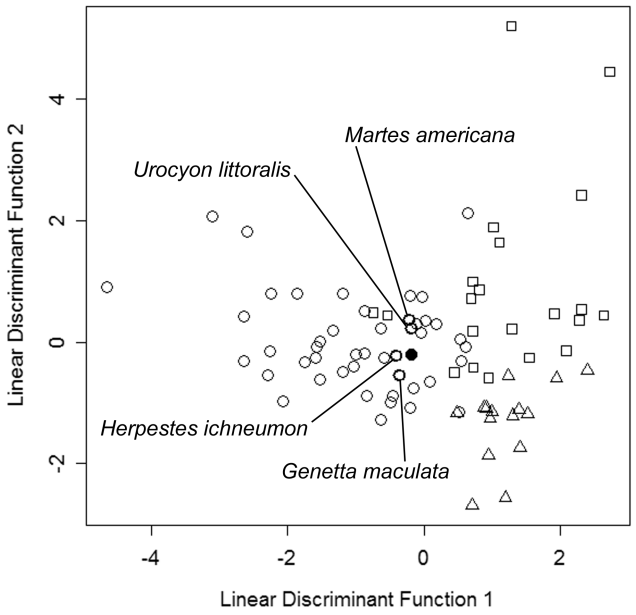

Figure 1.7: Discriminant function plot of extant carnivorans and *Lycophocyon hutchisoni*. Six ecomorphological variables were used to maximally separate three dietary groups: carnivores (open circles), omnivores/hard-object feeders (open squares), and insectivores (open triangles). Data for 82 extant taxa are from Friscia et al. (2007) and those for *L. hutchisoni* (filled circle) are based on holotype UCMP 85202. Four labeled taxa are the closest to *L. hutchisoni* in their posterior probabilities of dietary-group affiliations.

Figure 1.8: Cladistic position of *Lycophocyon hutchisoni*. *A*, strict consensus of 132 most-parsimonious trees (tree length = 488 steps, ensemble consistency index = 0.289, ensemble retention index = 0.667) obtained for 50 OTUs. *B*, strict consensus of 32 most-parsimonious trees (tree length = 280 steps, ensemble consistency index = 0.382, ensemble retention index = 0.664) obtained for 33 taxa that are known from the Paleogene. Numbers next to branches indicate Bremer support values followed by bootstrap support values. Bootstrap support values below 50% are denoted as "<".

Chapter 2

On the scaling of supraspecific extinction risk with body size: information from North American Oligo-Pleistocene mammals

Introduction

Understanding the link between ecological properties and extinction risk is critical to preservation of mammalian diversity. Considerable work has been from the perspectives of population biology and macroecology to identify intrinsic traits of individual organisms, emergent properties of species, and environmental factors that contribute to population declines and threaten species with extinction (McKinney, 1997; Cardillo et al., 2005, 2008; Burger and Ginzburg, 2009; Fritz et al., 2009; Ginzburg et al., 2010; Collen et al., 2011). Importantly, much of our current knowledge of extinction selectivity among mammals comes from population statuses of living species (e.g., Cardillo et al., 2008), late-Pleistocene megafaunal extinctions (e.g., Barnosky et al., 2004; Lyons et al., 2004; Koch and Barnosky, 2006; Carrasco et al., 2009; Polishchuk, 2010; Barnosky et al., 2011*a*), and Holocene extinctions on islands (e.g., Turvey and Fritz, 2011). In this context, the rich fossil record of Cenozoic mammals in North America is particularly valuable for investigating ecological patterns of extirpation at the continental scale in the absence of human impacts. In this paper, I use this record to examine the relationship between body size and extinction probability in terrestrial placental mammals, focusing on the durations of genera—many of which belong to extant families—that disappeared from the continent between 29 and 1 million years (Ma) ago.

Phylogenetic comparative analyses of living and recently-extinct mammalian species frequently show large body size to be significantly correlated with elevated risk of extinction under exploitative and environmental pressures, although the mechanistic explanation for this pattern lies variably in size-biased hunting practices by humans, low population densities, or life-history traits that characterize slow reproduction (Cardillo et al., 2005, 2008; Fritz et al., 2009). Similarly, the late-Quaternary collapses of megafaunas on multiple continents have been interpreted in terms of the vulnerability of populations (Johnson, 2002; Lyons et al., 2004; Polishchuk, 2010). It should be emphasized that these studies demonstrated large body size as a correlate of high probability of extinction and not necessarily its determinant. For example, Johnson (2002) showed through a comprehensive analysis of late-Quaternary extinctions that the negative effect of increase in body size was greater in clades (at the level of families and above) with low reproductive rates (quantified as the number of offspring produced by a female per year), and that a species with a slow reproductive rate is expected to have greater risk of extinction than another, larger species with a faster reproductive rate (but note that reproductive rates generally decrease with increasing body weight at the scale of present study; Fig. 2.1). Direct reconstruction of population densities and life-history traits is not feasible for most of the extinct mammals in the fossil record (but see Cartlett et al., 2010), but the strong correlations between these variables and body size (the latter of which can be estimated from skeletal measurements) makes it possible to assess their bearing on extinction selectivity, whether at the level of species or genera (Fig. 2.1). For example, if properties such as population density, home-range size, and reproductive rate were primary determinants of extinction probability, a negative correlation would be expected between estimated body weights and durations of fossil taxa. On the other hand, if large geographic ranges—which are correlated

with large body size (Fig. 2.1; see also Brown and Maurer, 1989)—directly buffer species and genera from extinction pressures (see e.g., Cardillo et al. (2008) on recent mammals and McKinney (1997) for a more general review), they may compensate for the greater risk for large mammals that stems from lower population densities and reproductive rates.

Testing for correlation between body weights and taxonomic durations, however, may be confounded by variations in the relationship between the two variables (weights and durations) in different ecological groups or in different times, reflecting variable causes of extinctions (Fig. 2.2). Indeed, previous paleontological studies have uncovered apparently discordant patterns of association between body size and extinction risk in mammals, possibly because of differences in their taxonomic and spatio-temporal scopes as well as analytical methods (Table 2.1). As explained below (see Materials and Methods), these issues were partly addressed in this study by partitioning the data set into major trophic groups and temporal subsets, and by conducting multiple linear regression analyses where applicable.

From the analytical standpoint, it was more feasible in the present study to work at the level of genera rather than species because (1) the taxonomy of fossil mammalian species is considerably less stable (Alroy, 2003), (2) the dearth of cladistic hypotheses makes it practically impossible to conduct phylogenetic comparative analyses of fossil species at the scale of this study, (3) the specific identities of fossils are often indeterminate with available material and existing taxonomic knowledge, the consequences of which are many fossil species that are known from too few occurrences for robust statistical analyses (see e.g., Liow et al. (2008) on a similar problem with the European record of fossil mammals), and (4) in much of the North American Cenozoic fossil record, the temporal resolution based on the traditional mammalian biochronology is roughly equivalent to, or substantially coarser than, the median species duration of 1.5 million years (Alroy, 1996). Furthermore, the correspondence between morphologically-recognized fossil species and true species as segments of independent evolutionary lineages (cf. de Queiroz, 2007) is often questionable at the scale of this study, such that analyses of fossil species could lead to misleading comparisons with neontological studies at the species level (see Carrasco, in press). It is acknowledged that, within the deep-historical context of present study, at least some (and possibly many) of the genera are inevitably paraphyletic. For the present study, however, the key question is not whether the genera are monophyletic but whether they are non-polyphyletic so as to represent phylogenetically continuous sets of lineage segments. This question cannot be directly answered for the fossil genera unless true species can be identified as such, but it is noteworthy that molecular phylogenetic data generally support non-polyphyly of morphologically-diagnosed genera among extant mammals (Jablonski and Finarelli, 2009).

In fact, one of the strengths of the fossil record is that it offers macroevolutionary insights into biological patterns of extinction above the level of species, which are difficult to discern from the limited historical data for living and recently-extinct mammals. The question of how patterns and processes of extinction scale up from the level of species to higher taxa has largely eluded neontological studies of extinction selectivity but is important for predicting losses of ecological types and clusters of unique evolutionary history (Erwin, 2008). Therefore, the present study aims to address, albeit indirectly, whether extinctions of genera (a) can be adequately characterized as phenomena resulting from additive losses of their constituent species, or (b) are not necessarily predictable from information on individuals species alone, as might be expected from distinct geographic-range dynamics at specific and generic levels (Hadly et al., 2009) and disproportionately high extinction risk among species-poor genera of birds and mammals (Russell et al., 1998).

The geographic scope of the study was limited to the contiguous 48 states of the United States because adequate data are only available for that region. In fact, the vast majority of the fossil-bearing localities considered here are in the western United States and the Gulf Coast region (Fig. 2.3). As such, the findings of this study may be conservatively interpreted as pertaining to inter-regional extirpations rather than true (by definition, global) extinctions. However, considering that many extant genera have geographic ranges within—and smaller than—this area, it seems plausible that many of the extirpations at this spatial scale in fact represented global extinctions.

In essence, the objective of this study is to determine, within the constraints of fossil data, whether the kinds of strong relationships observed between body size and ecological and life-history parameters in mammalian species (Fig. 2.1) translate into similarly clear-cut patterns of survival of genus-level morphotypes in macroevolutionary time.

Materials and Methods

Unless otherwise noted, all computations were performed in the R programming environment (R Developement Core Team, 2009).

Taxonomic Occurrence Data

North American fossil occurrence data from the Oligocene through the present (34-0 million years ago) were compiled from the MIOMAP and FAUNMAP databases (Carrasco et al., 2005; Graham and Lundelius, 2010). The raw data sets were downloaded from the NEOMAP web portal (www.ucmp.berkeley.edu/neomap/) on March 6, 2012. Because the geographic coverage of MIOMAP is restricted to the contiguous 48 states of the United States, FAUNMAP data from outside this area (i.e., occurrence records in Alaska and Canada) were excluded from the analyses. In addition, the following elements of the raw data set were removed: (1) the genus *Homo*; (2) primarily volant and marine-aquatic groups, namely, Chiroptera, Cetacea, Sirenia, Desmostylia, and pinnipedimorph carnivorans); (3) taxonomic occurrences of unknown or uncertain generic identities (noted as "aff.", "cf.", "nr", or "?" in the databases); (4) generic occurrences from localities that lack maximum or minimum age estimates. Occurrences of multiple congeneric species at a given locality were counted as a single generic occurrence. Thus, 48,947 occurrences of 675 genera from 9,690 localities formed the basis of present study, and the sampling-adjusted durations (see below) of 221 of these genera (represented by 8,450 occurrences of at least 621 species at 2,733 localities) were included in comparative analyses. Of these, 80 genera are each potentially (i.e., when unidentified species are disregarded) represented in the data set by a single fossil species. The classifications of all extinct species in the data set were cross-checked with—and, when necessary, modified after—those of Janis et al. (1998, 2008). The full data set is available as Supporting Material (Appendix S2.1).

Size data

Measurements of the anteroposterior length and mediolateral width of the lower first molar (m1) for 935 species were obtained from the Paleobiology Database (http://www.pbdb.org) on January

6, 2012. The generic taxonomy of these species was standardized with that for the combined MIOMAP/FAUNMAP data set.

Determination of Observed Temporal Ranges

Each locality and all generic occurrences from that locality are assigned a range of possible ages that were obtained by radioisotopic, magnetostratigraphic, or, most frequently, biochronologic dating. For the purpose of present study, the following assumptions were made with regard to locality ages: (1) The true age of a locality is geologically instantaneous (or practically so relative to durations of genera, which are generally on the order of 10^6 years or greater in the data set analyzed here); (2) The uncertainty in the age of a locality is sufficiently captured by its age range reported in the MIOMAP and FAUNMAP databases; (3) The age of each locality i is assumed to have a continuous uniform distribution with the probability density function (Fig. 2.4A):

$$f_i(t) = \begin{cases} \dfrac{1}{T_{max,i} - T_{min,i}} & \text{if } T_{max,i} > t > T_{min,i} \\ 0 & \text{otherwise} \end{cases} \qquad (1),$$

where $T_{min,i}$ and $T_{max,i}$ are the minimum and maximum ages for the locality, respectively, and the unit of time is million years ago (e.g., $t = 20$ is equivalent to 20 Ma ago; note that, following the paleontological convention, the time axis is reversed such that the value of t decreases as time progresses, and $t = -\infty$ stands for time at ∞). Then, for each taxon, the joint probability of at least one occurrence across all localities $i = 1, \ldots, n$ (only the localities that have yielded the taxon are considered) by time t is:

$$p(t) = 1 - \prod_{i=1}^{n} \int_{t}^{-\infty} f_i(t)\mathrm{d}t \qquad (2).$$

The median-unbiased estimate for the first appearance date $t = T_{FAD}$ of the taxon is the point in time at which the probability $p(t)$ reaches 0.5. Thus $\hat{T}_{FAD}$ was obtained by solving (Fig. 2.4B):

$$p(\hat{T}_{FAD}) = 1 - \prod_{i=1}^{n} \int_{\hat{T}_{FAD}}^{-\infty} f_i(t)\mathrm{d}t = 0.5 \qquad (3).$$

Similarly, the last appearance date $t = T_{LAD}$ for each taxon was estimated by solving:

$$q(\hat{T}_{LAD}) = \prod_{i=1}^{n} \int_{\infty}^{\hat{T}_{LAD}} f_i(t)\mathrm{d}t = 0.5 \qquad (4),$$

which represents the probability of the taxon's last occurrence before $\hat{T}_{FAD}$.

In the special cases in which (1) a taxon is known from only one locality, or (2) there exists a locality age range whose midpoint predates or postdates the age ranges of all other localities from which the taxon is known, the estimate for the first or last appearance date is simply the midpoint of this locality age range. For the genera that are known from multiple localities, the above equations were numerically solved with the precision of 2.8×10^{-7} to 7.3×10^{-2} million years, depending on the genus.

The first and last appearance dates of a taxon thus obtained are merely the age estimates for the observed first and last appearances. Realistically, the sampling of taxonomic occurrences in the fossil record is expected to be incomplete, which makes the observed temporal range from T_{FAD} to T_{LAD} a truncated subset of the taxon's true temporal range. Further, it is likely that taxonomic ranges are differentially truncated because of ecological and taphonomic variations, as discussed below.

Adjustment of Temporal Ranges for Sampling Bias

Confidence-interval Method. Unless the sampling of taxonomic occurrences is complete, the observed duration of a taxon in the fossil record underestimates its true duration in geologic time. Although the present study is primarily concerned with relative durations of genera across a body-weight spectrum, it is important to derive sampling-adjusted durations because (1) incomplete sampling disproportionately shortens truly-short temporal ranges (Fig. 2.5; see also Foote and Raup, 1996), and (2) fossil recovery potential (sensu Marshall, 2010) may vary substantially across taxa and over time at the scale of millions of years. My approach therefore follows Marshall's (1997; 2010) generalized confidence-interval method, first deriving fossil recovery potential functions and then using this information to calculate the 50% confidence interval for the temporal range of each genus, extending the observed first and last appearance dates.

Of particular concern here is the possible body-size bias in fossil recovery potential. Such a bias may stem from different methods that are employed to collect large versus small mammalian fossils, and the relative ease of finding large mammalian fossils in the field. It should also be noted that intensive collecting of small mammalian fossils using screen-washing techniques commenced relatively late in the history of North American vertebrate paleontology with the work of Claude W. Hibbard in the 1930s (McKenna et al., 1994). Based on these field-practical and historical factors, the Cenozoic fossil record of small mammals may be suspected to be less complete than that of large mammals. To date, however, such a bias has not been quantitatively demonstrated at the scale of present study, and previous studies of diversity dynamics in the mammalian fossil record have generally avoided these problems by conducting separate analyses for large and small mammals (e.g., Barry et al., 2002) or by focusing on large mammals only (e.g., Jernvall and Fortelius, 2004; Carotenuto et al., 2010; Raia et al., 2011). I addressed this issue instead by quantifying the per-million-year sampling probability separately for classes of small (estimated body weight of less than 1,000 g) and large ($\geq 1,000$ g) taxa (see the next section on body-weight estimation). Some of the genera for which m1 measurements were not available were assigned to one of the two classes based on their taxonomic affiliations: specifically, all dipodids, heteromyids, murids, lagomorphs, and lipotyphlans were placed in the small-size class, and all non-mustelidan carnivoramorphans, artiodactyls, perissodactyls, xenarthrans, and proboscideans were placed in the large-size class. A few canids in the data set have estimated body weights of less than 1,000 g, but those lacking m1 measurements, namely *Caedocyon* and *Epicyon*, can securely be placed in the large-size class based on other skeletal measurements reported by Wang (1994) and Wang, X. and Tedford, R. H. and Taylor, B. E. (1999). In addition, the following genera were assigned to the large-size class based on the size ranges of their extant species: *Enhydra*, *Lutra*, *Nasua*, *Hydrochoerus*, and *Myocastor*. Other genera lacking body-weight estimates (e.g., some castorid rodents) were excluded from the present study. Separate estimation of range-through sampling probability for finer categories (e.g., herbivores and carnivores within large mammals) would be ideal, but further subdivision of the data set would substantially increase the uncertainties in the estimates.

The fossil recovery potential was approximated based on the range-through sampling probability R_j (cf. Paul, 1982; Foote, 2000, and references therein). The latter was calculated for 1 million-year intervals $j = 1, \ldots, m$ as:

$$R_j = N_{j,rts}/N_{j,rt} \qquad (5),$$

where $N_{j,rt}$ is the number of genera that range all the way through the given time interval j and

$N_{j,rts}$ is their subset that were actually sampled. Thus, occurrences of a taxon in the 1 million-year intervals that contain the taxon's first and last appearances are not counted; consequently, those genera whose observed temporal ranges lie within two consecutive time intervals are not informative for the calculation of R_j and are therefore excluded from this step. In the cases of genera that are extant in the contiguous 48 states of the United States (e.g., *Sorex* but not *Alopex*), all of the complete 1 million-year intervals between their observed fist appearance dates and the present were considered as intervals through which they ranged, regardless of their last appearance dates in the fossil record. Because the sampling probability R_j concerns only those genera that are assumed to have been present, its estimation should not be biased by the fact that the true range endpoints are unknown at this stage.

For each 1 million-year interval, the value of R_j estimates the probability of at least one occurrence of a taxon being ultimately reported in the MIOMAP or FAUNMAP database, assuming the taxon's existence throughout the interval (cf. Foote, 2000). This probability likely reflects diverse paleontological factors such as taxonomic abundance, paleoenvironmental potentials for fossil preservation, sizes and geographic distributions of accessible outcrops, fossil collection methods, and intensities of collection and reporting efforts. The calculation of range-through sampling probabilities assumes the continuous presence of each genus in the continental United States between its first and last appearances there. Although major shifts and contractions in geographic ranges could cause temporary disappearances of genera from the study area, this is (1) difficult to demonstrate with incomplete data and (2) unlikely if the typically inter-regional distributions of extant mammalian genera in North America also characterized the fossil genera considered here (see also Hadly et al. (2009) on the stability of genus-level geographic ranges in North America through the last glacial-interglacial transition). Indeed, the faunal inertia at the million-year time scale that renders the framework of North American Land Mammal Ages biologically meaningful also supports the above assumption, if only in the most general sense.

As mentioned above, locality ages are known with varying levels of uncertainty, affecting the estimation of range-through sampling probability. To take these uncertainties into account, 1,000 sets of instantaneous ages for 9,685 localities were drawn from the set of probability density functions for these localities (eq. 1). Then, for each set of locality ages, the sampling probability through time was estimated separately for large and small mammals. For each 1 million-year interval, the median of 1,000 estimates was selected for use in the calculation of sampling-adjusted temporal-range endpoints, as explained below. In addition, the bootstrap estimate of bias-corrected 95% confidence interval (cf. Efron, 1981) was calculated separately for large and small mammals in each time interval, as well as for the difference in sampling probability between the two size classes to test its statistical significance.

Assuming that taxonomic occurrences (i.e., instances of positive sampling) within each 1 million-year interval follow the Poisson process, the discrete range-through sampling probability R_j described above can be converted to a continuous-time function (Foote, 2000):

$$r_j(t) = 1 - e^{-\lambda_j(T_j - t)} \qquad (6),$$

such that $R_j = r_j(t = T_j - 1)$, where λ_j is the expected number of occurrences of a taxon per million years ("preservation rate" of Foote (2000)), and T_j is the age of the beginning of interval j. Equation 6 is a cumulative distribution function, so the corresponding probability density function—which is adopted here as the fossil recovery potential function (cf. Marshall, 2010)—can be expressed as:

$$g_j(t) = \frac{\mathrm{d}}{\mathrm{d}t} r_j(t) = \lambda_j e^{-\lambda_j (T_j - t)} \qquad (7)$$

within a time interval j, where $\lambda_j = -\ln(1 - R_j)$. Graphically, $r_j(t)$ corresponds to the area under the curve defined by the function $g_j(t)$ (Fig. 2.6). By extension, the sampling probability $r(t)$ across multiple time intervals can be obtained from the function $g(t)$ that combines $g_j(t)$ for different intervals.

Using the generalized confidence-interval method of Marshall (1997, 2010), the amount of temporal extension x for an observed range endpoint (in the present study, the first or last appearance date of a genus) for the fossil recovery potential function $g(t)$, confidence level C, and number of fossil horizons H can be derived as:

$$x^* = r^*[(1 - C)^{\frac{1}{H-1}} - 1] \qquad (8),$$

where $r^* = \int_{T_{FAD}}^{T_{LAD}} g(t)\mathrm{d}t$ and $x^* = x^*_{FAD} = \int_{T_{FAD}+x_{FAD}}^{T_{FAD}} g(t)\mathrm{d}t$ for the extension of first appearance date or $x^* = x^*_{LAD} = \int_{T_{LAD}}^{T_{LAD}-x_{LAD}} g(t)\mathrm{d}t$ for the extension of last appearance date. Note that, for the extension of first appearance date backwards in time, both the fossil recovery potential function and the corresponding cumulative distribution function must be inverted along the time axis, such that $g_j(t) = \lambda_j e^{-\lambda_j (t-(T_j-1))}$ and $r_j(t) = 1 - e^{-\lambda_j (t-(T_j-1))}$ (Fig. 2.6). For joint estimation of sampling-adjusted range endpoints, Equation 8 can be modified (after Strauss and Sadler (1989)) as:

$$C = 1 - 2\left(\frac{r^*}{r^* + x^*}\right)^{H-1} + \left(\frac{r^*}{r^* + 2x^*}\right)^{H-1} \qquad (9),$$

where $x^* = x^*_{FAD} = x^*_{LAD}$ but x_{FAD} does not necessarily equal x_{LAD} (see Fig. 2.6 for illustration).

The sampling-adjusted duration of a genus is here defined as the length of time encompassed by the median-unbiased estimates for its temporal-range endpoints. These endpoints, henceforth denoted as T_{FAD50} and T_{LAD50}, correspond to the 50% confidence interval for the temporal range of the genus and are obtained by numerically solving:

$$\left(\frac{\int_{T_{FAD}}^{T_{LAD}} g(t)\mathrm{d}t}{\int_{T_{FAD}+x_{FAD}}^{T_{LAD}} g(t)\mathrm{d}t}\right)^{H-1} + \left(\frac{\int_{T_{FAD}}^{T_{LAD}} g(t)\mathrm{d}t}{\int_{T_{FAD}}^{T_{LAD}-x_{LAD}} g(t)\mathrm{d}t}\right)^{H-1} - \left(\frac{\int_{T_{FAD}}^{T_{LAD}} g(t)\mathrm{d}t}{\int_{T_{FAD}+x_{FAD}}^{T_{LAD}-x_{LAD}} g(t)\mathrm{d}t}\right)^{H-1}$$

$$= 1 - C = 0.5 \qquad (10)$$

for the values of x_{FAD} and x_{LAD} that satisfy $\int_{T_{FAD}+x_{FAD}}^{T_{LAD}} g(t)\mathrm{d}t = \int_{T_{FAD}}^{T_{LAD}-x_{LAD}} g(t)\mathrm{d}t$. The precision of numerical solution was set to 0.01 million years. Note that this method is not applicable to genera that are known from a single occurrence (which makes the area $r* = 0$). Sampling-adjusted ranges were thus calculated for 221 genera that are each represented by multiple occurrences, and for which body size data were available.

In reality, fossil recovery potential may vary significantly over time within each 1 million-year bin or across genera within each size class. Analytical compromises had to be made, however, between estimating the temporal and cross-taxonomic variations in sampling probability and attaining reasonable precision for these estimates because the latter is limited by the amount of taxonomic occurrence data. Indeed, the data at hand are insufficient for the assessment of temporal

fluctuations in sampling probability for individual genera without making major assumptions such as constancy of non-taxon-specific components of sampling probability through time, which turns out to be untenable (see Results below).

Nevertheless, the effect of potential fluctuations in fossil recovery potential of a genus during its existence is worth consideration. For examaple, it is conceivable that the fossil recovery potential of a taxon starts low at its first appearance, rises subsequently, and declines toward its last appearance, reflecting the rise and fall in its abundance, and in a manner that is significant at the 1 million-year time scale of this study (cf. Alroy (1996) on sampling gaps, Jernvall and Fortelius (2004) and Carotenuto et al. (2010) on site occupancy; but see Vrba and DeGusta (2004) and Jones et al. (2005) on the dynamics of mammalian geographic ranges that suggest alternative patterns of taxonomic rise and fall, at least at the species level). If this were true—that is, if taxa persisted outside their observed temporal ranges at much lower levels of abundance compared to within their observed ranges—the range extension as described above could be based on values of fossil recovery potential that are too high and, consequently, underestimates true durations. Conservatively, then, the duration estimates analyzed in this study should be regarded simply as sampling-adjusted durations rather than estimates of true durations. There is, however, no obvious reason to suspect that such underestimation of true durations would be body-size biased.

Body-weight Estimation

Estimates of adult body weights (in natural-log scale) for 932 species belonging to 405 out of 674 fossil species in the data set were obtained based on measurements of the occlusal surface areas of their lower first molars (m1), which were calculated as the products of anteroposterior length and labiolingual width, and Legendre's (1986) allometric equations derived for extant mammals. Proboscideans were excluded from the analysis because estimation of their body weights based on dental elements would be problematic. For some mammalian groups, allometric equations for other skeletal elements (or combinations of multiple skeletal elements) have been derived that have higher predictive precisions, but here I use only the m1 data to maximize the taxonomic breadth of analysis and because accurate prediction of relative rather than absolute body weights is of primary importance for the purpose of analysis. For example, when the body-weight estimate for one genus is based on its m1 size while that of another genus is based on its humeral cross-sectional area, the estimated relative weights of the two genera can be distorted because of systematic differences in parameter (slope and intercept) values between the two allometric equations used.

Although the analysis is conducted at the genus level, simply using the average (geometric mean of untransformed weights or, equivalently, arithmetic mean of natural-log transformed weights) estimated body weight of multiple species in each genus would ignore interspecific variation and may introduce additional inaccuracy to the analysis. Inaccuracy in body-weight estimates for the genera may come from (1) measurement errors, (2) measured species not yielding average generic body weight that is representative of the genus, (3) measured specimen not yielding average specific body weight that is representative of the species (because of biased representation of ages, sexes, or populations), and (4) allometric equations that: do not take into account phylogeny; are based on poor predictors of body weights; or suffer from any of the above-listed problems with extant species data. Because original measurements used to derive allometric equations are rarely published, it was not possible to directly assess the extent of these sources of errors at the scale of present study. With regard to the 244 genera in the data set that are represented by multiple

species with body-weight estimates, the median standard deviation of weights in the natural-log scale is 0.388 units; in the non-logarithmic scale, this would correspond to a 95% confidence interval bounded by 46.7 and 214% of the geometric mean weight (in grams) for a genus, assuming a log-normal distribution of body weights among congeneric species.

Comparative Method

Phylogenetic Data. The cladistic relationships among extant mammalian clades follow the supertree of Bininda-Emonds et al. (2007, 2008). The cladistic relationships among fossil genera were primarily adopted from the compilations by Janis et al. (1998, 2008). It must be emphasized that many of the cladograms used here are hypotheses proposed by taxonomic experts and are not directly supported by numerical (e.g., parsimony) analyses. For some groups, cladograms presented in Janis et al. (1998, 2008) were supplanted by more recent ones of comparable or greater taxonomic scope based on quantitative analyses (e.g., Hopkins (2008*a*) for Aplodontidae). Recent taxonomic changes that were not incorporated into Janis et al. (2008) were followed here except when the generic identity of a given taxon was uncertain (see Appendix 2.1 for details).

The 50% confidence-interval estimates for the first appearance dates were adopted as the ages of terminal nodes on the composite phylogeny (Fig. 2.7). In addition, the ages of 20 internal nodes corresponding to divergence points at and above the level of families were fixed using molecular divergence-date estimates by Bininda-Emonds et al. (2007, 2008). The ages of remaining internal nodes and their associated branch lengths were randomly selected within these constraints, and this process was iterated to produce 1,000 sets of branch lengths for the entire tree to simulate a variety of phylogenetic scenarios with the same tree topology.

Analytical Procedure. To accommodate the possible phylogenetic correlations among generic durations (or, more precisely, correlations that remain in the residual error of the regression model described below), comparative analyses were conducted within the framework of generalized least-squares regression. The basic linear model considered here has the form of:

$$D_i = \beta W_i + \varepsilon_i,$$

where D_i and W_i are the natural-log transformed duration and body weight of taxon i, and ε_i represents the residual error. The phylogenetic structure of the data, if present, is incorporated into the regression analysis through the specification of the residual variance-covariance matrix, in which the diagonal elements are:

$$\mathbf{var}(\varepsilon)_i = t_i \sigma^2,$$

and the off-diagonal elements are:

$$\mathbf{cov}(\varepsilon)_{ij} = \lambda t_{ij} \sigma^2,$$

where t_i is the branch length from the root of phylogeny to the terminal node represented by the taxon i, t_{ij} is the branch length on the phylogeny that is shared between a pair of taxa i and j, σ^2 is the variance expected from the constant-variance random-walk model of trait evolution for a unit time, and λ is a parameter that measures the strength of phylogenetic signal relative to the expectation from the random-walk model; thus, $\lambda = 0$ would indicate no phylogenetic structure

in the residual error, and $0 < \lambda < 1$ would correspond to a mode of constrained evolution (Pagel, 1999; Freckleton et al., 2002). The regression slope β and the parameter λ were simultaneously estimated (the latter to the nearest 0.005) by the maximum-likelihood method (cf. Revell, 2010), using the functions *corPagel*, *gls*, and *Gls* of packages *ape* (Paradis et al., 2012), *nlme* (Pinheiro et al., 2012), and *rms* (Harrell, 2012) for the R programming environment (R Developement Core Team, 2009).

In the cases where the maximum-likelihood estimates for λ are invariably zero for all 1,000 sets of simulated branch lengths, ordinary least-squares regression analyses were conducted, in which all diagonal elements of the residual variance-covariance matrix were identical (i.e., equal variances) and all off-diagonal elements were set to zero (because the residuals are not phylogenetically correlated), representing a non-evolutionary model for generic durations.

Analysis was first conducted with the above regression model for the set of 221 genera for which both sampling-adjusted durations and body weights are available and its five temporal and six ecological subsets. The temporal subsets are reverse cohorts that are broadly united by the timing of their extinction (or, more conservatively, extirpation in the North American regions covered by the data set), consisting of those genera whose sampling-adjusted last appearance dates fall between (1) 29 and 15 Ma ago, (2) 15 and 12 Ma ago, (3) 12 and 9 Ma ago, (4) 9 and 5 Ma ago, and (5) 5 and 1 Ma ago. The ecological subsets are as follows: (1) herbivores, consisting of rodents, lagomorphs, artiodactyls, and perissodactyls; (2) ungulates, consisting of artiodactyls and perissodactyls as large herbivores; (3) glires, consisting of rodents and lagomorphs as small herbivores; (4) secondary consumers, consisting of lipotyphlans and carnivorans; (5) carnivorans as generally faunivorous secondary consumers; and (6) lipotyphlans as small secondary consumers that generally feed on invertebrates. These categories are taxonomically delineated and are each diverse in ecological attributes; nevertheless, they represent broadly coherent trophic groups for which sufficient data are available for the present study.

Finally, a more direct assessment of the link between the tempos of life history and taxonomic durations was made by repeating the above analyses with expected inter-birth interval lengths (in natural-log scale) as the predictive variable. This variable represents the time between successive births given by the same female and has been shown to capture an important component of the multidimensional fast-slow continuum of life history in extant mammals (Bielby et al., 2007). Using the data from the PanTHERIA data base (Jones et al., 2009), least-squares regression equations describing the relationship between body weight and inter-birth interval length were derived separately for a group of generally small mammals (rodents, lagomorphs, and lipotyphlans), ungulates (artiodactyls and perissodactyls), and carnivorans (Fig. 2.8). These equations were then used to calculate the inter-birth interval lengths of the fossil genera expected from their estimated body weights (app. 2.2). The use of same predictive equation for lipotyphlans, lagomorphs, and rodents was perhaps not ideal but necessitated by the scarcity of data for lipotyphlans and lagomorphs. Note that, if a single predictive equation were used to estimate the inter-birth interval lengths of all fossil genera, the results of regression analyses would be identical to those of the previous analyses for weights and durations except for the linearly-transformed predictive variable. Instead, by using separate predictive equations for different groups of mammals, some of the essential variations in the scaling of the tempo of life history across the body-size axis were taken into account (Fig. 2.8).

Results

Body-size Bias in Sampling Probability

Taking into account uncertainties in locality ages, significantly lower range-through sampling probability was observed for small mammals compared to large mammals during much of the Miocene Epoch (Fig. 2.9A-C). Between 20 Ma and 5 Ma, the median per-million-year sampling probability for small mammals was lower than that for large mammals by 2.3 to 25.9%, with the mean difference of 13.5%. On the other hand, the post-Miocene (5-1 Ma) sampling probability was roughly comparable between the two groups. The values for the latest Oligocene to the earliest Miocene are difficult to compare mainly because of the poor fossil record for this time period (cf. Alroy, 2009). In no time interval did the sampling probability for small mammals significantly exceed that for large mammals. The adjustment of observed durations to correct for these sampling disparities resulted in the median extension of observed temporal ranges by 17.1% or 0.79 Ma for small mammals and 6.4% or 0.34 Ma for large mammals (Figs. 2.7, 2.9D-E).

Correlation between Body Weights and Sampling-adjusted Generic Durations

The maximum-likelihood estimates for λ are generally low (Table 2.2, Fig. 2.10). The value of $\lambda_{ML} = 0$ was obtained for the reverse cohort of genera with sampling-adjusted last appearance dates of 29 to 15 Ma ago, secondary consumers, and carnivorans across all 1,000 sets of partly simulated branch lengths.

Significant regression slopes (at the significance level of $\alpha = 0.05$) were obtained for secondary consumers (from ordinary least-squares regression as well as generalized least-squares regression for all 1,000 sets of branch lengths) and for 26.3% of 1,000 sets of branch lengths generated for lipotyphlans (Table 2.2, Figs. 2.12, 2.14). The slopes for all other groups, including the full set of 221 genera, were not significantly different from zero for all sets of branch lengths (Table 2.2, Fig. 2.12). While the correlation between estimated body weights and sampling-adjusted durations within carnivorans is non-significant, their durations were found to be significantly shorter than those of lipotyphlans (Mann-Whitney *U* test, *P*-value = 0.023) and "ungulates" (*P*-value = 0.017). When the comparison was limited to the 41 large carnivoran genera with estimated body weights of greater than 7 kg, their durations were still found to be significantly shorter (*P*-value = 0.012) than those of ungulates.

A preliminary examination using local regression (Fig. 2.16A) suggested a possible shift in the relationship between estimated body weights and durations of secondary consumers, which represent the only group that showed significant correlation between the two variables (Fig. 2.14). Consequently, additional regression analyses using the ordinary least-squares method (since the maximum-likelihood estimate for λ was invariably zero; Fig. 2.10) were conducted for this group to compare the relative fit of three models to the data: (1) multiple regression model with body weights, sampling-adjusted last appearance dates, and an interaction term for the two variables as the predictors; (2) multiple regression model with body weights and sampling-adjusted last appearance dates as the predictors (no interaction term); (3) simple regression model with body weights as the sole predictor. All three of the alternative models received more than negligible support measured by sample-size corrected Akaike information criteria (Table 2.3, Fig. 2.16B-D). However, no significant correlation was detected between durations and last appearance dates or between

durations and estimated values of the interaction between body weights and last appearance dates (Table 2.2).

Correlation between Expected Inter-birth Interval Lengths and Sampling-adjusted Generic Durations

The regression analyses of durations and inter-birth interval lengths that are expected from estimated body weights produced results that are quantitatively similar and qualitatively identical to those from the analyses of body weights and durations (Table 2.3, Figs. 2.11, 2.13, 2.15; compare with Table 2.2, Figs. 2.10, 2.12, 2.14). Thus, the maximum-likelihood estimates of phylogenetic signal λ were generally low, and estimates of zero were obtained, once again, for the reverse cohort that included those genera with their last appearance dates falling between 29 and 15 Ma ago, secondary consumers, and carnivorans (Table 2.3, Fig. 2.11). The slope of regression line was significantly different from zero in secondary consumers for all sets of simulated branch lengths, and in lipotyphlans for some of the simulated sets of branch lengths (Table 2.3, Fig. 2.13).

Discussion

In this study, it was not possible to assess the effects of life-history traits, abundance, and spatial distribution by controlling for body size. Rather, the aim was to use estimated body weights as a proxy for the combined effect of these unmeasurable (in the fossil record) variables to determine how generic durations scaled across 7 orders of magnitude along the body weight spectrum, as well as within trophic and temporal subsets of the 221 genera.

In interpreting the results, it is assumed that the sampling-adjusted duration of each genus in the fossil record primarily reflects its extinction probability—or, more precisely, the probability of extirpation from the regions covered by the data set at hand—averaged over the timespan of its existence, regardless of how extinction pressures are distributed over time. An alternative approach to the main question of this study might examine survival of genera across predefined temporal boundaries using logistic regression (cf. Polishchuk (2010) for late-Quaternary species), but such analyses would be more sensitive to inaccuracies in the estimation of temporal-range end points, nor are mammalian extinctions in the Cenozoic fossil record characterizable as belonging to geologically-instantaneous mass extinction events (cf. Alroy, 1996).

Because the fossil genera are morphologically recognized (based entirely on skeletal features), durations of genera can, in theory, be determined solely (i.e., without involving true extinctions) by the rate of taxonomically-significant morphological evolution that may or may not have extrinsic causes. Such instances, however, are likely to be rare, judging from the commonly overlapping temporal ranges of closely related genera (Fig. 2.7). It is also important to bear in mind that mammalian genera are not entirely arbitrary constructs of taxonomists. On the contrary, discordant patterns of lineage diversification at the generic and familial levels support evolutionary coherence and distinctiveness of genera as clusters on the tree of mammals (Stanley, 1998).

Across the range of trophic and temporal groups analyzed, the phylogenetic signal λ in the regression-model residual is generally weak (Table 2.2, Fig. 2.10), suggesting that evolutionary distances as measured by branch lengths in time do not have strong influence on the persistence of genera when body weights are controlled for. In fact, body weights themselves were found

to be a poor predictor of generic durations in most of the cases considered here (Table 2.2, Figs. 2.12, 2.14), and this pattern does not appear to result from temporal or ecological variations in the relationship between the two variables (Fig. 2.14). Furthermore, the general lack of correlation is robust to the considerable uncertainties in phylogenetic branch lengths (Table 2.2, Figs. 2.12, 2.14). Many of the shortest-lived genera in the fossil record—for example, those with single occurrences (precluding the estimation of range end points using the confidence interval method) and those that left no fossils—are no doubt excluded from the present study, but it is difficult to see how such omissions alone would produce the pattern observed here. Thus, although small sample sizes may have limited the statistical power of hypothesis tests for some of the data subsets, the conclusion seems inescapable that, overall, there is little, if any, scaling of generic extinction probability along the body-size axis from shrews to rhinoceroses.

Furthermore, because many ecological and life-history traits of key importance to extinction risk in mammalian species have strong and essentially monotonic relationships with body weights in ways that make large mammals more vulnerable (Fig. 2.1), it follows that these traits, too, are unlikely to have had dominant effects on the survival of genera. It is conceivable that the lack of detectable correlation between body weights and durations is a result of opposing effects of life-history traits and abundance on one hand and geographic range size on the other, but this scenario would require the positive effect of geographic range size on generic survival to be much stronger than is expected from the relatively weak positive correlation between body size and geographic range size (Brown and Maurer (1989); also see Fig. 2.1). Unfortunately, meaningful comparison of geographic range sizes for the fossil mammals included in this study is precluded by the uneven and restricted spatial distribution of fossil-bearing localities in North America (Fig. 2.3).

Similarly, it is not feasible to assess the effect of site occupancy (as a proxy for local and regional abundance; see Jernvall and Fortelius (2004)) as there is presently no method to correct for the sampling disparity between large and small mammals across space. Assuming that total abundance of genera can be reasonably approximated by multiplying their local population densities (that are reported in the literature) by their geographic range sizes, a negative correlation is expected between body weights and total abundance (since geographic rage size increases more slowly than population density declines; see Fig. 2.1), and so extinction probability would show positive correlation with body weights if total abundance were of paramount importance to the survival of genera. Such a pattern was not observed in this study except for secondary consumers (Fig. 2.14).

The exploratory analyses using expected inter-birth interval lengths instead of estimated body weights require more provisional interpretation as additional errors in the predictor variable are introduced when this life-history trait is estimated from body weights that are themselves estimated from tooth sizes. Even with the use of separate predictive equations for different groups within the data set, the estimated inter-birth interval lengths are probably inaccurate in many cases, particularly in small mammals (Fig. 2.8). Nevertheless, the distinct scaling of the tempo of reproduction across the body-size spectrum in different ecological groups (e.g., carnivorans are generally characterized by long inter-birth intervals) renders these analyses instructive. In effect, the conversion of weights into inter-birth lengths results in heterogeneous re-scaling of the predictor variable, which could, in principle, reveal patterns of correlation with durations that are not apparent in the observed relationships between weights and durations. The analyses, however, essentially replicated the patterns of correlation between weights and durations (Figs. 2.11, 2.13, 2.15), providing additional, albeit non-independent, support to the claim above that the general lack of correlation

between body weights and durations implies the lack of strong effect of life-history traits on the survivorship of genera. Certainly, additional reproductive data for living mammals (those for lipotyphlans are severely limited at present) as well as improved cladistic hypotheses that relate living and extinct genera would enable more sophisticated treatment of this subject.

The set of secondary consumers merits special attention as the only group for which significant (negative) correlation was detected between body weights and durations. When the relationship between the two variable are examined separately within each of the two component groups of secondary consumers, the lipotyphlans and carnivorans, it was found to be non-significant at the significance level of $\alpha = 0.05$ (carnivorans) or equivocally significant (lipotyphlans) depending on the set of branch lengths that was used in the generalized least-squares regression analysis (Table 2.2, Figs. 2.12, 2.14). This, combined with the results of nonparametric tests, suggests that the observed negative correlation among secondary consumers primarily reflects the significantly shorter durations of carnivorans as a group relative to those of lipotyphlans as well as those of ungulates of similar sizes (N.B. The durations of large carnivorans may, in fact be underestimated here by applying the same set fossil-recovery potential functions through time to both large carnivores and large herbivores). The latter observation in itself appears to mirror the lower population densities and greater individual home-range sizes of carnivoran species and genera compared to those of large herbivores (Fig. 2.1), but again, such an explanation cannot be readily extended beyond these specific comparisons; small herbivores, for example, do not have longer durations than large herbivores despite their substantially higher population densities. The multiple linear regression analysis using a model with an interaction term for body weights and last appearance dates suggests the possibility that the shorter durations of carnivorans, presumably reflecting their elevated extinction risk, is a relatively recent trend in the post-early-Oligocene history of North American mammals (Table 2.2, Fig. 2.14), although the statistical support for this hypothesis is limited (Table 2.2).

The great variation in durations across the full spectrum of body weights implies that the determinants of extinction probability (or interactions among them) are far more complex than can be described in a bivariate space. With regard to large mammals, the findings of the present study are generally consistent with those of previous studies (see Table 2.1) by Viranta (2003), Carotenuto et al. (2010), and Raia et al. (2011), and extend the observation of no correlation to small mammals. Comparison of the results with those reported by Flynn et al. (1995), which showed longer durations of small species in the Miocene of northern Pakistan, is difficult because of the differences in geographic extent (being orders of magnitude smaller), likely environmental conditions, and taxonomic resolution.

In terms of the taxonomic and spatiotemporal scales, the present study is comparable to that of Liow et al. (2008) on Neogene mammals of Europe. Using a capture-mark-recapture method, Liow et al. (2008) demonstrated a negative effect of greater body size (taxonomically categorized as large or small rather than using body-weight estimates for individual taxa) on the persistence of genera. Interestingly, their analysis yielded inconclusive evidence for under-sampling of small mammals relative to large mammals. In the European fossil record, the observed durations of large genera (not adjusting for sampling bias, since the latter was not substantiated), with the median of 2.90 Ma, were found to be significantly shorter than those of small genera, with the median of 4.04 Ma. In contrast, the median observed durations (prior to adjustment) of large and small mammals in the North American record are rather similar 6.12 and 5.58 Ma, while the adjustment for sampling bias brings these statistics even closer, giving median durations of 7.20 and 7.13

Ma, respectively. Thus, it is unlikely that the disparate findings of the present study and those reported by Liow et al. (2008) stem from methodological differences because the raw data from the two continents (i.e., observed durations prior to any adjustment) are already quite dissimilar in the relative durations of large versus small taxa. To put this into perspective, in order for the North American data to exhibit the proportional difference of 39% between the two size classes as seen in the European data, the durations of North American small mammals would need to be further extended by 41 (sampling-adjusted durations) to 53% (observed durations) while keeping the durations of large genera unchanged. In essence, the North American and European fossil records appear not only to have different qualities with respect to size bias in sampling but also to paint contrasting pictures of the relationship between body size and extinction probability. Liow et al. (2008) proposed the physiological and behavioral advantages of small mammals (specifically, their ability to cope with environmental stress through torpor, hibernation, or use of shelters) as the primary reason for their lower extinction rates—a hypothesis that, if correct, should have produced a similar pattern of extinction selectivity in the North American fossil record. The findings of the present study, however, suggest that the mechanistic explanation for the elevated extinction risk of large mammals in Europe may lie not in intrinsic properties of organisms but in the biogeographic context of extinctions. Notably, the discordant diversity trends of large and small mammals in the Mio-Pliocene of the Iberian Peninsula demonstrate the key importance of the "mobility" of geographic ranges in understanding patterns of regional extirpations in Europe (Casanovas-Vilar et al., 2010). It may be postulated that the connection of Europe to the rest of Eurasia and the biotic influence of Afro-Arabia may have contributed to more dynamic (i.e., characterized by short durations in the region) biogeoraphic history of mobile large mammals in the Neogene of Europe compared to North America (cf. Pickford, 1989; van der Made, 1999). In contrast, while a number of genera dispersed from Eurasia to North America during the Miocene, dispersal out of North America was much more limited (Dawson, 1999).

Given that body size is strongly correlated with—and, in many ways, governs—a suite of fundamental ecological properties in mammals (Eisenberg, 1981), the lack of scaling of extinction probability (as inferred from durations) with body weights in the fossil record is striking and is at apparent odds with the elevated extinction risk of large living mammals. Two hypotheses may be advanced to explain this apparent incongruity between theoretical expectation and empirical observation. First, environmental modifications and hunting by humans since the late Quaternary may have presented a radically new threat to large mammals in particular and fundamentally altered the extinction regime of the previous 29 million years, which had been non-selective with respect to body size. There is little doubt that characteristics such as low reproductive rates, low growth rates, and low population densities predispose large mammals to extinction by demographic or environmental stochasticity (including "catastrophes" of Lande (1993)) alone once the minimal viable population size is reached (Lande, 1993). While this is an inevitable and proximate component of any extinction, perhaps the key to understanding the patterns of mammalian extinction prior to the advent of human influence lies in the earlier phase of a taxon's history in which its (meta)population size falls from a sustainable level to a critical threshold. The indistinguishable distributions of durations of large versus small mammal during much of the last 29 million years can be explained if, for instance, the elevated risk for large mammals during the last phase leading to their extinction is balanced by lower likelihood of reaching the minimum viable population size in the first place compared to small mammals. Extrinsic factors that disturb this balance would create size-biased extinction risk. Indeed, the rate of mammalian extinction for the last 500 years

at the global scale is anomalously high when compared to extinction-rate estimates obtained from the Cenozoic fossil record of North America (Barnosky et al., 2011*b*). It may be speculated that, under non-anthropogenic environmental pressures, thriving populations of large mammals are less likely than those of small mammals to decline to critical levels, perhaps because of their traits such as wide ranges of physiological tolerance, great mobility, and typically large geographic ranges.

An alternative—but not mutually exclusive—interpretation of the findings of present study would invoke distinct processes of extinction across phylogenetic hierarchy. Under this scenario, size-biased species extinction risk since the late Quaternary may have applied to the deeper past as well but did not manifest at the genus level because generic extinctions were not simply added sums of specific extinctions. Such a pattern may be anticipated from, for example, the discordant geographic-range dynamics of mammalian species and genera in North America across glacial-interglacial transition (Hadly et al., 2009). Importantly, Hadly et al. (2009) point out that the environmental tolerance of a multispecific genus as a whole is often greater than that of any one of its constituent species; thus, loss of species is often accompanied or followed by expansion of their congeners, resulting in the maintenance of generic range size and perhaps abundance as well. If this pattern of internal compensation is adequately strong, it can override extinction selectivity at the level of species. For such a mechanism to work, it must involve (a) higher speciation rates for large mammals or (b) different modes of speciation in large versus small mammals. Corroboration of this hypothesis would require high-resolution data on temporal ranges of extinct species.

The possibility remains that, for some complex reason, the negative effect of large body size on the survival of taxa manifests at finer scales of phylogeny rather than across the spectrum of body weights of land mammals. In the well-studied phylogeny of fossil canids, for example, evolutionary increase in body size is apparently accompanied by reduction in durations of species, although this may have resulted from concomitant trophic specialization towards increased carnivory (Van Valkenburgh et al., 2004). As stated earlier, the dearth of species-level phylogenetic hypotheses and the problems of identifying true species in the fossil record make it difficult to assess the generality of such a pattern in most other mammalian groups.

The effect of potential errors in the adopted tree topology was not directly assessed because of the difficulty of delineating the range of plausible alternatives. Nevertheless, the generally consistent pattern observed for the various subsets of the data (each with a different combination of genera) indicates that the conclusions of this study do not depend precariously on the precise topology of the tree that was used in the comparative analyses. Certainly, additional taxonomic occurrence data, refinement of body-weight estimation, and advancement in taxonomy, phylogenetic hypotheses, and biochronology would warrant renewed investigation in the future of the subject discussed here. In addition, extension of the present study deeper into the fossil record may provide new insights into biological patterns of mammalian extinction, although both the comparative analyses and body-weight estimation would become increasingly challenging with greater phylogenetic and morphological distances between fossil taxa and their closest living relatives.

Conclusions

Small mammalian genera are under-sampled relative to large mammals in much of the Miocene fossil record of North America. When observed generic durations are adjusted for this sampling bias, no correlation between body weights and durations was found among 221 genera ranging

7 orders of magnitude in estimated weights. Nor was a significant relationship between the two variables detected within most of the ecological and temporal subsets of the data examined. The only exception was the secondary consumers, in which a significant correlation arose from shorter durations of carnivorans relative to those of primarily invertebrate-feeding lipotyphlans. Qualitatively identical results were obtained when expected inter-birth interval lengths were analyzed instead of estimated weights themselves, suggesting that this important aspect of fast-slow continuum of mammalian life history is not strongly correlated with the persistence of genera in deep time, either.

The variation in generic durations cannot be explained satisfactorily by the variation in body weights, defying population-biological expectations from the data on late-Quaternary (including living) species. Moreover, the generally low phylogenetic signal in the regression model residual implies that intrinsic traits that are inherited at the level of genera may not be reliable indicators of generic extinction risk. Crucially, these findings are compatible with the interpretation that the size-biased extinction selectivity since the late Quaternary is an anomaly in the evolutionary history of North American mammals in the past 29 million years. Alternatively, or in addition to this, the observed patterns may reflect decoupling of extinctions at the levels of species and genera. The reason for this cannot be deduced from the presently available data, but the results of this study call for further investigation of extinctions as multi-phase processes and caution against extrapolation of species extinction risk across phylogenetic hierarchy.

Supporting Material

The following Supporting Material is available in the .csv file format in the accompanying CD.

Appendix S2.1. MIOMAP/FAUNMAP generic occurrence data. Additional data for the taxonomic occurrences included in this appendix are publically available at http://www.ucmp.berkeley.edu/neomap/.

Table 2.1: Paleontological evidence for size-selective extinction in mammals

Study	Taxonomic scope (size range)	Spatiotemporal scale	Response variable	PCM	Relevant conclusion
Flynn et al. 1995	108 terrestrial species ($10^1 \sim 10^7$ g)	M: northern Pakistan	Duration	n/a	Large species generally have longer durations than small species
Johnson 2002	184 extinct and extant terrestrial species ($10^2 \sim 10^6$ g)	LQ: Au, Madagascar, northern Eu, NA, SA	LQ extinction	PIC	Within clades, body size is correlated with extinction probability through low reproductive rates
Viranta 2003	366 carnivoran species ($10^3 \sim 10^4$ g)	M: western Eu, NA	Duration	n/a	No differences in durations (2 classes) among 3 body-size classes
Lyons et al. 2004	2,130 extinct and extant terrestrial species ($10^{0.27} \sim 10^7$ g)	LQ: NA, SA, Af, Au	LQ extinction	n/a	Extinct species are significantly larger than surviving species
Van Valkenburgh et al. 2004	42 canid species (m1L = $5 \sim 40$ mm)	E-P: NA	Duration	n/a	Large, ecologically-specialized species have shorter durations than small, ecologically-generalized species
Liow et al. 2008	554 terrestrial genera ($10^0 \sim 10^6$ g)	M-Q: western E	Duration, extinction rate, survivorship	n/a	Large genera have shorter durations, higher extinction rates, and lower survivorships than small genera
Polishchuk 2010	2,534 extinct and extant species ($10^0 \sim 10^6$ g)	LQ: Af, Au, NA, SA	LQ extinction	n/a	Extinction is correlated with body weight through population density
Carotenuto et al. 2010	54 terrestrial species in 20 genera ($10^3 \sim 10^6$ g)	P-Q: western Eu	Duration	PIC	No correlation between body weights and generic/specific durations
Raia et al. 2011	72 terrestrial species ($10^3 \sim 10^7$ g)	M-Q: western Eu, Af	Duration	GLS	No correlation between body weights and specific durations
This study	220 terrestrial genera ($10^0 \sim 10^6$ g)	O-Q: NA	Duration	GLS	See Discussion

NOTE—Af = Africa; Au = Australia; E = Eocene; Eu = Eurasia; GLS = generalized least-squares regression; LQ = late Quaternary; M = Miocene; NA = North America; O = Oligocene; P = Pliocene; PCM = phylogenetic comparative method; PIC = phylogenetically-independent contrast method Q = Quaternary, SA = South America.

Table 2.2: Regression statistics for estimated body weights

Included genera	λ_{ML}	Slope β_{ML}	*P*-value for slope
All	0.129 (0.114, 0.156)	-0.025 (-0.028, -0.022)	0.232 (0.19, 0.281)
$T_{LAD50} = [29, 15)$	0.000 (0.000, 0.000)	-0.005[a]	0.890[a]
$T_{LAD50} = [15, 12)$	0.100 (0.020, 0.490)	-0.049 (-0.055, -0.037)	0.187 (0.103, 0.485)
$T_{LAD50} = [12, 9)$	0.065 (0.040, 0.205)	0.017 (0.016, 0.020)	0.492 (0.472, 0.516)
$T_{LAD50} = [9, 5)$	0.575 (0.470, 1.000)	-0.052 (-0.062, -0.022)	0.246 (0.198, 0.848)
$T_{LAD50} = [5, 1)$	0.220 (0.205, 0.245)	-0.025 (-0.028, -0.021)	0.482 (0.435, 0.546)
Herbivores	0.145 (0.125, 0.200)	0.002 (-0.003, 0.006)	0.936 (0.827, 0.996)
"Ungulates"	0.220 (0.140, 0.486)	-0.011 (-0.032, 0.001)	0.887 (0.686, 0.987)
Glires	0.145 (0.130, 0.170)	-0.010 (-0.022, -0.002)	0.881 (0.729, 0.979)
Secondary consumers	0.000 (0.000, 0.000)	-0.067[a]	0.003[a]
Carnivorans	0.000 (0.000, 0.000)	-0.066[a]	0.150[a]
Lipotyphlans	0.100 (0.050, 1.000)	-0.083 (-0.393, -0.067)	0.478 ($<10^{-3}$, 0.575)

NOTE—a, Estimates from ordinary least-squares regression analyses . All other values are medians and bias-corrected 95% confidence intervals (in parentheses) from generalized least-squares regression analyses for 1,000 sets of partly simulated branch lengths.

Table 2.3: Regression statistics for inter-birth interval lengths

Included genera	λ_{ML}	Slope β_{ML}	*P*-value for slope
All	0.127 (0.115, 0.156)	-0.074 (-0.084, -0.064)	0.310 (0.268, 0.372)
$T_{LAD50} = [29, 15)$	0.000 (0.000, 0.000)	0.003[a]	0.982[a]
$T_{LAD50} = [15, 12)$	0.098 (0.000, 0.389)	-0.158 (-0.177, -0.125)	0.181 (0.083, 0.433)
$T_{LAD50} = [12, 9)$	0.095 (0.065, 0.271)	0.072 (0.066, 0.087)	0.396 (0.376, 0.416)
$T_{LAD50} = [9, 5)$	0.540 (0.455, 1.000)	-0.110 (-0.165, -0.080)	0.476 (0.405, 0.927)
$T_{LAD50} = [5, 1)$	0.235 (0.213, 0.250)	-0.109 (-0.121, -0.093)	0.383 (0.344, 0.443)
Herbivores	0.145 (0.130, 0.232)	0.006 (-0.014, 0.020)	0.949 (0.809, 0.993)
"Ungulates"	0.215 (0.140, 0.500)	-0.038 (-0.132, -0.011)	0.899 (0.682, 0.978)
Glires	0.150 (0.130, 0.170)	-0.037 (-0.089, -0.012)	0.875 (0.710, 0.962)
Secondary consumers	0.000 (0.000, 0.000)	-0.206[a]	0.005[a]
Carnivorans	0.000 (0.000, 0.000)	-0.705[a]	0.123[a]
Lipotyphlans	0.105 (0.050, 1.000)	-0.308 (-1.433, -0.242)	0.470 ($<10^{-3}$, 0.587)

NOTE—a, Estimates from ordinary least-squares regression analyses . All other values are medians and bias-corrected 95% confidence intervals (in parentheses) from generalized least-squares regression analyses for 350 sets of partly simulated branch lengths. The results for "ungulates," glires, carnivorans, and lipotyphlans are expected to be identical to those for body weights (Table 2.3) except for the different scales of predictor variable and randomness of simulations.

Table 2.4: Regression model comparison for secondary consumers

Model	$\hat{\beta}_0$	$\hat{\beta}_1$	$\hat{\beta}_2$	$\hat{\beta_{12}}$	R^2	AIC_c	Relative likelihood
$D = \beta_0 + \beta_1 W + \beta_2 T_{LAD50} + \beta_{12}(W \times T_{LAD50}) + \varepsilon$	2.876	-0.117*	-0.066	0.006	0.088	-63.18	0.105
$D = \beta_0 + \beta_1 W + \beta_2 T_{LAD50} + \varepsilon$	2.387	-0.060**	-0.012		0.080	-63.78	0.191
$D = \beta_0 + \beta_1 W + \varepsilon$	2.279	-0.059**			0.087	-65.43	1.00

NOTE—D, natural-log transformed duration; W, natural-log transformed body weight. Asterisks denote significant correlations with body weights at the significance levels of $\alpha = 0.05$ (*) and $\alpha = 0.01$ (**). All analyses were conducted with the ordinary least-squares method.

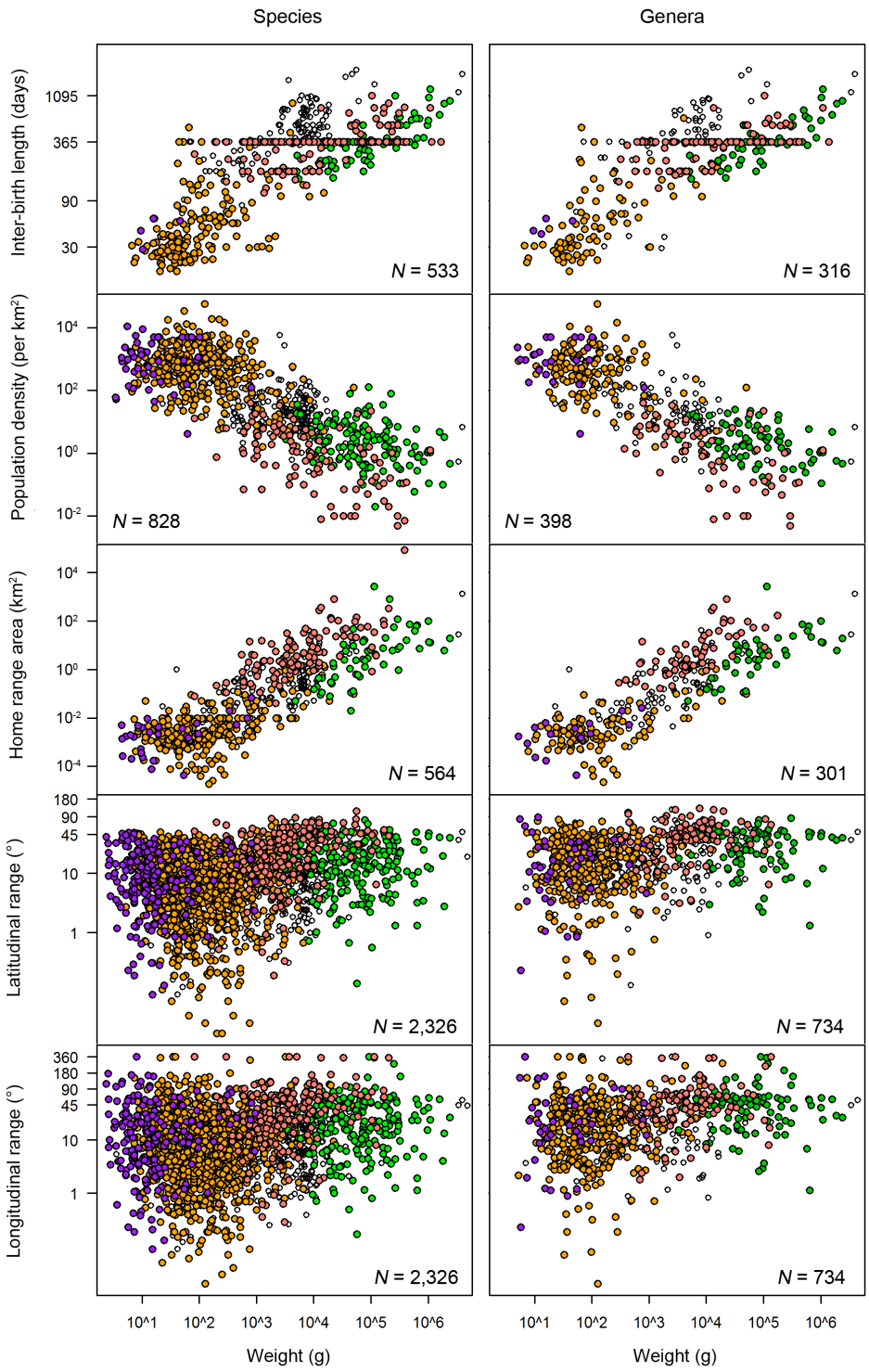

Figure 2.1: Relationships of body weight with ecological properties and life-history traits at the specific and generic levels. Data for extant rodents and lagomorphs (orange), artiodactyls and perissodactyls (green), lipotyphlans (purple), carnivorans (pink), and other terrestrial eutherian mammals from the PanTHERIA database (Jones et al., 2009). The latitudinal and longitudinal ranges for genera are the differences between the maximum and minimum ranges of their constituent species for which data are available; all other variables for genera are the means of natural-log transformed values for their constituent species for which data are available. The home ranges are those of individual organisms.

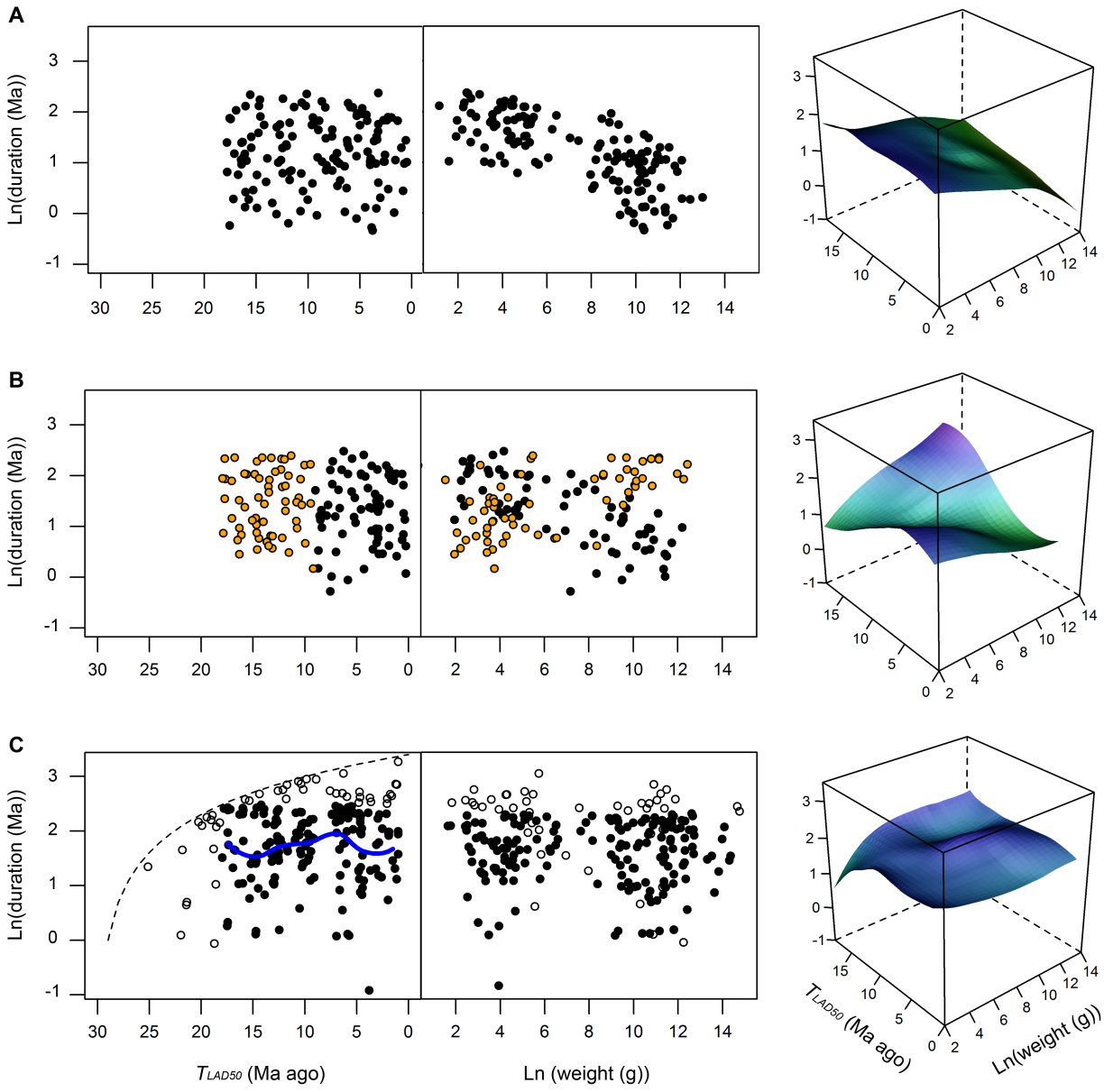

Figure 2.2: Illustration of alternative hypotheses. Each circle represents a hypothetical (*A* and *B*) or actual (*C*) genus. *A*, Extinction is size-biased in a consistent manner throughout the time span of study. *B*, Extinction is size-biased, but the direction of bias changes over time, depending on changing causes of extinction. In this example, small taxa are more vulnerable earlier in time (orange circles) but this pattern is reversed later (black circles). *C*, Preliminary examination of the empirical data for this study suggests general lack of size selectivity in extinction. Surface plots and the blue line in *C* were generated by locally-weighted scatter-plot smoothing (LOWESS) with the smoothing parameter of $\alpha = 0.5$ and second-degree polynomial fitting. Because the sampling-adjusted first appearance dates for the genera in the data set do not go back by more than 29 million years, the maximum possible duration is inevitably correlated with the last appearance date (dashed line in *C*); therefore, to address the relationship between last appearance dates and durations, only those genera are considered here whose (1) last appearance dates fall in the last 18 million years and (2) durations do not exceed 12 million years (filled circles in *C*).

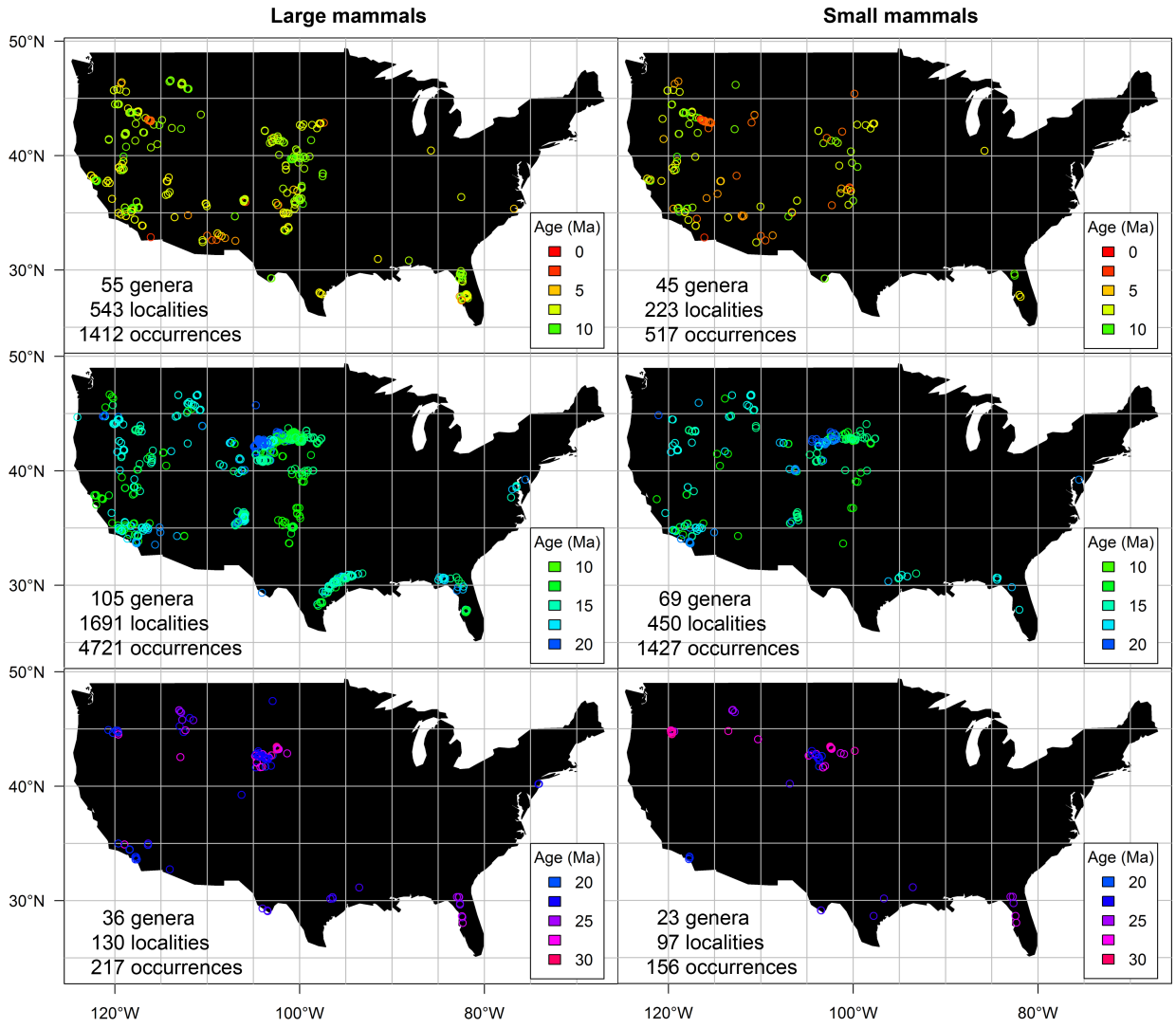

Figure 2.3: Geographic distributions of fossil-bearing localities. Data from the MIOMAP and FAUNMAP databases (see Materials and Methods). A total of 2,733 localities are shown that have collectively yielded the 221 genera considered in the comparative analysis of the present study. Additional localities (not shown) were included in the derivation of fossil recovery potential curves (see text). For comparison, localities are plotted separately for large (left column) and small (right column) mammals, and for three successive time intervals: 29-20 Ma ago (bottom row); 20-10 Ma ago (middle row); and 10-1 Ma ago (top row). Each locality is color-coded according to its midpoint age (i.e., the mean of maximum and minimum possible ages)

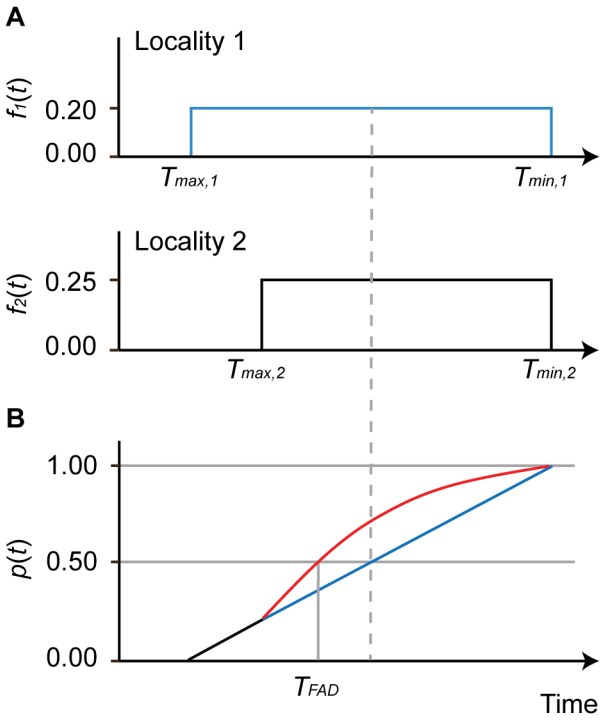

Figure 2.4: Determination of median-unbiased first/last observed taxonomic occurrence. *A*, probability density functions $f(t)$ for ages of two localities that have yielded a taxon of interest. Each locality age is bounded by the maximum (T_{max}) and minimum (T_{min}) possible ages. *B*, cumulative density functions $p(t)$ describing the probability of the first occurrence taking place before the time T at Locality 1 alone (blue) versus across Localities 1 and 2 (red). The median-unbiased estimate for the first occurrence T_{FAD} corresponds to the cumulative density of 0.5.

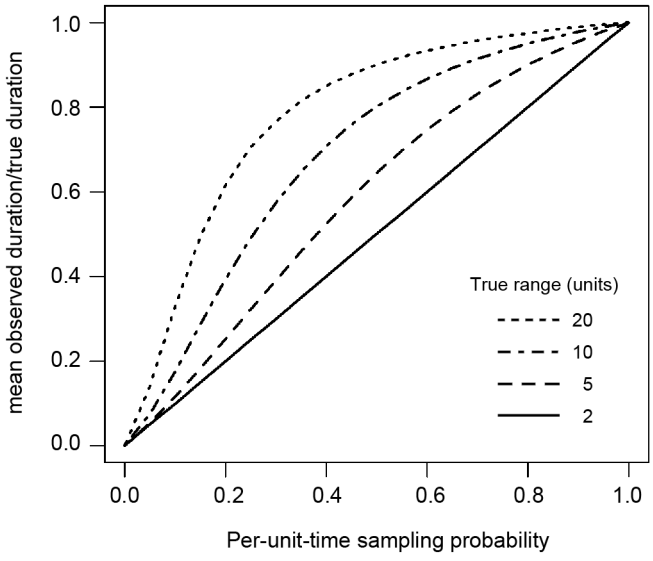

Figure 2.5: Disproportionate impact of incomplete sampling on short temporal ranges. The same probability of sampling results in proportionately greater range truncation for truly short ranges. Consequently, both absolute and relative durations of taxa can be distorted by incomplete sampling.

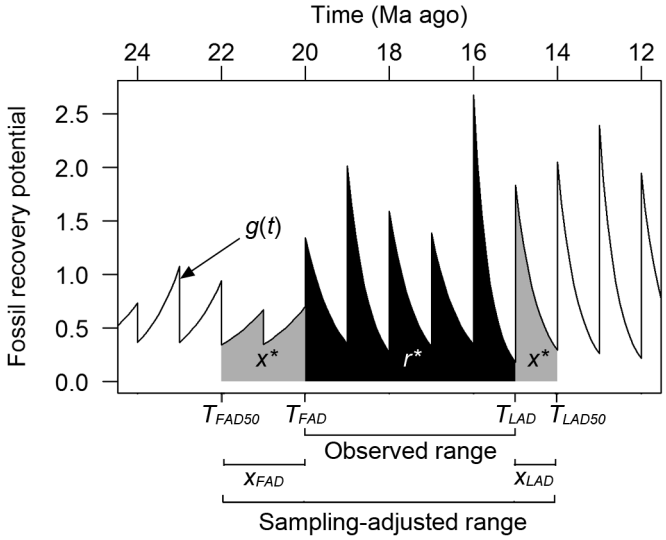

Figure 2.6: Illustration of Marshall's 2010 generalized confidence-interval method as applied to the present study. The fossil recovery potential curve $g(t)$ is derived from per-million-year range-through sampling probabilities and the assumption of a constant sampling probability within each 1 million-year interval. T_{FAD} and T_{LAD} are observed first and last appearance dates, respectively, and x_{FAD} and x_{LAD} are their corresponding temporal extensions for a given confidence level. T_{FAD50} and T_{LAD50} mark the median-unbiased confidence-interval estimates for the first and last appearance dates. The gray and black areas under the curve represent $x*$ and $r*$, as discussed in the text.

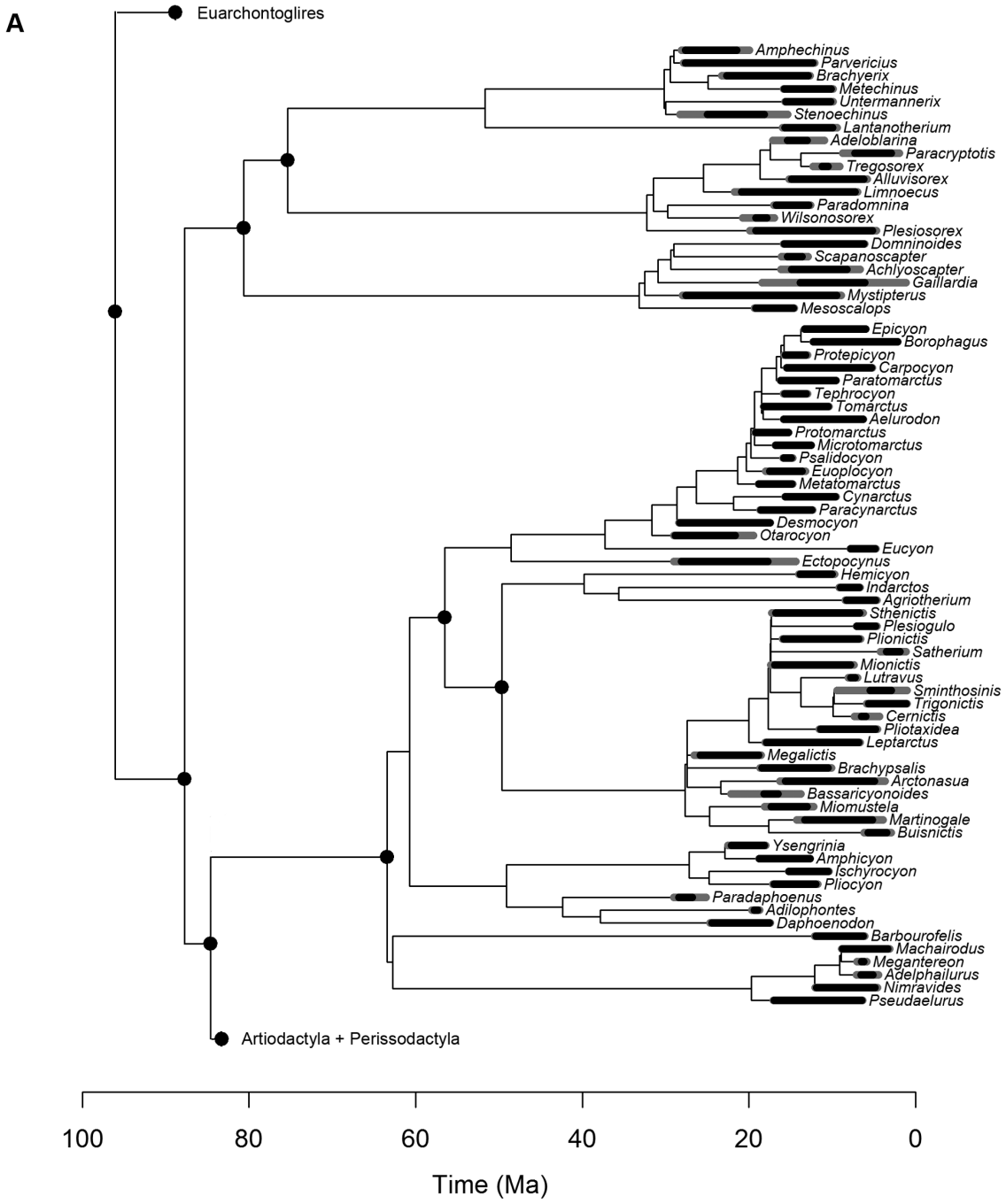

Figure 2.7: One example of time-calibrated cladogram for 221 genera. *A*, lipotyphlans and carnivorans; *B*, artiodactyls and perissodactyls; *C*, rodents and lagomorphs. Filled circles indicate the nodes whose ages are fixed by molecular divergence-date estimates of Bininda-Emonds et al. (2007, 2008). The ages of remaining nodes and their associated branch lengths were randomly selected in each simulation. Black and gray bars represent the observed and sampling-adjusted temporal ranges, respectively.

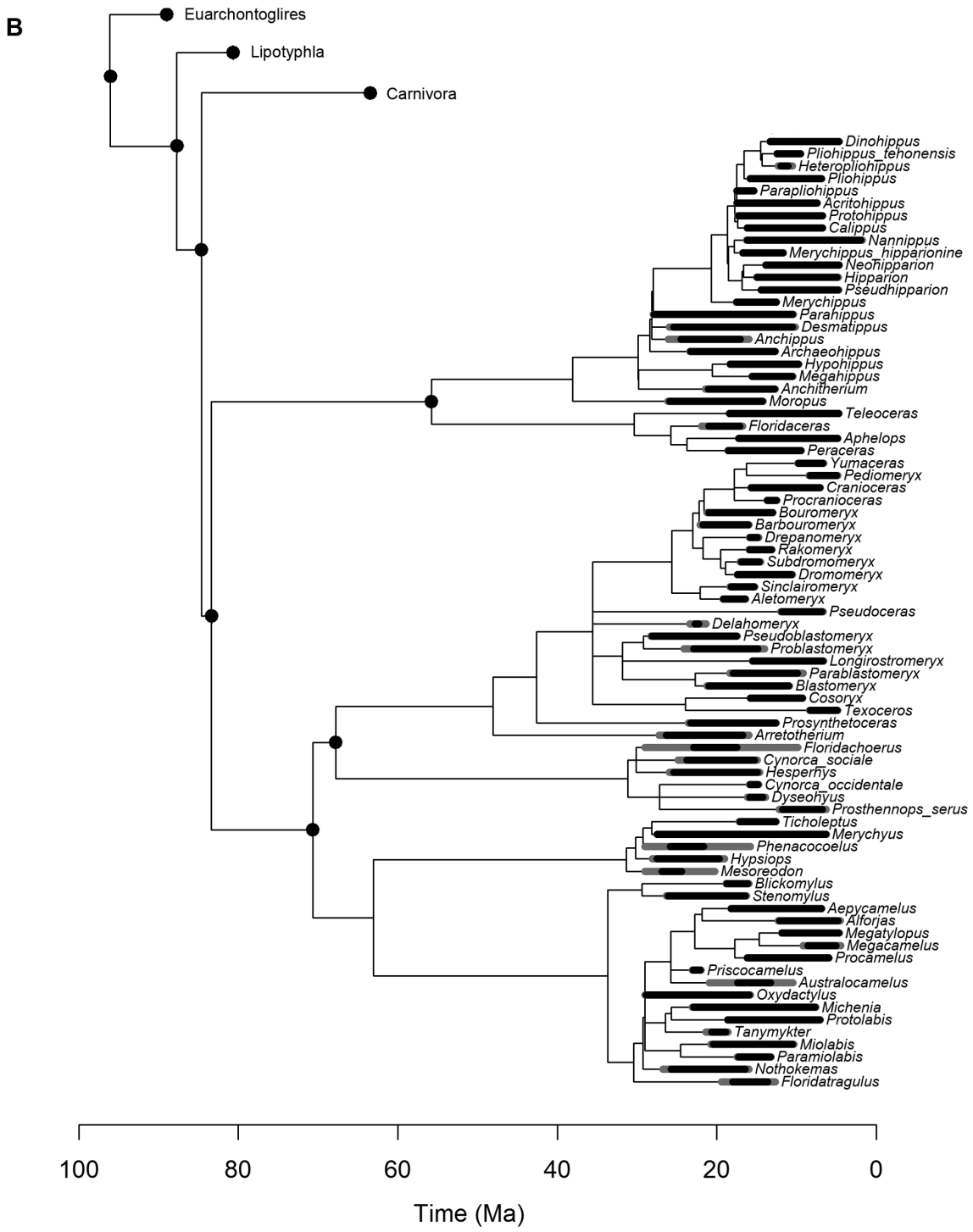
B
Euarchontoglires
Lipotyphla
Carnivora
Dinohippus
Pliohippus_tehonensis
Heteropliohippus
Pliohippus
Parapliohippus
Acritohippus
Protohippus
Calippus
Nannippus
Merychippus_hipparionine
Neohipparion
Hipparion
Pseudhipparion
Merychippus
Parahippus
Desmatippus
Anchippus
Archaeohippus
Hypohippus
Megahippus
Anchitherium
Moropus
Teleoceras
Floridaceras
Aphelops
Peraceras
Yumaceras
Pediomeryx
Cranioceras
Procranioceras
Bouromeryx
Barbouromeryx
Drepanomeryx
Rakomeryx
Subdromomeryx
Dromomeryx
Sinclairomeryx
Aletomeryx
Pseudoceras
Delahomeryx
Pseudoblastomeryx
Problastomeryx
Longirostromeryx
Parablastomeryx
Blastomeryx
Cosoryx
Texoceros
Prosynthetoceras
Arretotherium
Floridachoerus
Cynorca_sociale
Hesperhys
Cynorca_occidentale
Dyseohyus
Prosthennops_serus
Ticholeptus
Merychyus
Phenacocoelus
Hypsiops
Mesoreodon
Blickomylus
Stenomylus
Aepycamelus
Alforjas
Megatylopus
Megacamelus
Procamelus
Priscocamelus
Australocamelus
Oxydactylus
Michenia
Protolabis
Tanymykter
Miolabis
Paramiolabis
Nothokemas
Floridatragulus
100
80
60
40
20
0
Time (Ma)

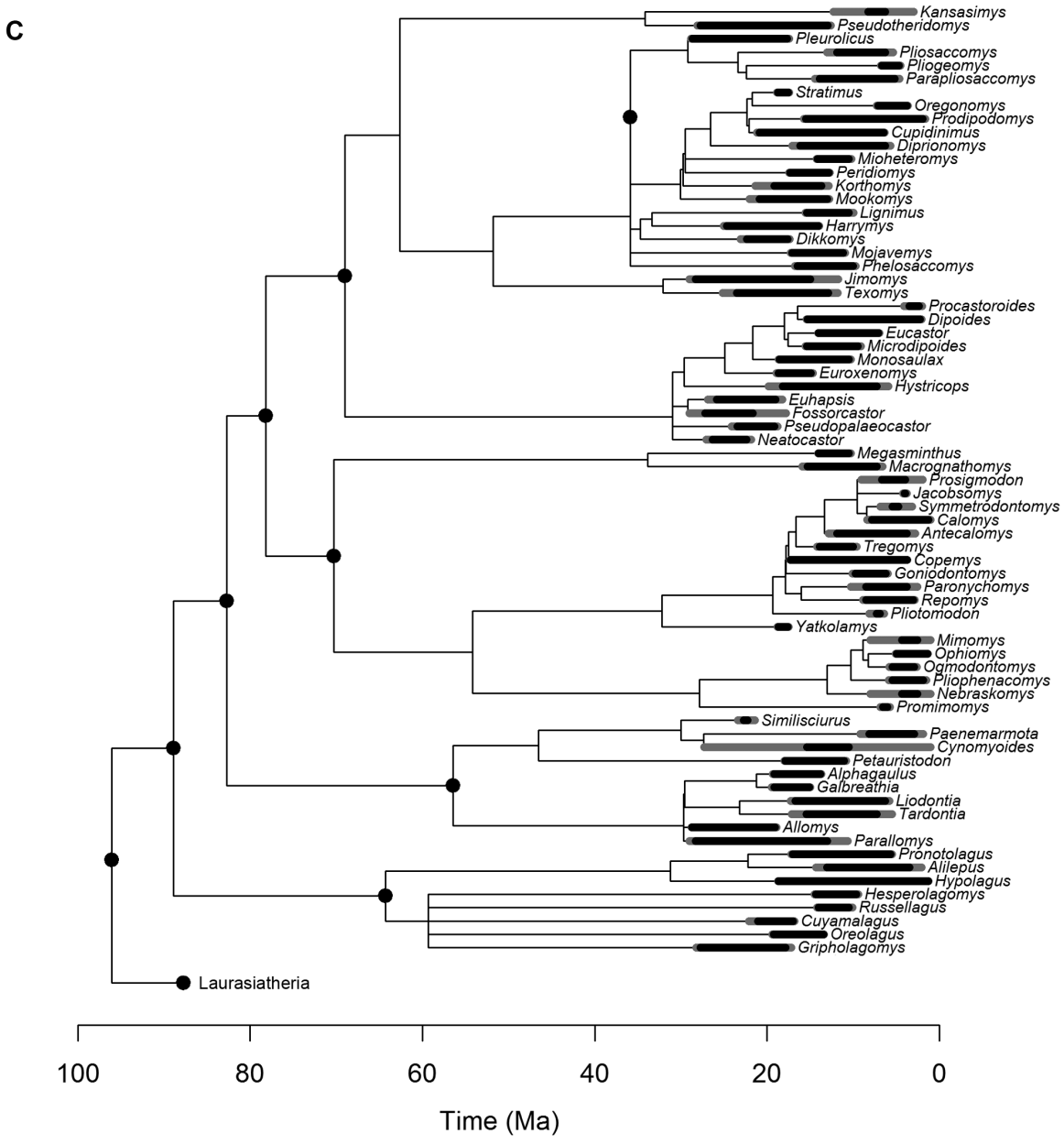
C
Kansasimys
Pseudotheridomys
Pleurolicus
Pliosaccomys
Pliogeomys
Parapliosaccomys
Stratimus
Oregonomys
Prodipodomys
Cupidinimus
Diprionomys
Mioheteromys
Peridiomys
Korthomys
Mookomys
Lignimus
Harrymys
Dikkomys
Mojavemys
Phelosaccomys
Jimomys
Texomys
Procastoroides
Dipoides
Eucastor
Microdipoides
Monosaulax
Euroxenomys
Hystricops
Euhapsis
Fossorcastor
Pseudopalaeocastor
Neatocastor
Megasminthus
Macrognathomys
Prosigmodon
Jacobsomys
Symmetrodontomys
Calomys
Antecalomys
Tregomys
Copemys
Goniodontomys
Paronychomys
Repomys
Pliotomodon
Yatkolamys
Mimomys
Ophiomys
Ogmodontomys
Pliophenacomys
Nebraskomys
Promimomys
Similisciurus
Paenemarmota
Cynomyoides
Petauristodon
Alphagaulus
Galbreathia
Liodontia
Tardontia
Allomys
Parallomys
Pronotolagus
Allolepus
Hypolagus
Hesperolagomys
Russellagus
Cuyamalagus
Oreolagus
Gripholagomys
Laurasiatheria
100
80
60
40
20
0
Time (Ma)

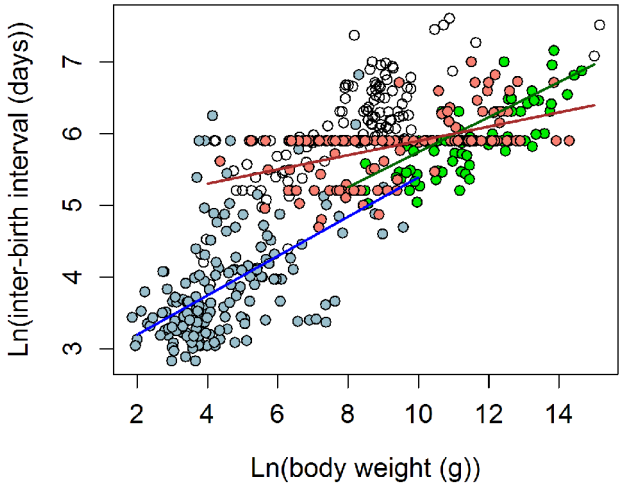

Figure 2.8: Least-squares regression lines for prediction of inter-birth interval lengths (L) from body weights (W). Rodents, lagomorphs, and lipotyphlans (blue, $N = 165$): $L = 0.275W + 2.643$, $R^2 = 0.303$. Artiodactyls and perissodactyls (green, $N = 94$): $L = 0.244W + 3.301$, $R^2 = 0.552$. Carnivorans (pink, $N = 145$): $L = 0.099W + 4.901$, $R^2 = 0.261$. Data from PanTHERIA data base (Jones et al., 2009)

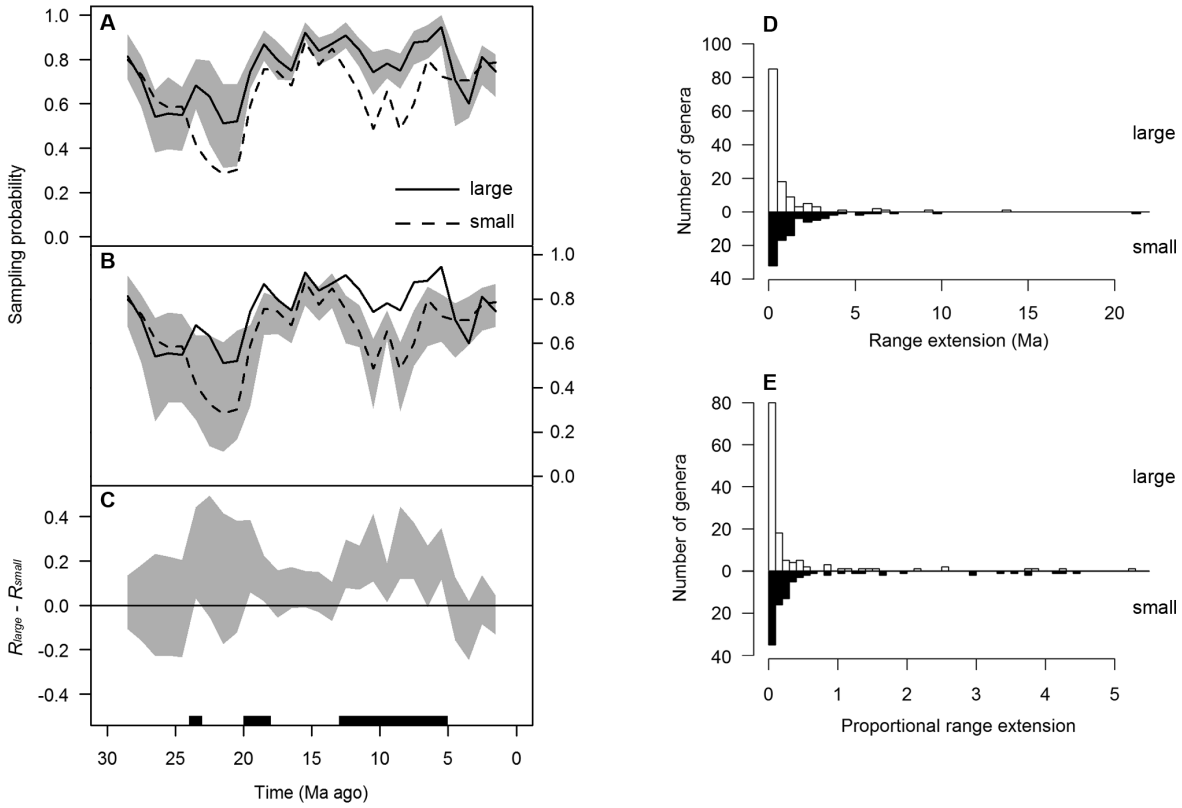

Figure 2.9: Range-through sampling probability through time for large and small mammals. *A* and *B*: The median values are plotted for large (solid line) and small (dashed line) mammals along with their bias-corrected 95% confidence intervals (shaded regions) that reflect uncertainties in locality ages. The sampling probability for the youngest time interval (1-0 Ma ago) is necessarily 1 and is not shown here. *C*: Shaded region shows the 95% confidence intervals for differences in sampling probability between large and small mammals. The time intervals in which small mammals are significantly less sampled than large mammals are indicated by black bars along the temporal axis. *D* and *E*: Temporal-range extensions obtained by the generalized confidence-interval method measured in millions of years (*C*) and as proportions of observed temporal ranges (*D*).

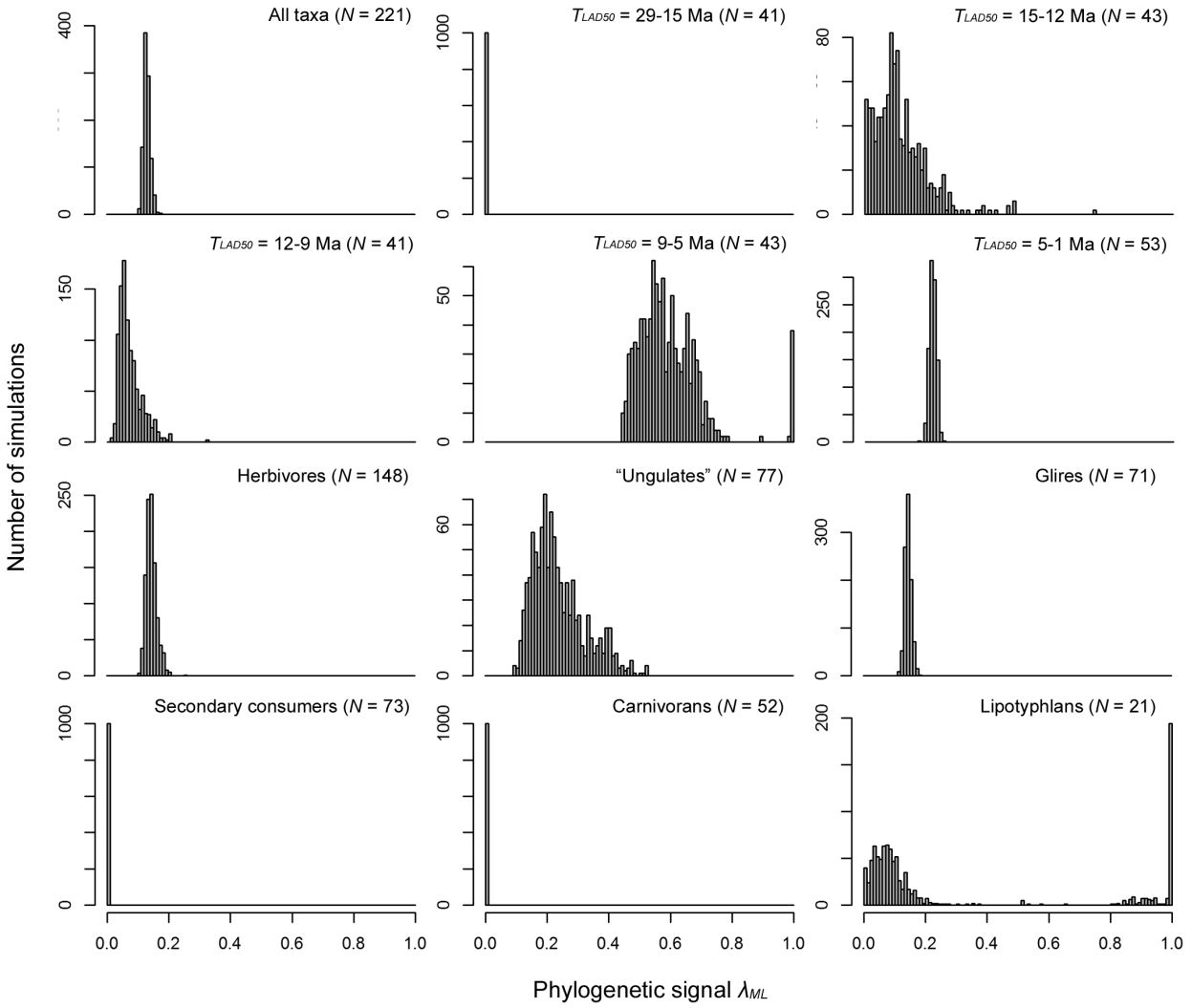

Figure 2.10: Maximum-likelihood estimates of phylogenetic signal (Pagel's λ) in the residual error ε of the regression model for body weights and durations. The results for 1,000 simulated sets of branch lengths are shown for each data subset.

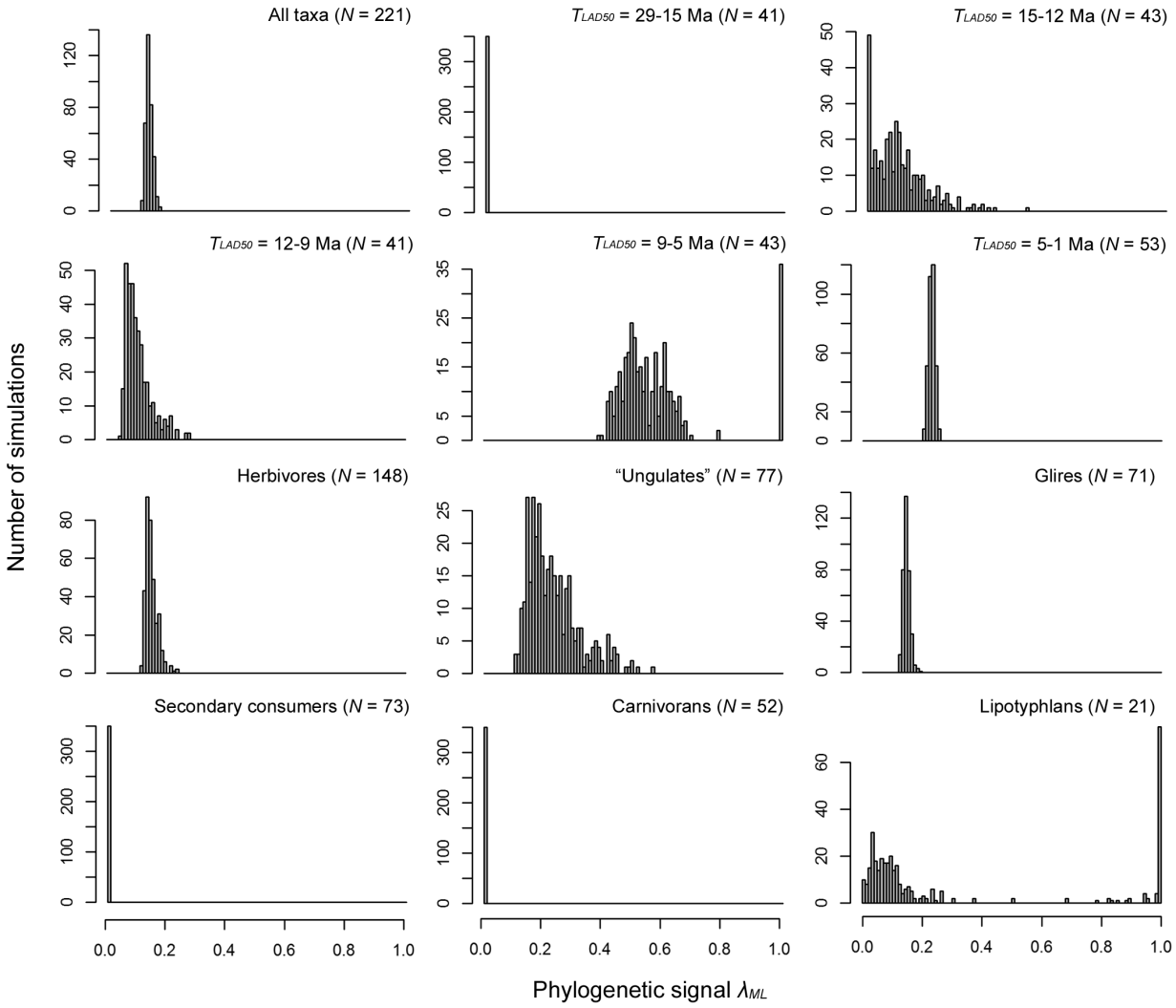

Figure 2.11: Maximum-likelihood estimates of phylogenetic signal (Pagel's λ) in the residual error ε of the regression model for inter-birth intervals lengths and durations. The results for 350 simulated sets of branch lengths are shown for each data subset.

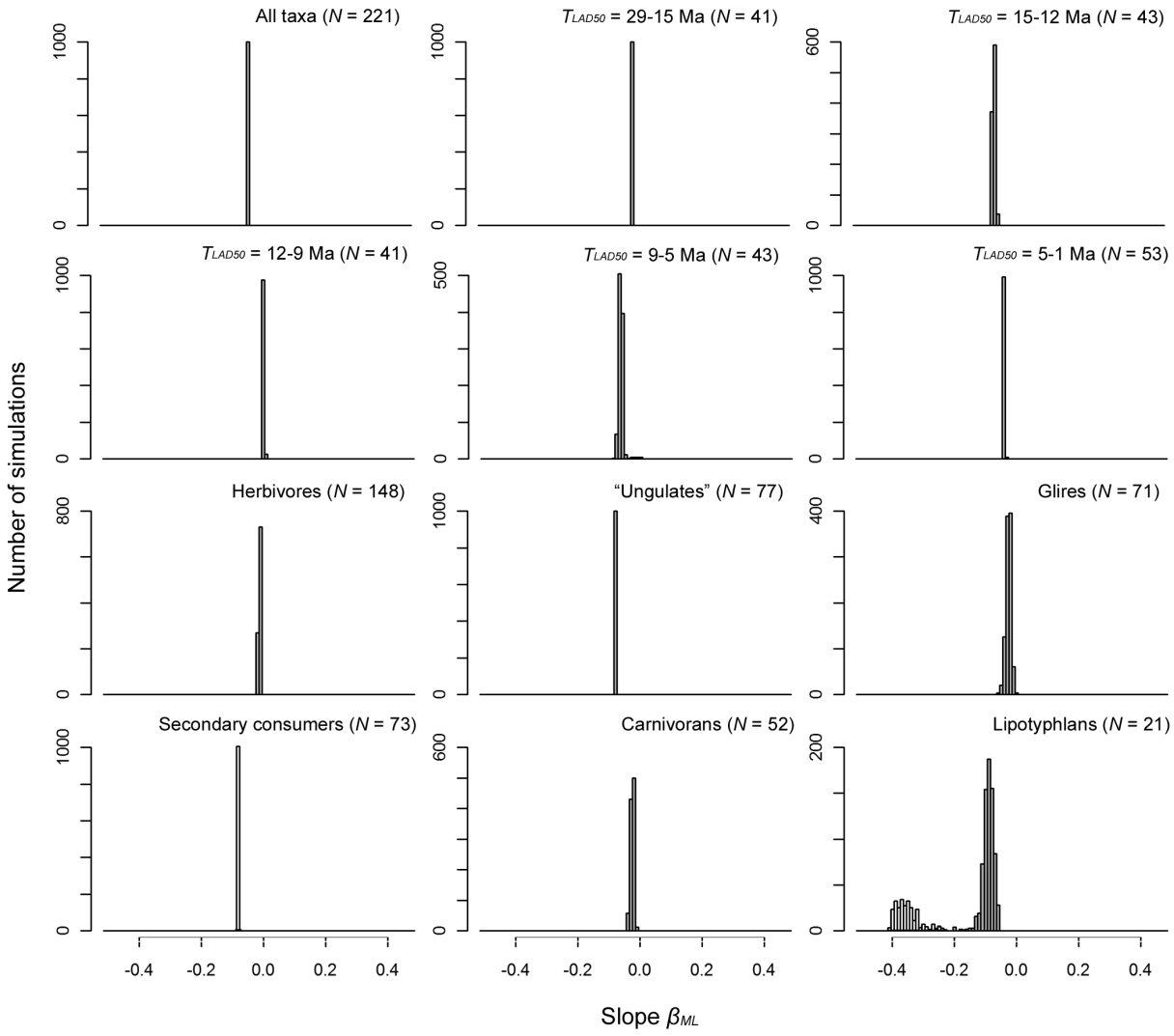

Figure 2.12: Maximum-likelihood estimates of slope for regression of body weights and durations. The results for 1,000 sets of simulated branch lengths are shown for each data subset. White bars represent estimated slopes that differ from zero at the significance level of $\alpha = 0.05$.

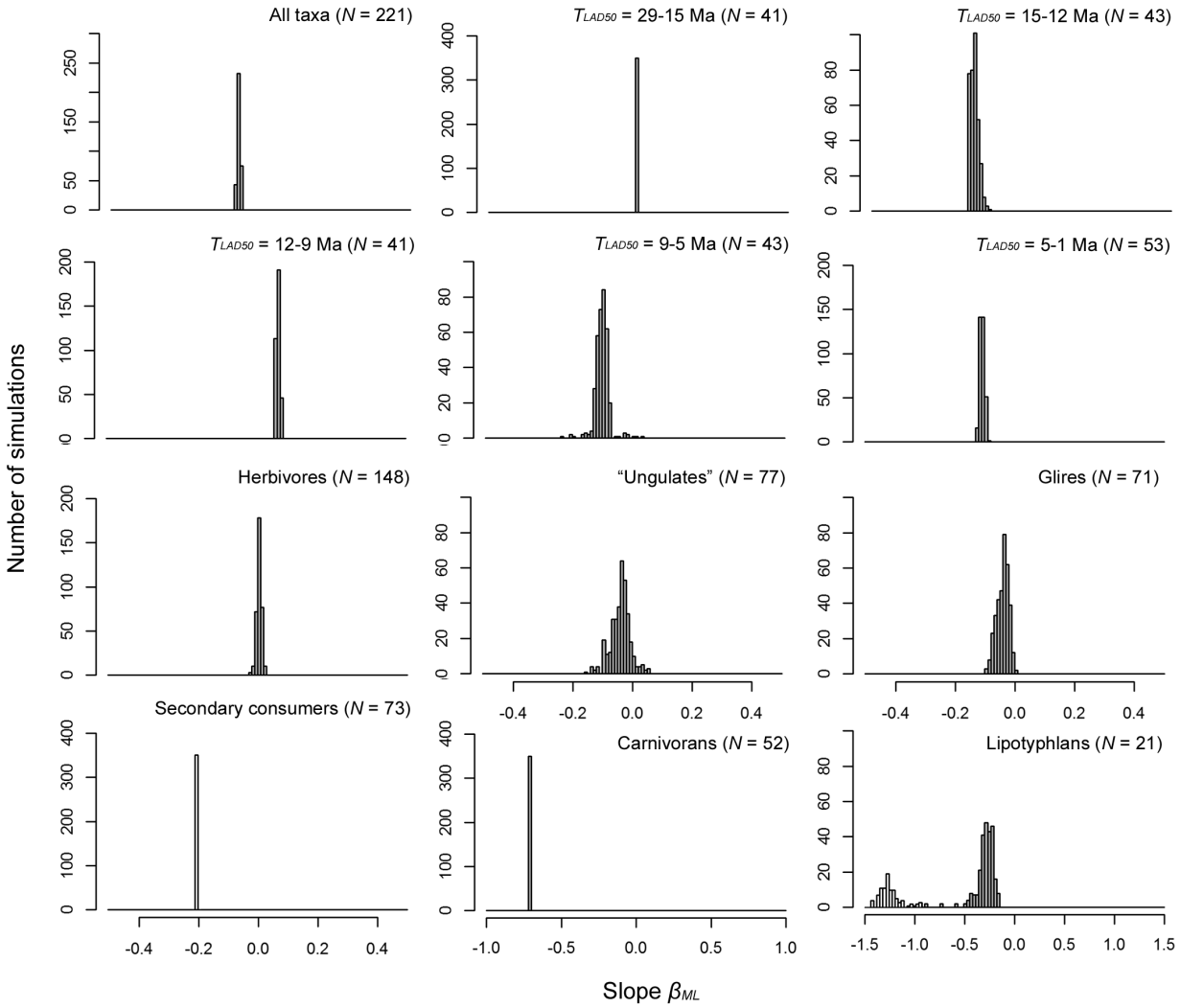

Figure 2.13: Maximum-likelihood estimates of slope for regression of inter-birth interval lengths and durations. The results for 350 sets of simulated branch lengths are shown for each data subset. White bars represent estimated slopes that differ from zero at the significance level of $\alpha = 0.05$.

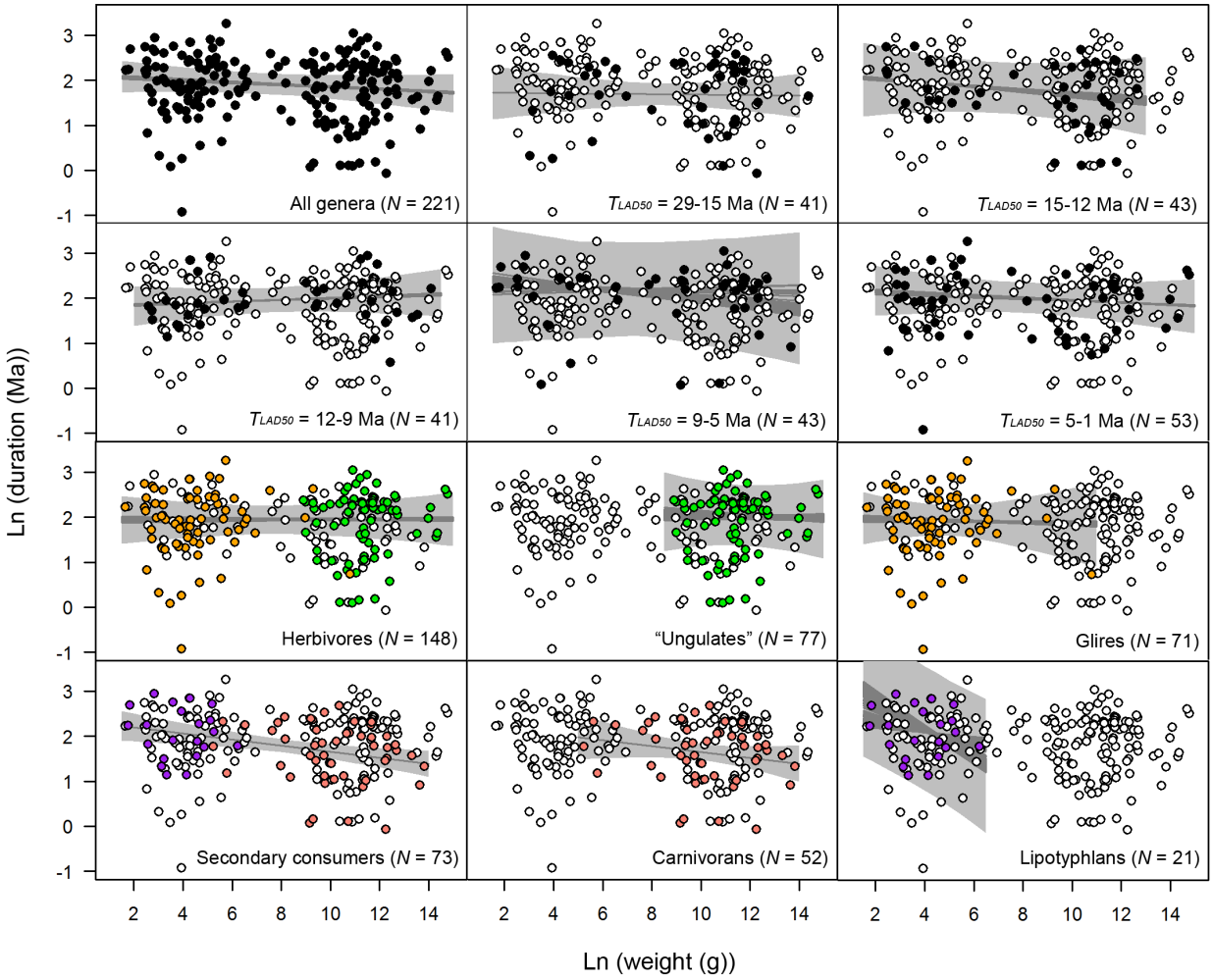

Figure 2.14: Relationships between estimated body weights and sampling-adjusted durations. In each plot, filled circles represent the subset of data that was selected for regression analysis; the regression lines (dark gray lines) and 95% confidence intervals (light gray areas) for 1,000 sets of simulated branch lengths are overlaid. Taxonomic groups that approximate major ecological divisions among terrestrial mammals are color-coded as in figure 1.

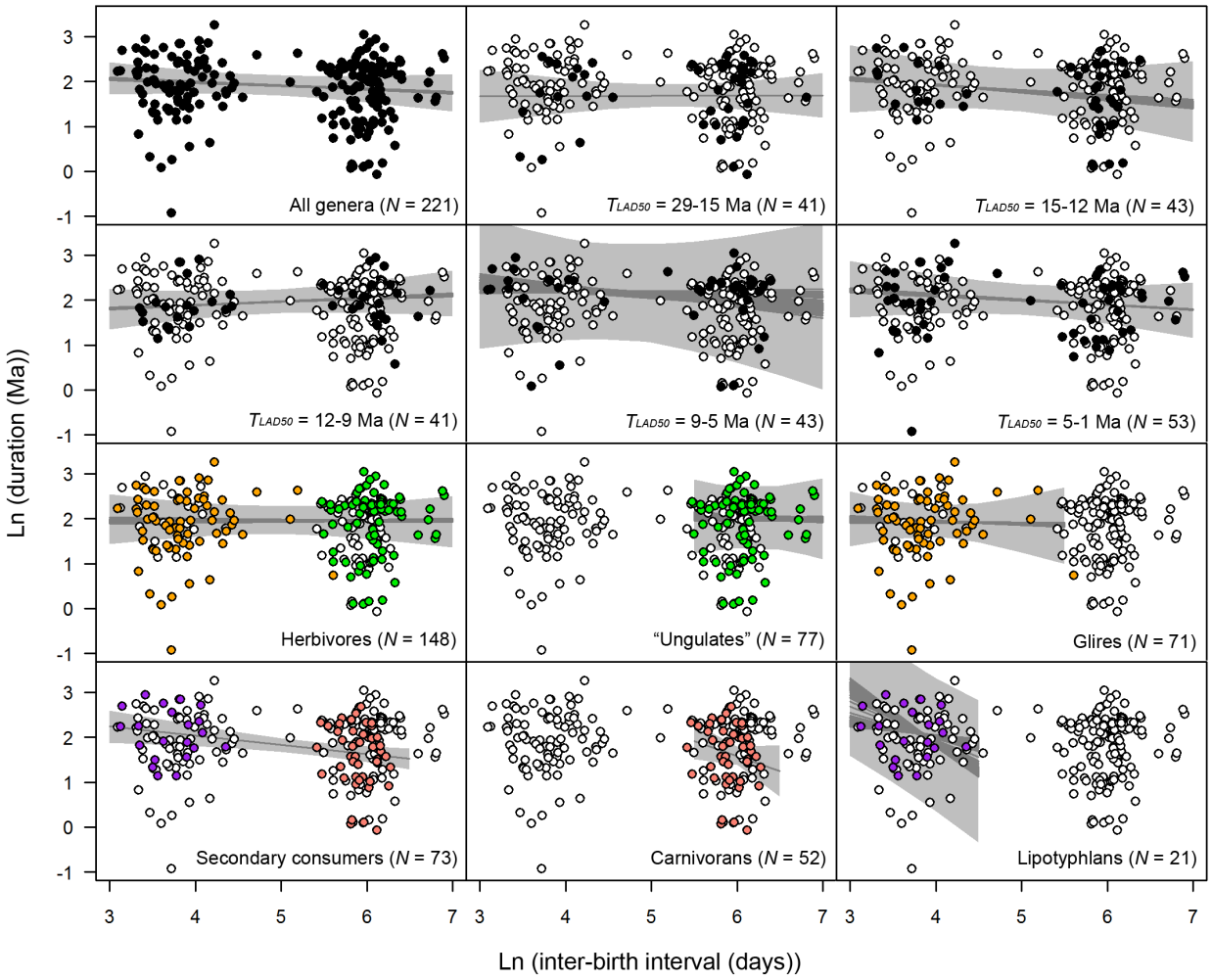

Figure 2.15: Relationships between expected inter-birth interval lengths and sampling-adjusted durations. Symbols and presentation of regression results (here based on 350 sets of simulated branch lengths) as in Figure 2.14. The results for "ungulates," glires, carnivorans, and lipotyphlans are expected to be identical to those for body weights (Fig. 2.14) except for the different scales of predictor variable and randomness of simulations.

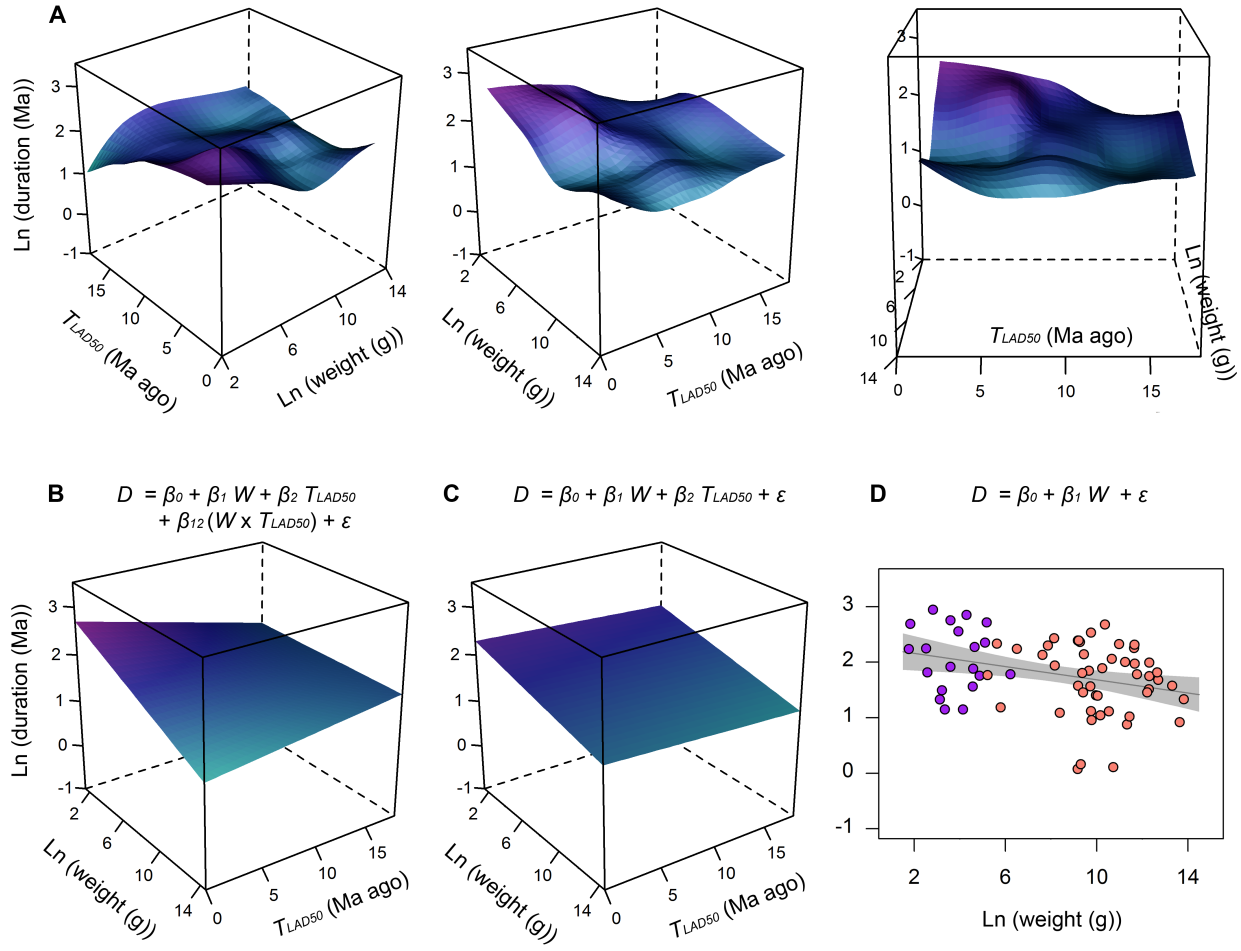

Figure 2.16: Results of additional analyses for secondary consumers. *A*, locally-weighted scatter-plot smoothing (LOWESS) surface shown from 3 different angles; *B*, ordinary least-squares (OLS) regression surface for a model with an interaction term; *C*, OLS regression surface for an additive model; *D*, OLS regression line and 95% confidence interval for the 2-variable model for lipotyphlans (purple) and carnivorans (pink) combined. Here, unlike in Figs. 2.14-2.15, only those genera ($N = 68$) with their last appearance dates in the last 18 Ma and durations of 12 Ma or less are considered (see Fig. 2.2). See Table 2.3 for regression statistics.

Chapter 3

Concordance and discordance of diversity dynamics across mammalian trophic groups in the middle Eocene of coastal southern California

Introduction

The degree to which trophic interactions influence the macroevolution of mammalian carnivores is poorly understood. While modern ecological studies have uncovered the often-critical roles played by mammalian predators in local community assembly to landscape-level ecosystem processes (see e.g., Estes et al., 2011; Roemer et al., 2009), dynamics that play out over longer time scales require looking at the fossil record. Such long-term investigations of fossil carnivores have typically been confined to the predators themselves (e.g., Van Valkenburgh, 1985, 1989; Morlo, 1999; Wesley-Hunt, 2005). Comparative examination of temporal changes in the ecological structures of carnivores in concert with their potential prey can potentially illuminate ecological underpinnings of diversity dynamics that manifest at the level of multi-trophic taxonomic assemblages, although only certain kinds of information on specific predator-prey interactions can be extracted from the mammalian fossil record.

An impetus for the present study came from an earlier work by Van Valkenburgh and Janis (1993), which compared the diversity trajectories of large mammalian carnivores and herbivores in North America over the last 44 million years (Ma). The authors found statistically-significant correlation between the shifts in large carnivore and herbivore species richness. However, the herbivore richness was shown to be more volatile, contributing to substantial fluctuations in the predator-prey ratio at the continental scale over geologic time. These observations suggest a certain degree of mechanistic decoupling of carnivore and herbivore diversity dynamics. The present study subjects this hypothesis to further testing by tracking shifts in the morphological compositions of carnivores and other mammals at a regional scale, which benefits from greater ecological coherence in terms of taxonomic associations than studies at the continental scale. In addition, I expand the scope of investigation to include small to medium-sized mammals in an attempt to (1) detect key environmental changes and (2) take into account their indirect but possibly crucial interactions with large mammals (see e.g., Keesing, 1998). The rich terrestrial fossil record of the middle Eocene of southern California (encompassing the period of roughly 47-37 Ma ago) provides an ideal data set for this study, and is made particularly valuable because of the intensive efforts to screen-wash bulk sediment (cf. Lillegraven and Wilson, 1975; Novacek, 1976; Kelly et al., 1991; Walsh, 1996, 2010), which enhances the recovery of small mammalian fossils (cf. Wolff, 1975). From the paleobiological perspective, the middle Eocene marks an important period for the early diversification of crown-clade carnivorans (Chapter 1, Tomiya, 2011).

The immediate goals of this study are (1) to infer the chronological sequence of the southern California fossil assemblages at as fine a scale as possible by reconstructing their relative ages from lithologically-disconnected areas within the study region (i.e., Ventura County, northwestern San Diego County, and southwestern San Diego County) and (2) to analyze the ecological patterns of faunal change at the regional scale.

Geographic Context

The middle-Eocene fossil assemblages considered in the present study come from 188 localities in the counties of San Diego and Ventura, California, and encompass a distance of approximately 300 km along a northwest-southeast axis that more or less parallels the present-day coastline (Fig. 3.1). Of these, most of the San Diego localities belong to the Friars and Mission Valley Formations in the southwestern part of the county in and around the city of San Diego, and to member C of the Santiago Formation in the northwestern part of the county including the cities of Carlsbad and Oceanside. All of the localities in the Ventura County belong to the middle member of Sespe Formation in the Simi Valley area.

The paleobiogeographical aspects of the middle-Eocene mammalian fauna of southern California have been reviewed extensively by Lillegraven (1976), Golz and Lillegraven (1977), Novacek and Lillegraven (1979), Kelly (1990),Walsh (1996), and Kelly et al. (2012). Palinspastic reconstructions along the regional fault systems suggest the placement of the San Diego area at paleolatitudes of 28-30 degrees north, possibly several hundred kilometers to the southeast of its current position (Lillegraven, 1976; Myers, 1991).

Geologic Context

The lithology of the geologic formations included in this study varies from claystone to conglomerate (see Walsh et al., 1996, for the most recent overview), and corresponding depositional environments have been inferred to have ranged from subtidal zones (with associated marine invertebrate fossils) to lagoons (for example, with reed impressions and brackish molluscan fossils), stream channels, and floodplains. It is therefore plausible on the basis of sedimentary information alone that the vertebrate fossil assemblages recovered from the various localities represent elements of the regional fauna with a variety of environmental affinities. This would be important to consider in identifying patterns of regional faunal succession through time, as assemblages at the level of individual localities are likely (1) dominated by signals of their proximal mammalian communities and (2) influenced by hydrodynamic sorting of skeletal elements (Wolff, 1973). Nevertheless, geographic and stratigraphic proximity to marine sediments suggests that all of these lithologic units were probably deposited close (in the biogeographic sense) to the ancient coast (cf. Howell and Link, 1979; Kelly, 1990; Eisenberg and Abbott, 1991) and, as such, are likely associated with broadly similar ranges of habitats for mammals.

The current understanding of the relative and absolute ages of these lithologic units (Fig. 3.2; reviewed in Walsh et al., 1996; Kelly et al., 2012) are based directly on: (1) lithostratigraphy where superpositional relationships can be observed; (2) biochronological correlation using planktic foraminifers, calcareous nannoplankton, and mollusks from marine sediments; (3) mammalian biostratigraphy that relies on inter-regional correlation with the fossil record of the Western Interior; (4) pollen biostratigraphic correlation with the record from the Transverse Ranges of California (Frederiksen, 1991); (5) magnetostratigraphy; and (6) a single radioisotopic $^{40}Ar/^{39}Ar$ date of 42.83 ± 0.24 Ma from a bentonite (a mineral product of altered volcanic ash) layer within the Mission Valley Formation. Despite these efforts on multiple fronts, the overall temporal resolution of the middle-Eocene mammalian fossil record of southern California remains rather low for various reasons, and the absolute-age ranges of lithologic units as depicted in Figure 2 should not, in general, be taken precisely to within one million years (Walsh, 1996). First, it is important to

note that most of the fossil localities of San Diego County were discovered during paleontological mitigation of land-development projects from the late 1960s to the present (locality records on file at the San Diego Natural History Museum and the University of California Museum of Paleontology) on increasingly urbanized landscapes. Fossil-bearing rock exposures are generally limited in their depths (cf. Walsh et al., 1996), frequently isolated from one another, and are usually destroyed by development subsequent to collecting of fossils, making it difficult to determine the stratigraphic relationships of localities both within each formation and among formations in different areas of the county. Additional uncertainties in relative locality ages are introduced by the prevalence of gradational and intergradational contacts between superposed lithostratigraphic units (see e.g., Walsh and Deméré, 1991; Walsh et al., 1996).

Likewise, the temporal correlation between various localities in San Diego County and those in the Sespe Formation of Ventura County (separated by $>$150 km) has been hampered by the lack of a unified lithostratigraphic framework. For example, a group of paleobiologically-important assemblages collectively known as the Laguna Riviera local fauna from northwestern San Diego County has variously been assigned to the late Uintan North American Land Mammal Age (NALMA) based on the perceived stage of dental evolution among artiodactyls similar to that seen in assemblages from the lower portion of the middle member of Sespe Formation (Golz, 1976; Golz and Lillegraven, 1977; but see Kelly et al., 1991), or to the early Duchesnean NALMA based on shared occurrences of a few taxa both in Laguna Riviera local fauna and in the upper portion of the middle member of Sespe Formation but nowhere else (Walsh, 1996). Such conflicting assessments cannot be readily resolved without knowing which taxa are chronologically more informative than others. In an attempt to increase the temporal resolution of the pertinent fossil occurrence data for subsequent analyses, I first conducted numerical ordination of fossil localities and their associated taxonomic assemblages.

Paleoenvironmental Context

The global paleoclimate of the middle Eocene is characterized by gradual cooling from the hot tropical condition of the earlier Eocene (Zachos et al., 2001). Against this backdrop, a geologically-brief period (ca. 100,000-500,000 years in duration) of 4-6°Cwarming took place around 40 Ma ago and is known as the middle-Eocene Climatic Optimum (Bohaty et al., 2009). Much of the mammalian fossil record examined here, however, likely predates this event if the recent chronological revision of the mammalian fauna from the Sespe Formation of Ventura County is accepted (Kelly et al., 2012).

Studies of palynological samples from the Delmar Formation, Ardath Shale, and the lower portion of Mission Valley Formation (Frederiksen, 1991, and references therein; see also Walsh, 1996) as well as plant macrofossils from the Torrey Sandstone and localities tentatively assigned to the Friars Formation (Myers, 1991, 2003*a*) suggest relative stability from the ?Bridgerian to the latter part of Uintan NALMA (prior to ca. 43 Ma ago if the single radioisotopic date from the Mission Valley Formation is correct) of a regional flora that is indicative of a thermally equable, summer-wet paratropical climate. For example, based on the environmental requirements of nearest living relatives and the proportion of species with entire-margined leaves, the mean annual temperature of at least 20°C, mean annual temperature range of perhaps around 7°C, and mean annual precipitation of 1,200-1,500 mm have been estimated from the plant assemblage of the Torrey Sandstone, which closely resembles the present-day floras of southeastern China and, to

a lesser extent, the Gulf Coast of North America (Myers, 1991). Of additional paleoecological importance are macrofossil assemblages presumably belonging to the Friars Formation that have yielded abundant lianas and possible epiphytes, indicating the presence of multi-tiered rainforests at least in the coastal areas of the region under a climate similar to that associated with the Torrey flora (Myers, 2003*a*).

These climatic interpretations are supported for the early part of middle Eocene by well-developed paleosol with abundant quartz, kaolinite, and iron oxide from the Mount Soledad Formation (roughly contemporaneous with the Delmar Formation, Torrey Sandstone, and Ardath Shale; Fig. 3.2), which indicate a warm, wet climate (Peterson and Abbott, 1979). Although common occurrence of a particular type of woody particles (considered to be products of wildfires) in the Ardath Shale and Mission Valley Formation has led Frederiksen (1991) to hypothesize the existence of a presumably short dry season, such a scenario may not be incompatible with the paratropical climatic reconstruction. Additional support, if preliminary, for at least moderately-high precipitation during the time of deposition of a part of the member C of Santiago Formation comes from a morphological analysis of land-snail shells collected at the vertebrate-rich "Jeff's Discovery" site (Roth, 1991, locality unit labeled "SJD" in Figs. 3.5, 3.6).

It is worth noting, however, that the apparent persistence of a moderately-wet climate into at least part of the Mission Valley time conflicts with sedimentological studies (e.g., Peterson and Abbott, 1979) that suggest a semi-arid climate with mean annual precipitation of less than 630 mm for the time period represented by the Friars and Mission Valley Formations. This latter estimate stems from the typical thickness of prevalent caliche horizons in the two geologic formations, and a seasonally-dry environment was further inferred from (1) clay minerals from the Friars and Mission Valley Formations that are chiefly represented by vermiculite and smectite (reflecting weak weathering in contrast to the severe weathering that produces kaolinite, as mentioned above for the Mount Soledad Formation) and (2) the depositional system for the Stadium and Pomerado Conglomerates interpreted as a river system with generally low water discharge punctuated by episodic large floods. Because published paleobotanical data are few and sparsely distributed in the Friars and Mission Valley Formations, the possibility cannot be discounted that this time period witnessed substantial climatic fluctuations. Such an ad hoc explanation, however, is inconsistent with the previous sedimentological descriptions (Peterson and Abbott, 1979) that portray these formations as rather uniform with respect to their climatically-informative characteristics. In any case, the precipitation estimate by Peterson and Abbott (1979) warrants re-examination. If, as I am inclined to believe, the climatic reconstruction based on paleobotanical evidence is accurate, then it may not be necessary to invoke the kind of complex savanna vegetation envisioned by Novacek and Lillegraven (1979) as the context for the regional mammalian fauna.

The most significant paleoenvironmental event of the middle Eocene in the region is probably the drastic loss of floral diversity that is indicated by approximately 40% reduction in the number of angiosperm pollen taxa that took place roughly between 40 and 38 Ma (the first two-thirds of Bartonian age according to Frederiksen, 1991; also see Walsh, 1996 regarding the age of this event). Frederiksen (1991) interpreted the floral decline as indicative of reduced precipitation and called this episode the "middle-Eocene Climatic Deterioration" (Frederiksen, 1991), which may represent the aftermath of the middle-Eocene Climatic Optimum mentioned above.

Materials and Methods

Institutional Abbreviations

AMNH, American Museum of Natural History, New York, New York; CIT, California Institute of Technology, Pasadena, California (vertebrate paleontology collection currently housed at the Natural History Museum of Los Angeles County); LACM, Natural History Museum of Los Angeles County, Los Angeles, California; SDSNH, San Diego Natural History Museum, San Diego, California; UCMP, University of California Museum of Paleontology, Berkeley, California.

Morphological and taxonomic-occurrence data

Linear measurements were taken with digital calipers, an ocular micrometer, or an Ehrenreich Photo-Optical Industries Shopscope to the nearest 0.01 mm.

Taxonomic-occurrence data for localities in San Diego County were primarily taken from the vertebrate fossil specimen records of the San Diego Natural History Museum (SDSNH) and the University of California Museum of Paleontology (UCMP), and those for localities in Ventura County were compiled from taxonomic lists of Kelly (1990); Kelly et al. (1991); Kelly (1992); Kelly and Whistler (1994), respectively. The taxonomic classification adopted here generally follows those of Janis et al. (1998, 2008). All currently-accessible specimens (originals or casts) of the carnivoramorphans, hyaenodontid creodonts, and mesonychians that are included in the analyses below were directly examined by the author. Although the identifications of specimens representing other groups of mammals have been checked for accuracy so far as possible, a large portion of the >30,000 cataloged specimens analyzed here have yet to be directly examined by the author.

The analyses below are based on the combination of: (1) 33,026 mammalian fossil specimens (mostly in the SDSNH and UCMP collections) that are identified at the level of genus or below, representing 93 genera and possibly up to 193 species from 177 localities; and (2) additional taxonomic occurrence data for the Simi Valley localities of the Sespe Formation, which were adopted from published lists of Kelly (1990), Kelly et al. (1991), and Kelly and Whistler (1994) (see also Kelly, 1992; Kelly and Whistler, 1998). The taxonomic occurrence data analyzed in this study are available as Supporting Material Appendix S3.1.

Temporal Ordination of Fossil Assemblages

Appearance event ordination (Alroy, 1994) was conducted to infer the relative ages of fossil assemblages based on their taxonomic compositions and, where available, known stratigraphic superpositions of the fossil-bearing localities. Briefly, the method involves the following steps: (1) temporal ordering of first and last appearances of all the taxa in the data set in a way that minimizes the number of invoked but unobserved taxonomic (co-)occurrences (Fig. 3.3A-C); (2) determination of relative ages (or, more precisely, possible ranges of relative ages) of localities based on the oldest last appearance date and the youngest first appearance date for their respective taxonomic assemblages (Fig. 3.3D). For the purpose of temporally correlating fossil assemblages, this approach is preferable to phenetic techniques (e.g., cluster analysis), since the latter is influenced

by the selection of similarity index, and because overall similarity of taxonomic compositions between assemblages, however quantified, is more sensitive to taphonomic variations (Alroy, 1992). Of course, no biochronological method is immune to taphonomic biases, and the relative locality ages inferred from the appearance event ordination should be interpreted carefully.

Although not required, prior knowledge of relative ages of some of the localities based on stratigraphic information can be incorporated into the ordination process so as to constrain the parsimonious optimization of the sequence of first and last appearance events (Fig. 3.3B; see Alroy, 1994, for computational details). To this end, the following ascending order of lithostratigraphic units was adopted from the literature (reviewed in Walsh et al., 1996, and Kelly et al., 2012; see also Fig. 3.2): (1) Delmar Formation; (2) Ardath Shale, Scripps Formation, and Friars Formation; (3) Mission Valley Formation, Pomerado Conglomerate, and Sweetwater Formation. Further, all fossil assemblages from the middle member of Sespe Formation were designated as younger in ages than those from the Delmar Formation, Ardath Shale, Scripps Formation, Friars Formation, and Stadium Conglomerate based on previous bio- and magnetostratigraphic studies (Walsh, 1996; Kelly et al., 2012). Within the formations, the following relationships were accepted (cf. Walsh et al., 1996): (1) the upper tongue of Friars Formation overlies the lower tongue; (2) the upper member of Pomerado Conglomerate overlies the lower tongue; (3) the upper member of Stadium Conglomerate overlies the lower member; (4) the member C of Santiago Formation overlies the member B. Additional superpositional relationships at finer stratigraphic scales (generally within local stratigraphic sections) were adopted from Walsh (1996), Walsh et al. (1996), Kelly (1990), Kelly et al. (1991), andMihlbachler and Deméré (2009), and the locality records on file at SDSNH for pairs of localities that are lithologically distinct (Appendix S3.2).

In the original ordination procedure of Alroy 1994, stratigraphic information, where available, was used to identify the precedence of the first appearance of one taxon over the last appearance of another (which is otherwise only apparent when the two taxa are known from the same locality). In the present study, the ranges of possible locality ages obtained through this method was, where applicable, further and directly constrained by the known superpositional relationships of localities, thus utilizing the stratigraphic information in two separate steps (Fig. 3.3B, D).

As mentioned above, relative ages of localities and their associated assemblages are tied to taxonomic first and last appearances. Each first or last appearance represents—and is counted as—a distinct event. However, it is more useful to reference locality ages to informal time steps that are defined by sets of taxonomic events rather than individual taxonomic events themselves, since the relative ages of certain taxonomic events are indistinguishable using the ordination method. Thus, the earliest set of taxonomic first appearance events marks Step 1, the next earliest set of events defines Step 2, and so forth, and the estimated age of an assemblage from a locality is given as, for instance, "between Step 4 and Step 7" (Fig. 3.3C) It is important to note that only the order of time steps can be hypothesized; neither their absolute ages nor their durations relative to one another can be deduced without additional information.

Generally, fossil assemblages from individual localities were treated as the minimum unit for appearance event ordination. In some cases, however, assemblages from separate localities were combined as "locality units" for the ordination when (1) localities belonged to the same lithologically-distinct stratum in a local setting according to the SDSNH record, (2) some localities were stratigraphic subsets of others, or (3) localities were located in the same local stratigraphic section, not separated by an unconformity, and have previously been assigned to the same local fauna based on similarities in lithology or taxonomic compositions. These include (Walsh, 1996):

the SDSNH "Jeff's Discovery" localities 3560-3564; SDSNH "Mission del Oro" localities 3570, 3572, and 3574; SDSNH "Mesa Drive" localities 3440 and 3448 (grouped as one assemblage) and 3443, 3447, 3450, and 3465 (grouped as a second assemblage). Those taxa that are known from only a single locality are not informative for biochronological purpose, but such carnivores (e.g., "*Miacis*" *gracilis*) were included in analyses of taxonomic and morphological compositions of assemblages on the ground that the rarity of carnivore specimens are naturally expected. Localities that have yielded fewer than 4 taxa that are identified at the level of genus or below were excluded from this study as recommended by Alroy (1994), since assemblages with few taxa can unduly affect the result of numerical ordination.

The choice of taxonomic unit is important in inferring the relative ages of fossil localities and their associated mammalian assemblages from geographically-isolated stratigraphic sections. In principle, finer scales of taxonomic unit could enable temporal correlation of fossil localities with greater resolutions. In practice, however, the diagnostic traits at the finest taxonomic scale (generally species but occasionally subspecies) are often missing in fossil materials due to incomplete preservation, resulting in many specimens whose species-level identities are indeterminate. Furthermore, taxonomic "over-splitting" of true species (defined as a segment of an evolving metapopulation; cf. de Queiroz, 2007) stemming from failure to recognize intraspecific morphological variations in time or space can limit or mislead biochronological analyses. Indeed, as was common in the early history of vertebrate paleontology, many of the taxa apparently endemic to the middle Eocene of southern California were erected based on a few specimens. In cases where sufficiently large fossil samples have subsequently become available, consideration of intraspecific variations in dental morphology has tended to result in taxonomic unification of what had originally been regarded as distinct species (see e.g., Lillegraven and Wilson (1975) on the rodent *Simimys* and Wesley and Flynn (2003) on the carnivoramorphan *Tapocyon*; see also Rose and von Koenigswald (2007) for general comments on the taxonomy of ischyromyid rodents). For these reasons, a non-overlapping combination of 64 genera and potentially informative 20 species (totalling 84 taxa) was used in the appearance event ordination.

All computations for the appearance event ordination were performed in the R programming environment (R Developement Core Team, 2009).

Analysis of Morphological Composition

Determination of Ecomorphological Categories

Changes in the ecological structure within the carnivore and non-carnivore components of the regional mammalian fauna were inferred from shifts in the distribution of taxonomic diversity and abundance across morphological categories. Two types of morphological-compositional matrices (Fig. 3.3E) were constructed in which each row i and column j corresponded to a taxonomic assemblage from a locality unit (see above) and a morphological category, respectively, and each matrix element represented either the number of cataloged specimens of all the taxa from locality i that are classified into the category j (specimen-count matrix) or the number of taxa from locality i that are classified into the category j (taxon-count matrix). The specimen-count matrix is intended to capture the abundance of taxa in each broadly-defined morphological category without regard to their taxonomic identities, whereas the taxon-count matrix should reflect the division of regional faunal diversity into various ecological types. Elements of the specimen-count matrix

were natural-log transformed prior to analysis in order to reduce the undue influence of extremely large specimen counts, which are sometimes associated with separate numbering of dissociated skeletal elements in museum collections that may well have belonged to a much smaller number of individual organisms (e.g., specimens of the brontothere *Duchesneodus californicus* from Pearson Ranch local fauna (CS20 in the data set); author's personal observation). An alternative measure of relative abundance would be based on the minimum numbers of individuals estimated from skeletal-element counts, but the required data have not been gathered. In constructing the taxon-count matrix, unidentified species of a genus were treated as a taxon that is distinct from all other identified species of the same genus (see Appendix 3.2 for the list of taxa that were treated as distinct from one another).

Carnivores: The mammalian carnivores were grouped into 6 categories defined by combinations of estimated body weight and diet inferred from dentition (Table 3.1, Appendices 3.1, 3.2). Only two dietary types were recognized: (a) carnivory, which may be supplemented by consumption of food other than mammalian prey (e.g., eggs, invertebrates, plants); (b) hypercarnivory, with greater dependence on mammalian prey. These two types were distinguished by the presence (a) or absence (b) of molar talonid basins that are important for grinding of food material other than vertebrate tissues; the correlation between this functional morphology and diet is well established for living carnivorans of various body size (Van Valkenburgh, 1989; Friscia et al., 2007). The superficially cat-like nimravids and species of the creodont genus *Hyaenodon* were assigned to the hypercarnivorous type; all other carnivoramorphans and the creodont *Limnocyon* were placed in the more generalized carnivore group. While living carnivorans are characterized by a wide range of diet and, consequently, dental morphology, it is intriguing that all of the middle-Eocene carnivoramorphans included here possess at least one pair of teeth with well-developed blades for shearing; none of them exhibits clear adaptation for omnivory as in extant bears and raccoons, for example, or herbivory as in the kinkajou. The mesonychian *Harpagolestes* was assigned to the hypercarnivorous type following the interpretation by Szalay and Gould (1966) of their dentition as conductive to bone crushing.

Although locomotor habit is potentially important for understanding the diversity dynamics of mammalian predators (cf. Van Valkenburgh, 1985), postcranial skeletal elements have not been described for the majority of carnivores in this study. It is worth noting, however, that postcranial skeletons of early to middle Eocene carnivoramorphans have generally been compared to those of terretrial and scansorial (i.e., capable of climbing but spends substantial amount of time on the ground) extant representatives (Heinrich and Rose, 1995, 1997; Spaulding and Flynn, 2009; Tomiya, 2011). Skeletal modifications for sustained high-speed running (i.e., cursoriality), predominantly arboreal mode of life (as in the extant kinkajou), or semi-fossorial habit (as in the extant North American badger) is unknown in most of the mammalian carnivores from before the Oligocene Epoch (see e.g., Janis and Wilhelm, 1993).

Non-carnivores: Temporal patterns of the distribution of non-carnivore dietary types (inferred from dental morphology) could provide insights into the environmental history of the region. On the other hand, it is questionable whether the diet of potential prey species directly influences the predation behavior of mammalian carnivores, except in cases of intraguild predation among carnivores. Thus, two morphological classification systems were employed for separate analyses: (1) combinations of estimated body weight and arboreal or non-arboreal habit; (2) combinations of the variables in (1) plus dental morphology or inferred diet (grouped into 8 types). In total, 11 and 30 non-carnivore categories were established by the first and the second classification systems,

respectively (Table 3.1).

The purpose of distinguishing arboreal from non-arboreal taxa is to recognize a set of non-carnivores that are generally outside the reach of terrestrial carnivores. To this end, the "arboreal" taxa are here restricted to those that are primarily tree-dwelling, and do not include animals that are capable climbers but likely spend substantial amount of time on the ground (e.g., scansorial rodents). The locomotor classification is necessarily provisional, since postcranial material is poorly known for many of the rodents. For the purpose of this study, a taxon was classified as non-arboreal unless there was strong evidence to the contrary. Thus, the arboreal category included all primates (plesiadapiforms and euprimates; cf. Silcox and Gunnell, 2008, and Gunnell et al., 2008), the apatemyid *Apatemys* (cf. von Koenigswald et al., 2005), and the peradectine marsupial *Peradectes* (cf. Rose, 2006, and references therein).

The classification of ungulate dental types into "bunodont" (low-cusped), "semi-lophed" (equivalent to bunoselenodont and bunolophodont, showing intermediate developement of ridges on cheek teeth), and "lophed" (cheek teeth with well-developed ridges) follows that of Janis (2000). Among living ungulates, these dental morphotypes show close correspondence with a spectrum of hebivorous diet ranging from fruits to more fibrous plant tissues (e.g., leaves and shoots; Janis, 2000). A few rodents were classified into the semi-lophed and lophed dental types to distinguish them from their typically-bunodont relatives; it is not implied here that these rodents necessarily had diets similar to those of semi-/lophed ungulates. With regard to primates, dietary inferences were adopted primarily from Strait (2001), Gunnell and Rose (2002), and Gilbert (2005). The assignment here of the enigmatic pantolestan *Simidectes* to the bunodont type is not entirely accurate as its dentition (lower molars in particular) shows some gross-structural similarities to those of carnivoramorphans. Coombs (1971), however, noted the lack of precise shearing action between the upper and lower cheek teeth (as occurs in most carnivoramorphans) and suggested that they functioned primarily for crushing rather than slicing of food items. The postcranial skeleton of an European Eocene pantolestan has been interpreted as indicative of a river otter-like semi-aquatic habit (Rose, 2006, and references therein), and the extreme dental wear that is present on multiple specimens of *Simidectes merriami* (author's personal observation) certainly seems consistent with a diet dominated by hard-shelled aquatic invertebrates.

Body-weight Estimation

So far as possible, body weights were estimated based on original and published craniodental measurements of specimens from the middle Eocene of southern California; for those taxa for which these data are presently unavailable, published measurements for the same taxon from outside southern California or measurements for their closest relatives (generally other species of the same genus) were adopted from the Paleobiology Database (www.paleodb.org) as surrogates. From these measurements, weights were predicted using least-squares regression equations of: Gordon (2003) for marsupials; Legendre (1986) and, when the lower tooth-row length was available, Hopkins (2008*b*) for rodents; Bloch et al. (1998) for lipotyphlans and the apatotherian *Apatemys*; Conroy (1987) for primates (including plesiadapiforms); Damuth (1990) for artiodactyls and perissodactyls; and Van Valkenburgh (1990) for carnivorans, the pantolestan *Simidectes*, and the mesonychian *Harpagolestes*. Among the carnivores, body-weight estimation based on dental measurements is particularly problematic with creodonts and mesonychians—two groups with unique dentition and no extant representatives. The estimate for *Harpagolestes* is therefore based

on the approximate cranial length of a specimen of *H. uintensis* (Osborn, 1895) whose dental dimensions are similar to those of the specimens from southern California. In the case of creodonts, the body weight of *Limnocyon* sp. was predicted based on the humeral length and the equation of Egi (2001); the weights of two species of *Hyaenodon* that are not included in the study by Egi (2001)) were predicted via linear regression using her postcrania-based estimates for *H. crucians* and *H. horridus* and published measurements of the lengths of the lower third molars of these four species (Mellet, 1977). Body size classes were defined broadly enough (such that each class spans an order of magnitude in weight in grams) to accommodate intraspecific variation and frequently substantial errors associated with weight estimation based on a single tooth (cf. Damuth, 1990; Van Valkenburgh, 1990). All metric data and predictive equations used for body-weight estimation are presented in Appendix 3.1.

Analyses of Aggregated and Locality-level Assemblages

The incompleteness of fossil record presents an acute problem to quantitative investigation focused on community paleoecology of mammalian carnivores. For example, despite the diversity of carnivores known from the middle Eocene of southern California, only 24 out of 177 localities subjected to the appearance event ordination have yielded at least one cataloged specimen of carnivore that is identified at the level of genus or below. It would be unreasonable to accept their absence at the majority of fossil sites as reflection of their true absence from the regional fauna (or even local community), and so reasonable extension of their observed ranges, whether in time or space, is desirable. Unfortunately, probabilistic approaches such as the one used in Chapter 2 are not readily applicable to the case at hand because the absolute ages of the fossil assemblages considered here are poorly known. As discussed below, the statistical analyses conducted in this study requires assignment of locality-level assemblages to time bins such that each bin—which encompasses one or more time steps as defined above—contains multiple assemblages as samples (albeit non-independent ones) of the regional fauna from that time interval. For the purpose of analyses, each carnivore is assumed to have ranged through one or more of these time bins. Thus, the question of how much extension of the observed temporal ranges of carnivores is reasonable essentially translates to how long the durations of time bins should be set to. To minimize the subjectivity, and because the carnivore diversity dynamics is the focus of this study, a set of time bins was initially designated in reference to the inferred first and last appearance events of carnivores included in the ordination (dashed lines in Figs. 3.3C-D, 3.4), which mark biologically significant points in time.

This resulted in seven bins with various numbers of steps. Of these, the time bin corresponding to Steps 5-22 (during which no first or last appearance event of a carnivore takes place) was divided into three subsets to keep track of the changes in the non-carnivore component of the regional fauna. Thus, a total of 9 bins were established: Time Bin 1, Step 1; Time Bin 2, Steps 2-4; Time Bin 3, Steps 5-7; Time Bin 4, Steps 8-15; Time Bin 5, Steps 16-22; Time Bin 6, Steps 23-26; Time Bin 7, Steps 27-32; Time Bin 8, Steps 33-34; Time Bin 9, Steps 35-36. Of the 177 assemblages, 57 could be placed entirely within one of these bins. The locality-level assemblages in each bin were then combined to form an aggregated assemblage (heretofore "meta-assemblage") for the time interval. To this, four carnivore taxa that are known from only a single locality (and thus could not be included in the ordination process) were added based on the relative age-estimates for the localities that have yielded them.

The degree of concordance between changes in the morphological compositions of carnivores on one hand and those of non-carnivores on the other was assessed by a set of Mantel tests as follows: (1) separate matrices were constructed for carnivores (9 x 6) and non-carnivores (9 x 11 for weight-locomotion categories; 9 x 30 for weight-locomotion-dental morphology categories), in which the rows i and columns j represented the meta-assemblages and morphological categories, respectively (Fig. 3.3E); (2) the difference in carnivore or non-carnivore composition between every pair of meta-assemblages was quantified by Jaccard (= Ružička) dissimilarity index and, alternatively, Manhattan distance (Fig. 3.3F); (3) the rank-order correlation between the resulting two dissimilarity/distance matrices (one based on carnivores, the other based on non-carnivores) was calculated, and its statistical significance was determined by permutation test. In addition, the compositional differences among the meta-assemblages were visualized through non-metric multidimensional scaling, and the plots obtained were Procrustes superimposed to compare carnivore and non-carnivore compositional variations. The two measures of compositional differences were used to compare patterns based on relative (Jaccard) and absolute taxon counts (Manhattan).

All statistical computations were performed with the *vegan* package for the R programming environment (Oksanen et al., 2009).

Results and Discussion

Temporal Ordination of Fossil Assemblages

A total of 36 distinct time steps were identified through the ordination of 168 taxonomic appearance events (Fig. 3.4). It should be noted that, although their relative ages are indistinguishable by the ordination, the taxonomically unique Simi Valley Landfill Local Fauna (SVLFLF) and SDSNH localities 4041-4042 are almost certainly younger than all other localities (cf. Kelly et al., 1991; Walsh, 2010) and are here considered as such.

Of biochronological importance, locality age estimates suggest that absolute-age ranges of lithologic units in gradational contact frequently overlap (Fig. 3.5). For example, although the conglomerate tongue of Friars Formation as a whole overlies the lower tongue of the same formation, some of the assemblages from the conglomerate tongue are likely older in age than some of the assemblages from the lower tongue. Similarly, at least some of the assemblages from the Mission Valley Formation may well be contemporaneous with those from the underlying Stadium Conglomerate. With regard to the temporal relationships among lithologic units in different areas, member B of the Santiago Formation in northwestern San Diego County appears to be largely correlative with the Friars Formation of southwestern San Diego County, although the SDSNH locality 4567 may be younger than any of the localities of Friars Formation. Among the major lithologic units, the member C of Santiago Formation most clearly encompasses a wide range of time steps, temporally bridging the record of the Sespe Formation in Ventura County with that of the southwestern San Diego County. Overall, the result of ordination demonstrates that lithostratigraphic boundaries are of limited value in an attempt to demarcate successive phases of the faunal change in this region.

General pattern of taxonomic turnover

Although the absolute ages of the time steps are unknown (that is, with a level of precision that would be informative for this study), the relative temporal pattern of first and last appearance events recovered from the appearance event ordination is generally consistent with gradual faunal turnover, since appearance events are spread across many steps (Fig. 3.4A, B, D). The only notable exception is the appearances of 14 new taxa at Step 3, causing 62% increase in the number of taxa that are included in the ordination. Since appearance event ordination as conducted here operates on the principle of parsimony—essentially minimizing the number of implied but unobserved presence of taxa, it is expected to be sensitive to incomplete sampling at early stages of the faunal sequence. For instance, if the second earliest assemblage is a taxonomic subset of the earliest one, the truly earliest assemblage will likely be inferred to be the second earliest assemblage because, in a sense, it is "pulled" toward more recent assemblages that contain subsequent occurrences of some of the taxa found in the earliest assemblage—positioning it as the earliest would invoke extra cases of presence without fossil evidence and thus be counter to the parsimony principle.

Indeed, inspection of taxonomic compositions of the hypothesized earliest and the second earliest sets of assemblages reveals that the former is largely a subset of the latter (Fig. 3.6; compare e.g., localities S3788-S3655 with S3785-S3784). The difference in taxonomic diversity between these two sets of localities may reflect difference in taphonomic (depositional or preservational) environment rather than separation in time, since (1) a substantial proportion (5 out of 13) of the additional taxa in the second earliest set of assemblages are likely arboreal taxa (see locality S3784 in Fig. 3.6), whereas perhaps only 2 (out of 21) are known from the presumed earliest set of assemblages, and (2) two of the arboreal taxa missing in the earliest set (marsupial *Peradectes* and euprimate *Washakius*) are relatively common elsewhere. In the absence of stratigraphic evidence to the contrary, however, the apparently sudden rise in diversity at this early stage of faunal sequence is tentatively accepted as a genuine pattern that possibly reflects a change in the flora and, concomitantly, macrohabitat structure. Although beyond the scope of present study, this assumption may be tested through detailed taphonomic analyses of these assemblages.

Ecological patterns of regional faunal succession

Different aspects of compositional shifts were examined through analyses of various combinations of ecological factors, including: (a) distribution of taxonomic diversity across morphotypes versus distribution of numbers of specimens (as a proxy for relative abundance) across morphotypes; (b) morphotypes defined by estimated body weight and arboreal/non-arboreal locomotor type versus morphotypes defined by these variables plus dental morphology/inferred diet; (c) distribution of taxa across morphotypes measured in relative terms (using Jaccard index) versus distribution measured in a way that included the information on the absolute numbers of taxa (using Manhattan distance).

The history of carnivore diversity in the region (Figs. 3.4, 3.7A) appears to be characterized by (1) persistently low taxon counts through Step 22, that is, throughout the period of deposition of Friars Formation (and possibly Stadium Conglomerate and Mission Valley Formation as well), followed by (2) steady increase from 3 to 10 taxa toward the upper end of the faunal sequence, (3) increase in the number of body-size classes occupied by this trophic group (4) increase in the relative share of carnivore diversity in the small size class (estimated weight of less than 10 kg),

(4) general absence until the last time bin of hypercarnivores that are not specialized for bone-crushing (i.e., *Harpagolestes*) and (5) persistence throughout the faunal sequence of mesonychian *Harpagolestes*, which is the sole representative of the very large size class (estimated weight of greater than 100 kg).

The changes in the relative taxonomic diversity of morphotypes (i.e., the compositional differences measured by Jaccard dissimilarity index) does not correlate with changes in the non-carnivore composition regardless of how the latter is measured (Fig. 3.10, top row). In contrast, when the absolute as well as relative taxonomic diversity of carnivores was taken into account (i.e., the compositional differences measured by Manhattan distance), statistically significant rank-order correlation was observed between the shifts in carnivore composition on one hand and shifts in (a) the distribution of non-carnivore specimen counts (as a proxy for relative abundance) across morphological categories that reflected dental-morphological divisions (Fig. 3.10J), and (b) the distribution of absolute numbers of non-carnivore taxa across morphological categories that, again, reflected dental-morphological divisions (Fig. 3.10L). It should be noted that the significance values reported here (Table 3.2) are not adjusted for multiple testing, as it could be argued that each test concerns a distinct data set. Bonferroni correction for more than two multiple tests would, if applied, make the above observations statistically non-significant at the significance level of $\alpha = 0.1$ or below. More importantly, meta-assemblage pairs exist in both of these cases (Analyses J and L) that are similar in carnivore composition but differ considerably in non-carnivore composition (note data points in the lower right-hand corners of Fig. 3.10J, L). Some of these cases of discordance are related to the above mentioned episode of pronounced diversity increase at Step 3, which, in fact, is not accompanied by any change in the taxonomic (and hence morphological) composition of the carnivores (Fig. 3.4).

The compositional changes in non-carnivores that are possibly correlated with the shifts in carnivores (Analyses J and L, Fig. 3.10J, L) do not appear to be readily interpretable in terms of possible trophic interactions (Figs. 3.7-3.9). Arboreal taxa are initially (Time Bin 1) relatively rare both in taxonomic diversity and specimen counts, then become considerably more common and occupy an increased number of morphological categories (Time Bins 2-7). The arboreal taxa decline towards the upper end of faunal sequence (Figs. 3.7-3.9). This pattern is roughly mirrored by a similar waxing and waning of small non-arboreal taxa (Figs. 3.7-3.9), with increasingly even distribution of specimen counts across the body size spectrum of non-arboreal taxa as a whole (Figs. 3.7C, 3.9). The youngest meta-assemblage from the Time Bin 9 is also marked by a sudden increase in the number of large herbivores with lophed cheek teeth (Fig. 3.8). For the most part, neither the tempo nor the directionality of shifts in carnivores and non-carnivores seems to be in clear accord.

Finally, the possibility that these apparent patterns reflect taphonomic variations—in particular, differential preservation and recovery of fossils at different localities—more than true temporal succession of the regional fauna was addressed by assessing the correlation between non-carnivore composition at the locality-level and a set of predictive variables consisting of: (1) the age of locality in terms of its affiliation with a time bin (treated as an ordered factor); (2) basic lithology of the sedimentary deposit at the fossil locality (mudstone, mud and siltstone, siltstone, sandstone, or conglomerate); (3) natural-log transformed number of specimens (identified at the level of genus or below) collected from the locality; and (4) natural-log transformed weight (originally in kilograms) of the sedimentary matrix that was collected from the locality and screen-washed to recover small vertebrate remains (these data were extracted from the locality record on file at the SDSNH).

Permutational multivariate analysis of variance (conducted with the *vegan* package of Oksanen et al., 2009) shows that compositional variation is in fact best explained by locality ages (Table 3.3, Fig. 3.12), suggesting that, at the scale of present study, the regional mammalian fossil record under consideration is not so heavily biased as to preclude chronological interpretation of the morphological differences observed among the sets of localities. Of note, the amounts of screen-washed sediment significantly correlates with compositional variations based on specimen counts, but its explanatory power is far more limited than that of the locality ages (Table 3.3).

The above observations as well as the result of appearance event ordination are, of course, subject to further testing through new fossil discoveries, refinement of taxonomy, and improved understanding of the palebiology of the animals.

Conclusions

The main finding of the present study is that morphological-compositional shifts of carnivores are largely decoupled from those of non-carnivores so long as the compositional shifts are measured as changes in the numbers of taxa or abundance of specimens across combined categories of body size, arboreal/non-arboreal habit, and dental ecomorphology. At the most coarse temporal scale, the monotonic increase in the number of carnivore taxa from the early Uintan through Duchesnean North American Land Mammal Ages of southern California does mirror that of non-carnivorous mammals. However, when the fundamental ecological compositions within the carnivore and non-carnivore trophic groups were examined in juxtaposition, only two cases (Analyses J and L above) of possible statistical correlation between carnivore and non-carnivore morphological shifts were found, when the non-carnivore composition incorporated dental ecomorphological categories. Thus, the abundance of individual organisms of non-carnivores and perhaps their biomass within each dietary category, rather than their taxonomic diversity, are more closely associated with the succession of carnivore guild. However, the statistical support for theses cases is modest at best, and, more problematically, the ecological link between the diversity dynamics of carnivores and their potential prey—if there is one—is obscure, even though clear compositional changes are detectable separately in carnivores and non-carnivores. Although the importance of trophic interactions in the structuring of mammalian assemblages is undeniable at the ecological time scale, the driving force for diversification and extinction of mammalian carnivores at the macroevolutionary time scale may need to be sought elsewhere—for instance, in competition among predators themselves and in aspects of predator-prey interactions that were not considered here, such as prey behaviors and distribution of biomass (rather than taxonomic diversity or abundance of individual organisms) across morphological types. In addition, the roles of non-mammalian vertebrate predators (e.g., boid snakes) may be a key to understanding the ecological diversity dynamics of mammals.

Supporting Material

The following Supporting Material is available in the .csv file format in the accompanying CD.

Appendix S3.1. Taxonomic occurrence data. A compilation of data from the collection records of the SDSNH and the UCMP and author's original list of specimens from certain localities of the

Sespe Formation (in the collection of LACM). Additional data for the specimens and localities included in this appendix are publically available at http://ucmpdb.berkeley.edu/ (UCMP) and http://www.sdnhm.org/archive/research/paleontology/searchdata.html (SDSNH).

Appendix S3.2. Stratigraphic superpositional relationships of localities. Each entry of "1" in Row i and Column j represents known stratigraphic position of locality i above locality j. See main text for the sources of information.

Table 3.1: Morphological Categories

Estimated weight (g)	10^0-10^1		10^1-10^2		10^2-10^3		10^3-10^4		10^4-10^5		10^5-10^6		$>10^6$	
Locomotor mode	Arboreal	Non-arboreal	Arboreal	Non-arboreal	Arboreal	Non-arboreal	Arboreal	Non-arboreal	Arboreal	Non-arboreal	Arboreal	Non-arboreal	Arboreal	Non-arboreal
All dental types[1]	A0	N0	A1	N1	A2	N2	A3	N3	A4	N4	A5	N5	A6	N6
Acute-cusped[2]		N0-ac	A1-ac	N1-ac										
Semi-acute-cusped[2]				N1-sa		N2-sa								
Bunodont[2]		N0-bu	A1-bu	N1-bu		N2-bu		N3-bu		N4-bu		N5-bu		
Semi-lophed[2]						N2-sl		N3-sl		N4-sl		N5-sl	A6-sl	
Lophed[2]				N1-lo		N2-lo		N3-lo		N4-lo		N5-lo		
Sectorial[2]														
Hyper-sectorial[2]														
Faunivore-frugivore[2,*]	A0-ff		A1-ff		A2-ff		A3-ff							
Frugivore[2,*]					A2-fr		A3-fr							
Folivore[2,*]					A2-fo		A3-fo							

NOTE—[1]Classification system for one set of analyses. [2]Classification for the second set of analyses. *Dietary categories for primates, including plesiadapiforms.

Table 3.2: List of analyses and Mantel test statistics

Analysis	Carnivore	Non-carnivore					
	Difference measure	Dental types	Difference measure	Counts	Procrustes square distance m^2	Mantel statistic r	Significance
A	Jaccard	N	Jaccard	taxa	0.603	-0.057	0.587
B	Jaccard	Y	Jaccard	taxa	0.554	0.178	0.162
C	Jaccard	N	Jaccard	specimen	0.881	0.113	0.239
D	Jaccard	Y	Jaccard	specimen	0.724	0.250	0.104
E	Jaccard	N	Manhattan	taxa	0.602	-0.112	0.726
F	Jaccard	Y	Manhattan	taxa	0.555	0.185	0.162
G	Manhattan	N	Jaccard	taxa	0.587	-0.012	0.418
H	Manhattan	Y	Jaccard	taxa	0.492	0.280	0.114
I	Manhattan	N	Jaccard	specimen	0.868	0.192	0.161
J	Manhattan	Y	Jaccard	specimen	0.603	0.326	0.083
K	Manhattan	N	Manhattan	taxa	0.587	0.004	0.455
L	Manhattan	Y	Manhattan	taxa	0.492	0.382	0.045

Table 3.3: Permutational MANOVA for non-carnivore composition

Analysis	Variable	d.f.	F	R^2	P
J (taxon counts)	Time Bin (9 ordered factors)	7	1.909	0.316	0.013
	Lithology (5 ordered factors)	4	1.168	0.110	0.271
	Ln (NISP)	1	0.554	0.013	0.756
	Ln (matrix weight (kg) + 1)	1	1.737	0.041	0.137
	Residual	22		0.520	
L (specimen counts)	Time Bin (9 ordered factors)	7	1.214	0.223	0.091
	Lithology (5 ordered factors)	4	1.213	0.128	0.143
	Ln (NISP)	1	0.920	0.024	0.496
	Ln (matrix weight (kg) + 1)	1	1.724	0.045	0.048
	Residual	22		0.579	

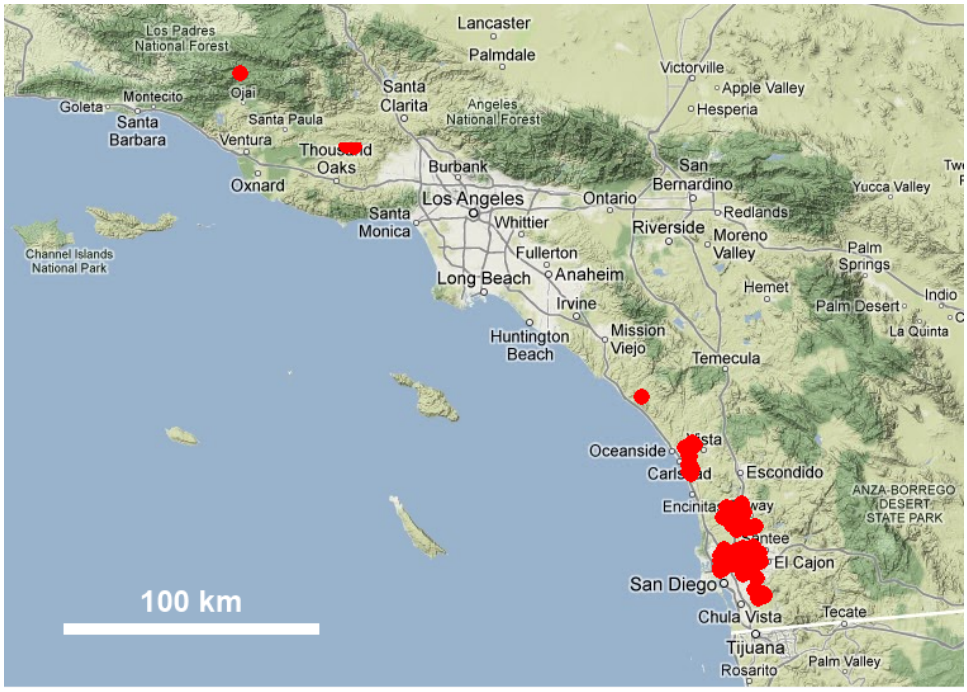

FIGURE 3.1: Map of southern California showing the distribution of fossil localities included in this study. Map generated by BerkeleyMapper (http://berkeleymapper.berkeley.edu/).

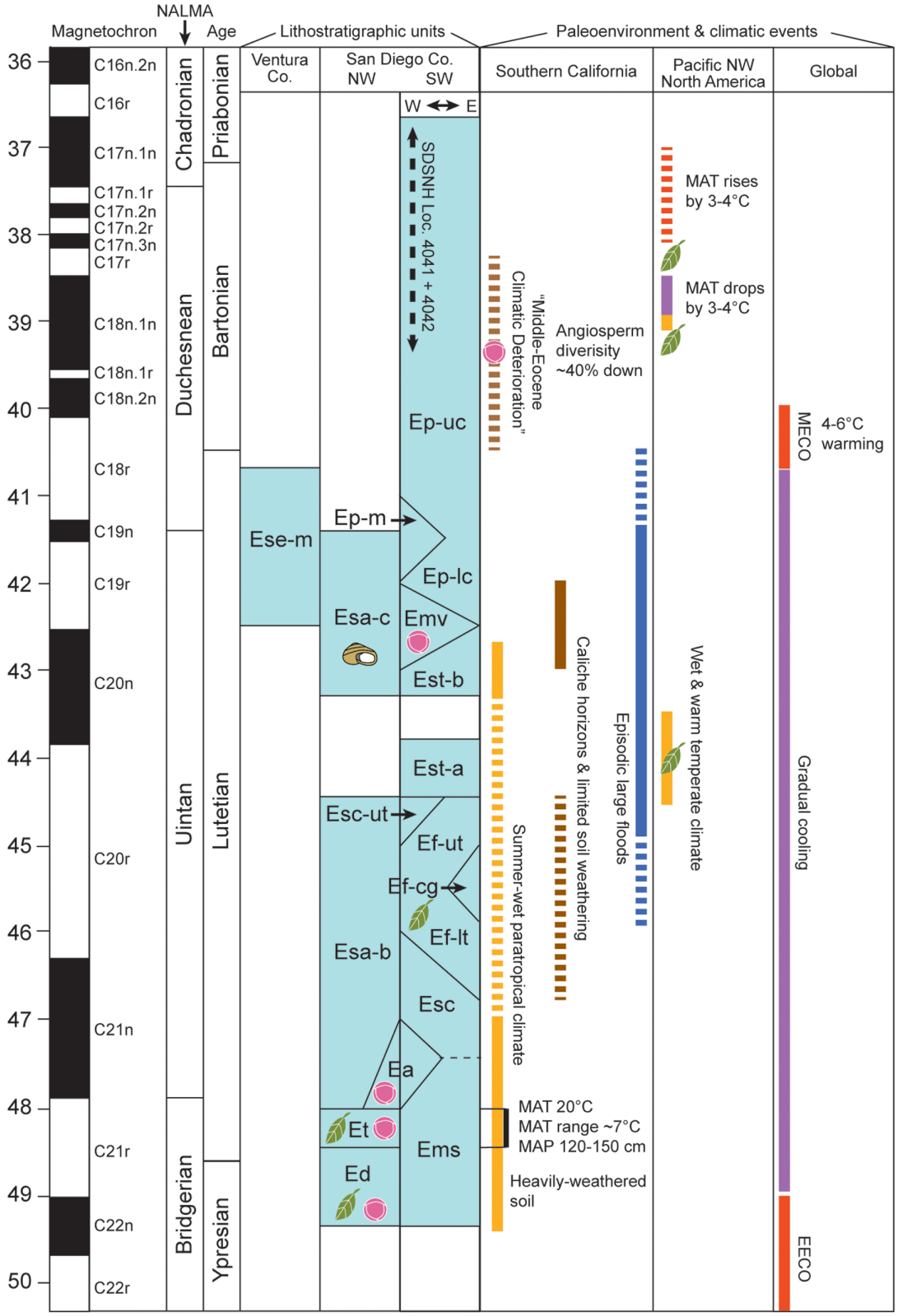

FIGURE 3.2: Preliminary chronological correlation chart for geologic formations discussed in the text. Icons show the stratigraphic distribution of molluscan (land snail; see Roth, 1991), plant macrofossil (leaves), and palynological (pollen grains) data of paleoenvironmental significance discussed in the text. Paleoclimatic reconstructions for the Pacific Northwest after Myers (2003*b*).

FIGURE 3.3: Overview of methods. Raw data consist of taxonomic occurrences from each locality (*A*). From this, the "F/L matrix" of Alroy (1994) is derived, in which the sign "$<$" indicates the observation that the first appearance of taxon i predates the last appearance of taxon *j* (*B*). This relationship is demonstrated whenever two taxa are known from the same locality (and thus their temporal ranges are assumed to have overlapped) or relative stratigraphic positions of two localities are known. In this hypothetical example, suppose Locality y, which has yielded Assemblage y, is stratigraphically higher (and thus younger in age) than Locality z. From this information, it can be deduced that the first appearance of Taxon D predated the last occurrence of Taxon B (brown "$<$" in *B*). Appearance event ordination seeks the sequence of first and last apperance events that minimizes the number of implied "$<$" (in gray in *B*). Events are grouped into time steps (*C*), and time bins are defined by first and last appearance events of carnivores (gray dashed lines in *C* and *D*). The range of possible ages for each locality is bounded by the oldest last appearance event and the youngest first appearance event of taxa known from that locality (*D*). In the case of Locality y, the age range thus determined (gray line in *D*) can be further constrained by the available stratigraphic information (brown line in *D* based on the fact that y cannot be older than z). Separate morphological-compositional matrices are then constructed (*E*) for carnivores (directly from their inferred temporal ranges) and non-carnivores (from locality-level occurrence data). Based on this, the compositional difference for every pair of meta-assemblages are quantified and tabulated (*F*) in Jaccard dissimilarity matrix (for taxon counts) or Manhattan distance matrix (for speciment counts). Finally, the rank-order correlation between the carnivore-compositional dissimilarity matrix and non-carnivore compositional dissimilarity/distance matrix is tested.

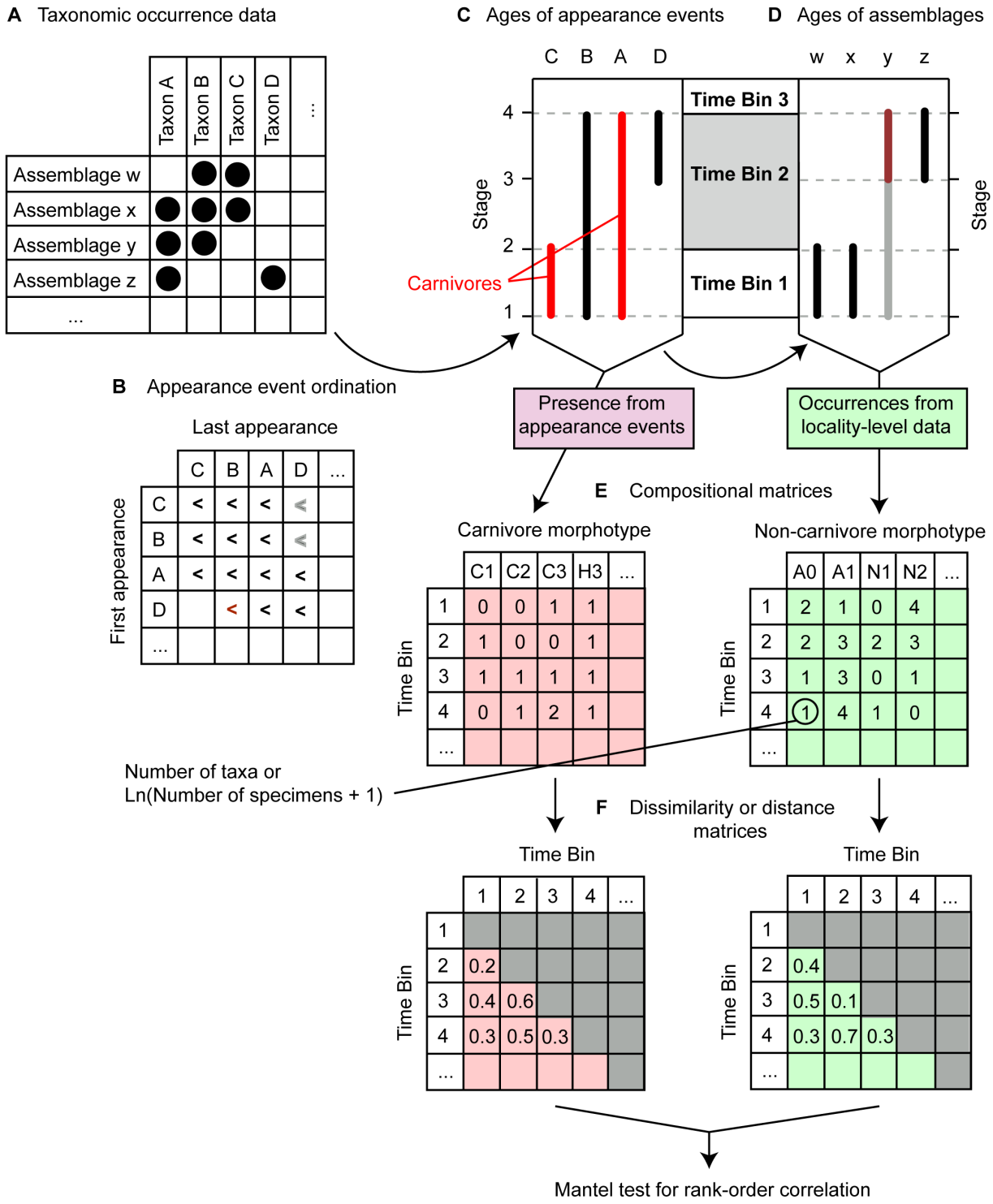
A Taxonomic occurrence data
Taxon A
Taxon B
Taxon C
Taxon D
...
Assemblage w
Assemblage x
Assemblage y
Assemblage z
...
C Ages of appearance events
D Ages of assemblages
C B A D
w x y z
Time Bin 3
Time Bin 2
Time Bin 1
Stage
Carnivores
B Appearance event ordination
Last appearance
First appearance
Presence from appearance events
Occurrences from locality-level data
E Compositional matrices
Carnivore morphotype
Non-carnivore morphotype
Time Bin
C1 C2 C3 H3
A0 A1 N1 N2
Number of taxa or
Ln(Number of specimens + 1)
F Dissimilarity or distance matrices
Mantel test for rank-order correlation

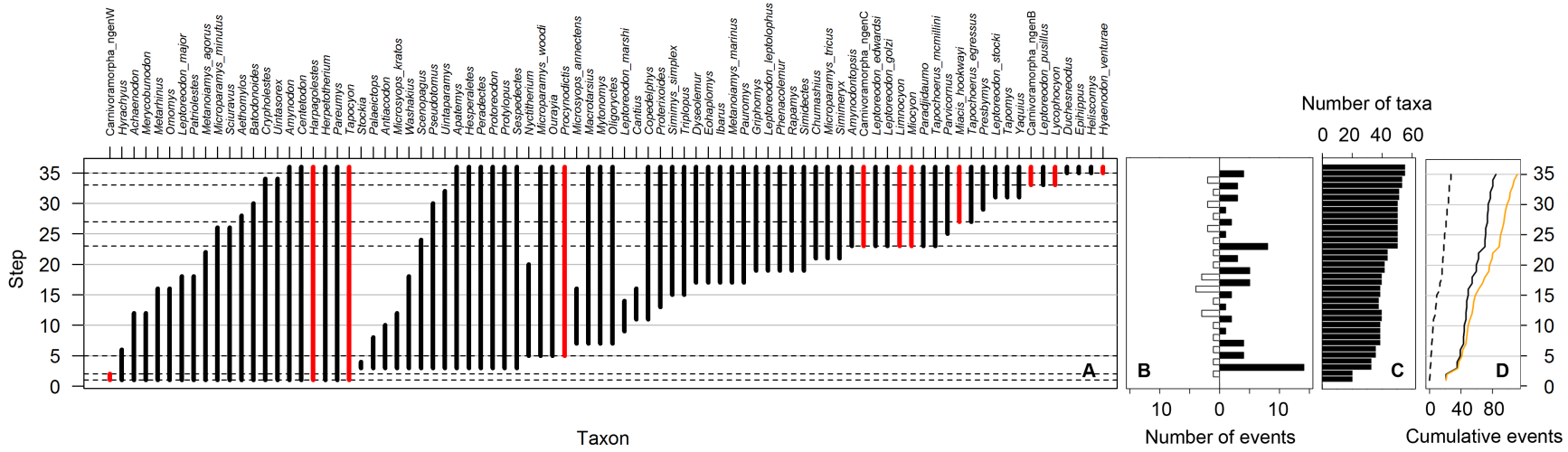

FIGURE 3.4: Relative timing of taxonomic first and last appearance events inferred from appearance event ordination. *A*, Carnivorous mammals are indicated by red lines, and their appearance events are marked by dashed lines. *B*, numbers of first (black bars) and last (white bars) appearance events in each Step. *C*, total number of taxa included in the ordination. *D*, cumulative numbers of first (black line), last (dashed line), and combined first and last (orange line) appearance events.

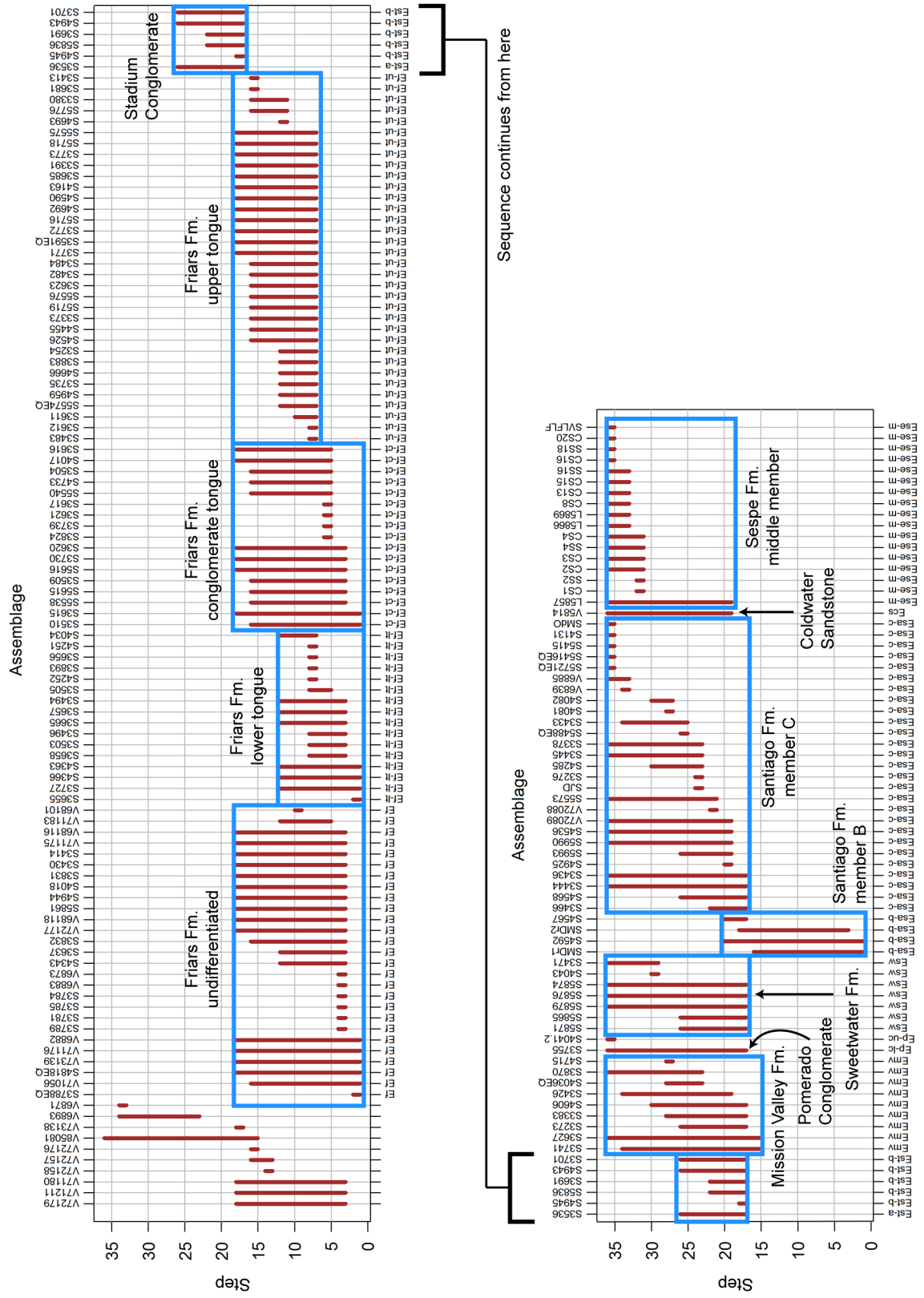

FIGURE 3.5: Ranges of possible ages for 177 localities (grouped into 168 units) and associated fossil assemblages.

FIGURE 3.6: Taxonomic occurrence data arranged in order of inferred locality ages. Filled black circles mark observed occurrences, and filled orange circles indicate localities where a taxon is expected (from appearance event ordination) to have been present but was not sampled. In the plot of locality-age ranges, the gray lines indicate ranges of possible locality ages inferred from the appearance event ordination, and the red lines represent their subsets where stratigraphic superpositional information was used to further constrain the possible-age ranges.

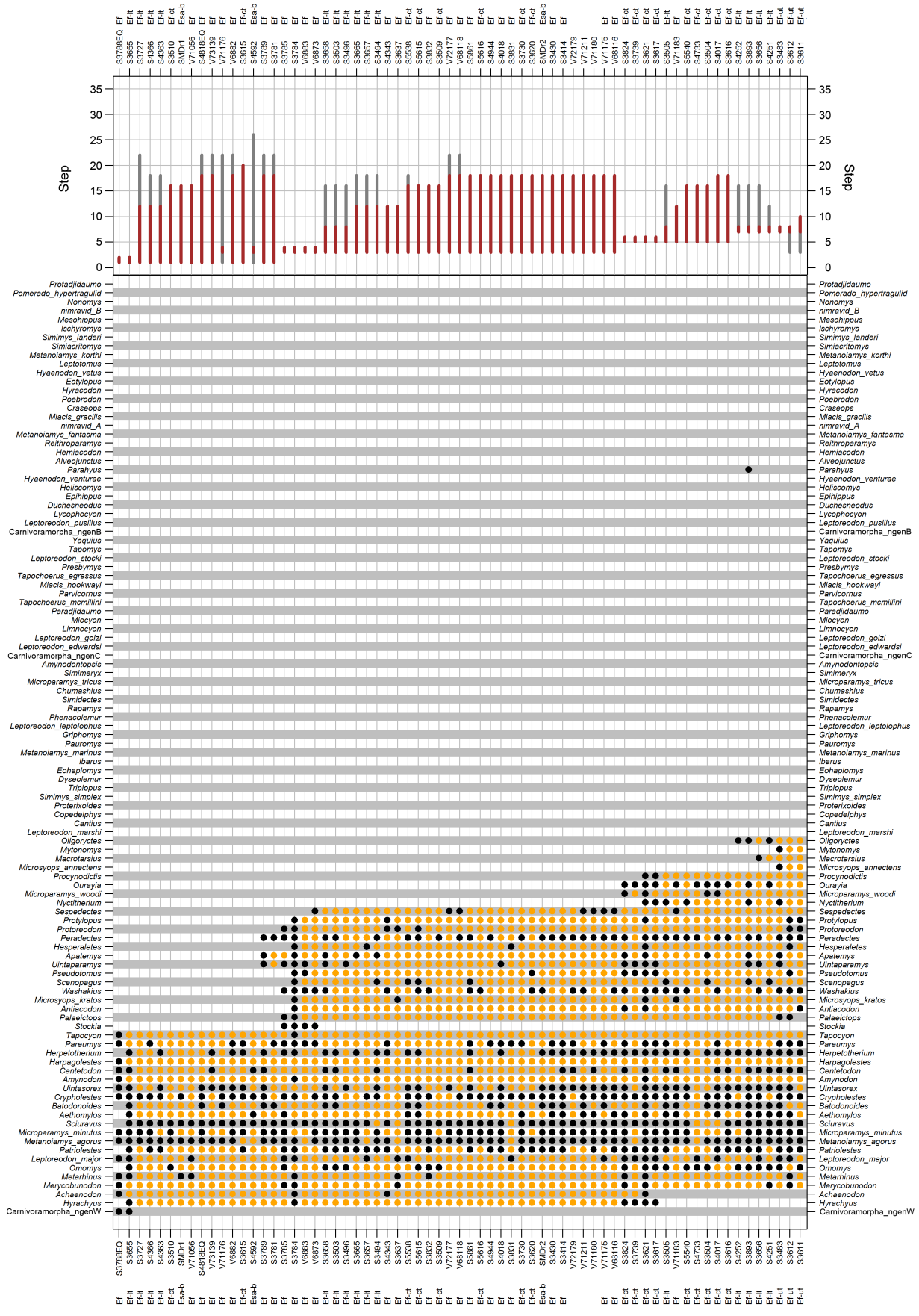
Step
Step
S3788EQ Ef
S3655 Ef-lt
S3727 Ef-lt
S4366 Ef-lt
S4363 Ef-lt
S3510 Ef-ct
SMDr1 Esa-b
V71056 Ef
S4818EQ Ef
V73139 Ef
V71176 Ef
V6882 Ef
S3615 Ef-ct
S4592 Esa-b
S3789 Ef
S3781 Ef
S3785 Ef
S3784 Ef
V6883 Ef
V6873 Ef
S3658 Ef-lt
S3503 Ef-lt
S3496 Ef-lt
S3665 Ef-lt
S3657 Ef-lt
S3494 Ef-lt
S4343 Ef
S3637 Ef
S5538 Ef-ct
S5615 Ef-ct
S3832 Ef
S3509 Ef-ct
V72177 Ef
V68118 Ef
S5861 Ef
S5616 Ef-ct
S4944 Ef
S4018 Ef
S3831 Ef
S3730 Ef-ct
S3620 Ef-ct
SMDr2 Esa-b
S3430 Ef
S3414 Ef
V72179
V71211
V71180 Ef
V71175 Ef
V68116 Ef
S3824 Ef-ct
S3739 Ef-ct
S3621 Ef-ct
S3617 Ef-ct
S3505 Ef-lt
V71183 Ef
S5540 Ef-ct
S4733 Ef-ct
S3504 Ef-ct
S4017 Ef-ct
S3616 Ef-ct
S4252 Ef-lt
S3893 Ef-lt
S3656 Ef-lt
S4251 Ef-lt
S3483 Ef-ut
S3612 Ef-ut
S3611 Ef-ut
Protadjidaumo
Pomerado_hypertragulid
Nonomys
nimravid_B
Mesohippus
Ischyromys
Simimys_landeri
Simiacritomys
Metanoiamys_korthi
Leptotomus
Hyaenodon_vetus
Eotylopus
Hyracodon
Poebrodon
Craseops
Miacis_gracilis
nimravid_A
Metanoiamys_fantasma
Reithroparamys
Hemiacodon
Alveojunctus
Parahyus
Hyaenodon_venturae
Heliscomys
Epihippus
Duchesneodus
Lycophocyon
Leptoreodon_pusillus
Carnivoramorpha_ngenB
Yaquius
Tapomys
Leptoreodon_stocki
Presbymys
Tapochoerus_egressus
Miacis_hookwayi
Parvicornus
Tapochoerus_mcmillini
Paradjidaumo
Miocyon
Limnocyon
Leptoreodon_golzi
Leptoreodon_edwardsi
Carnivoramorpha_ngenC
Amynodontopsis
Simimeryx
Microparamys_tricus
Chumashius
Simidectes
Rapamys
Phenacolemur
Leptoreodon_leptolophus
Griphomys
Pauromys
Metanoiamys_marinus
Ibarus
Eohaplomys
Dyseolemur
Triplopus
Simimys_simplex
Proterixoides
Copedelphys
Cantius
Leptoreodon_marshi
Oligoryctes
Mytonomys
Macrotarsius
Microsyops_annectens
Procynodictis
Ourayia
Microparamys_woodi
Nyctitherium
Sespedectes
Protylopus
Protoreodon
Peradectes
Hesperaletes
Apatemys
Uintaparamys
Pseudotomus
Scenopagus
Washakius
Microsyops_kratos
Antiacodon
Palaeictops
Stockia
Tapocyon
Pareumys
Herpetotherium
Harpagolestes
Centetodon
Amynodon
Uintasorex
Cryptolestes
Batodonoides
Aethomylos
Sciuravus
Microparamys_minutus
Metanoiamys_agorus
Patriolestes
Leptoreodon_major
Omomys
Metarhinus
Merycobunodon
Achaenodon
Hyrachyus
Carnivoramorpha_ngenW

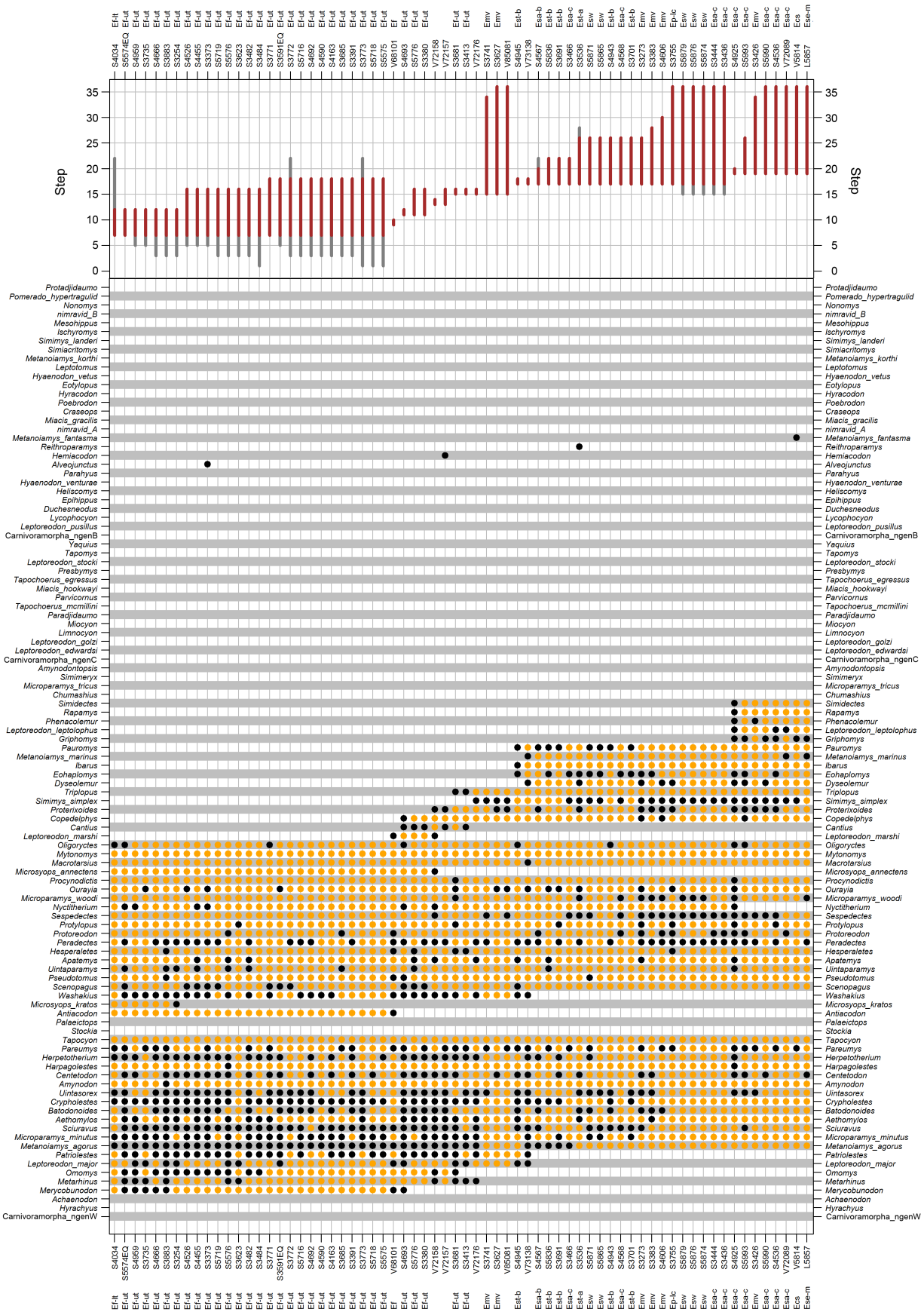
Step
Steps
0
5
10
15
20
25
30
35
Protadjidaumo
Pomerado_hypertragulid
Nonomys
nimravid_B
Mesohippus
Ischyromys
Simimys_landeri
Simiacritomys
Metanoiamys_korthi
Leptotomus
Hyaenodon_vetus
Eotylopus
Hyracodon
Poebrodon
Craseops
Miacis_gracilis
nimravid_A
Metanoiamys_fantasma
Reithroparamys
Hemiacodon
Alveojunctus
Parahyus
Hyaenodon_venturae
Heliscomys
Epihippus
Duchesneodus
Lycophocyon
Leptoreodon_pusillus
Carnivoramorpha_ngenB
Yaquius
Tapomys
Leptoreodon_stocki
Presbymys
Tapochoerus_egressus
Miacis_hookwayi
Parvicornus
Tapochoerus_mcmillini
Paradjidaumo
Miocyon
Limnocyon
Leptoreodon_golzi
Leptoreodon_edwardsi
Carnivoramorpha_ngenC
Amynodontopsis
Simimeryx
Microparamys_tricus
Chumashius
Simidectes
Rapamys
Phenacolemur
Leptoreodon_leptolophus
Griphomys
Pauromys
Metanoiamys_marinus
Ibarus
Eohaplomys
Dyseolemur
Triplopus
Simimys_simplex
Proterixoides
Copedelphys
Cantius
Leptoreodon_marshi
Oligoryctes
Mytonomys
Macrotarsius
Microsyops_annectens
Procynodictis
Ourayia
Microparamys_woodi
Nyctitherium
Sespedectes
Protylopus
Protoreodon
Peradectes
Hesperaletes
Apatemys
Uintaparamys
Pseudotomus
Scenopagus
Washakius
Microsyops_kratos
Antiacodon
Palaeictops
Stockia
Tapocyon
Pareumys
Herpetotherium
Harpagolestes
Centetodon
Amynodon
Uintasorex
Cryptolestes
Batodonoides
Aethomylos
Sciuravus
Microparamys_minutus
Metanoiamys_agorus
Patriolestes
Leptoreodon_major
Omomys
Metarhinus
Merycobunodon
Achaenodon
Hyrachyus
Carnivoramorpha_ngenW
Ef-lt S4034
Ef-ut S5574EQ
Ef-ut S4959
Ef-ut S3735
Ef-ut S4666
Ef-ut S3883
Ef-ut S3254
Ef-ut S4526
Ef-ut S4455
Ef-ut S3373
Ef-ut S5719
Ef-ut S5576
Ef-ut S3623
Ef-ut S3482
Ef-ut S3484
Ef-ut S3771
Ef-ut S3591EQ
Ef-ut S3772
Ef-ut S5716
Ef-ut S4692
Ef-ut S4590
Ef-ut S4163
Ef-ut S3885
Ef-ut S3391
Ef-ut S3773
Ef-ut S5718
Ef-ut S5575
Ef V6810
Ef-ut S4693
Ef-ut S5776
Ef-ut S3380
Ef-ut V72158
V72157
Ef-ut S3681
Ef-ut S3413
V72176
Emv S3741
Emv S3627
V85081
Est-b S4945
V73138
Esa-b S4567
Est-b S5836
Est-b S3691
Esa-c S3466
Est-a S3536
Esw S5871
Esw S5865
Est-b S4943
Esa-c S4568
Est-b S3701
Emv S3273
Emv S3383
Emv S4606
Ep-lc S3755
Esw S5879
Esw S5876
Esw S5874
Esa-c S3444
Esa-c S3436
Esa-c S4925
Esa-c S5993
Emv S3426
Esa-c S5990
Esa-c S4536
Esa-c V72089
Ecs V5814
Ese-m L5857

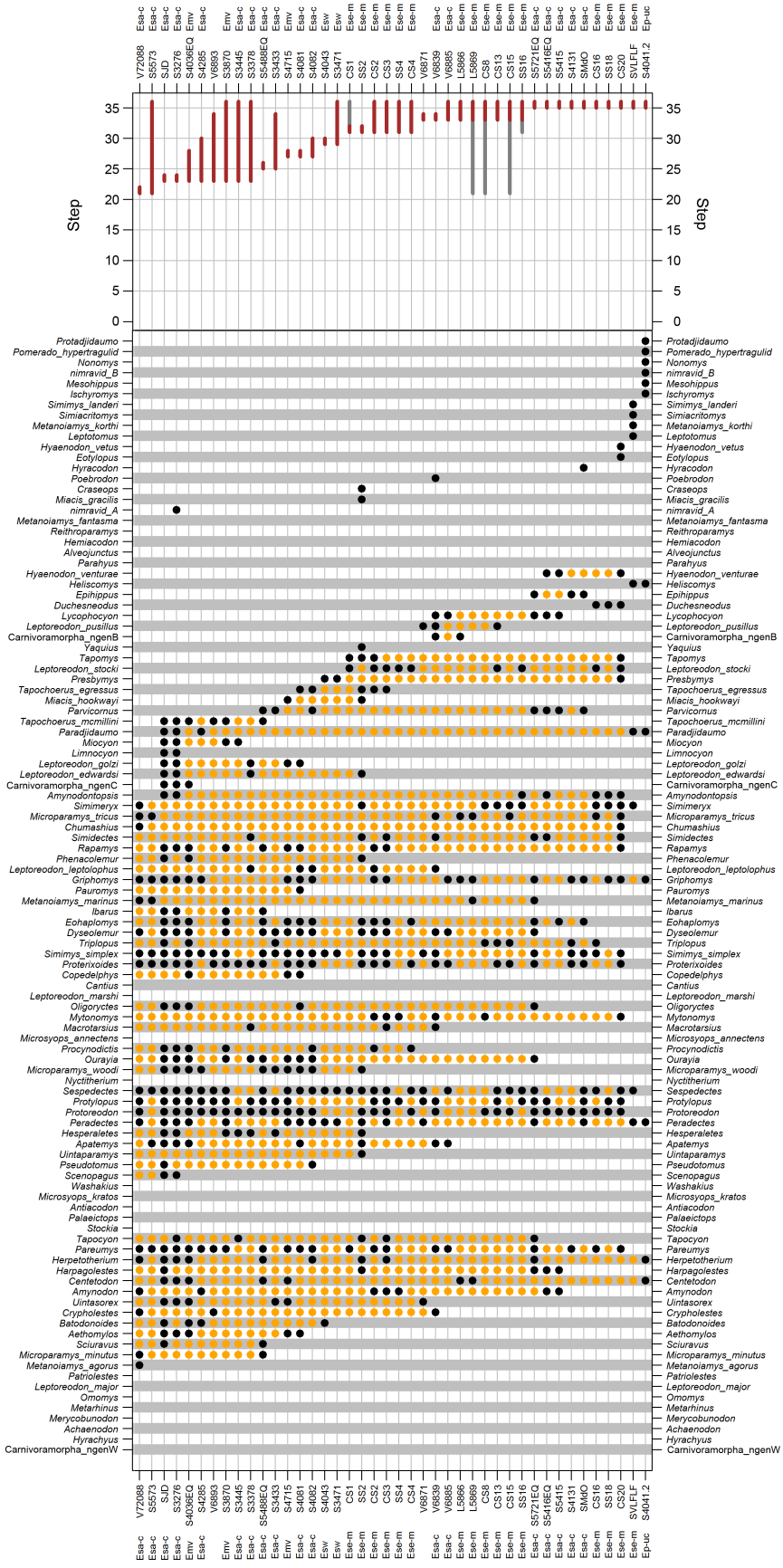
Step
Step
0
5
10
15
20
25
30
35
V72088 S5573 SJD S3276 S4036EQ S4285 Emv V6893 S3870 S3445 S3478 S5489EQ S3433 S4715 S4081 S4082 S4043 S3471 CS1 SS2 CS2 CS3 SS4 CS4 V6871 V6839 V6885 L5866 L5869 CS8 CS13 CS15 SS16 S5721EQ S5416EQ S5415 S4131 SMdO CS16 SS18 CS20 SVLFLF S4041.2
Esa-c Esa-c Esa-c Esa-c Emv Esa-c Emv Esa-c Esa-c Esa-c Esa-c Esa-c Emv Esa-c Esa-c Esw Esw Ese-m Ese-m Ese-m Ese-m Ese-m Ese-m Esa-c Esa-c Ese-m Ese-m Ese-m Ese-m Ese-m Ese-m Esa-c Esa-c Esa-c Esa-c Esa-c Esa-c Ese-m Ese-m Ese-m Ese-m Ese-m Ep-uc
Protadjidaumo
Pomerado_hypertragulid
Nonomys
nimravid_B
Mesohippus
Ischyromys
Simimys_landeri
Simiacritomys
Metanoiamys_korthi
Leptotomus
Hyaenodon_vetus
Ectylopus
Hyracodon
Poebrodon
Craseops
Miacis_gracilis
nimravid_A
Metanoiamys_fantasma
Reithroparamys
Hemiacodon
Alveojunctus
Parahyus
Hyaenodon_venturae
Heliscomys
Epihippus
Duchesneodus
Lycophocyon
Leptoreodon_pusillus
Carnivoramorpha_ngenB
Yaquius
Tapomys
Leptoreodon_stocki
Presbymys
Tapochoerus_egressus
Miacis_hookwayi
Parvicornus
Tapochoerus_mcmillini
Paradjidaumo
Miocyon
Limnocyon
Leptoreodon_golzi
Leptoreodon_edwardsi
Carnivoramorpha_ngenC
Amynodontopsis
Simimeryx
Microparamys_tricus
Chumashius
Simidectes
Rapamys
Phenacolemur
Leptoreodon_leptolophus
Griphomys
Pauromys
Metanoiamys_marinus
Ibarus
Eohaplomys
Dyseolemur
Triplopus
Simimys_simplex
Proterixoides
Copedelphys
Cantius
Leptoreodon_marshi
Oligoryctes
Mytonomys
Macrotarsius
Microsyops_annectens
Procynodictis
Ourayia
Microparamys_woodi
Nyctitherium
Sespedectes
Protylopus
Protoreodon
Peradectes
Hesperaletes
Apatemys
Uintaparamys
Pseudotomus
Scenopagus
Washakius
Microsyops_kratos
Antiacodon
Palaeictops
Stockia
Tapocyon
Pareumys
Herpetotherium
Harpagolestes
Centetodon
Amynodon
Uintasorex
Crypholestes
Batodonoides
Aethomylos
Sciuravus
Microparamys_minutus
Metanoiamys_agorus
Patriolestes
Leptoreodon_major
Omomys
Metarhinus
Merycobunodon
Achaenodon
Hyrachyus
Carnivoramorpha_ngenW

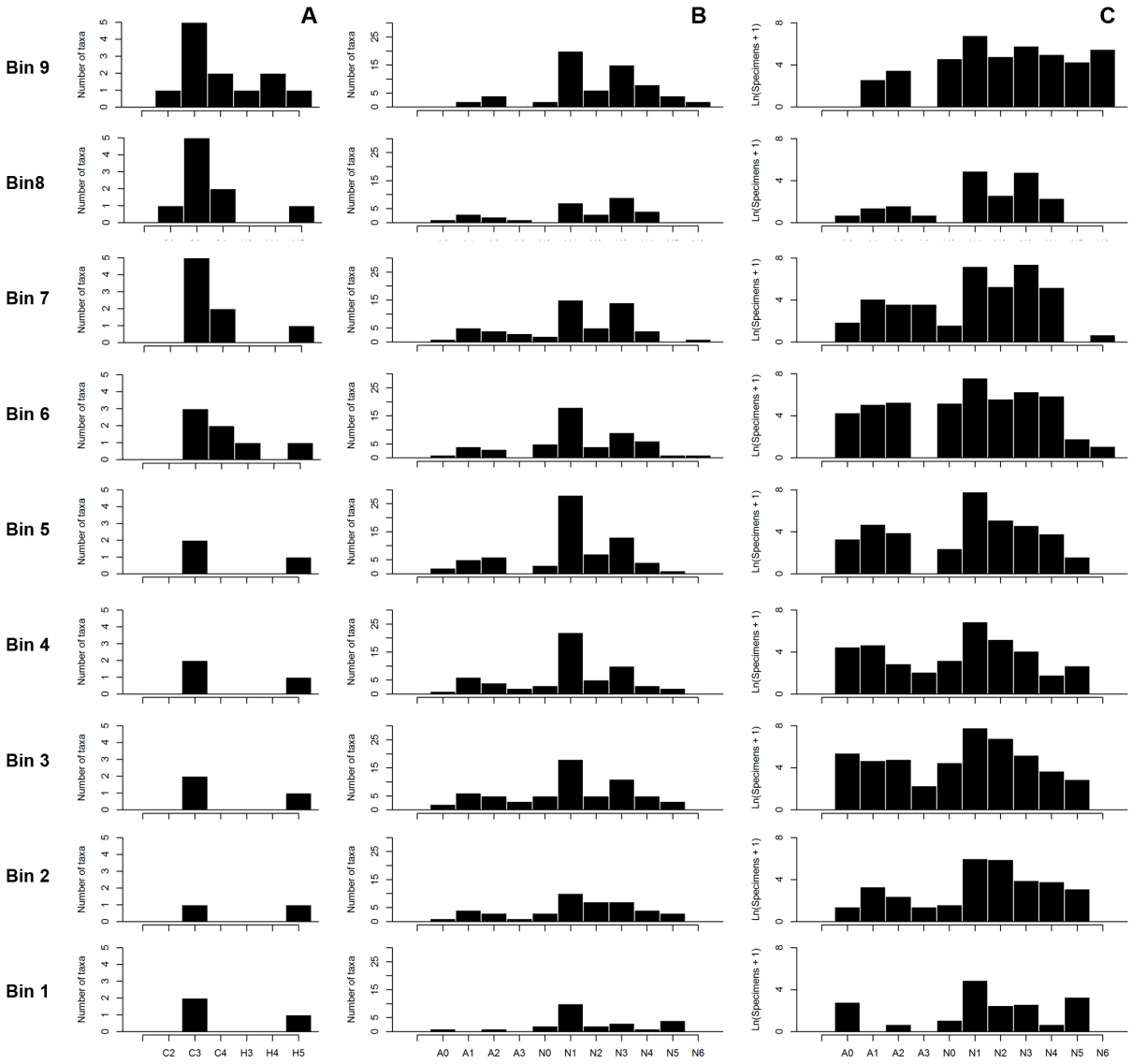

FIGURE 3.7: Distributions through time of specimens and taxa across morphological categories, not including non-carnivore dental types. *A*, carnivores. *B*, taxon counts for non-carnivores. *C*, natural-log transformed specimen counts for non-carnivores. See Table 3.1 for notations and definitions of categories.

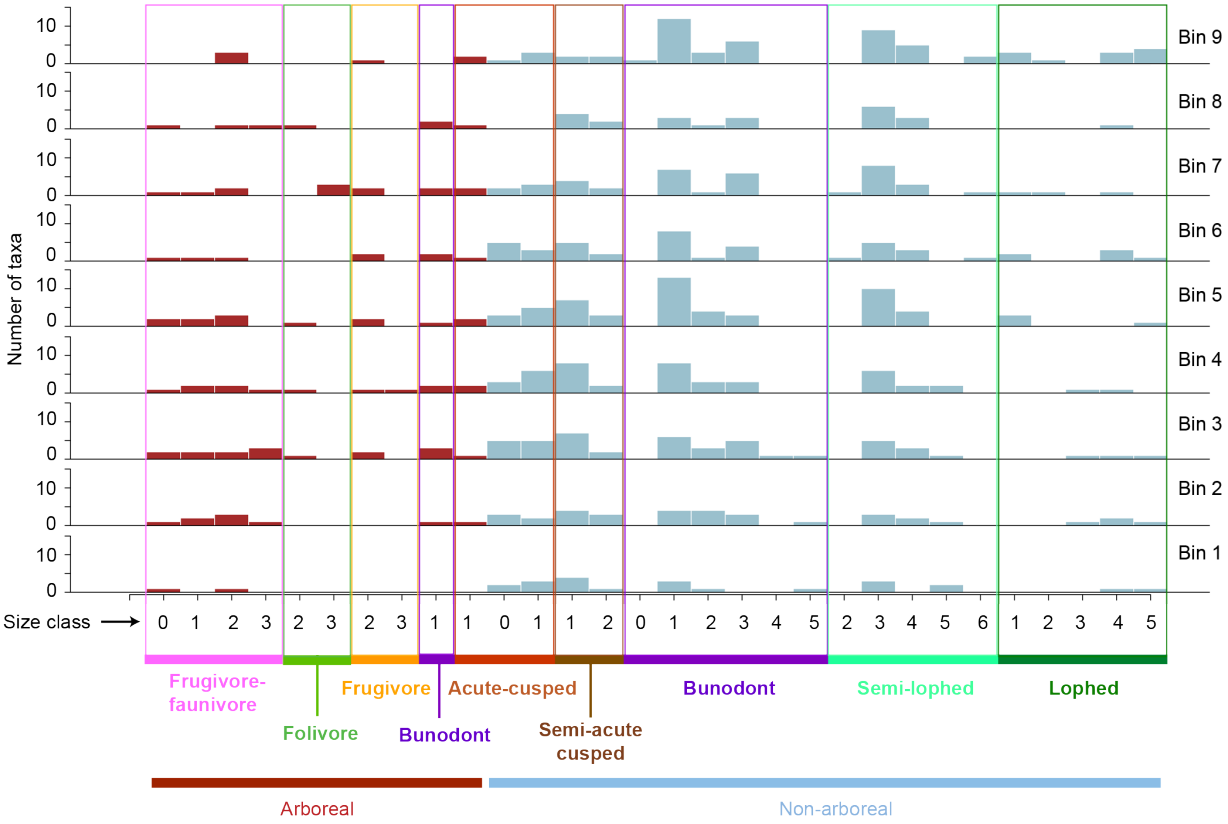

FIGURE 3.8: Distributions through time of taxa across non-carnivore morphological categories, including dental types.

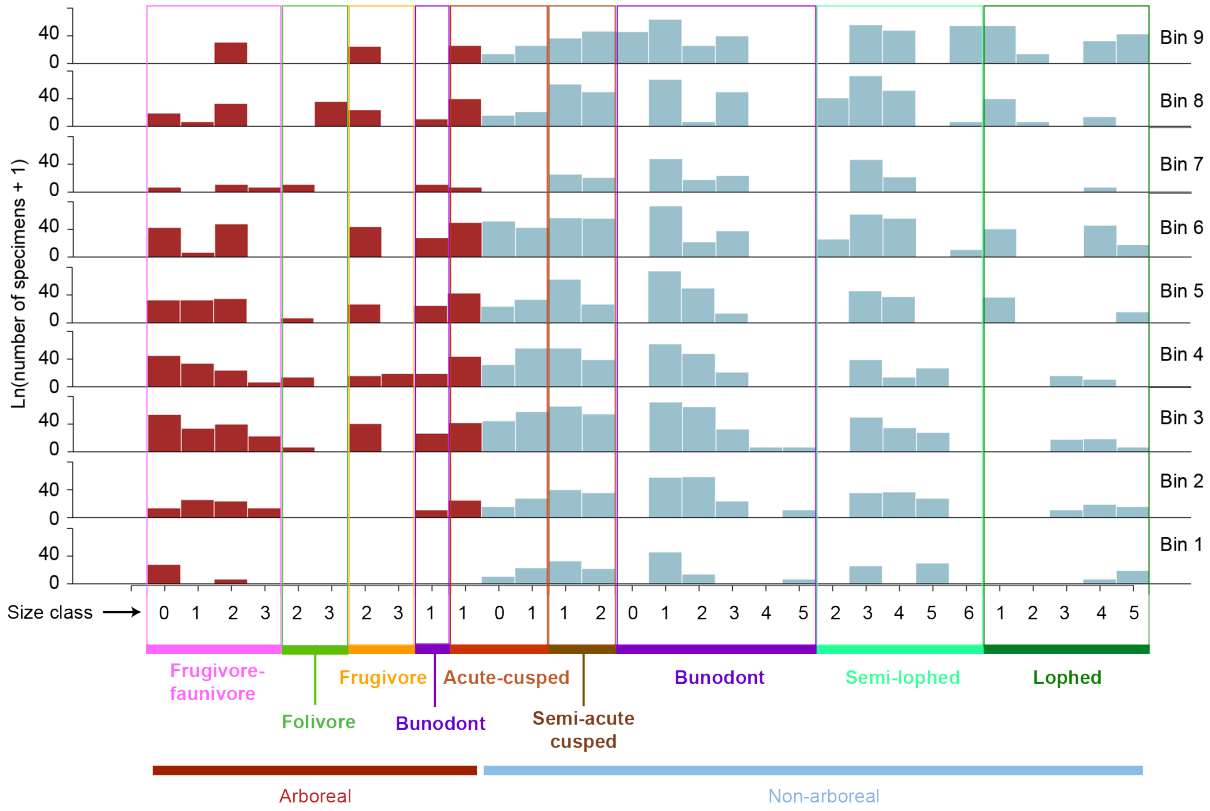

FIGURE 3.9: Distributions through time of specimens across non-carnivore morphological categories, including dental types.

FIGURE 3.10: Assessment of concordance between shifts in carnivore and non-carnivore compositions across time bins. Letters correspond to Analyses A-L (see Table 3.2). In the top two rows, pairs of meta-assemblages are plotted with respect to their differences in carnivore composition (horizontal axis) and non-carnivore composition (vertical axis). Plots with black circles correspond to analyses that showed rank-order correlation at the significance level of $\alpha = 0.10$. The bottom two rows show Procrustes superimposed non-metric multidimensional scaling plots of 9 meta-assemblages. Each labeled box (e.g., "int1" = Time Bin 1) represents a meta-assemblage plotted according to its carnivore composition. Orange arrows indicate the displacements that would be required to re-plot the same meta-assemblages based on their non-carnivore compositions. The sum of squared arrow-lengths reflects discordance between carnivore and non-carnivore compositions. Black axes show rotation of one plot superimposed on another. See Table 3.2 for statistics.

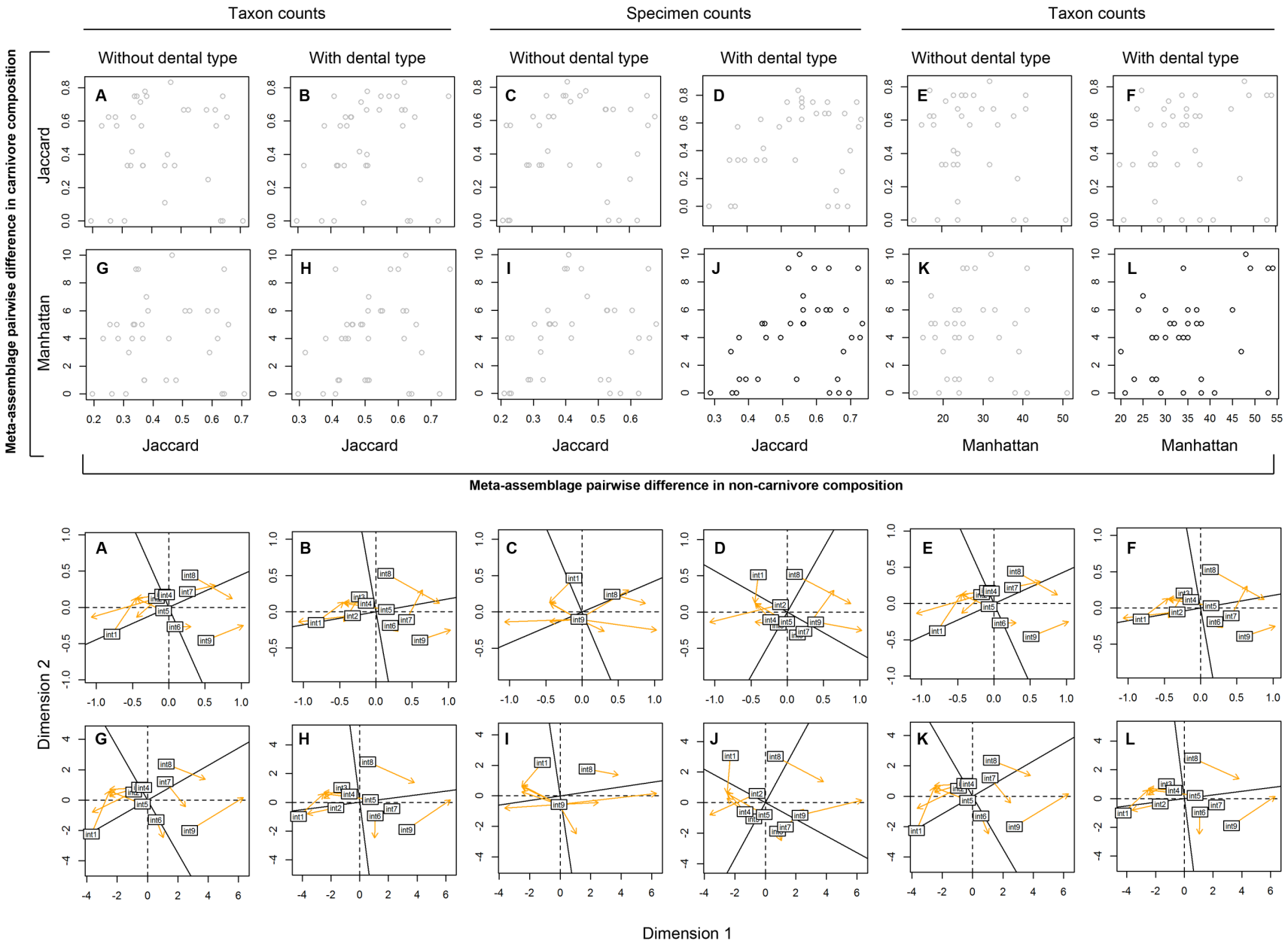
Taxon counts
Specimen counts
Taxon counts
Without dental type
With dental type
Without dental type
With dental type
Without dental type
With dental type
Meta-assemblage pairwise difference in carnivore composition
Jaccard
Manhattan
Jaccard
Jaccard
Jaccard
Jaccard
Manhattan
Manhattan
Meta-assemblage pairwise difference in non-carnivore composition
Dimension 2
Dimension 1

FIGURE 3.11: Compositional shifts examined in Analyses J and L. Here, variation in non-carnivore composition (middle three columns) is plotted by non-metric multidimensional scaling for 54 localities belonging to the 9 time bins. The far-right and far-left plots reflect the distribution of 30 non-carnivore morphotypes in the same space based on their distribution across time bins. Thus, morphotypes that characterize certain time bins are located close to the localities belonging to these bins. *A*. Composition based on taxon counts in morphological categories that included dental types, and differences measured in Jaccard dissimilarity; corresponds to Fig. 3.10J. *B*. Same as *A* but based instead on specimen counts, and differences measured in Manhattan distance to take into account absolute taxonomic diversity; corresponds to Fig. 3.10L. Color coding and labels for arboreal (A) and non-arboreal (N) morphotypes, time bins (numbers), and weight classes (yellow-red; each class encompasses an order of magnitude in weight in grams).

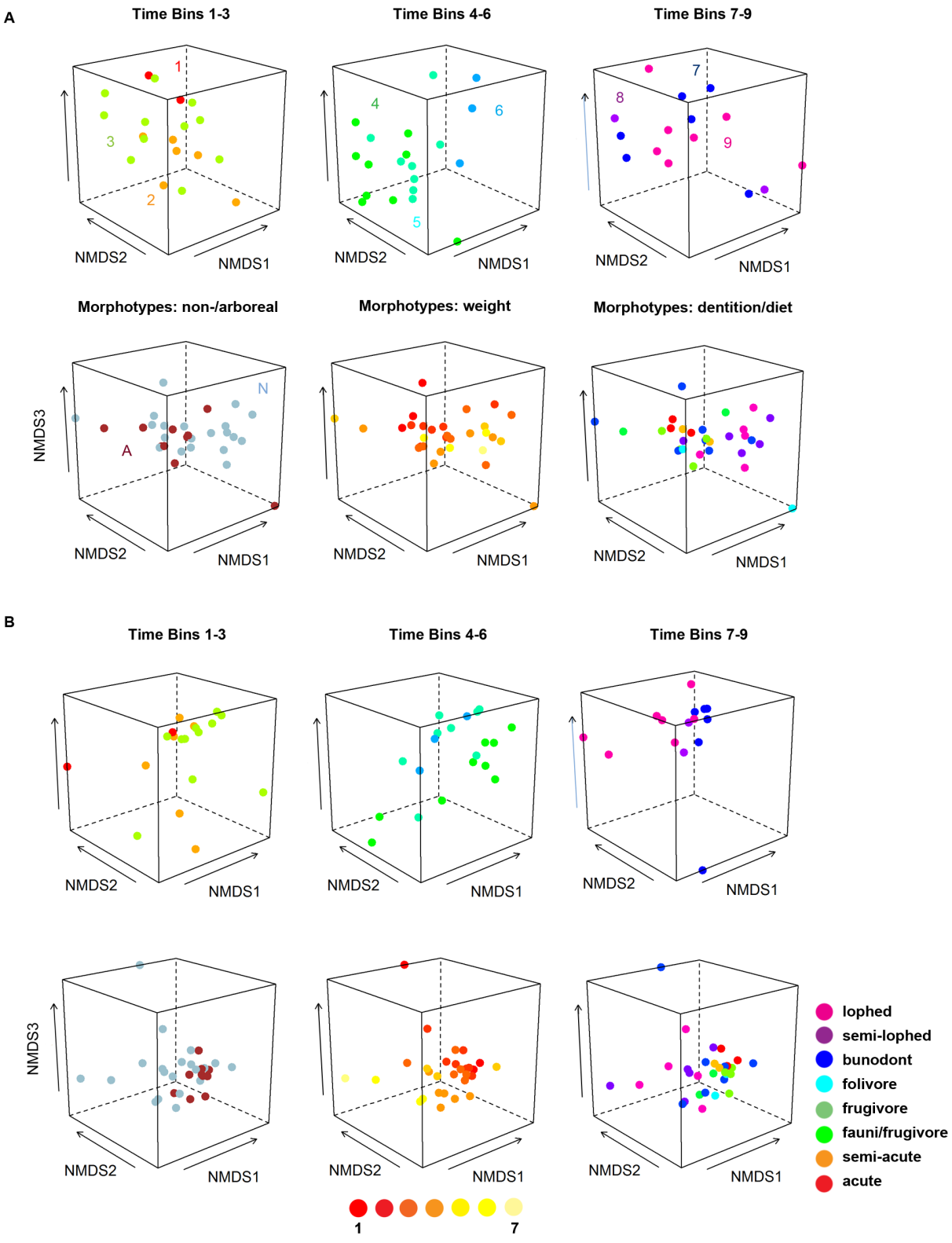
A
Time Bins 1-3
Time Bins 4-6
Time Bins 7-9
1
2
3
4
5
6
7
8
9
NMDS1
NMDS2
NMDS3
Morphotypes: non-/arboreal
Morphotypes: weight
Morphotypes: dentition/diet
A
N
B
1
7
lophed
semi-lophed
bunodont
folivore
frugivore
fauni/frugivore
semi-acute
acute

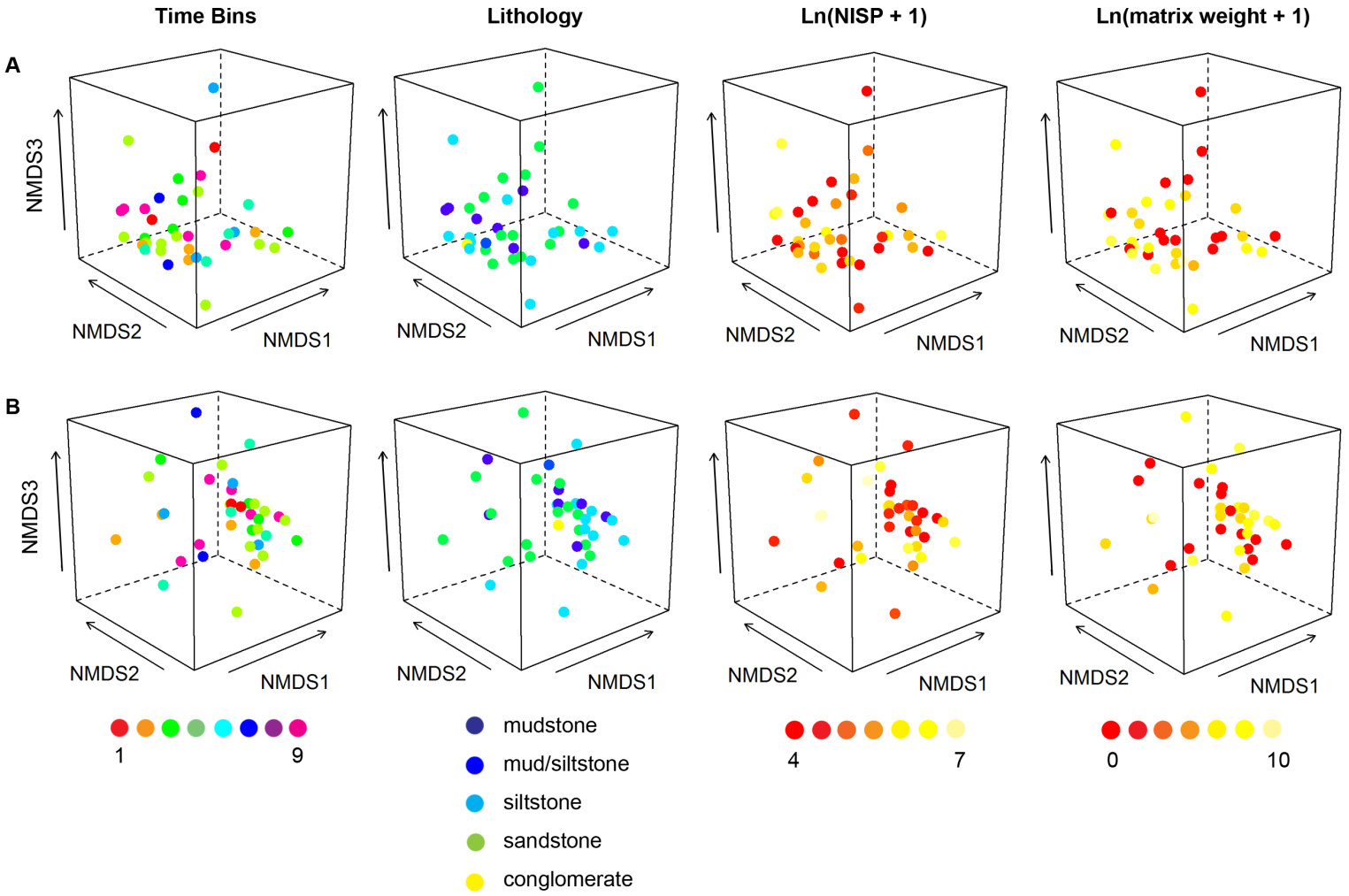

FIGURE 3.12: Potential factors influencing non-carnivore compositional variations. locality-level assemblages are color-coded based on its age, characteristic lithologic type, number of identified specimens, and the weight of sedimentary matrix that was screen-washed to recover small mammals. *A*, composition based on Jaccard dissimilarity index and taxon counts in morphological categories that included dental types. *B*. composition based on Manhattan distance and specimen counts in morphological categories that included dental types. A and B correspond to Figure 11A and B, respectively. See Table 3.3 for related statistics.

References

Albright, L. B. 1998. New genus of tapir (Mammalia: Tapiridae) from the Arikareean (earliest Miocene) of the Texas Coastal Plain. Journal of Vertebrate Paleontology 18:200–217.

Alroy, J. 1992. Conjunction among taxonomic distributions and the Miocene mammalian biochronology of the Great Plains. Paleobiology 18:326–343.

———. 1994. Appearance event ordination: a new biochronologic method. Paleobiology 20:191–207.

———. 1996. Constant extinction, constrained diversification, and uncooridnated stasis in North American mammals. Palaeogeography, Palaeoclimatology, Palaeoecology 127:285–311.

———. 2003. Taxonomic inflation and body mass distributions in North American fossil mammals. Journal of Mammalogy 84:431–443.

———. 2009. Speciation and extinction in the fossil record of North American mammals. Pages 301–333 *in* R. K. Butlin, J. R. Bridle, and D. Schluter, eds. Speciation and patterns on diversity. Cambridge University Press, Cambridge.

Angelici, F. M. 2000. Food habits and resource partitioning of carnivores (herpestidae, viverridae) in the rainforests of southeastern nigeria: preliminary results. La Terre et la Vie-Revue d'écologie 55:67–76.

Arnason, U., J. A. Adegoke, A. Gullberg, E. H. Harley, A. Janke, and M. Kullberg. 2008. Mitogenomic relationships of placental mammals and molecular estimates of their divergences. Gene 421:37–51.

Arnason, U., A. Gullberg, A. Janke, and M. Kullberg. 2007. Mitogenomic analysis of caniform relationships. Molecular Phylogeny and Evolution 45:863–874.

Arnason, U., A. Gullberg, A. Janke, M. Kullberg, N. Lehman, E. A. Petrov, and R. Väinölä. 2006. Pinniped phylogeny and a new hypothesis for their origin and dispersal). Molecular Phylogenetics and Evolution 41:345–354.

Barnosky, A. D., M. A. Carrasco, and R. W. Graham. 2011*a*. Collateral mammal diversity loss associated with late Quaternary megafaunal extinctions and implications for the future. Pages 179–189 *in* A. J. McGowan and A. B. Smith, eds. Comparing the geological and fossil records: implications for biodiversity studies. Geological Society of London, London.

Barnosky, A. D., P. L. Koch, R. S. Feranec, S. L. Wing, and A. B. Shabel. 2004. Assessing the causes of late Pleistocene extinctions on the continents. Science 306:70–75.

Barnosky, A. D., N. Matzke, S. Tomiya, G. O. U. Wogan, B. Swartz, T. B. Quental, C. Marshall, J. L. McGuire, E. L. Lindsey, K. C. Maguire, B. Mersey, and E. A. Ferrer. 2011*b*. Has the Earth's sixth mass extinction already arrived? Nature 471:51–57.

Barry, J. C., M. E. Morgan, L. J. Flynn, D. Pilbeam, A. K. Behrensmeyer, S. M. Raza, I. A. Khan, C. Badgley, J. Hicks, and J. Kelley. 2002. Faunal and environmental change in the late Miocene Siwaliks of northern Pakistan. Paleobiology 28 (Special Issue 3):1–71.

Baskin, J. A. 1998*a*. Mustelidae. Pages 152–173 *in* C. M. Janis, K. M. Scott, and L. L. Jacobs, eds. Evolution of tertiary mammals of North America: volume 1, terrestrial carnivores, ungulates, and ungulatelike mammals. Cambridge University Press , Cambridge.

———. 1998*b*. Procyonidae. Pages 144–151 *in* C. M. Janis, K. M. Scott, and L. L. Jacobs, eds. Evolution of tertiary mammals of North America: volume 1, terrestrial carnivores, ungulates, and ungulatelike mammals. Cambridge University Press , Cambridge.

———. 2004. *Bassariscus* and *Probassariscus* (Mammalia, Carnivora, Procyonidae) from the early Barstovian (middle Miocene). Journal of Vertebrate Paleontology 24:709–720.

Benton, M. J., and P. C. J. Donoghue. 2007. Paleontological evidence to date the tree of life. Molecular Biology and Evolution 24:26–53.

Bergsten, J. 2005. A review of long-branch attraction. Cladistics 21:163–193.

Bielby, J., G. M. Mace, O. R. P. Bininda-Emonds, M. Cardillo, J. L. Gittleman, K. E. Jones, C. D. L. Orme, and A. Purvis. 2007. The fast-slow continnum in mammalian life history: an empirical reevaluation). American Naturalist 169:748–757.

Bininda-Emonds, O. R. P., M. Cardillo, K. E. Jones, R. D. E. MacPhee, R. M. D. Beck, R. Grenyer, S. A. Price, R. A. Vos, J. L. Gittleman, and A. Purvis. 2007. The delayed rise of present-day mammals. Nature 446:507–512.

———. 2008. Corrigendum: The delayed rise of present-day mammals (vol 446, pg 507, 2007). Nature 456:274.

Bloch, J. I., K. D. Rose, and P. D. Gingerich. 1998. New species of *Batodonoides* (Lipotyphla, Geolabididae) from the early Eocene of Wyoming. Journal of Mammalogy 79:804–827.

Bohaty, S. M., J. C. Zachos, F. Florindo, and M. L. Delaney. 2009. Coupled greenhouse warming and deep-sea acidification in the middle Eocene. Paleoceanography 24:1–16.

Bremer, K. 1994. Branch support and tree stability. Cladistics 10:295–304.

Brown, J. H., and B. A. Maurer. 1989. Macroecology: the division of food and space among species on continents. Science 243:1145–1150.

Bryant, H. N. 1991. Phylogenetic relationships and systematics of the Nimravidae (Carnivora). Journal of Mammalogy 72:56–78.

———. 1992. The Carnivora of the Lac Pelletier Lower Fauna (Eocene: Duchesnean), Cypress Hills Formation, Saskatchewan. Journal of Paleontology 66:847–855.

———. 1996. Explicitness, stability, and universality in the phylogenetic definition and usage of taxon names: a case study of the phylogenetic taxonomy of the Carnivora (Mammalia). Systematic Biology 45:174–189.

Burger, O., and L. Ginzburg. 2009. On size and extinction: a random walk model predicts the body size of lowest risk for mammals. Evolutionary Ecology Research 11:1017–1029.

Cardillo, M., G. M. Mace, J. L. Gittleman, K. E. Jones, J. Bielby, and A. Purvis. 2008. The predictability of extinction: biological and external correlates of decline in mammals. Proceedings of the Royal Society B-Biological Sciences 275:1441–1448.

Cardillo, M., G. M. Mace, K. E. Jones, J. Bielby, O. R. P. Bininda-Emonds, W. Sechrest, C. D. L. Orme, and A. Purvis. 2005. Multiple causes of high extinction risk in large mammal species. Science 309:1239–1241.

Carotenuto, F., C. Barbera, and P. Raia. 2010. Occupancy, range size, and phylogeny in Eurasian Pliocene to Recent large mammals. Paleobiology 36:399–414.

Carrasco, M. A. in press. The impact of taxonomic bias when comparing past and present species diversity. Palaeogeography, Palaeoclimatology, Palaeoecology :. DOI: 10.1016/j.palaeo.2012.06.010.

Carrasco, M. A., A. D. Barnosky, and R. W. Graham. 2009. Quantifying the extent of North American mammal extinction relative to the pre-anthropogenic baseline. PLoS ONE 4:e8331.

Carrasco, M. A., B. P. Kraatz, E. B. Davis, and A. D. Barnosky. 2005. Miocene mammal mpping project (MIOMAP). University of California Museum of Paleontology. Available at http://www.ucmp.berkeley.edu/miomap/.

Carroll, R. L. 1988. Vertebrate paleontology and evolution. Freeman, New York.

Cartlett, K. K., G. T. Schwartz, L. R. Godfrey, and W. L. Jungers. 2010. "Life history space": a multivariate analysis of life history variation in extant and extinct Malagasy lemurs. American Journal of Physical Anthropology 142:391–404.

Casanovas-Vilar, I., I. García-Paredes, D. M. Alba, L. W. van den Hoek Ostende, and S. Moyà-Solà. 2010. The European Far West: Miocene mammal isolation, diversity and turnover in the Iberian Peninsula. Journal of Biogeography 37:1079–1093.

Chiment, J. J., and W. W. Korth. 1996. A new genus of eomyid rodent (Mammalia) from the Eocene (Uintan-Duchesnean) of southern California. Journal of Vertebrate Paleontology 16:116–124.

Clark, H. O., Jr. 2005. *Otocyon megalotis*. Mammalian Species 766:1–5.

Clark, J. 1939. *Miacis gracilis*, a new carnivore from the uinta eocene. Annals of the Carnegie Museum 27:349–371.

Colbert, M. W. 2006. Variation and species recognition in Eocene tapirs form southern California. Journal of Vertebrate Paleontology 26:712–719.

Colbert, M. W., and R. M. Schoch. 1998. Tapiroidea and other moropomorphs. Pages 569–582 *in* C. M. Janis, K. M. Scott, and L. L. Jacobs, eds. Evolution of tertiary mammals of North America: volume 1, terrestrial carnivores, ungulates, and ungulatelike mammals. Cambridge University Press , Cambridge.

Collen, B., L. McRae, S. Deinet, A. De Palma, T. Carranza, N. Cooper, J. Loh, and J. E. M. Baillie. 2011. Predicting how populations decline to extinction. Philosophical Transactions of the Royal Society B-Biological Sciences 366:2577–2586.

Conroy, G. C. 1987. Problems of body-weight estimation in fossil primates. International Journal of Primatology 8:125–137.

Coombs, M. C. 1971. Status of *Simidectes* (Insectivora, Pantolestoidea) of the late Eocene of North America. American Museum Novitates 2455:1–41.

Cooper, N., J. Rodríguez, and A. Purvis. 2008. A common tendency for phylogenetic overdispersion in mammalian assemblages). Proceedings of the Royal Society B, Biological Sciences 275:2031–2037.

Corneli, P. S. 2003. Complete mitochondrial genomes and eutherian evolution. Journal of Mammalian Evolution 9:281–305.

Crooks, K. R., and D. Van Vuren. 1995. Resource utilization by two insular endemic mammalian carnivores, the island fox and island spotted skunk. Oecologia 104:301–307.

Czaplewski, N. J. 1990. The Verde local fauna: small vertebrate fossils from the Verde Formation, Arizona. Quarterly, San Bernardino County Museum Association 37:1–39.

Daitch, D. J., and R. P. Guralnick. 2007. Geographic variation in tooth morphology of the arctic fox, *Vulpes* (*Alopex*) *lagopus*. Journal of Mammalogy 88:384–393.

Damuth, J. 1990. Problems in estimating body masses of archaic ungulates using dental measurements. Pages 229–253 *in* Damuth, John and MacFadden, Bruce J., ed. Body size in mammalian paleobiology: estimation and biological implications. Cambridge University Press, Cambridge.

Dawson, M. R. 1999. Bering down: Miocene dispersals of land mammals between North America and Europe. Pages 473–483 *in* G. E. Rössner and K. Heissig, eds. The Miocene land mammals of Europe. Munich, Verlag Dr. Friedrich Pfeil.

Dayan, T., D. Wool, and D. Simberloff. 2002. Variation and covariation of skulls and teeth: modern carnivores and the interpretation of fossil mammals. Paleobiology 28:508–526.

de Queiroz, K. 2007. Species concepts and species delimitation. Systematic Biology 56:879–886.

Diniz-Filho, J. A. F. 2004. Phylogenetic diversity and conservation priorities under distinct models of phenotypic evolution). Conservation Biology 18:698–704.

Donoghue, M. J., J. A. Doyle, J. Gauthier, A. G. Kluge, and T. Rowe. 1989. The importance of fossils in phylogeny reconstruction. Annual Review of Ecology and Systematics 20:431–460.

Efron, B. 1979. Bootstrap methods: another look at the jackknife. Annals of Statistics 7:1–26.

———. 1981. Nonparametric standard errors and confidence intervals. Canadian Journal of Statistics 9:139–158.

Egi, N. 2001. Body mass estimates in extinct mammals from limb bone dimensions: the case of North American hyaenodontids. Palaeontology 44:497–528.

Egi, N., M. Takai, N. Shigehara, and T. Tsubamoto. 2004. Body mass estimates for Eocene eosimiid and amphipithecid primates using prosimian and anthropoid scaling models. International Journal of Primatology 25:211–236.

Eisenberg, J. F. 1981. The mammalian radiations: an analysis of trends in evolution, adaptation, and behavior. University of Chicago Press, Chicago.

Eisenberg, L. I., and P. L. Abbott. 1991. Middle Eocene paralic facies, northern San Diego County, CA. Pages 55–72 *in* P. L. Abbott and J. A. May, eds. Eocene geologic history: San Diego region. Pacific Section, Society of Economic Paleontologists and Mineralogists, Los Angeles.

Eizirik, E., W. J. Murphy, K.-P. Koepfli, W. E. Johnson, J. W. Dragoo, R. K. Wayne, and S. J. O'Brien. 2010. Pattern and timing of diversification of the mammalian order Carnivora inferred from multiple nuclear gene sequences. Molecular Phylogenetics and Evolution 56:49–63.

Eizirik, E., W. J. Murphy, and S. J. O'Brien. 2001. Molecular dating and biogeography of the early placental mammal radiation. Journal of Heredity 92:212–219.

Emry, R. J., and W. W. Korth. 2007. A new genus of squirrel (Rodentia, Sciuridae) from the mid-Cenozoic of North America). Journal of Vertebrate Paleontology 27:693–698.

Erwin, D. H. 2008. Extinction as the loss of evolutionary history. Proceedings of the National Academy of Sciences of the United States of America 105:11520–11527.

Estes, J. A., J. Terborgh, J. S. Brashares, M. E. Power, J. Berger, W. J. Bond, S. R. Carpenter, T. E. Essington, R. D. Holt, J. B. C. Jackson, R. J. Marquis, L. Oksanen, T. Oksanen, R. T. Paine, E. K. Pikitch, W. J. Ripple, S. A. Sandin, M. Scheffer, T. W. Schoener, J. B. Shurin, A. R. E. Sinclair, M. E. Soulé, R. Virtanen, and D. A. Wardle. 2011. Trophic downgrading of planet Earth. Science 333:301–306.

Farris, J. S. 1989. The retention index and the rescaled consistency index. Cladistics 5:417–419.

Felsenstein, J. 1985. Confidence limits on phylogenies: an approach using the bootstrap. Evolution 39:783–791.

Finarelli, J. A. 2008. A total evidence phylogeny of the Arctoidea (Carnivora: Mammalia): relationships among basal taxa. Journal of Mammalian Evolution 15:231–259.

Flynn, J. J., J. A. Finarelli, S. Zehr, J. Hsu, and M. A. Nedbal. 2005. Molecular phylogeny of the Carnivora (Mammalia): assessing the impact of increased sampling on resolving enigmatic relationships. Systematic Biology 54:317–337.

Flynn, J. J., and H. Galiano. 1982. Phylogeny of early Tertiary Carnivora, with a description of a new species of Protictis from the middle Eocene of northwestern Wyoming. American Museum Novitates 2725:1–64.

Flynn, J. J., and M. A. Nedbal. 1998. Phylogeny of the Carnivora (Mammalia): congruence vs incompatibility among multiple data sets. Molecular Phylogenetics and Evolution 9:414–426.

Flynn, J. J., and G. D. Wesley-Hunt. 2005. Carnivora. Pages 175–198 *in* K. D. Rose and J. D. Archibald, eds. The rise of placental mammals: origins and relationships of the major extant clades. Johns Hopkins University Press, Baltimore.

Flynn, L. J. 2008*a*. Eomyidae. Pages 415–427 *in* C. M. Janis, G. F. Gunnell, and M. D. Uhen, eds. Evolution of tertiary mammals of North America: volume 2, small mammals, xenarthrans, and marine mammals. Cambridge University Press , Cambridge.

———. 2008*b*. Hystricognathi and Rodentia incertae sedis. Pages 498–506 *in* C. M. Janis, G. F. Gunnell, and M. D. Uhen, eds. Evolution of tertiary mammals of North America: volume 2, small mammals, xenarthrans, and marine mammals. Cambridge University Press, Cambridge.

Flynn, L. J., J. C. Barry, M. E. Morgan, D. Pilbeam, L. L. Jacobs, and E. H. Lindsay. 1995. Neogene Siwalik mammalian lineages: species longevities, rates of change, and modes of speciation). Palaeogeography, Palaeoclimatology, Palaeoecology 115:249–264.

Flynn, L. J., and L. L. Jacobs. 2008. Castoroidea. Pages 391–405 *in* C. M. Janis, G. F. Gunnell, and M. D. Uhen, eds. Evolution of tertiary mammals of North America: volume 2, small mammals, xenarthrans, and marine mammals. Cambridge University Press , Cambridge.

Flynn, L. J., H. Lindsay, Everett, and R. A. Martin. 2008. Geomorpha. Pages 428–455 *in* C. M. Janis, G. F. Gunnell, and M. D. Uhen, eds. Evolution of tertiary mammals of North America: volume 2, small mammals, xenarthrans, and marine mammals. Cambridge University Press , Cambridge.

Foote, M. 2000. Origination and extinction components of taxonomic diversity: general problems. Paleobiology 26:74–102.

Foote, M., and D. M. Raup. 1996. Fossil preservation and the stratigraphic ranges of taxa. Paleobiology 22:121–140.

Foss, S. E. 2007. Family Entelodontidae. Pages 120–129 *in* D. R. Prothero and S. E. Foss, eds. The Evolution of Artiodactyls. Johns Hopkins University Press, Baltimore.

Freckleton, R. P., P. H. Harvey, and M. Pagel. 2002. Phylogenetic analysis and comparative data: A test and review of evidence. American Naturalist 160:712–726.

Frederiksen, N. O. 1991. Age determination for Eocene formations of the San Diego, California, area, based on pollen data. Pages 195–200 *in* P. L. Abbott and J. A. May, eds. Eocene geologic history: San Diego region. Pacific Section, Society of Economic Paleontologists and Mineralogists, Los Angeles.

Friscia, A. R., B. Van Valkenburgh, and A. R. Biknevicius. 2007. An ecomorphological analysis of extant small carnivorans. Journal of Zoology 272:82–100.

Fritz, S. A., O. R. P. Bininda-Emonds, and A. Purvis. 2009. Geographical variation in predictors of mammalian extinction risk: big is bad, but only in the tropics. Ecology Letters 12:538–549.

Fritzell, E. K., and K. J. Haroldson. 1982. *Urocyon cinereoargenteus*. Mammalian Species 189:1–8.

Fulton, T. L., and C. Strobeck. 2010. Multiple fossil calibrations, nuclear loci and mitochondrial genomes provide new insight into biogeography and divergence timing for true seals (Phocidae, Pinnipedia). Journal of Biogeography 37:814–829.

Garland, T., Jr., P. H. Harvey, and A. R. Ives. 1992. Procedures for the analysis of comparative data using phylogenetically independent contrasts). Systematic Biology 41:18–32.

Garland, T., Jr., and C. M. Janis. 1993. Does metatarsal/femur ratio predict maximal running speed in cursorial mammals? Journal of Zoology 229:131–151.

Gaubert, P., and P. Cordeiro-Estrela. 2006. Phylogenetic systematics and tempo of evolution of the Viverrinae (Mammalia, Carnivora, Viverridae) within feliformians: implications for faunal exchange between Asia and Africa. Molecular Phylogenetics and Evolution 41:266–278.

Gaubert, P., and G. Veron. 2003. Exhaustive sample set among viverridae reveals the sister-group of felids: the linsangs as a case of extreme morphological convergence within feliformia. Proceedings of the Royal Society of London B 270:2523–2530.

Gaubert, P., W. C. Wozencraft, P. Cordeiro-Estrela, and G. Veron. 2005. Mosaics of convergences and noise in morphological phylogenies: what's in a viverrid-like carnivoran? Systematic Biology 54:865–894.

Gazin, C. L. 1958. A review of the middle and upper Eocene primates of North America. Smithsonian Miscellaneous Collections 136:1–112.

Geisler, J. H., J. M. Theodor, M. D. Uhen, and S. E. Foss. 2007. Phylogenetic relationships of cetaceans to terrestrial artiodactyls. Pages 19–31 *in* D. R. Prothero and S. E. Foss, eds. The Evolution of Artiodactyls. Johns Hopkins University Press, Baltimore.

Geisler, J. H., and M. D. Uhen. 2005. Phylogenetic relationships of extinct cetartiodactyls: results of simultaneous analyses of molecular, morphological, and stratigraphic data. Journal of Mammalian Evolution 12:145–159.

Gilbert, C. C. 2005. Dietary ecospace and the diversity of Euprimates during the early and middle Eocene. American Journal of Physical Anthropology 126:237–249.

Gingerich, P. D. 1974. Size variability of the teeth in living mammals and the diagnosis of closely related sympatric fossil species. Journal of Paleontology 48:895–903.

———. 1983. Systematics of early Eocene Miacidae (Mammalia, Carnivora) in the Clark's Fork Basin, Wyoming. Contributions from the Museum of Paleontology, University of Michigan 26:197–225.

Gingerich, P. D., and D. A. Winkler. 1979. Patterns of variation and correlation in the dentition of the red fox, *Vulpes vulpes*. Journal of Mammalogy 60:691–704.

Ginzburg, L. R., O. Burger, and J. Damuth. 2010. The May threshold and life-history allometry. Biology Letters 6:850–853.

Goloboff, P. A., J. S. Farris, and K. C. Nixon. 2003. T.N.T.: tree analysis using new technology, Willi Hennig Society Edition. TNT website. Available at www.zmuc.dk/public/phylogeny/tnt. Accessed March 4, 2010.

———. 2008. TNT: a free program for phylogenetic analysis. Cladistics 24:774–786.

Golz, D. J. 1976. Eocene Artiodactyla of southern California. Natural History Museum of Los Angeles County, Science Bulletin 26:1–85.

Golz, D. J., and J. A. Lillegraven. 1977. Summary of known occurrences of terrestrial vertebrates from Eocene strata of southern California. University of Wyoming Contributions to Geology 15:43–65.

Gompper, M. E. 1995. *Nasua narica*. Mammalian Species 487:1–10.

Gonyea, W., and R. Ashworth. 1975. The form and function of retractile claws in the Felidae and other representative carnivorans. Journal of Morphology 145:229–238.

Goodwin, H. T. 2008. Sciuridae. Pages 355–376 *in* C. M. Janis, G. F. Gunnell, and M. D. Uhen, eds. Evolution of tertiary mammals of North America: volume 2, small mammals, xenarthrans, and marine mammals. Cambridge University Press , Cambridge.

Gordon, C. L. 2003. A first look at estimating body size in dentally conservative marsupial. Journal of Mammalian Evolution 10:1–21.

Graham, R. W., and E. L. Lundelius. 2010. FAUNMAP II: new data for North America with a temporal extension for the Blancan, Irvingtonian and early Rancholabrean. Available at http://www.ucmp.berkeley.edu/faunmap/.

Graur, D., and W. Martin. 2004. Reading the entrails of chickens: molecular timescales of evolution and the illusion of precision. Trends in Genetics 20:80–86.

Guilday, J. E. 1962. Supernumerary molars of *Otocyon*. Journal of Mammalogy 43:455–462.

Gunnell, F., Gregg, T. M. Bown, J. H. Hutchison, and J. I. Bloch. 2008. Lipotyphla. Pages 89–125 *in* C. M. Janis, G. F. Gunnell, and M. D. Uhen, eds. Evolution of tertiary mammals of North America: volume 2, small mammals, xenarthrans, and marine mammals. Cambridge University Press , Cambridge.

Gunnell, G. F. 1995. New notharctine (Primates, Adapiformes) skull from the Uintan (middle Eocene) of San Diego County, California. American Journal of Physical Anthropology 98:447–470.

Gunnell, G. F., and K. D. Rose. 2002. Tarsiiformes: evolutionary history and adaptation. Pages 45–82 *in* Hartwig, Wlater C., ed. The primate fossil record. Cambridge University Press, Cambridge.

Gustafson, E. P. 1986. Carnivorous mammals of the late Eocene and early Oligocene of Trans-Pecos Texas. Bulletin of the Texas Memorial Museum 33:1–66.

Hadly, E. A., P. A. Spaeth, and C. Li. 2009. Niche conservatism above the species level. Proceedings of the National Academy of Sciences of the United States of America 106:19707–19714.

Haldane, J. B. S. 1955. The measurement of variation. Evolution 9:484.

Hall, E. R. 1930. Three new genera of Mustelidae from the later Tertiary of North America). Journal of Mammalogy 11:146–155.

Hanson, C. B. 1996. Stratigraphy and vertebrate faunas of the Bridgerian-Duchesnean Clarno Formation, northern Oregon. Pages 206–239 *in* Prothero, D. R. and Emry, R. J., ed. The terrestrial Eocene-Oligocene transition in North America. Cambridge University Press, Cambridge.

Harrell, F. E. 2012. Regression modeling strategies (Package 'rms'), Version 3.5-0. Available at http://cran.r-project.org/web/packages/rms/index.html.

Hatcher, J. B. 1902. Oligocene Canidae. Memoirs of the Carnegie Museum 1:65–108.

Hayes, F. G. 2000. The Brooksville 2 Local Fauna (Arikareean, latest Oligocene): Hernando County, Florida). Bulleting of the Florida Museum of Natural History 43:1–47.

Heinrich, R. E., and P. Houde. 2006. Postcranial anatomy of viverravus (mammalia, carnivora) and implications for substrate use in basal carnivora. Journal of Vertebrate Paleontology 26:422–435.

Heinrich, R. E., and K. D. Rose. 1995. Partial skeleton of the primitive carnivoran *Miacis petilus* from the early Eocene of Wyoming. Journal of Mammalogy 76:148–162.

———. 1997. Postcranial morphology and locomotor behaviour of two early Eocene miacoid carnivorans, *Vulpavus* and *Didymictis*. Palaeontology 40:279–305.

Heinrich, R. E., S. G. Strait, and P. Houde. 2008. Earliest eocene miacidae (mammalia: Carnivora) from northwestern wyoming. Journal of Paleontology 82:154–162.

Hildebrand, M., and G. E. Goslow. 2001. Analysis of vertebrate structure, Fifth edition. John Wiley, New York.

Hooker, J. J., and D. Dashzeveg. 2004. The origin of chalicotheres (Perissodactyla, Mammalia). Palaeontology 47:1363–1386.

Hopkins, S. S. B. 2008*a*. Phylogeny and evolutionary history of the Aplodontoidea (Mammalia : Rodentia). Zoological Journal of the Linnean Society 153:769–838.

———. 2008*b*. Reassessing the mass of exceptionally large rodents using toothrow length and area as proxies for body mass. Journal of Mammalogy 89:232–243.

Hough, J. R. 1948. A systematic revision of *Daphoenus* and some allied genera. Journal of Paleontology 22:573–600.

Howell, D. G., and M. H. Link. 1979. Eocene conglomerate sedimentology and basin analysis, San Diego and the southern California borderland. Journal of Sedimentary Petrology 49:517–540.

Hug, L. A., and A. J. Roger. 2007. The impact of fossil and taxon sampling on ancient molecular dating analyses. Molecular Biology and Evolution 24:1889–1897.

Hunt, G. 2004*a*. Phenotypic variance inflation in fossil samples: an empirical assessment. Paleobiology 30:487–506.

———. 2004*b*. Phenotypic variation in fossil samples: modeling the consequences of time-averaging. Paleobiology 30:426–443.

Hunt, R. M., Jr. 1977. Basicranial anatomy of *Cynelos* Jourdan (Mammalia: Carnivora), an Aquitanian Amphicyonid from the Allier Basin, France. Journal of Paleontology 51:826–843.

———. 1989. Evolution of the aeluroid carnivora: significance of the ventral promontorial process of the petrosal, and the origin of basicranial patterns in the living families. American Museum Novitates 2930:1–32.

———. 1996*a*. Amphicyonidae. Pages 476–485 *in* D. R. Prothero and R. J. Emry, eds. The terrestrial Eocene-Oligocene transition in North America. Cambridge University Press, Cambridge.

———. 1996*b*. Biogeography of the order Carnivora. Pages 485–541 *in* J. L. Gittleman, ed. Carnivore behavior, ecology, and evolution, Volume 2. Cornell University Press, Ithaca.

———. 1998*a*. Amphicyonidae. Pages 196–227 *in* C. M. Janis, K. M. Scott, and L. L. Jacobs, eds. Evolution of tertiary mammals of North America: volume 1, terrestrial carnivores, ungulates, and ungulatelike mammals. Cambridge University Press , Cambridge.

———. 1998*b*. Ursidae. Pages 174–195 *in* C. M. Janis, K. M. Scott, and L. L. Jacobs, eds. Evolution of tertiary mammals of North America: volume 1, terrestrial carnivores, ungulates, and ungulatelike mammals. Cambridge University Press , Cambridge.

———. 2001. Small Oligocene amphicyonids from North America (*Paradaphoenus*, Mammalia, Carnivora). American Museum Novitates 3331:1–20.

———. 2002. New amphicyonid carnivorans (Mammalia, Daphoeninae) from the early Miocene of southeastern Wyoming. American Museum Novitates 3385:1–41.

Isaac, N. J. B., S. T. Turvey, B. Collen, C. Waterman, and J. E. M. Baillie. 2007. Mammals on the EDGE: conservation priorities based on threat and phylogeny. PLoS ONE 2:e296.

Jablonski, D., and J. A. Finarelli. 2009. Congruence of morphologically-defined genera with molecular phylogenies. Proceedings of the National Academy of Sciences of the United States of America 106:8262–8266.

Janis, C. M. 2000. Patterns in the evolution of herbivory in large terrestrial mammals: the Paleogene of North America. Pages 168–222 *in* Sues, H. -D., ed. Evolution of herbivory in terrestrial vertebrates: perspectives from the fossil record. Cambridge University Press, Cambridge.

Janis, C. M., G. F. Gunnell, and M. D. Uhen. 2008. Evolution of tertiary mammals of North America: volume 2, small mammals, xenarthrans, and marine mammals. Cambridge University Press, Cambridge.

Janis, C. M., K. M. Scott, and L. L. Jacobs. 1998. Evolution of tertiary mammals of North America: volume 1, terrestrial carnivores, ungulates, and ungulatelike mammals. Cambridge University Press, Cambridge.

Janis, C. M., and P. B. Wilhelm. 1993. Were there mammalian pursuit predators in the Tertiary? Dances with wolf avatars. Journal of Mammalian Evolution 1:103–125.

Jenkins, F. A., Jr., and D. McClearn. 1984. Mechanisms of hindfoot reversal in climbing mammals. Journal of Morphology 182:197–219.

Jernvall, J., and M. Fortelius. 2004. Maintenance of trophic structure in fossil mammal communities: Site occupancy and taxon resilience. American Naturalist 164:614–624.

Johnson, C. N. 2002. Determinants of loss of mammal species during the Late Quaternary 'megafauna' extinctions: life history and ecology, but not body size. Proceedings of the Royal Society of London Series B-Biological Sciences 269:2221–2227.

Johnson, W. E., E. Eizirik, J. Pecon-Slattery, W. J. Murphy, A. Antunes, E. Teeling, and S. J. O'Brien. 2006. The late Miocene radiation of modern Felidae: a genetic assessment. Science 311:73–77.

Jones, K. E., J. Bielby, M. Cardillo, S. A. Fritz, J. O'Dell, C. D. Orme, K. Safi, W. Sechrest, E. H. Boakes, C. Carbone, C. Connolly, M. J. Cutts, J. K. Foster, R. Grenyer, M. Habib, C. A. Plaster, S. A. Price, E. A. Rigby, J. Rist, A. Teacher, O. R. P. Bininda-Emonds, J. L. Gittleman, G. M. Mace, and A. Purvis. 2009. PanTHERIA: a species-level database of life history, ecology, and geography of extant and recently extinct mammals.). Ecology 90:2648. Available at http://esapubs.org/archive/ecol/E090/184/metadata.htm.

Jones, K. E., W. Sechrest, and J. L. Gittleman. 2005. Age and area revisited: identifying global patterns and implications for conservation. Pages 141–165 *in* A. Purvis, J. L. Gittleman, and T. Brooks, eds. Phylogeny and Conservation. Cambridge University Press, Cambridge.

Keesing, F. 1998. Impacts of ungulates on the demography and diversity of small mammals in central Kenya. Oecologia 116:381–389.

Kelly, T. S. 1990. Biostratigraphy of Uintan and Duchesnean land mammal assemblages from the Middle Member of the Sespe Formation, Simi Valley, California. Natural History Museum of Los Angeles County, Contributions in Science 419:1–42.

———. 1992. New Uintan and Duchesnean (middle and late Eocene) rodents from the Sespe Formation, Simi Valley, California. Bulletin of the Southern California Academy of Science 91:97–120.

———. 2007. A new species of *Bensomys* (Rodentia, Cricetidae) from the late early Hemphillian (late Miocene), Coal Valley Formation, Smith Valley, Nevada. Paludicola 6:125–138.

Kelly, T. S., E. B. Lander, D. P. Whistler, M. A. Roeder, and R. E. Reynolds. 1991. Preliminary report on a paleontologic investigation of the lower and middle Members, Sespe Formation, Simi Valley Landfill, Ventura County, California. PaleoBios 13:1–13.

Kelly, T. S., P. C. Murphey, and S. L. Walsh. 2012. New records of small mammals from the middle Eocene Duchesne River Formation, Utah, and their implications for the Uintan-Duchesnean North American Land Mammal Age transition. Paludicola 8:208–251.

Kelly, T. S., and D. P. Whistler. 1994. Additional Uintan and Duchesnean (middle and late Eocene) mammals from the Sespe Formation, Simi Valley, California. Natural History Museum of Los Angeles County, Contributions in Science 439:1–29.

———. 1998. A new eomyid rodent from the Sespe Formation of southern California. Journal of Vertebrate Paleontology 18:440–443.

Kitazoe, Y., H. Kishino, P. J. Waddell, N. Nakajima, T. Okabayashi, T. Watabe, and O. Yoshiyasu. 2007. Robust time estimation reconciles views of the antiquity of placental mammals. PLoS ONE 2:e384.

Kluge, A. G., and J. S. Farris. 1969. Quantitative phyletics and the evolution of anurans. Systematic Zoology 18:1–32.

Koch, P. L., and A. D. Barnosky. 2006. Late Quaternary extinctions: state of the debate. Annual Review of Ecology, Evolution, and Systematics 37:215–250.

Koepfli, K. P., K. A. Deere, G. J. Slater, C. Begg, K. Begg, L. Grassman, M. Lucherini, G. Veron, and R. K. Wayne. 2008. Multigene phylogeny of the Mustelidae: resolving relationships, tempo and biogeographic history of a mammalian adaptive radiation). BMC Biology 6:10.

Koepfli, K. P., M. E. Gompper, E. Eizirik, C. C. Ho, L. Linden, J. E. Maldonado, and R. K. Wayne. 2007. Phylogeny of the Procyonidae (Mammalia: Carnivora): molecules, morphology and the Great American Interchange). Molecular Phylogenetics and Evolution 43:1076–1095.

Korth, W. W. 1999. A new species of beaver (Rodentia, Castoridae) from the earliest Barstovian (Miocene) of Nebraska and the phylogeny of *Monosaulax* Stirton. Paludicola 2:258–264.

———. 2001. Comments on the systematics and classification of the beavers (Rodentia, Castoridae). Journal of Mammalian Evolution 8:279–296.

———. 2002. Review of the castoroidine beavers (Rodentia, Castoridae) from the Clarendonian (Miocene) of northcentral Nebraska. Paludicola 4:15–24.

———. 2007*a*. A new genus of beaver (Rodentia, Castoridae) from the Miocene (Clarendonian) of North America and systematics of the Castoroidinae based on comparative cranial anatomy. Annals of Carnegie Museum 76:117–134.

———. 2007*b*. A new species of *Ansomys* (Rodentia, Aplodontidae) from the late Oligocene (latest Whitneyan-earliest Arikareean) of South Dakota). Journal of Vertebrate Paleontology 27:740–743.

———. 2007*c*. Mammals from the Blue Ash local fauna (late Oligocene), South Dakota. Rodentia, Part 1: families Eutypomyidae, Eomyidae, Heliscomyidae, and *Zetamys*. Paludicola 6:31–40.

———. 2008. Early Arikareean (late Oligocene) Eomyidae (Mammalia, Rodentia) from Nebraska. Paludicola 6:144–154.

Korth, W. W., and B. E. Bailey. 2006. Earliest castoroidine beaver (Rodentia, Castoridae) from the late Arikareean (early Miocene) of Nebraska. Annals of Carnegie Museum 75:237–245.

Korth, W. W., and C. Branciforte. 2007. Geomyoid rodents (Mammalia) from the Ridgeview Local Fauna, early-early Arikareean (late Oligocene) of wetern Nebraska. Annals of Carnegie Museum 76:177–201.

Kotsakis, T. 1980. Revisione sistematica e distribuzione stratigrafica e geografica del genere *Cynodictis* bravard pomel (carnivora, mammalia). Bollettino della Societ Paleontologica Italiana 19:259–273.

Kumar, S., and S. B. Hedges. 1998. A molecular timescale for vertebrate evolution. Nature 392:917–920.

Lande, R. 1993. Risks of population extinction from demographic and environmental stochasticity and random catastrophes. American Naturalist 142:911–927.

Lander, E. B., and C. B. Hanson. 2006. *Agriochoerus matthewi crassus* (Artiodactyla, Agriochoeridae) of the late middle Eocene Hancock Mammal Quarry Local Fauna, Clarno Formation, John Day Basin, north-central Oregon. PaleoBios 26:19–34.

Larson, S. D., and J. T. Stern. 1989. Role of supraspinatus in the quadrupedal locomotion of vervets (*Cercopithecus ethiops*): implications for the interpretation of humeral morphology. American Journal of Physical Anthropology 79:369–377.

Leach, D. 1977. The descriptive and comparative osteology of marten (*Martes americana* Turton) and fisher (*Martes pennanti* Erxleben): the appendicular skeleton. Canadian Journal of Zoology 55:199–214.

Legendre, S. 1986. Analysis of mammalian communities from the Late Eocene and Oligocene of southern France. Palaeovertebrata (Montpellier) 16:191–212.

Lillegraven, J. A. 1976. A biogeographical problem involving comparisons of later Eocene terrestrial vertebrate faunas of western North America. Pages 333–347 *in* J. Gray and A. J. Boucot, eds. Historical biogeography, plate tectonics, and the changing environment. Oregon State University Press, Corvallis, Oregon.

———. 1977. Small rodents (Mammalia) from Eocene deposits of San Diego County, California. Bulletin of the American Museum of Natural History 158:221–262.

———. 1980. Primates from later Eocene rocks of southern California. Journal of Mammalogy 61:181–204.

Lillegraven, J. A., M. C. McKenna, and L. Krishtalka. 1981. Evolutionary relationships of middle Eocene and younger species of *Centetodon* (Mammalia, Insectivora, Geolabididae) with a description of the dentition of *Ankylodon* (Adapisoricidae). University of Wyoming Publications 45:1–113.

Lillegraven, J. A., and R. W. Wilson. 1975. Analysis of *Simimys simplex*, an Eocene rodent (?Zapodidae). Journal of Paleontology 49:856–874.

Lindsay, E. 1968. Rodents from the Hartman Ranch local fauna, California. PaleoBios 6:1–22.

Lindsay, E. H. 2008. Cricetidae. Pages 456–479 *in* C. M. Janis, G. F. Gunnell, and M. D. Uhen, eds. Evolution of tertiary mammals of North America: volume 2, small mammals, xenarthrans, and marine mammals. Cambridge University Press , Cambridge.

Liow, L. H., M. Fortelius, E. Bingham, K. Lintulaakso, H. Mannila, L. Flynn, and N. C. Stenseth. 2008. Higher origination and extinction rates in larger mammals. Proceedings of the National Academy of Sciences of the United States of America 105:6097–6102.

Lockwood, C. A., B. G. Richmond, W. L. Jungers, and W. H. Kimbel. 1996. Randomization procedures and sexual dimorphism in *Australopithecus afarensis*. Journal of Human Evolution 31:537–548.

Ludtke, J. A., and D. R. Prothero. 2004. Taxonomic revision of the middle Eocene (Uintan-Duchesnean) protoceratid *Leptoreodon* (Mammalia: Artiodactyla). New Mexico Museum of Natural History and Science Bulletin 26:101–111.

Lyons, S. K., F. A. Smith, and J. H. Brown. 2004. Of mice, mastodons and men: human-mediated extinctions on four continents. Evolutionary Ecology Research 6:339–358.

Mac Intyre, G. T. 1966. The miacidae (mammalia, carnivora): part 1, the systematics of *Ictidopappus* and *Protictis*. Bulletin of the American Museum of Natural History 131:117–209.

MacFadden, B. J. 1998. Equidae. Pages 537–559 *in* C. M. Janis, K. M. Scott, and L. L. Jacobs, eds. Evolution of tertiary mammals of North America: volume 1, terrestrial carnivores, ungulates, and ungulatelike mammals. Cambridge University Press , Cambridge.

Maddison, W. P., and D. R. Maddison. 2009. Mesquite: a modular system for evolutionary analysis, version 2.72. Mesquite website. Available at mesquiteproject.org/mesquite/mesquite.html. Accessed March 23, 2010.

Marshall, C. R. 1997. Confidence intervals on stratigraphic ranges with nonrandom distributions of fossil horizons. Paleobiology 23:165–173.

———. 2010. Using confidence intervals to quantify the uncertainty in the end-points of stratigraphic ranges. Pages 291–316 *in* J. Alroy and G. Hunt, eds. Quantitative methods in paleobiology (Paleontological Society Papers 16). Paleontological Society.

Martin, L. D. 1998. Felidae. Pages 236–242 *in* C. M. Janis, K. M. Scott, and L. L. Jacobs, eds. Evolution of tertiary mammals of North America: volume 1, terrestrial carnivores, ungulates, and ungulatelike mammals. Cambridge University Press , Cambridge.

Martin, L. D., and J. D. Lim. 2004. New insectivores from the Early Miocene of Nebraska, USA and the Hemingfordian faunal exchange). Mammalian Biology 69:202–209.

Martin, R. A. 2008. Arvicolinae. Pages 480–497 *in* C. M. Janis, G. F. Gunnell, and M. D. Uhen, eds. Evolution of tertiary mammals of North America: volume 2, small mammals, xenarthrans, and marine mammals. Cambridge University Press , Cambridge.

Mason, M. A. 1990. New fossil primates from the Uintan (Eocene) of southern California. PaleoBios 13:1–7.

Matthew, W. D. 1909. The Carnivora and Insectivora of the Bridger Basin, middle Eocene. Memoirs of the American Museum of Natural History 9:289–576.

McKenna, M. C., and S. K. Bell. 1997. Classification of mammals above the species level. Columbia University Press, New York.

McKenna, M. C., A. R. Bleefeld, and J. S. Mellett. 1994. Microvertebrate collecting: large-scale wet sieving for fossil microvertebrates in the field. Pages 93–112 *in* P. Leiggi and P. May, eds. Vertebrate paleontological techniques, Volume 1. Cambridge University Press, Cambridge.

McKinney, M. L. 1997. Extinction vulnerability and selectivity: combining ecological and paleontological views. Annual Review of Ecology and Systematics 28:495–516.

Meachen-Samuels, J., and B. Van Valkenburgh. 2009. Forelimb indicators of prey-size preference in the felidae. Journal of Morphology 270:729–744.

Mellet, J. S. 1977. Paleobiology of North American Hyaenodon. Contributions to Vertebrate Evolution 1:1–134.

Mihlbachler, M. C., and T. A. Deméré. 2009. A new species of Brontotheriidae (Perissodactyla, Mammalia) from the Santiago Formation (Duchesnean, middle Eocene) of southern California. Proceedings of the San Diego Society of Natural History 41:1–36.

Morlo, M. 1999. Niche structure and evolution in creodont (Mammalia) faunas of the European and North American Eocene. Geobios 32:297–305.

Murphey, P. C., A. Lester, B. Bohor, P. Robinson, E. Evanoff, and E. Larson. 1999. $^{40}\mathrm{Ar}/^{39}\mathrm{Ar}$ dating of volcanic ash deposits in the Bridger Formation (middle Eocene) southwestern Wyoming. Geological Society of America Abstracts with Programs 31:A233.

Murphy, W. J., E. Eizirik, S. J. O'Brien, O. Madsen, M. Scally, C. J. Douady, E. Teeling, O. A. Ryder, M. J. Stanhope, W. W. de Jong, and M. S. Springer. 2001. Resolution of the early placental mammal radiation using Bayesian phylogenetics. Science 294:2348–2351.

Myers, J. A. 1991. The early middle Eocene Torrey Flora, Del Mar, California. Pages 201–216 *in* P. L. Abbott and J. A. May, eds. Eocene geologic history: San Diego region. Pacific Section, Society of Economic Paleontologists and Mineralogists, Los Angeles.

———. 2003*a*. Fossil leaf remains from the middle Eocene Westview High School and 4S Ranch localities, San Diego County, California. *In* G. L. Kennedy and G. I. Shiller, eds., Paleontological mitigation investigation, construction of Westview High School Rancho Peñasquitos, San Diego, San Diego County, California. Brian F. Smith and Associates, Poway, California. Unpublished paleontological report prepared for the Poway Unified School District.

———. 2003*b*. Terrestrial Eocene-Oligocene vegetation and climate in the Pacific Northwest. Pages 171–185 *in* D. R. Prothero, L. C. Ivany, and E. A. Nesbitt, eds. From greenhouse to icehouse: the marine Eocene-Oligocene transition. Columbia University Press, New York.

Novacek, M. J. 1976. Insectivora and Proteutheria of the later Eocene (Uintan) of San Diego County, California. Contributions in Science, Natural History Museum of Los Angeles County 283:1–52.

———. 1985. The Sespedectinae, a new subfamily of hedgehog-like insectivores). American Museum Novitates 2822:1–24.

Novacek, M. J., and J. A. Lillegraven. 1979. Terrestrial vertebrates from the later Eocene of San Diego County, California: a conspectus. Pages 69–79 *in* P. L. Abbott, ed. Eocene depositional systems: San Diego, California. Pacific Section, Society of Economic Paleontologists and Mineralogists, Los Angeles.

Oksanen, J., R. Kindt, P. Legendre, B. O'Hara, G. L. Simpson, P. Solymos, M. H. H. Stevens, and H. Wagner. 2009. Community ecology package 'vegan', Version 1.15-2 Available at http://cran.r-project.org/, http://vegan.r-forge.r-project.org/.

O'Leary, M. A., and J. Gatesy. 2008. Impact of increased character sampling on the phylogeny of Cetartiodactyla (Mammalia): combined analysis including fossils. Cladistics 24:397–442.

Osborn, H. F. 1895. Fossil mammals of the Uinta Basin: expedition of 1894. Bulletin of the American Museum of Natural History 7:71–105.

Pagel, M. 1999. Inferring the historical patterns of biological evolution. Nature 401:877–884.

Palomares, F. 1993. Opportunistic feeding of the egyptian mongoose, *Herpestes ichneumon*, (l.) in southwestern spain. La Terre et la Vie-Revue d'écologie 48:295–304.

Paradis, E., B. Bolker, J. Claude, H. S. Cuong, R. Desper, B. Durand, J. Dutheil, O. Gascuel, C. Heibl, D. Lawson, V. Lefort, P. Legendre, J. Lemon, Y. Noel, J. Nylander, R. Opgen-Rhein, A.-A. Popescu, K. Schliep, K. Strimmer, and D. de Vienne. 2012. Linear and nonlinear mixed effects models (Package 'nlme'), Version 3.0-3. Available at http://cran.r-project.org/web/packages/ape/index.html.

Pasitschniak-Arts, M., and S. Larivière. 1995. *Gulo gulo*. Mammalian Species 499:1–10.

Paul, C. R. C. 1982. The adequacy of the fossil record. Pages 75–117 *in* K. A. Joysey and A. E. Friday, eds. Problems of phylogenetic reconstruction. Academic Press, London.

Peterson, G. L., and P. L. Abbott. 1979. Mid-Eocene climatic change, southwestern California and northwestern Baja California. Palaeogeography, Palaeoclimatology, Palaeoecology 26:73–87.

Petter, G. 1966. *Cynodictis*, canidé oligocène d'Europe: région tympanique et affinités. Annales de Paléontologie 52:1–19.

Phillips, R. B., C. S. Winchell, and R. H. Schmidt. 2007. Dietary overlap of an alien and native carnivore on san clemente island, california. Journal of Mammalogy 88:173–180.

Pickford, M. 1989. Dynamics of Old World biogeographic realms during the Neogene: implications for biostratigraphy. Pages 413–442 *in* E. H. Lindsay, V. Fahlbusch, and P. Mein, eds. European Neogene mammal chronology. Plenum Press, New York.

Pinheiro, J., D. Bates, S. DebRoy, D. Sarkar, and R Development Core Team. 2012. Linear and nonlinear mixed effects models (Package 'nlme'), Version 3.1-103. Available at http://cran.r-project.org/web/packages/nlme/index.html.

Plavcan, J. M., and D. A. Cope. 2001. Metric variation and species recognition in the fossil record. Evolutionary Anthropology 10:204–222.

Polishchuk, L. V. 2010. The three-quarter-power scaling of extinction risk in Late Pleistocene mammals, and a new theory of the size selectivity of extinction. Evolutionary Ecology Research 12:1–22.

Polly, P. D. 1996. The skeleton of *Gazinocyon vulpeculus* gen. et comb. nov. and the cladistic relationships of Hyaenodontidae (Eutheria, Mammalia). Journal of Vertebrate Paleontology 16:303–319.

———. 1997. Ancestry and species definition in paleontology: a stratocladistic analysis of Viverravidae (Carnivora, Mammalia) from Wyoming. Contributions from the Museum of Paleontology, University of Michigan 30:1–53.

———. 1998. Variability in mammalian dentitions: size-related bias in the coefficient of variation. Biological Journal of the Linnean Society 64:83–99.

Polly, P. D., G. D. Wesley-Hunt, R. E. Heinrich, G. Davis, and P. Houde. 2006. Earliest known carnivoran auditory bulla and support for a recent origin of crown-group Carnivora (Eutheria, Mammalia). Palaeontology 49:1019–1027.

Poux, C., O. Madsen, J. Glow, W. W. Jong, and M. Vences. 2008. Molecular phylogeny and divergence times of Malagasy tenrecs: influence of data partitioning and taxon sampling on dating analyses. BMC Evolutionary Biology 8:102.

Prothero, D. R. 1998. Hyradocontidae. Pages 589–594 *in* Evolution of tertiary mammals of North America: volume 1, terrestrial carnivores, ungulates, and ungulatelike mammals. Cambridge University Press .

———. 2005. The evolution of North American rhinoceroses. Cambridge University Press, Cambridge.

———. 2008. Systematics of the musk deer (Artiodactyla: Moschidae: Blastomerycinae) from the Miocene of North America). New Mexico Museum of Natural History and Science Bulletin 44:207–224.

Prothero, D. R., and M. R. Liter. 2007. Family Palaeomerycidae. Pages 241–248 *in* D. R. Prothero and S. E. Foss, eds. The Evolution of Artiodactyls. Johns Hopkins University Press, Baltimore.

———. 2008. Systematics of the dromomerycines and aletomerycines (Artiodactyla: Palaeomerycidae) from the Miocene and Pliocene of North America). New Mexico Museum of Natural History and Science Bulletin 44:273–298.

Prothero, D. R., and D. L. Rasmussen. 2008. New giant rhinoceros from the Arikareean (Oligocene-Miocene) of Montana, South Dakota and Wyoming. New Mexico Museum of Natural History and Science Bulletin 44:323–330.

R Developement Core Team. 2009. R: a language and environment for statistical computing, Version 2.10.1. Available at http://www.R-project.org.

Raia, P., F. Passaro, D. Fulgione, and F. Carotenuto. 2011. Habitat tracking, stasis and survival in Neogene large mammals. Biology Letters 8:64–66.

Repenning, C. A., and F. Grady. 1988. The microtine rodents of the Cheetah Room Fauna, Hamilton Cave, West Virginia, and the spontaneous origin of *Synaptomys*. U. S. Geological Survey Bulletin 1853:1–32.

Revell, L. J. 2010. Phylogenetic signal and linear regression on species data. Methods in Ecology and Evolution 1:319–329.

Robinson, P., G. F. Gunnell, S. L. Walsh, W. C. Clyde, J. E. Storer, R. K. Stucky, D. J. Froehlich, I. F. Villafranca, and M. C. McKenna. 2004. Wasatchian through Duchesnean biochronology. Pages 106–155 *in* Woodburne, M. O., ed. Late Cretaceous and Cenozoic mammals of North America: biostratigraphy and geochronology. Columbia University Press, New York.

Roemer, G. W., M. E. Gompper, and B. Van Valkenburgh. 2009. The ecological role of the mammalian mesocarnivore. BioScience 59:165–173.

Rosalino, L. M., M. J. Santos, I. Pereira, and M. Santos-Reis. 2009. Sex-driven differences in egyptian mongoose s (*Herpestes ichneumon*) diet in its northwestern european range. European Journal of Wildlife Research 55:293–299.

Rose, K. D. 2006. The beginning of the age of mammals. Johns Hopkins University Press, Baltimore.

Rose, K. D., and W. von Koenigswald. 2007. The marmot-sized paramyid rodent *Notoparamys costilloi* from the early Eocene of Wyoming, with comments on dental variation and occlusion in paramyids. Bulletin of Carnegi Museum of Natural History 39:111–125.

Roth, B. 1991. Tropical "physiognomy" of a land snail faunule from the Eocene of southern California. Malacologia 33:281–288.

Rowe, T. 1988. Definition, diagnosis, and origin of Mammalia. Journal of Vertebrate Paleontology 8:241–264.

Russell, G. J., T. M. Brooks, M. M. McKinney, and C. G. Anderson. 1998. Present and future taxonomic selectivity in bird and mammal extinctions. Conservation Biology 12:1365–1376.

Scott, W. B. 1898. Notes on the Canidae of the White River Oligocene. Transactions of the American Philosophical Society 19:325–416.

Silcox, M. T., and G. F. Gunnell. 2008. Plesiadapiformes. Pages 207–238 *in* C. M. Janis, G. F. Gunnell, and M. D. Uhen, eds. Evolution of tertiary mammals of North America: volume 2, small mammals, xenarthrans, and marine mammals. Cambridge University Press , Cambridge.

Simpson, G. G., A. Roe, and R. C. Lewontin. 1960. Quantitative zoology, Revised edition. Harcourt, New York.

Spaulding, M., and J. J. Flynn. 2009. Anatomy of the postcranial skeleton of *"Miacis" uintensis* (Mammalia: Carnivoramorpha). Journal of Vertebrate Paleontology 29:1212–1223.

Spaulding, M., J. J. Flynn, and R. K. Stucky. 2010. A new basal carnivoramorphan (Mammalia) from the 'Bridger B' (Black's Fork Member, Bridger Formation, Bridgerian NALMA, middle Eocene) of Wyoming, USA. Palaeontology 53:815–832.

Springer, M. S., W. J. Murphy, E. Eizirik, and S. J. O'Brien. 2003. Placental mammal diversification and the Cretaceous-Tertiary boundary. Proceedings of the National Academy of Sciences of the United States of America 100:1056–1061.

Stanley, S. M. 1998. Macroevolution. Johns Hopkins University Press, Baltimore. Paperback edition.

Stock, C. 1938*a*. A tarsiid primate and a mixodectid from the Poway Eocene, California. Proceedings of the National Academy of Sciences of the United States of America 24:288–293.

———. 1938*b*. A titanothere from the type Sespe of California. Proceedings of the National Academy of Sciences of the United States of America 24:507–512.

Strait, S. G. 2001. Dietary reconstruction of small-bodied omomyoid primates. Journal of Vertebrate Paleontology 21:322–334.

Strauss, D., and P. M. Sadler. 1989. Classical confidence-intervals and Bayesian probability estimates for ends of local taxon ranges. Mathematical Geology 21:411–421.

Stucky, R. K., and M. C. McKenna. 1993. Mammalia. Pages 739–771 *in* Benton, M. J., ed. The fossil record 2. Chapman Hall, London.

Szalay, F. S., and R. L. Decker. 1974. Origins, evolution, and function of the tarsus in Late Cretaceous Eutheria and Paleocene Primates. Pages 223–259 *in* F. A. Jenkins, Jr., ed. Primate locomotion. Academic Press, New York.

Szalay, F. S., and S. J. Gould. 1966. Asiatic Mesonychidae (Mammalia, Condylarthra). Bulletin of the American Museum of Natural History 132:127–174.

Szuma, E. 2004. Evolutionary implications of morphological variation in the lower carnassial of red fox *Vulpes vulpes*. Acta Theriologica 49:434–447.

———. 2007. Geography of dental polymorphism in the red fox *Vulpes vulpes* and its evolutionary implications. Biological Journal of the Linnean Society 90:61–84.

———. 2008. Geographic variation of tooth and skull sizes in the arctic fox *Vulpes* (*Alopex*) *lagopus*. Annales Zoologici Fennici 45:185–199.

Taylor, M. E. 1974. The functional anatomy of the forelimb of some African Viverridae (Carnivora). Journal of Morphology 143:307–335.

———. 1976. The functional anatomy of the hindlimb of some African Viverridae (Carnivora). Journal of Morphology 148:227–253.

Tedford, R. H., X. Wang, and B. E. Taylor. 2009. Phylogenetic systematics of the North American fossil Caninae (Carnivora: Canidae). Bulletin of the American Museum of Natural History pages 1–218.

Teilhard de Chardin, P. 1914-1915. Les carnassiers des Phosphorites du Quercy. Annales de Paléontologie 9:101–192.

Tomiya, S. 2011. A new caniform (Carnivora: Mammalia) from the middle Eocene of North America and remarks on the phylogeny of early carnivorans). PLoS ONE 6:e24146.

Turvey, S. T., and S. A. Fritz. 2011. The ghosts of mammals past: biological and geographical patterns of global mammalian extinction across the Holocene. Philosophical Transactions of the Royal Society B-Biological Sciences 366:2564–2576.

van der Made, J. 1999. Intercontinental relationship Europe-Africa and the Indian Subcontinent. Pages 457–472 *in* G. E. Rössner and K. Heissig, eds. The Miocene land mammals of Europe. Munich, Verlag Dr. Friedrich Pfeil.

Van Valen, L. 1964. Nature of the supernumerary molars of *Otocyon*. Journal of Mammalogy 45:284–286.

———. 1966. Deltatheridia, a new order of mammals. Bulletin of the American Museum of Natural History 132:1–126.

Van Valkenburgh, B. 1985. Locomotor diversity within past and present guilds of large predatory mammals. Paleobiology 11:406–428.

———. 1987. Skeletal indicators of locomotor behavior in living and extinct carnivores. Journal of Vertebrate Paleontology 7:162–182.

———. 1989. Carnivore dental adaptations and diet: a study of trophic diversity within guilds. Pages 410–436 *in* J. L. Gittleman, ed. Carnivore behavior, ecology, and evolution. Cornell University Press, Ithaca, New York.

———. 1990. Skeletal and dental predictors of body mass in carnivores. Pages 181–205 *in* Damuth, John and MacFadden, Bruce J., ed. Body size in mammalian paleobiology: estimation and biological implications. Cambridge University Press, Cambridge.

———. 2007. Déjà vu: the evolution of feeding morphologies in the carnivora. Integrative and Comparative Biology 47:147–163.

Van Valkenburgh, B., and M. Janis, Christine. 1993. Historical diversity patterns in North American large herbivores and carnivores. Pages 330–340 *in* R. E. Ricklefs and D. Schluter, eds. Species diversity in ecological communities: historical and geographical perspectives. University of Chicago Press, Chicago.

Van Valkenburgh, B., X. Wang, and J. Damuth. 2004. Cope's Rule, hypercarnivory, and extinction in North American canids. Science 306:101–104.

Venables, W. N., and B. D. Ripley. 2010. Main package of venables and ripley's mass, version 7.3-5. Available at www.stats.ox.ac.uk/pub/MASS4. Accessed January 17, 2010.

Viranta, S. 2003. Geographic and temporal ranges of middle and late Miocene carnivorans. Journal of Mammalogy 84:1267–1278.

von Koenigswald, W., K. D. Rose, L. Grande, and R. D. Martin. 2005. First apatemyid skeleton from the lower Eocene Fossil Butte Member, Wyoming (USA), compared to the European apatemyid from Messel, Germany. Paläontologische Abteilung A 272:149–169.

Vrba, E. S., and D. DeGusta. 2004. Do species populations really start small? New Perspectives from the Late Neogene fossil record of African mamamls. Philosophical Transactions of the Royal Society B 359:285–293.

Wallace, S. C., and X. Wang. 2004. Two new carnivores from an unusual late Tertiary forest biota in eastern North America. Nature 431:556–559.

Walsh, S. L. 1996. Middle Eocene mammal faunas of San Diego County, California. Pages 75–119 *in* D. R. Prothero and R. J. Emry, eds. The terrestrial Eocene-Oligocene transition in North America. Cambridge University Press, Cambridge.

———. 1997. New specimens of *Metanoiamys*, *Pauromys*, and *Simimys* (Rodentia: Myomorpha) from the Uintan (middle Eocene) of San Diego County, California, and comments on the relationships of selected Paleogene Myomorpha. Proceedings of the San Diego Society of Natural History 32:1–20.

———. 1998. Notes on the anterior dentition and skull of *Proterixoides* (Mammalia: Insectivora: Dormaaliidae), and a new dormaaliid genus from the early Uintan (Middle Eocene) of southern California . Proceedings of the San Diego Society of Natural History 34:1–26.

———. 2000. Bunodont artiodactyls (Mammalia) from the Uintan (middle Eocene) of San Diego County, California. Proceedings of the San Diego Society of Natural History 37:1–27.

———. 2010. New myomorph rodents from the Eocene of southern California. Journal of Vertebrate Paleontology 30:1610–1621.

Walsh, S. L., and T. A. Demeré. 1991. Age and stratigraphy of the Sweetwater and Otay formations, San Diego County, California. Pages 131–148 *in* P. L. Abbott and J. A. May, eds. Eocene geologic history: San Diego region. Pacific Section, Society of Economic Paleontologists and Mineralogists, Los Angeles.

Walsh, S. L., D. R. Prothero, and D. J. Lundquist. 1996. Stratigraphy and paleomagnetism of the middle Eocene Friars Formation and Poway Group, southwestern San Diego County, California. Pages 120–154 *in* D. R. Prothero and R. J. Emry, eds. The terrestrial Eocene-Oligocene transition in North America. Cambridge University Press, Cambridge.

Wan, Q. H., C. J. Zeng, X. W. Ni, H. J. Pan, and S. J. Fang. 2009. Giant panda genomic data provide insight into the birth-and-death process of mammalian major histocompatibility complex class II genes. PLoS ONE 4:e4147.

Wang, X. 1993. Transformation from plantigrady to digitigrady: functional morphology of locomotion in *Hesperocyon* (Canidae: Carnivora). American Museum Novitates 3069:1–23.

———. 1994. Phylogenetic systematics of the Hesperocyoninae (Carnivora: Canidae). Bulletin of the American Museum of Natural History 221:1–207.

Wang, X., M. C. McKenna, and D. Dashzeveg. 2005. *Amphicticeps* and *Amphicynodon* (Arctoidea, Carnivora) from Hsanda Gol Formation, central Mongolia and phylogeny of basal arctoids with comments on zoogeography. American Museum Novitates 3483:1–57.

———. 2005*a*. *Amphicticeps* and *Amphicynodon* (Arctoidea, Carnivora) from Hsanda Gol Formation, central Mongolia and phylogeny of basal arctoids with comments on zoogeography. American Museum Novitates 3483:1–57.

Wang, X., Z. Qiu, and B. Wang. 2004. A new leptarctine (Carnivora: Mustelidae) from the early Miocene of the northern Tibetan Plateau: implications for the phylogeny and zoogeography of basal mustelids. Zoological Journal of the Linnean Society 142:405–421.

Wang, X., and R. H. Tedford. 1994. Basicranial anatomy and phylogeny of primitive canids and closely related miacids (Carnivora: Mammalia). American Museum Novitates 3092:1–34.

———. 1996. Canidae. Pages 433–452 *in* D. R. Prothero and R. J. Emry, eds. The terrestrial Eocene-Oligocene transition in North America. Cambridge University Press, Cambridge.

Wang, X., D. P. Whistler, and G. T. Takeuchi. 2005*b*. A new basal skunk *Martinogale* (Carnivora, Mephitinae) from Late Miocene Dove Spring Formation, California, and origin of New World mephitines. Journal of Vertebrate Paleontology 25:936–949.

Wang, X. and Tedford, R. H. and Taylor, B. E. 1999. Phylogenetic systematics of the Borophaginae (Carnivora: Canidae). Bulletin of the American Museum of Natural History 243:1–391.

Webb, S. D. 2008. Revision of the extinct Pseudoceratinae (Artiodactyla: Ruminantia: Gelocidae). Bulletin of the Florida Museum of Natural History 48:17–58.

Webb, S. D., and J. Meachen. 2004. On the origin of lamine Camelidae including a new genus from the late Miocene of the High Plains). Bulletin of the Carnegie Museum of Natural History 36:349–362.

Wesley, G. D., and J. J. Flynn. 2003. A revision of *Tapocyon* (Carnivoramorpha), including analysis of the first cranial specimens and identification of a new species. Journal of Paleontology 77:769–783.

Wesley-Hunt, G. D. 2005. The morphological diversification of carnivores in North America. Paleobiology 31:35–55.

Wesley-Hunt, G. D., and J. J. Flynn. 2005. Phylogeny of the Carnivora: basal relationships among the carnivoramorphans, and assessment of the position of 'Miacoidea' relative to Carnivora. Journal of Systematic Palaeontology 3:1–28.

Wesley-Hunt, G. D., and L. Werdelin. 2005. Basicranial morphology and phylogenetic position of the upper Eocene carnivoramorphan *Quercygale*. Acta Palaeontologica Polonica 50:837–846.

Wilson, D. E., and D. M. Reeder. 1993. Mammal species of the world: a taxonomic and geographic reference, Second edition. Smithsonian Institution Press, Washington, D. C.

———. 2005. Mammal species of the world: a taxonomic and geographic reference, Third edition. Johns Hopkins University Press, Baltimore.

Wilson, K. L. 1972. Eocene and related geology of a portion of the San Luis Rey and Encinitas quadrangles, San Diego County, California. Unpublished M. S. thesis, University of California, Riverside.

Wilson, R. W. 1940*a*. California paramyid rodents. Carnegie Institution of Washington Publication 514:59–83.

———. 1940*b*. *Pareumys* remains from the later Eocene of California. Carnegie Institution of Washington Publication 514:97–108.

———. 1949. Additional Eocene rodent material from southern California. Carnegie Institution of Washington Publication 584:1–25.

Wolff, R. G. 1973. Hydrodynamic sorting and ecology of a Pleistocene mammalian assemblage from California (U.S.A.). Palaeogeography, Palaeoclimatology, Palaeoecology 13:91–101.

———. 1975. Sampling and sample size in ecological analyses of fossil mammals. Paleobiology 1:195–204.

Wood, A. E., and H. E. Wood. 1933. The genetic and phylogenetic significance of the presence of a third upper molar in a modern dog. American Midland Naturalist 14:36–48.

Woodburne, M. O. 2007. Phyletic diversification of the *Cormohipparion occidentale* complex (Mammalia; Perissodactyla, Equidae), late Miocene, North America, and the origin of the Old World *Hippotherium Datum*. Bulletin of the American Museum of Natural History 306:1–138.

Woodburne, M. O., T. H. Rich, and M. S. Springer. 2003. The evolution of tribospheny and the antiquity of mammalian clades. Molecular Phylogenetics and Evolution 28:360–385.

Wortman, J. L., and W. D. Matthew. 1899. The ancestry of certain members of the Canidae, the Viverridae, and Procyonidae. Bulletin of the American Museum of Natural History 7:109–138.

Wyss, A. R., and J. J. Flynn. 1993. A phylogenetic analysis and definition of the Carnivora. Pages 32–52 *in* F. S. Szalay, M. J. Novacek, and M. C. McKenna, eds. Mammal phylogeny: placentals, Volume 2. Springer-Verlag, New York.

Yoder, A. D., M. M. Burns, S. Zehr, T. Delefosse, G. Veron, S. M. Goodman, and J. J. Flynn. 2003. Single origin of Malagasy Carnivora from an African ancestor. Nature 421:734–737.

Youlatos, D. 2003. Osteological correlates of tail prehensility in carnivorans. Journal of Zoology 259:423–430.

Zachos, J., M. Pagani, L. Sloan, E. Thomas, and K. Billups. 2001. Trends, rhythms, and aberrations in global climate 65 Ma to present. Science 292:686–693.

Zielinski, W. J., and N. P. Duncan. 2004. Diets of sympatric populations of american martens (*Martes americana*) and fishers (*Martes pennanti*) in california. Journal of Mammalogy 85:470–477.

Appendices

Appendix 2.1: Additional Notes on Taxonomy, Cladistic Hypotheses, and Size Measurements

In the present study, occurrences reported in the MIOMAP data base of unpublished new genera were excluded from analyses, and those of unpublished new species belonging to known genera were included as unidentified species. Generic classifications primarily follow those of Janis et al. (1998, 2008), and modified generic identities of MIOMAP and FAUNMAP data are indicated as such in Appendix S2.1. Measurements of m1 length and width obtained from sources other than the Paleobiology Database are noted below.

Artiodactyla

Although the cladistic relationships among some of the extant families of artiodactyls were adopted from Bininda-Emonds et al. (2007, 2008), it should be noted that many parts of the family-level phylogeny of Artiodactyla are at present highly uncertain (see e.g., Geisler and Uhen (2005); Geisler et al. (2007); O'Leary and Gatesy (2008)). Furthermore, no single cladogram is currently available in the literature that includes all families of extant and extinct artiodactyls as recognized in Janis et al. (1998). With respect to extinct families, I followed the combined molecular and morphological tree of Spaulding et al. (2009:fig. 2) and placed: (1) protoceratids and anthracotheres as successive outgroups to Ruminantia within Ruminantiamorpha; (2) oreodonts as the outgroup to camelids; (3) entelodonts as the outgroup to the clade consisting of Cetaceamorpha and Hippopotamidamorpha. Included in Ruminantia are (1) the family Palaeomerycidae as the sister group to the Cervidae (Prothero and Liter, 2007, and references therein) and (2) gelocids *Pseudoceras* and *Floridameryx* (Webb, 2008). Two representatives of leptochoerines were placed outside all other artiodactyls in the data set following the placement of family suggested by Geisler et al. (2007).

Camelidae: Following Webb and Meachen (2004), the genus *Pleiolama* was tentatively placed in a multichotomy with other lamines. The problematic genus *Pliauchenia* was removed from the data set.
Entelodontidae: The genus *Dinohyus* is regarded here as a junior synonym of *Daeodon* (Foss, 2007).
Moschidae: Additional measurements of m1 were obtained from Prothero (2008).
Palaeomerycidae: Additional measurements of m1 were obtained from Prothero and Liter (2008).

Perissodactyla

Chalicotheriidae: Following Hooker and Dashzeveg (2004), chalicotheres were placed outside the clade containing all other perissodactyls in the data set.
Tapiridae: The classification and cladistic hypothesis of Colbert and Schoch (1998) and additional information from Albright (1998) and Janis et al. (2008).
Rhinocerotoidea: The classification and cladistic hypothesis for Hyracodontidae and Rhinocerotidae were adopted from Prothero (1998, 2005), with the addition of *Diceratherium radtkei* (Prothero and Rasmussen, 2008). Two poorly-known genera, *Gulfoceras* and *Woodoceras*, could not be placed on the cladogram (cf. Prothero, 2005). Additional measurements of m1 were obtained from Prothero (2005).
Equidae: The classification and cladistic hypotheis of MacFadden (1998) and additional information from Janis et al. (2008) were adopted. In addition, 5 new species of *Cormohipparion*, *C. fricki*, *C. johnsoni*, *C. matthewi*, *C. merriami*, and *C. skinneri* were recognized (Woodburne, 2007). The cladistic positions of *Acritohippus*, *Parapliohippus*, *Heteropliohippus*, and *"Pliohippus" tehonensis* follow those proposed by Kelly (1998:fig. 9).

Carnivora

The family-level cladistic relationships and lineage divergence dates proposed by Bininda-Emonds et al. (2007, 2008) were adopted. The family Amphicyonidae was positioned as a sister group to all other caniforms in the data set (Tomiya, 2011).

Amphicyonidae: The classification and cladistic hypothesis of Hunt (1998*a*) were adopted. In addition, the daphoenine *Adilophontes* was provisionally positioned as the sister taxon to *Daphoenodon* following Hunt (2002).
Canidae: The classifications and cladistic hypotheses of Wang (1994), Wang, X. and Tedford, R. H. and Taylor, B. E. (1999), and Tedford et al. (2009) were adopted.
Ursidae: The classification and cladistic hypothesis of Hunt (1998*b*) were adopted. Note that Hunt (1998*b*) considered the North American species *"Hemicyon" barbouri* to be generically distinct from the Old World *Hemicyon*.
Mustelida: Two Arikareean genra, *Acheronictis* and *Arikarictis*, were tentatively place in a polytomy at the base of Mustelida (Hayes, 2000). Following Wang et al. (2005*a*), leptarctines and oligobunines were placed as successive outgroups to the crown-group mustelids.
The classification and cladistic hypothesis for Mustelidae followed those of Baskin (1998*a*). The genus *Arctomeles* was positioned as a member of Melinae (Wallace and Wang, 2004). The genus *Schultzogale* was paired with the leptarctine *Leptarctus* (cf. Wang et al., 2004). The genus *Miomustela* was here allied with Mephitidae rather than Mustelidae (cf. Hall, 1930).
The classification and cladistic hypothesis for Mephitidae followed those of Baskin (1998*a*, originally considered as subfamily Mephitinae within Mustelidae). Although Wang et al. (2005*b*) presented an alternative hypothesis regarding basal skunks, the absence of several genera in their cladogram precluded it from being incorporated into the present study.
As for procyonids, the classifications and cladograms of Baskin (1998*b*, 2004) were generally adopted. However, simocyonines were positioned as the sister group to Ailuridae instead of within Procyonidae (but see Wang et al., 2005*a*; Baskin, 1998*b*).
Felidae: The classification and cladogram of Martin (1998) were adopted.

Rodentia

Sciuridae: *Hesperopetes blacki* and *H. jamesi* (Emry and Korth, 2007) were added to the taxonomic list of Goodwin (2008).
Aplodontidae: The "preferred phylogeny" of Hopkins (2008:fig. 7) was followed, with the addition of *Ansomys cyanotephrus* and *A. nevadensis* (Korth, 2007*b*).
Castoroidea: The classification and cladistic hypothesis within the family in general follow those of Flynn and Jacobs (2008), and those within the Tribe Castoridini (Korth, 2001) were modified according to Korth (2007*a*). Thus, *Eucastor dividerus*, *E. lecontei*, and *E. phillisi* of Flynn and Jacobs (2008) were here treated as *Prodipoides dividerus*, *P. lecontei*, and *P. phillisi*, respectively, and two additional species, *P. burgensis* and *P. katensis*, were recognized (Korth, 2002, 2007*a*). The genus *Priusaulax* was tentatively placed in a polytomy with *Monosaulax* and other members of Castoridini (cf. Korth and Bailey, 2006). In addition, *Euroxenomys galushai* (Korth, 2002) and *Eutypomys wilsoni* Korth (2007*c*), and *Monosaulax tedi* (Korth, 1999).
Cricetidae (non-Arvicoline): The classification and cladistic hypothesis of Lindsay (2008) were adopted. Lindsay (2008) considered *Bensomys* to be a subgenus of *Callomys*; thus, *Bensomys*

lindsayi (Kelly, 2007) was classified as *Callomys lindsayi*. Two Pleistocene species, *"Synaptomys" borealis* and *"S." meltoni*, were assigned to the genus *Mictomys* following Repenning and Grady (1988).
Arvicolinae: The genus *Loupomys* could not be placed on the cladogram for this study (cf. Martin, 2008).
Eomyidae: *Pentabuneomys* sp. (cf. Korth, 2008) and *Zophoapeomys indicum* (Korth, 2007*c*) were added to the taxonomic list by Flynn (2008*a*).
Heteromyidae: The classification and caldistic hypothesis of Flynn (2008) were adopted. The genus *Tylionomys* (Korth and Branciforte, 2007) was tentatively considered as the sister taxon to *Mookomys* (*Heliscomys* of Korth and Branciforte (2007)).
Geomorpha: The following taxa were added to the taxonomic list of Flynn et al. (2008): *Cupidinimus smaragdinus* (Korth 1996), *Perognathus strigipredus* (Czaplewski, 1990), *Proharrymys fedti*, *Pr. schlaikjeri*, and *Pr. wahlerti* (Korth and Branciforte, 2007) *Tenudomys ridgeviewensis* and *Te. titanus*, and *Tylionomys voorhiesi* and *Ti. woodi* (Korth and Branciforte, 2007).
Erethizontidae: Following Flynn (2008*b*), occurrences of the genus *Coendou* are here recognized as those of *Erethizon*.

Lipotyphla

Amphechinus ellicottae and *Brachyerix richi* (Martin and Lim, 2004) were added to the taxonomic list of Gunnell et al. (2008).

Appendix 2.2: Generic Data for Comparative Analyses

Appendix 2.2: Generic Data for Comparative Analyses

	Genus (Occurrences)	T_{FAD}	T_{LAD}	T_{FAD50}	T_{LAD50}	W	L
Lipotyphla							
Erinaceidae	*Amphechinus* (9)	27.6	21.5	28.1	19.9	5.2	4.1
	Brachyerix (33)	22.6	12.9	23.2	12.7	5.1	4.0
	Lantanotherium (13)	15.7	10	16	9.4	4.6	3.9
	Metechinus (28)	15.7	10.1	15.9	9.9	6.2	4.3
	Parvericius (41)	27.6	12.4	27.8	12.1	3.6	3.6
	Plesiosorex (27)	19.2	5.2	19.9	4.7	5.2	4.1
	Stenoechinus (3)	25	18.2	28.3	15.4	3.9	3.7
	Untermannerix (22)	15.6	10.2	15.7	9.9	4.9	4.0
Proscalopidae	*Mesoscalops* (28)	19.2	14.7	19.4	14.6	4.6	3.9
Soricidae	*Adeloblarina* (3)	15.4	13.1	17.1	11	2.6	3.4
	Alluvisorex (15)	14.9	6.3	15.2	5.8	1.8	3.1
	Limnoecus (43)	20.9	7.3	21.7	7	1.8	3.1
	Paracryptotis (6)	7.3	2.9	8.7	1.9	3.6	3.6
	Paradomnina (13)	16.7	12.9	17	12.6	3.2	3.5
	Tregosorex (2)	11.2	10.5	12.3	9.1	3.3	3.6
	Wilsonosorex (3)	19.2	17.9	20.7	16.9	3.1	3.5
Talpidae	*Achlyoscapter* (6)	14.9	8.3	16.1	6.6	2.5	3.3
	Domninoides (43)	15.7	6.3	15.8	6.1	4.6	3.9
	Gaillardia (3)	13.8	6.1	18.4	1.1	4.3	3.8
	Mystipterus (32)	27.5	9.5	28	8.9	2.8	3.4
	Scapanoscapter (4)	15.4	13.7	16.1	12.9	4.1	3.8
Carnivora							
Amphicyonidae	*Adilophontes* (3)	19.4	18.9	19.7	18.7	12.2	6.1
	Amphicyon (76)	18.8	12.7	18.8	12.6	12.6	6.2
	Daphoenodon (34)	24.4	17.6	24.7	17.5	11.7	6.1
	Ischyrocyon (35)	15.2	10.5	15.2	10.4	13.3	6.2
	Paradaphoenus (3)	28.4	26.8	29	25.1	8	5.7
	Pliocyon (20)	16.9	12	17.1	11.8	12.7	6.2
	Ysengrinia (12)	22.1	18.2	22.5	18	12.3	6.1
Canidae	*Aelurodon* (206)	15.8	6.3	15.8	6.3	11.6	6.1
	Borophagus (107)	12.3	2.2	12.3	2.1	11.7	6.1
	Carpocyon (56)	15.4	5.3	15.5	5.2	11	6.0
	Cynarctus (44)	15.6	9.7	15.6	9.6	9.4	5.8
	Desmocyon (72)	28.3	17.5	28.4	17.5	9.2	5.8
	Ectopocynus (4)	28.1	17.8	29	14.4	10.4	5.9
	Epicyon (162)	13.3	6	13.3	6	12.3	6.1
	Eucyon (22)	7.8	4.9	7.8	4.8	9.8	5.9
	Euoplocyon (9)	17.5	13.6	18	13.2	9.7	5.9
	Metatomarctus (30)	18.8	14.9	18.8	14.8	10	5.9
	Microtomarctus (64)	16.8	12.6	16.8	12.5	9.4	5.8
	Otarocyon (7)	28.9	21.7	29	19.5	6.5	5.5
	Paracynarctus (34)	18.6	12.5	18.7	12.4	9.7	5.9
	Paratomarctus (93)	16.1	9.6	16.2	9.6	10.2	5.9
	Protepicyon (9)	15.6	13.2	15.8	13	11.4	6.0
	Protomarctus (31)	19.2	15.3	19.3	15.2	10	5.9
	Psalidocyon (5)	15.8	14.9	15.9	14.7	9.3	5.8

NOTE—T_{FAD}, observed first appearance date; T_{FAD50}, sampling-adjusted first appearance date; T_{LAD}, observed last appearance date; T_{FAD50}, observed last appearance date. All dates in millions of years before present.

Appendix 2.2 (cont.)

	Genus (Occurrences)	T_{FAD}	T_{LAD}	T_{FAD50}	T_{LAD50}	W	L
	Tephrocyon (10)	15.7	13.2	15.8	13	10.2	5.9
	Tomarctus (59)	18.2	10.5	18.2	10.4	10.7	6.0
Felidae	*Adelphailurus* (4)	6.5	5.1	7.1	4.5	9.8	5.9
	Machairodus (30)	8.7	3.4	8.9	3.1	12.3	6.1
	Megantereon (2)	6.5	6.3	7	5.9	10.7	6.0
	Nimravides (26)	11.9	4.9	12	4.6	11.2	6.0
	Pseudaelurus (76)	17	6.5	17.1	6.4	9.3	5.8
Mustelidae	*Brachypsalis* (23)	18.4	10.5	18.7	10.1	9.4	5.8
	Buisnictis (5)	5.7	3.5	6.2	2.9	5.8	5.5
	Cernictis (2)	6.5	6	7.3	4.3	8.4	5.7
	Leptarctus (40)	17.9	6.9	18.1	6.7	8.1	5.7
	Lutravus (3)	7.8	7.3	8.1	7	9.2	5.8
	Martinogale (8)	13.3	5.2	14.2	3.9	5.6	5.5
	Megalictis (13)	25.9	18.9	26.5	18.6	10.8	6.0
	Miomustela (7)	17.3	13.1	18.1	12.2	5.2	5.4
	Mionictis (17)	16.9	7.9	17.4	7.4	7.9	5.7
	Plesiogulo (19)	7	4.8	7.1	4.7	11.3	6.0
	Plionictis (23)	15.8	6.9	16	6.6	6.5	5.5
	Pliotaxidea (24)	11.4	4.9	11.5	4.6	8.2	5.7
	Satherium (4)	3.5	1.9	4.2	1.2	10.5	5.9
	Sthenictis (19)	16.8	6.7	17.2	6.3	9.2	5.8
	Trigonictis (10)	5.6	1.2	5.9	1	9.2	5.8
Nimravidae	*Barbourofelis* (21)	11.9	6.3	12.1	6.1	11.8	6.1
Procyonidae	*Arctonasua* (13)	15.6	5	16.3	3.6	9.7	5.9
	Bassaricyonoides (2)	18.2	16.6	22.2	13.8	7.6	5.7
Ursidae	*Agriotherium* (21)	8.3	4.8	8.4	4.6	13.8	6.3
	Hemicyon (12)	13.8	10	14	9.7	12.2	6.1
	Indarctos (11)	9	6.8	9.2	6.7	13.6	6.3
Perissodactyla							
Chalicotheriidae	*Moropus* (53)	25.9	14.3	26.2	14.2	12.6	6.4
Equidae	*Acritohippus* (95)	17.4	7.5	17.5	7.4	11.7	6.2
	Anchippus (8)	24.5	17.1	26.1	16	11.3	6.1
	Anchitherium (37)	21.1	12.8	21.4	12.7	11.9	6.2
	Archaeohippus (82)	23.3	12.7	23.4	12.7	10.6	5.9
	Calippus (124)	16.2	6.8	16.2	6.7	10.9	6.0
	Desmatippus (39)	25.4	10.5	26	10.2	11.9	6.2
	Dinohippus (153)	13.3	4.7	13.3	4.7	12.7	6.4
	Heteropliohippus (3)	12	11.1	12.3	10.5	12.4	6.3
	Hipparion (62)	14.9	4.9	15	4.8	11.6	6.1
	Hypohippus (94)	18.3	9.8	18.3	9.7	12.5	6.4
	Megahippus (35)	15.6	10.6	15.6	10.5	13.5	6.6
	Merychippus (59)	17.5	12.6	17.6	12.5	11.2	6.0
	"Merychippus" (hipparionine) (74)	16.7	11.7	16.8	11.7	11.4	6.1
	Nannippus (77)	16.2	1.9	16.3	1.8	10.7	5.9
	Neohipparion (164)	13.9	4.7	13.9	4.7	11.7	6.2
	Parahippus (101)	27.8	10.5	28	10.4	11.2	6.0
	Parapliohippus (37)	17.5	15.4	17.5	15.4	11	6.0

Appendix 2.2 (cont.)

	Genus (Occurrences)	T_{FAD}	T_{LAD}	T_{FAD50}	T_{LAD50}	W	L
	Pliohippus (80)	15.8	6.9	15.8	6.9	12.1	6.3
	"Pliohippus" tehonensis (32)	12.4	9.6	12.5	9.5	11.8	6.2
	Protohippus (91)	17.3	6.8	17.4	6.7	11.7	6.2
	Pseudhipparion (135)	14.4	4.8	14.5	4.7	10.9	6.0
Rhinocerotidae	*Aphelops* (232)	17.2	4.9	17.3	4.8	14.8	6.9
	Floridaceras (9)	21	17.1	21.9	16.7	14.4	6.8
	Peraceras (105)	18.5	9.5	18.6	9.4	14.1	6.7
	Teleoceras (503)	18.4	4.7	18.4	4.7	14.7	6.9
Artiodactyla							
Anthracotheriidae	*Arretotherium* (13)	26.3	16.7	27.3	16	11.7	6.2
Antilocapridae	*Cosoryx* (115)	15.8	9.3	15.8	9.3	9.4	5.6
	Texoceros (30)	8.3	4.9	8.4	4.8	9.5	5.6
Camelidae	*Aepycamelus* (85)	18.2	6.9	18.2	6.9	12.7	6.4
	Alforjas (24)	12.1	4.9	12.3	4.5	12.7	6.4
	Australocamelus (3)	17.4	13.3	20.9	10.5	11.3	6.1
	Blickomylus (18)	18.7	16.1	18.8	16	9.4	5.6
	Floridatragulus (5)	18	13.7	19.4	12.7	10.6	5.9
	Megacamelus (7)	8.6	5.1	9.2	4.5	14.3	6.8
	Megatylopus (97)	11.8	4.7	11.8	4.6	14	6.7
	Michenia (72)	22.9	7.7	23.1	7.6	11	6.0
	Miolabis (51)	20.4	10.5	20.8	10.3	12.2	6.3
	Nothokemas (13)	25.7	16.5	26.8	15.9	10.5	5.9
	Oxydactylus (26)	28.9	16	29	15.8	11.4	6.1
	Paramiolabis (23)	17.3	13.3	17.4	13.2	11.6	6.1
	Priscocamelus (9)	23	22.1	23.1	22	10.9	6.0
	Procamelus (127)	16.2	6	16.2	5.9	12.3	6.3
	Protolabis (80)	18.6	7.1	18.7	7	11.7	6.2
	Stenomylus (43)	26.1	16.5	26.3	16.3	10.4	5.8
	Tanymykter (5)	20.7	18.9	21.4	18.6	11.3	6.1
Gelocidae	*Pseudoceras* (20)	11.8	6.8	12	6.7	9	5.5
Moschidae	*Blastomeryx* (68)	21	11	21.2	10.9	9	5.5
	Longirostromeryx (46)	15.5	6.7	15.6	6.6	9.3	5.6
	Parablastomeryx (14)	17.9	9.9	18.4	9.2	9.7	5.7
	Problastomeryx (10)	22.9	14.9	24.1	14	9.3	5.6
	Pseudoblastomeryx (37)	28.1	17.6	28.3	17.4	8.9	5.5
Oreodontoidea	*Hypsiops* (11)	27.5	19.7	28.1	19.1	11.7	6.2
	Merychyus (395)	27.5	6.3	27.5	6.3	10.9	6.0
	Mesoreodon (2)	26.9	24.4	29	20.3	11.3	6.1
	Phenacocoelus (2)	25.9	21.7	29	15.8	10.6	5.9
	Ticholeptus (48)	17.1	12.6	17.2	12.6	11.3	6.1
Palaeomerycidae	*Aletomeryx* (42)	19.2	16.5	19.2	16.4	10	5.8
	Barbouromeryx (20)	21.7	16.1	22.1	15.9	10.2	5.8
	Bouromeryx (56)	21	13	21.2	13	10.7	5.9
	Cranioceras (58)	15.7	7.1	15.7	7	11.4	6.1
	Drepanomeryx (5)	15.8	14.9	15.9	14.7	11.2	6.0

Appendix 2.2 (cont.)

	Genus (Occurrences)	T_{FAD}	T_{LAD}	T_{FAD50}	T_{LAD50}	W	L
	Dromomeryx (66)	17.4	10.6	17.4	10.6	11.7	6.1
	Pediomeryx (17)	8.3	5	8.5	4.8	11.8	6.2
	Procranioceras (18)	13.7	12.5	13.7	12.5	11.8	6.2
	Rakomeryx (21)	15.9	13.2	16	13.1	11.4	6.1
	Sinclairomeryx (12)	18.2	15.4	18.3	15.2	11.4	6.1
	Subdromomeryx (10)	16.9	14.7	17.1	14.5	10.7	5.9
	Yumaceras (17)	9.7	6.7	9.9	6.6	12.3	6.3
Protoceratidae	*Prosynthetoceras* (38)	23.3	12.7	23.6	12.6	11	6.0
(Ruminantia)	*Delahomeryx* (2)	22.7	22.3	23.4	21.4	10.3	5.8
Tayassuidae	*"Cynorca" occidentale* (8)	15.8	14.9	15.9	14.8	10.4	5.8
	"Cynorca" sociale (12)	23.7	15.3	24.9	14.9	10	5.7
	Dyseohyus (5)	15.9	14.2	16.2	13.9	10.7	5.9
	Floridachoerus (2)	22.9	17.5	29	9.9	11.5	6.1
	Hesperhys (26)	25.4	14.9	26	14.7	11.8	6.2
	"Prosthennops" serus (9)	11.8	6.8	12.2	6.3	11.3	6.1
Rodentia							
Aplodontidae	*Allomys* (39)	28.7	19.1	28.8	18.9	5.4	4.1
	Alphagaulus (33)	19.2	13.8	19.4	13.7	6.3	4.4
	Galbreathia (17)	19.2	15.1	19.5	15	5.1	4.0
	Parallomys (8)	28.3	13.1	29	10.6	5.1	4.0
	Liodontia (17)	16.7	6.3	17.3	5.8	5.3	4.1
	Tardontia (6)	15.4	7.3	17.1	5.5	5.1	4.0
Castoridae	*Dipoides* (52)	15.3	2.3	15.4	2.1	7.5	4.7
	Eucastor (33)	14	7.1	14.1	6.9	6.6	4.5
	Euhapsis (7)	25.9	19	26.9	18.2	5.7	4.2
	Euroxenomys (14)	18.7	14.9	18.9	14.7	6.1	4.3
	Fossorcastor (3)	27.2	21.7	29	17.8	6.1	4.3
	Hystricops (9)	18.2	7.3	19.8	6	9.3	5.2
	Microdipoides (18)	15.4	9.5	15.6	9.1	6.5	4.4
	Monosaulax (54)	18.6	10.5	18.7	10.3	6.4	4.4
	Neatocastor (8)	26.3	22.4	27	21.8	6.9	4.6
	Procastoroides (4)	3.5	2.4	4.1	2	10.8	5.6
	Pseudopalaeocastor (7)	23.4	19.2	24.1	18.8	5.8	4.2
Dipodidae	*Macrognathomys* (11)	15.3	7.3	15.9	6.6	1.6	3.1
	Megasminthus (23)	14	10.5	14.1	10.3	3.8	3.7
Eomyidae	*Kansasimys* (2)	8.3	6.3	12.3	3	4.9	4.0
	Pseudotheridomys (27)	27.7	13	28.1	12.6	2.4	3.3
Geomyidae	*Dikkomys* (12)	22.3	17.6	23.1	17.4	3.9	3.7
	Lignimus (15)	15.4	10.5	15.6	10	2.7	3.4
	Mojavemys (26)	17.1	11.2	17.3	11	3.7	3.7
	Parapliosaccomys (13)	13.9	5.2	14.4	4.6	3.2	3.5
	Phelosaccomys (22)	16.5	10	16.8	9.7	3.3	3.5
	Pleurolicus (30)	28.6	17.7	28.8	17.5	4.3	3.8
	Pliogeomys (11)	6.7	4.7	6.8	4.5	2.5	3.3
	Pliosaccomys (6)	11.9	6.3	13	5.4	3.1	3.5
(Geomyoidea)	*Jimomys* (5)	28.3	15	29	11.7	4.2	3.8
	Mookomys (21)	20.9	13.1	22	12.8	2.4	3.3
	Texomys (10)	23.5	12.9	25.2	11.8	4.6	3.9

Appendix 2.2 (cont.)

	Genus (Occurrences)	T_{FAD}	T_{LAD}	T_{FAD50}	T_{LAD50}	W	L
Heteromyidae	*Cupidinimus* (109)	20.9	6.5	21.2	6.4	2.7	3.4
	Diprionomys (13)	16.2	6.3	17.1	5.7	2.5	3.3
	Harrymys (31)	24.7	14.1	25	13.9	4.2	3.8
	Korthomys (7)	19.2	13.7	21.4	12.8	2.5	3.3
	Mioheteromys (19)	14.1	10.5	14.3	10.2	3.7	3.7
	Oregonomys (22)	7.1	3.8	7.3	3.7	3.3	3.5
	Peridiomys (33)	17.3	12.8	17.5	12.7	4.2	3.8
	Prodipodomys (36)	15.5	1.9	15.7	1.6	2.8	3.4
	Stratimus (9)	18.7	17.6	18.8	17.5	3	3.5
(Muroidea)	*Antecalomys* (9)	11.9	3.8	12.8	2.8	2.9	3.4
	Calomys (19)	7.9	1.3	8.4	1	2.9	3.4
	Copemys (121)	17.2	3.8	17.3	3.7	3.2	3.5
	Goniodontomys (10)	9.7	6.3	10.1	6	3.8	3.7
	Jacobsomys (2)	4	4	4.2	3.8	3.9	3.7
	Mimomys (2)	4.3	2.6	8	1	4.3	3.8
	Nebraskomys (2)	4.3	2.6	8	1	3.8	3.7
	Ogmodontomys (8)	5.5	2.9	5.8	2.6	4.6	3.9
	Ophiomys (34)	5	1.4	5.1	1.3	4.1	3.8
	Paronychomys (5)	8.5	3.8	10.3	2.6	3.2	3.5
	Pliophenacomys (10)	5.5	1.9	5.9	1.5	4.4	3.9
	Pliotomodon (2)	7.3	6.9	8.1	6.4	4.7	3.9
	Promimomys (3)	6.5	6.1	6.8	5.7	3.5	3.6
	Prosigmodon (3)	6.7	4	9	1.9	4.7	3.9
	Repomys (24)	8.5	3	8.9	2.9	4.3	3.8
	Symmetrodontomys (2)	5.5	4.8	6.9	3.2	3.2	3.5
	Tregomys (10)	13.9	10.1	14.2	9.6	2.7	3.4
	Yatkolamys (9)	18.7	17.6	18.8	17.5	3.9	3.7
Sciuridae	*Cynomyoides* (2)	15.4	10.5	27.3	1	5.7	4.2
	Paenemarmota (7)	8.1	3	9.2	1.9	9	5.1
	Petauristodon (36)	17.8	11.1	18	10.8	5.6	4.2
	Similisciurus (2)	22.7	22.3	23.4	21.5	5.6	4.2
Lagomorpha							
Leporidae	*Alilepus* (8)	13.1	3.5	14.3	2.1	5.3	4.1
	Gripholagomys (12)	27.7	17.9	28.2	17.2	4.6	3.9
	Hypolagus (238)	18.7	1.3	18.7	1.3	5.5	4.1
	Pronotolagus (49)	17	5.7	17.2	5.5	4.2	3.8
Ochotonidae	*Cuyamalagus* (11)	21	17	22.1	16.8	4.6	3.9
	Hesperolagomys (20)	14.3	9.7	14.5	9.4	4.2	3.8
	Oreolagus (40)	19.2	13.4	19.4	13.4	4.1	3.8
	Russellagus (14)	14	10.5	14.2	10.1	4.7	3.9

Appendix 3.1: Weight Estimation

Appendix 3.1: Weight Estimation

Taxon	Specimen	Locality	Predictor	APL (mm)	TW (mm)	Other (mm)	Weight (g)	Measurement source	Equation source
Marsupialia									
Copedelphys innominatum			m1L	1.7			41	PBDB	[7]
Herpetotherium knighti	UCMP 106719	V72157	m1L	2.0			65	original	[7]
Herpetotherium knighti	UCMP 106787	V72157	m1L	2.0			65	original	[7]
Herpetotherium valens			m1L	2.1			78	PBDB	[7]
Peradectes californicus	UCMP 106439	V72157	m1L	1.5			28	original	[7]
Peradectes californicus	UCMP 106644	V72158	m1L	1.7			41	original	[7]
Apatotheria									
Apatemys bellus	SDSNH 50574	3784	m1A	1.9	1.3		26	original	[10]
Apatemys downsi	LACM CIT 5202	CIT 180	m1A	2.5	1.8		68	Gazin 1958:91	[10]
Apatemys uintensis	UCMP 312832	RV6830	m1A	2.2	1.5		42	original	[10]
Mesonychia									
Harpagolestes uintensis	AMNH 1892	Uinta Fm.	cranial L			420	417609	Osborn 1895:79	[11]
Pantolesta									
Simidectes merriami	UCMP 83680	V6839	m1L	11.7			7949	original	[11]
Carnivoramorpha									
Tapocyon robustus	LACM CIT 1649	CIT 180	m1L	13.34			11795	original	[11]
Tapocyon robustus	LACM CIT 1652	CIT 180	m1L	15.2			17381	original	[11]
Tapocyon robustus	SDSNH 36000	4285	m1L	12.48			9677	original	[11]
Tapocyon dawsonae	SDSNH 35221	3276	m1L	11.61			7808	original	[11]
Miocyon sp.	SDSNH 40814	3464	m1L	15.16			17246	original	[11]
Miocyon sp.	SDSNH 54417	3870	m1L	15.19			17347	original	[11]
Lycophocyon hutchisoni	UCMP 170713	V6885	m1L	9.57			4399	original	[11]
Lycophocyon hutchisoni	UCMP 85202	V6839	m1L	10.72			6161	original	[11]
Lycophocyon hutchisoni	SDSNH 92094	4821	m1L	10.74			6196	original	[11]
Lycophocyon hutchisoni	SDSNH 107442	5721	m1L	9.91			4879	original	[11]
Lycophocyon hutchisoni	SDSNH 107446	5721	m1L	9.88			4835	original	[11]
Lycophocyon hutchisoni	SDSNH 107447	5721	m1L	9.36			4118	original	[11]
Lycophocyon hutchisoni	SDSNH 107448	5721	m1L	9.47			4263	original	[11]

PBDB, Paleobiology Database. References for predictive equations: 1, Bloch et al. (1998); 2, Conroy (1987); 3, Damuth (1990, non-selenodont); 4, Damuth (1990, selenodont browsers); 5, Egi (2001, all carnivorans); 6, Egi et al. (2004, prosimian); 7, Gordon (2003, pooled marsupials); 8, Hopkins (2008*b*, all rodents); 9, Legendre (1986, rodents); 10, Legendre (1986, small mammals); 11, Van Valkenburgh (1990, all carnivores)

.

Appendix 3.1: Weight Estimation (cont.)

Taxon	Specimen	Locality	Predictor	APL (mm)	TW (mm)	Other (mm)	Weight (g)	Measurement source	Equation source
Lycophocyon hutchisoni	SDSNH 107449	5721	m1L	9.87			4821	original	[11]
Lycophocyon hutchisoni	SDSNH 107450	5721	m1L	9.11			3800	original	[11]
Lycophocyon hutchisoni	SDSNH 107458	5721	m1L	10.81			6316	original	[11]
Miacis hookwayi	LACM CIT 1656	CIT 180	m1L	6.41			1338	original	[11]
Miacis hookwayi	LACM uncat.	CIT 180	m1L	6.89			1658	original	[11]
Miacis hookwayi	LACM 84969	4715	m1L	6.33			1289	original	[11]
Procynodictis progressus	LACM CIT 1776	CIT 207	m1L	8.8			3429	original	[11]
Procynodictis progressus	SDSNH 47642	3561	m1L	8.88			3522	original	[11]
Procynodictis progressus	SDSNH 43744	3564	m1L	9.26			3989	original	[11]
Procynodictis progressus	SDSNH 48100	3564	m1L	8.5			3093	original	[11]
Procynodictis progressus	SDSNH 55888	3621	m1L	8.6			3202	original	[11]
Procynodictis progressus	SDSNH 54413	3870	m1L	8.37			2955	original	[11]
Carnivoramorpha new gen. B	UCMP 141385	V6839	m1L	5.5			849	original	[11]
Carnivoramorpha new gen. C	SDSNH 42812	3562	m1L	6.2			1229	original	[11]
Carnivoramorpha new gen. W	SDSNH 50599	3788	m1L	6.2			1183	original	[11]
*Hoplophoneus**			m1L	19.1			34251	PBDB	[11]
Miacis gracilis	CM 11900	Uinta Fm.	m1L	8.4			2986	Clark 1939:362	[11]
Miacis gracilis	CM 12063	Uinta Fm.	m1L	10.0			5012	Clark 1939:362	[11]
Nimravidae gen. A	SDSNH 38343	3276	m1L	10.7			6127	original	[11]
Creodonta									
Limnocyon sp.	SDSNH 47965	3276	hunerus L			112.9	12287	original	[5]
Hyaenodon venturae	LACM CIT 1140	CIT 156	m3L	9.2			8783	Mellett 1977:43	
Hyaenodon vetus	LACM various	CIT 150	m3L	17.45			23538	Mellett 1977:19	
Leptictida									
Palaeictops sp.	SDSNH 47862	3612	m1A	4.5	4.3		688	original	[1]
Lipotyphla									
Aethomylos simplicidens	UCMP 101119	V72158	m1A	2.3	1.3		32	Novacek 1976:44	[1]
Aethomylos simplicidens	UCMP 101625	V72158	m1A	2.6	1.3		41	Novacek 1976:44	[1]
Aethomylos simplicidens	UCMP 101645	V71180	m1A	1.9	1.5		31	Novacek 1976:44	[1]
Aethomylos simplicidens	UCMP 101750	V71183	m1A	2.3	1.3		34	Novacek 1976:44	[1]
Batodonoides powayensis	UCMP 96138	V71181	m1A	1.0	0.6		2	Novacek 1976:31	[1]
Batodonoides powayensis	UCMP 96145	V71175	m1A	1.0	0.7		3	Novacek 1976:31	[1]

*Body-weight estimate for *Hoplophoneus* substituted for that for the unidentified nimravid "B," which is presently known only from the upper dentition.

Appendix 3.1: Weight Estimation (cont.)

Taxon	Specimen	Locality	Predictor	APL (mm)	TW (mm)	Other (mm)	Weight (g)	Measurement source	Equation source
Batodonoides powayensis	UCMP 96403	V71216	m1A	1.1	0.7		3	Novacek 1976:31	[1]
Batodonoides powayensis	UCMP 96432	V71211	m1A	1.0	0.6		3	Novacek 1976:31	[1]
Batodonoides powayensis	UCMP 96459	V71211	m1A	1.0	0.6		3	Novacek 1976:31	[1]
Centetodon aztecus	various various	various	m1A	1.6	1.0		13	Lillegraven et al 1981:44	[1]
Centetodon bembicophagus	various various	Bridger Fm.	m1A	1.5	0.9		9	Lillegraven et al 1981:39	[1]
Centetodon magnus	various various	various	m1A	2.1	1.2		25	Lillegraven et al 1981:60	[1]
Crypholestes vaughni	UCMP various	various	m1A	1.7	1.3		19	Novacek 1976:23	[1]
Nyctitherium			m1A	1.6	1.1		13	PBDB	[1]
Oligoryctes			m1A	1.0	0.9		4	PBDB	[1]
Patriolestes novaceki	SDSNH various	various	m1A	3.2	2.5		167	Walsh 1998:19	[1]
Proterixoides	LACM CIT 1883	CIT 207	m1A	3.6	3.6		360	original	[1]
Proterixoides	LACM CIT 1886	CIT 180	m1A	3.3	2.9		214	original	[1]
Proterixoides	LACM CIT 1887	CIT 180	m1A	3.4	2.6		185	original	[1]
Proterixoides	SDSNH various	various	m1A	3.1	2.5		159	Walsh 1998:8	[1]
Scenopagus cf. *S. priscus*	SDSNH 31715	3373	m1A	1.5	1.3		15	original	[1]
Sespedectes singularis	various	Sespe Fm.	m1A	1.8	1.3		23	Novacek 1985:6	[1]
Sespedectes singularis	various	San Diego	m1A	1.7	1.2		20	Novacek 1985:6	[1]
Sespedectes stocki	UCMP various	V72088	m1A	1.8	1.4		24	Novacek 1985:5	[1]
Artiodactyla									
Achaenodon robustus	SDSNH 47730	3737	M1A	22.7	29.5		252496	Walsh 2000:18	[3]
Antiacodon venustus	SDSNH 49170	3784	m1L	5.9			2996	original	[3]
Antiacodon venustus	SDSNH 50565	3784	m1L	5.5			2438	original	[3]
Eotylopus sp.	LACM 53560	CIT 150	m1L	8.5			12737	original	[4]
Ibarus sp.	SDSNH 47579	3564	m1L	5.3			2167	original	[3]
Leptoreodon edwardsi	various various	various	M1L	6.4			4548	Golz 1976:65	[4]
Leptoreodon golzi	SDSNH 47921	3621	M1L	5.1			2194	Ludtke and Prothero 2004:108	[4]
Leptoreodon leptolophus	various various	various	M1L	6.3			4324	Golz 1976:69	[4]
Leptoreodon major	SDSNH 55907	3621	M1L	7.8			8583	original	[4]
Leptoreodon cf. *L. marshi*	LACM various	CIT 249	M1L	6.6			5020	Golz 1976:73	[4]
Leptoreodon pusillus	various various	various	M1L	5.5			2796	Golz 1976:64	[4]
Leptoreodon stocki	LACM various	various	M1L	7.1			6204	Kelly 1990:19	[4]
Merycobunodon littoralis	SDSNH 49177	3784	m1L	7.2			5826	original	[3]

Appendix 3.1: Weight Estimation (cont.)

Taxon	Specimen	Locality	Predictor	APL (mm)	TW (mm)	Other (mm)	Weight (g)	Measurement source	Equation source
Merycobunodon littoralis	SDSNH 55894	3621	m1L	7.1			5575	original	[3]
Merycobunodon littoralis	SDSNH 55900	3621	M1L	7.1			6233	original	[4]
Parahyus sp.	SDSNH 55150	3893	M2A	16.3	20.5		64523	Walsh 2000:19	[3]
Poebrodon californicus	UCMP 314010	RV6830	M1L	8.2			10077	Golz 1976:56	[4]
Pomerado hypertragulid	SDSNH 69682	4042	m2L	6.0			2297	original	[4]
Protoreodon pacificus	various various	various	M1L	9.1			14077	Golz 1976:37	[4]
Protoreodon cf. *P. parvus*	various various	various	M1L	9.1			14077	Golz 1976:31	[4]
Protoreodon pumilus	various various	various	M1L	9.4			15622	Golz 1976:34	[4]
Protoreodon walshi	SDSNH 93838	4888	M1L	8.4			10763	original	[4]
Protoreodon walshi	SDSNH 105753	4730	M1L	10.0			19055	original	[4]
Protoreodon walshi	SDSNH 105754	4730	M1L	10.5			22285	original	[4]
Protylopus pearsonensis	various various	various	M1L	9.0			13587	Golz 1976:47	[4]
Protylopus cf. *P. petersoni*	various various	various	M1L	7.3			6939	Golz 1976:44	[4]
Protylopus stocki	various various	various	M1L	6.5			4780	Golz 1976:49	[4]
?Protylopus robustus	UCMP 312833	RV6830	m1L	8.5			12689	Golz 1976:51	[4]
Simimeryx hudsoni	LACM 53436	CIT 150	m1L	5.0			2340	original	[4]
Tapochoerus egressus	LACM 38058	CIT 202	m1L	6.7			4622	original	[3]
Tapochoerus egressus	LACM CIT 1292	CIT 180	m1L	7.2			5801	original	[3]
Tapochoerus egressus	LACM CIT 1587	CIT 180	m1L	7.2			5649	original	[3]
Tapochoerus egressus	LACM CIT 1588	CIT 180	m1L	7.5			6543	original	[3]
Tapochoerus egressus	LACM CIT 1590	CIT 180	m1L	7.3			6033	original	[3]
Tapochoerus mcmillini	SDSNH 47457	3562	m1L	5.5			2438	Walsh 2000:11	[3]
Tapochoerus mcmillini	SDSNH 47644	3276	m1L	5.6			2581	original	[3]
Tapochoerus mcmillini	SDSNH 52238	3564	M1A	5.5	6.7		3454	original	[3]
Tapochoerus mcmillini	SDSNH 52390	3564	M1A	5.5	6.6		3392	Walsh 2000:11	[3]
Tapochoerus mcmillini	SDSNH 52717	3564	m1L	5.7			2776	Walsh 2000:11	[3]
Tapochoerus mcmillini	SDSNH 52971	3564	m1L	5.7			2655	Walsh 2000:11	[3]
Tapochoerus mcmillini	SDSNH 54400	3870	M1A	5.7	6.9		3746	Walsh 2000:11	[3]
Perissodactyla									
Amynodon advenus	SDSNH 70960	4285	m1L	32.4			672322	original	[3]
Amynodon reedi	SDSNH 50557	3784	M1A	36.9	39.4		796581	original	[3]
Amynodontopsis bodei	SDSNH 92070	4732	M1A	41.1	38.7		906809	original	[3]
Amynodontopsis bodei	SDSNH 92070	4732	m2L	42.0			885064	original	[3]
Duchesneodus californicus	LACM 2143	CIT 292	M1A	39.0	45.0		1050824	Stock 1938*b*:512	[3]
Epihippus	SDSNH 105765	4730	m1L	8.3			8984	original	[3]
Hesperaletes borineyi	SDSNH various	various	M1A	8.3	9.5		10648	Colbert 2006:Sup. Data I	[3]

Appendix 3.1: Weight Estimation (cont.)

Taxon	Specimen	Locality	Predictor	APL (mm)	TW (mm)	Other (mm)	Weight (g)	Measurement source	Equation source
Hesperaletes walshi	SDSNH 55902	3621	M1A	8.1	9.0		9365	original	[3]
cf. *Hyrachyus* sp.	SDSNH 55887	3621	m1L	16.5			78568	original	[3]
cf. *Hyrachyus* sp.	UCMP 95848	V68161	m1L	15.3			62700	original	[3]
Hyracodon sp.	SDSNH 43478	3574	m1L	27.0			377940	original	[3]
Mesohippus sp.	SDSNH 60555	4042	m1L	10.5			18703	original	[3]
Metarhinus pater	SDSNH 98272	4566	M1A	26.0	28.4		291791	original	[3]
Metarhinus pater	SDSNH 98273	4566	m1L	27.8			414593	original	[3]
cf. *Metarhinus pater*	SDSNH 49313	3784	m1L	30.6			563749	original	[3]
Parvicornus occidentalis	SDSNH various	various	M1A	45.6	43.6		1263886	Mihlbachler and Demere 2009:7	[3]
Parvicornus occidentalis	SDSNH various	various	m1L	41.8			1510528	Mihlbachler and Demere 2009:7	[3]
Triplopus sp.	SDSNH 60386	4020	M1A	15.2	18.5		69631	original	[3]
Triplopus woodi	UCMP 134472	V88030	m1L	14.8			56320	original	[3]
Primates									
*Alveojunctus minutus**			m1A	1.8	1.3		51.0	PBDB	[2]
Cantius actius	SDSNH 35233	3413	M1A	5.2	6.2		2434	Gunnell 1995:463	[6]
Chumashius balchi	LACM CIT 1390	CIT 150 1/2	m1A	2.3	2.2		196	original	[2]
Chumashius balchi	LACM CIT 1392	CIT 150 1/2	m1A	2.3	1.9		150	original	[2]
Craseops sylvestris	LACM 40222	CIT 180	m1A	5.5	4.3		2365	original	[2]
Craseops sylvestris	LACM 40223	CIT 180	m1A	5.3	4.1		2092	original	[2]
Dyseolemur pacificus	LACM CIT 1395	CIT 180	m1A	2.0	1.9		127	original	[2]
Hemiacodon gracilis			m1A	3.6	3.0		661	PBDB	[2]
Macrotarsius cf. *M. roederi*	UCMP 113210	V73138	M1A	3.6	4.7		966	Lillegraven 1980:185	[6]
Microsyops annectens			m1A	4.7	3.4		1266	PBDB	[2]
Microsyops kratos	LACM CIT 2232	CIT 249	m1A	5.5	4.0		2120	Stock 1938*a*:292	[2]
Microsyops kratos	UCMP 99383	V71183	M2A	5.1	6.3		2495	Lillegraven 1980:199	[6]
Omomys cf. *O. carteri*	UCMP 101635	V72158	m1A	2.7	2.2		258	Lillegraven 1980:188	[2]
Omomys/Stockia	UCMP 106402	V72157	m1A	2.9	1.9		231	Lillegraven 1980:188	[2]
Ouraya sp.	UCMP 113214	V73138	m1A	3.7	3.1		712	Lillegraven 1980:195	[2]
Phenacolemur schifrae	LACM 40198	CIT 180	M1A	1.6	2.2		93	Mason 1990:2	[6]
Stockia powayensis	UCMP 94498	V6883	m1A	2.9	2.4		319	original	[2]

*Body weight estimate for *Alveojunctus minutus* substituted for that for *A. bowni*.

Appendix 3.1: Weight Estimation (cont.)

Taxon	Specimen	Locality	Predictor	APL (mm)	TW (mm)	Other (mm)	Weight (g)	Measurement source	Equation source
Uintasorex montezumicus	UCMP 106857	V72157	m1A	0.9	0.8		7	original	[2]
Uintasorex montezumicus	UCMP 109627	V72157	m1A	0.9	0.8		8	original	[2]
Washakius woodringi	various		m1A	2.0	1.6		90	Lillegraven 1980:196	[2]
Yaquius travisi	LACM 40202	CIT 180	m1A	4.3	3.8		1311	Mason 1990:4	[2]
Rodentia									
Eohaplomys matutinus	LACM CIT 3515	CIT 202	m1A	4.2	3.9		1227	Wilson 1949:18	[9]
Eohaplomys matutinus	LACM CIT 474	CIT 127	m1A	4.3	4.4		1564	original	[9]
Eohaplomys matutinus	LACM CIT3516	CIT 202	m1A	4.2	3.6		1066	Wilson 1949:18	[9]
Eohaplomys serus	LACM 5886	CIT 207	m1A	4.5	4.1		1476	original	[9]
Eohaplomys serus	LACM 5901	CIT 207	m1A	4.3	3.9		1281	original	[9]
Eohaplomys serus	LACM CIT 3509	CIT 207	m1A	4.2	4.1		1346	original	[9]
Eohaplomys serus	LACM CIT 3512	CIT 207	m1A	3.7	3.7		894	Wilson 1949:18	[9]
Eohaplomys serus	LACM CIT 3513	CIT 207	m1A	3.9	3.8		1028	Wilson 1949:18	[9]
Eohaplomys tradux	LACM CIT 1574	CIT 180	m1A	3.5	3.1		596	original	[9]
Eohaplomys tradux	LACM CIT 3521	CIT 180	m1A	3.6	3.5		772	Wilson 1949:18	[9]
Griphomys alecer	UCMP 85971	V72066	m1A	1.4	1.2		21	original	[9]
Griphomys toltecus	UCMP 104083	V72088	m1A	1.5	1.4		32	Lillegraven 1977:248	[9]
Heliscomys sp.	SDSNH 60436	4041	m1A	0.9	0.9		5.0	original	[9]
Ischyromys			m1A	3.5	3.4		687	PBDB	[9]
Leptotomus sp.	LACM CIT 2180	CIT 207	m1A	4.7	4.6		1989	original	[9]
Metanoiamys agorus	SDSNH various	various	m1A	1.1	1.0		11	Walsh 1997:6	[9]
Metanoiamys fantasma	UCMP various	various	m1A	1.3	1.2		19	Lindsay 1968:22	[9]
Metanoiamys korthi	LACM various	5876	m1A	1.2	1.1		14	Kelly and Whistler 1998:442	[9]
Metanoiamys marinus	UCMP various	various	m1A	1.1	1.0		10	Chiment and Korth 1996:122	[9]
Microparamys cf. *M. minutus*	UCMP various	various	m1A	1.2	1.3		19	Lillegraven 1977:229;232	[9]
Microparamys tricus	LACM CIT 1122	CIT 150	LTRL			7.9	154	Wilson 1940*a*:68	[8]
Microparamys tricus	various various	various	m1A	1.7	1.8		59	Lillegraven 1977:238	[9]
Microparamys woodi	LACM various	various	m1A	1.4	1.4		31	Kelly and Whistler 1994:439	[9]
Mytonomys burkei	UCMP 85833	V72065	m1A	5.1	4.8		2489	original	[9]
Nonomyinae new gen.	SDSNH 72232	4042	m1A	1.7	1.4		43	Walsh 2010:1617	[9]
Nonomys gutzleri	SDSNH various	various	m1A	1.3	1.1		19	Walsh 2010:1614	[9]
Paradjidaumo	PBDB		m1A	1.4	1.5		31		[9]

Appendix 3.1: Weight Estimation (cont.)

Taxon	Specimen	Locality	Predictor	APL (mm)	TW (mm)	Other (mm)	Weight (g)	Measurement source	Equation source
Pareumys nr. *P. grangeri*	LACM various	various	m1A	1.7	1.6		50	Lillegraven 1977:249	[9]
Pareumys nr. *P. milleri*	LACM CIT 2209	CIT 150	LTRL			7.4	129	Wilson 1940*b*:101	[8]
Pauromys lillegraveni	SDSNH various	various	m1A	1.2	0.9		11	Walsh 1997:11	[9]
Presbymys lophatus	UCMP 131875	V5368	LTRL			7.5	136	original	[8]
Protadjidaumo			m1A	1.3	1.2		20	PBDB	[9]
Pseudotomus californicus	LACM CIT 2185	CIT 249	LTRL			24.2	3538	Wilson 1940*a*:80	[8]
Pseudotomus californicus	UCMP 131823	V68101	m1A	6.1	5.0		3635	original	[9]
Pseudotomus littoralis	LACM CIT 2542	CIT 314	m1A	4.8	5.1		2496	Wilson 1949:7	[9]
Rapamys fricki	UCMP 85806	V72066	LTRL			16.3	1183	original	[8]
Reithroparamys			m1A	2.9	2.7		348	PBDB	[9]
Sciuravus powayensis	UCMP 85839	V6883	LTRL			9.1	231	original	[8]
Simimys landeri			m1A	1.8	1.3		39	PBDB	[9]
Simimys simplex	UCMP various	various	m1A	1.2	1.0		11	Lillegraven and Wilson 1975:868	[9]
Simimys simplex	UCMP various	V72088	m1A	1.4	1.0		15	Lillegraven and Wilson 1975:864	[9]
Tapomys tapensis	UCMP 85836	V6103	LTRL			19.4	1918	original	[8]
Uintaparamys caryophilus	UCMP 99989	V6883	m1A	3.8	3.4		795	original	[9]
Uriscus californicus	UCMP 99975	V6883	m1A	2.3	1.9		119	original	[9]

Appendix 3.2: Morphological Category Assignments

Appendix 3.2: Morphological Category Assignments

Taxon	Estimated Weight (g)	Dental type/diet	Locomotor habit	Category
Marsupialia				
Copedelphys innominatum	41	acute-cusped	non-arboreal	N1-ac
Herpetotherium knighti	65	acute-cusped	non-arboreal	N1-ac
Herpetotherium valens	78	acute-cusped	non-arboreal	N1-ac
Herpetotherium sp.	72	acute-cusped	non-arboreal	N1-ac
Peradectes californicus	35	acute-cusped	arboreal	A1-ac
Peradectes sp.	35	acute-cusped	arboreal	A1-ac
Apatotheria				
Apatemys bellus	26	bunodont	arboreal	A1-bu
Apatemys downsi	68	bunodont	arboreal	A1-bu
Apatemys uintensis	42	bunodont	arboreal	A1-bu
Apatemys sp.	46	bunodont	arboreal	A1-bu
Mesonychia				
Harpagolestes sp.	102873	hyper-sectorial	non-arboreal	H5
Pantolesta				
Simidectes merriami	7949	bunodont	non-arboreal	N3-bu
Simidectes sp.	7949	bunodont	non-arboreal	N3-bu
Carnivoramorpha				
Nimravidae gen. A	6127	hyper-sectorial	non-arboreal	H3
Nimravidae gen. B	34251	hyper-sectorial	non-arboreal	H4
Lycophocyon hutchisoni	4904	sectorial	non-arboreal	C3
Miacis gracilis	3999	sectorial	non-arboreal	C3
Miacis hookwayi	1419	sectorial	non-arboreal	C3
Miocyon sp.	17296	sectorial	non-arboreal	C4
Procynodictis progressus	3348	sectorial	non-arboreal	C3
Tapocyon dawsonae	7808	sectorial	non-arboreal	C3
Tapocyon robustus	12951	sectorial	non-arboreal	C4
Tapocyon sp.	10380	sectorial	non-arboreal	C4
Carnivoramorpha new gen. B	849	sectorial	non-arboreal	C2
Carnivoramorpha new gen. C	1229	sectorial	non-arboreal	C3
Carnivoramorpha new gen. W	1183	sectorial	non-arboreal	C3
Creodonta				
Hyaenodon venturae	8783	hyper-sectorial	non-arboreal	H3
Hyaenodon vetus	23538	hyper-sectorial	non-arboreal	H4
Limnocyon sp.	12287	sectorial	non-arboreal	C4
Leptictida				
Patriolestes sp.	167	semi-acute-cusped	non-arboreal	N2-sa

Appendix 3.2: Morphological Category Assignments (cont.)

Taxon	Estimated Weight (g)	Dental type/diet	Locomotor habit	Category
Lipotyphla				
Aethomylos new small sp.	35	semi-acute-cusped	non-arboreal	N1-sa
Aethomylos new sp.	35	semi-acute-cusped	non-arboreal	N1-sa
Aethomylos simplicidens	35	semi-acute-cusped	non-arboreal	N1-sa
Aethomylos sp.	35	semi-acute-cusped	non-arboreal	N1-sa
Batodonoides powayensis	3	acute-cusped	non-arboreal	N0-ac
Batodonoides sp.	3	acute-cusped	non-arboreal	N0-ac
Centetodon aztecus	13	acute-cusped	non-arboreal	N1-ac
Centetodon bembicophagus	9	acute-cusped	non-arboreal	N0-ac
Centetodon magnus	25	acute-cusped	non-arboreal	N1-ac
Centetodon sp.	16	acute-cusped	non-arboreal	N1-ac
Crypholestes major	19	semi-acute-cusped	non-arboreal	N1-sa
Crypholestes new large sp.	19	semi-acute-cusped	non-arboreal	N1-sa
Crypholestes new sp.	19	semi-acute-cusped	non-arboreal	N1-sa
Crypholestes sp.	19	semi-acute-cusped	non-arboreal	N1-sa
Crypholestes vaughni	19	semi-acute-cusped	non-arboreal	N1-sa
Nyctitherium sp.	13	acute-cusped	non-arboreal	N1-ac
Oligoryctes large sp.	4	acute-cusped	non-arboreal	N0-ac
Oligoryctes small sp.	4	acute-cusped	non-arboreal	N0-ac
Oligoryctes sp.	4	acute-cusped	non-arboreal	N0-ac
Palaeictops sp.	688	semi-acute-cusped	non-arboreal	N2-sa
Patriolestes novaceki	167	semi-acute-cusped	non-arboreal	N2-sa
Proterixoides davisi	230	semi-acute-cusped	non-arboreal	N2-sa
Proterixoides sp.	230	semi-acute-cusped	non-arboreal	N2-sa
Scenopagus priscus	15	semi-acute-cusped	non-arboreal	N1-sa
Scenopagus sp.	12	semi-acute-cusped	non-arboreal	N1-sa
Sespedectes singularis	22	semi-acute-cusped	non-arboreal	N1-sa
Sespedectes stocki	24	semi-acute-cusped	non-arboreal	N1-sa
Sespedectes sp.	23	semi-acute-cusped	non-arboreal	N1-sa
Artiodactyla				
Achaenodon robustus	252496	bunodont	non-arboreal	N5-bu
Achaenodon sp.	252496	bunodont	non-arboreal	N5-bu
Antiacodon venustus	2717	bunodont	non-arboreal	N3-bu
Eotylopus sp.	12738	lophed	non-arboreal	N4-lo
Ibarus sp.	2167	bunodont	non-arboreal	N3-bu
Leptoreodon edwardsi	4548	semi-lophed	non-arboreal	N3-sl
Leptoreodon golzi	2194	semi-lophed	non-arboreal	N3-sl
Leptoreodon leptolophus	4324	semi-lophed	non-arboreal	N3-sl
Leptoreodon major	8583	semi-lophed	non-arboreal	N3-sl
Leptoreodon marshi	5020	semi-lophed	non-arboreal	N3-sl
Leptoreodon pusillus	2796	semi-lophed	non-arboreal	N3-sl
Leptoreodon stocki	6204	semi-lophed	non-arboreal	N3-sl
Leptoreodon sp.	4810	semi-lophed	non-arboreal	N3-sl
Merycobunodon littoralis	5701	semi-lophed	non-arboreal	N3-sl
Merycobunodon sp.	5701	semi-lophed	non-arboreal	N3-sl
Parahyus sp.	64523	bunodont	non-arboreal	N4-bu
Poebrodon californicus	10077	lophed	non-arboreal	N4-lo
Pomerado hypertragulid	2297	semi-lophed	non-arboreal	N3-sl

Appendix 3.2: Morphological Category Assignments (cont.)

Taxon	Estimated Weight (g)	Dental type/diet	Locomotor habit	Category
Protoreodon new sp.	15286	semi-lophed	non-arboreal	N4-sl
Protoreodon new sp. 1	15286	semi-lophed	non-arboreal	N4-sl
Protoreodon new sp. 2	15286	semi-lophed	non-arboreal	N4-sl
Protoreodon pacificus	14077	semi-lophed	non-arboreal	N4-sl
Protoreodon parvus	14077	semi-lophed	non-arboreal	N4-sl
Protoreodon pumilus	15622	semi-lophed	non-arboreal	N4-sl
Protoreodon walshi	17368	semi-lophed	non-arboreal	N4-sl
Protoreodon sp.	15286	semi-lophed	non-arboreal	N4-sl
Protylopus pearsonensis	13587	semi-lophed	non-arboreal	N4-sl
Protylopus petersoni	6939	semi-lophed	non-arboreal	N3-sl
Protylopus robustus	12689	semi-lophed	non-arboreal	N4-sl
Protylopus stocki	4780	semi-lophed	non-arboreal	N3-sl
Protylopus sp.	9499	semi-lophed	non-arboreal	N3-sl
Simimeryx hudsoni	2340	semi-lophed	non-arboreal	N3-sl
Simimeryx sp.	2340	semi-lophed	non-arboreal	N3-sl
Tapochoerus egressus	5730	bunodont	non-arboreal	N3-bu
Tapochoerus mcmillini	2613	bunodont	non-arboreal	N3-bu
Tapochoerus new sp.	4172	bunodont	non-arboreal	N3-bu
Tapochoerus sp.	4172	bunodont	non-arboreal	N3-bu
Perissodactyla				
Amynodon advenus	672322	lophed	non-arboreal	N5-lo
Amynodon reedi	796581	lophed	non-arboreal	N5-lo
Amynodon sp.	734107	lophed	non-arboreal	N5-lo
Amynodontopsis bodei	906809	lophed	non-arboreal	N5-lo
Amynodontopsis sp.	906809	lophed	non-arboreal	N5-lo
Duchesneodus californicus	1050824	semi-lophed	non-arboreal	N6-sl
Epihippus sp.	8984	semi-lophed	non-arboreal	N3-sl
Hesperaletes borineyi	10648	lophed	non-arboreal	N4-lo
Hesperaletes walshi	9365	lophed	non-arboreal	N3-lo
Hesperaletes sp.	10007	lophed	non-arboreal	N4-lo
Hyrachyus sp.	70634	lophed	non-arboreal	N4-lo
Hyracodon sp.	377940	lophed	non-arboreal	N5-lo
Mesohippus sp.	18703	lophed	non-arboreal	N4-lo
Metarhinus fluviatilus	489171	semi-lophed	non-arboreal	N5-sl
Metarhinus pater	489171	semi-lophed	non-arboreal	N5-sl
Metarhinus sp.	489171	semi-lophed	non-arboreal	N5-sl
Parvicornus sp.	1510528	semi-lophed	non-arboreal	N6-sl
Triplopus sp.	62976	lophed	non-arboreal	N4-lo
Triplopus woodi	56320	lophed	non-arboreal	N4-lo
Primates				
Alveojunctus bowni	51	faunivore-frugivore	arboreal	A1-ff
Cantius actius	2434	frugivore	arboreal	A3-fr
Chumashius balchi	173	faunivore-frugivore	arboreal	A2-ff
Chumashius sp.	173	faunivore-frugivore	arboreal	A2-ff
Craseops sylvestris	2229	folivore	arboreal	A3-fo
Craseops sp.	2229	folivore	arboreal	A3-fo

Appendix 3.2: Morphological Category Assignments (cont.)

Taxon	Estimated Weight (g)	Dental type/diet	Locomotor habit	Category
Dyseolemur pacificus	127	faunivore-frugivore	arboreal	A2-ff
Dyseolemur new sp.	127	faunivore-frugivore	arboreal	A2-ff
Dyseolemur sp.	127	faunivore-frugivore	arboreal	A2-ff
Hemiacodon gracilis	661	folivore	arboreal	A2-fo
Macrotarsius roederi	966	folivore	arboreal	A2-fo
Macrotarsius sp.	966	folivore	arboreal	A2-fo
Microsyops annectens	1266	faunivore-frugivore	arboreal	A3-ff
Microsyops kratos	2308	faunivore-frugivore	arboreal	A3-ff
Microsyops sp.	1787	faunivore-frugivore	arboreal	A3-ff
Omomys/Stockia sp.	231	faunivore-frugivore	arboreal	A2-ff
Omomys carteri	258	faunivore-frugivore	arboreal	A2-ff
Omomys sp.	258	faunivore-frugivore	arboreal	A2-ff
Ourayia new sp.	712	frugivore	arboreal	A2-fr
Ourayia sp.	712	frugivore	arboreal	A2-fr
Ourayia uintensis	712	frugivore	arboreal	A2-fr
Phenacolemur shifrae	93	faunivore-frugivore	arboreal	A1-ff
Phenacolemur sp.	93	faunivore-frugivore	arboreal	A1-ff
Stockia powayensis	319	faunivore-frugivore	arboreal	A2-ff
Uintasorex montezumicus	8	faunivore-frugivore	arboreal	A0-ff
Uintasorex sp.	8	faunivore-frugivore	arboreal	A0-ff
Washakius woodringi	90	faunivore-frugivore	arboreal	A1-ff
Washakius sp.	90	faunivore-frugivore	arboreal	A1-ff
Yaquius travisi	1311	folivore	arboreal	A3-fo
Rodentia				
Eohaplomys matutinus	1286	semi-lophed	non-arboreal	N3-sl
Eohaplomys serus	1205	semi-lophed	non-arboreal	N3-sl
Eohaplomys tradux	684	semi-lophed	non-arboreal	N2-sl
Eohaplomys new sp.	1058	semi-lophed	non-arboreal	N3-sl
Eohaplomys sp.	1058	semi-lophed	non-arboreal	N3-sl
Griphomys alecer	21	lophed	non-arboreal	N1-lo
Griphomys toltecus	32	lophed	non-arboreal	N1-lo
Griphomys new sp.	27	lophed	non-arboreal	N1-lo
Griphomys sp.	27	lophed	non-arboreal	N1-lo
Heliscomys sp.	5	bunodont	non-arboreal	N0-bu
Ischyromys sp.	687	bunodont	non-arboreal	N2-bu
Metanoiamys agorus	11	bunodont	non-arboreal	N1-bu
Metanoiamys fantasma	19	bunodont	non-arboreal	N1-bu
Metanoiamys korthi	14	bunodont	non-arboreal	N1-bu
Metanoiamys marinus	10	bunodont	non-arboreal	N1-bu
Metanoiamys sp.	13	bunodont	non-arboreal	N1-bu
Microparamys minutus	19	bunodont	non-arboreal	N1-bu
Microparamys tricus	154	bunodont	non-arboreal	N2-bu
Microparamys woodi	31	bunodont	non-arboreal	N1-bu
Microparamys sp.	68	bunodont	non-arboreal	N1-bu
Mytonomys burkei	2489	bunodont	non-arboreal	N3-bu
Mytonomys sp.	2489	bunodont	non-arboreal	N3-bu
Nonomys gutzleri	19	bunodont	non-arboreal	N1-bu
Nonomys sp.	19	bunodont	non-arboreal	N1-bu
Nonomyinae new gen.	43	bunodont	non-arboreal	N1-bu

Appendix 3.2: Morphological Category Assignments (cont.)

Taxon	Estimated Weight (g)	Dental type/diet	Locomotor habit	Category
Paradjidaumo sp.	31	bunodont	non-arboreal	N1-bu
Pareumys grangeri	50	bunodont	non-arboreal	N1-bu
Pareumys milleri	129	bunodont	non-arboreal	N2-bu
Pareumys sp.	90	bunodont	non-arboreal	N1-bu
Pauromys lillegraveni	11	bunodont	non-arboreal	N1-bu
Pauromys new sp.	11	bunodont	non-arboreal	N1-bu
Pauromys sp.	11	bunodont	non-arboreal	N1-bu
Presbymys lophatus	136	lophed	non-arboreal	N2-lo
Presbymys sp.	136	lophed	non-arboreal	N2-lo
Protadjidaumo sp.	20	bunodont	non-arboreal	N1-bu
Pseudotomus californicus	3538	bunodont	non-arboreal	N3-bu
Pseudotomus littoralis	2496	bunodont	non-arboreal	N3-bu
Pseudotomus sp.	3017	bunodont	non-arboreal	N3-bu
Rapamys fricki	1183	bunodont	non-arboreal	N3-bu
Rapamys sp.	1183	bunodont	non-arboreal	N3-bu
Reithroparamys sp.	348	bunodont	non-arboreal	N2-bu
Sciuravus powayensis	231	bunodont	non-arboreal	N2-bu
Sciuravus new sp.	231	bunodont	non-arboreal	N2-bu
Sciuravus sp.	231	bunodont	non-arboreal	N2-bu
Simimys landeri	39	bunodont	non-arboreal	N1-bu
Simimys simplex	13	bunodont	non-arboreal	N1-bu
Simimys sp.	13	bunodont	non-arboreal	N1-bu
Tapomys tapensis	1918	bunodont	non-arboreal	N3-bu
Tapomys sp.	1918	bunodont	non-arboreal	N3-bu
Uintaparamys caryophilus	795	bunodont	non-arboreal	N2-bu
Uriscus californicus	119	bunodont	non-arboreal	N2-bu